HOST-PATHOGEN INTERACTIONS IN THE SPRING DEAD SPOT OF BERMUDAGRASS PATHOSYSTEM

By

NATHALIA GRAF-GRACHET

Bachelor of Science in Agricultural Engineering

Federal University of Sao Carlos

Araras, São Paulo, Brazil

2012

Master of Science in Entomology and Plant Pathology

Oklahoma State University

Stillwater, Oklahoma

2015

Submitted to the Faculty of the
Graduate College of the
Oklahoma State University
in partial fulfillment of
the requirements for
the Degree of
DOCTOR OF PHILOSOPHY
July, 2019

HOST-PATHOGEN INTERACTION IN THE SPRING DEAD SPOT OF

BERMUDAGRASS PATHOSYSTEM

Dissertation Approved:

Dr. Nathan R. Walker

Dissertation Adviser

Dr. Carla D. Garzon

Dr. Carolyn Young

Dr. Stephen Marek

Dr. Charles Fontanier

ACKNOWLEDGEMENTS

I would like to express my immense gratitude to my advisor, Dr. Nathan Walker, whose guidance and support has had a major impact in my life. It is certainly beyond everything I ever deserved. Thanks to all members of my committee, Dr. Stephen Marek, Dr. Carla Garzon, Dr. Carolyn Young, Dr. Charles Fontanier, and Dr. Matthew B. Couger, whose expertise helped me solve problems I found in the way. Thanks to Dr. Robert Hunger, Dr. Hassan Melouk, and Dr. Darren Hagen, who offered valuable advice whenever I needed it. I am very fortunate for having such an extraordinary mentors.

A special thank you to all faculty and staff members of the Department of Entomology and Plant Pathology. I extend this special thank you to all the friends I have made here in the US, and to my dearest friends in Brazil. I am extremely lucky for having such amazing people in my life.

Finally, I express my simple gratitude to my parents and sister, Mario, Roseli and Marina, who are the most important people in my life. None of this would have happened without your support.

NAME: NATHALIA GRAF-GRACHET

Date of Degree: JULY, 2019

Title of Study: HOST-PATHOGEN INTERACTIONS IN THE SPRING DEAD SPOT OF BERMUDAGRASS PATHOSYSTEM

Major Field: PLANT PATHOLOGY

Abstract: *Ophiosphaerella herpotricha, O. korrae* and *O. narmari* are the causal agents of spring dead spot of bermudagrass (*Cynodon* spp.). These pathogens colonize roots of susceptible bermudagrass causing necrosis and death of plants. Bermudagrass mortality is likely due to weakenening of rhizomes and stolons by means of nutrient depletion and reduced function of rotted roots that enhance cold temperature sensitivity. Limited information is available regarding host-pathogen interactions in this pathosystem. Although categorized as necrotrophs, the strategy of pathogenesis and genetic information of these pathogens has remained unknown. Additionally, the underlying genetics of root colonization by these pathogens has not been fully elucidated. Therefore, the goal of this research was to use a bioinformatic approach to elucidate the genes expressed by *Ophiosphaerella* spp. during colonization, and to identify gene(s) from bermudagrasses that determine host susceptibility and tolerance. This study produced the first report of draft genomes of eleven *Ophiosphaerella* isolates. Candidate necrotrophic effector genes were identified in their genomes, which were also found to be upregulated *in planta*. This might imply that *Ophiosphaerella*-induced necrosis is the result of pathogen-associated molecular pattern-triggered immunity (PTI). Expression profiling analysis of roots of susceptible bermudagrass cultivar 'Tifway' infected with *O. herpotricha* demonstrated activation of PTI mediated by jasmonic acid potentially resulting in necrosis. The tolerant 'U3' biotype showed activation of basal defense response mediated by salicylic acid. This salicylic acid-mediated signaling could be involved in enhanced resistance to nutrient starvation and cold tolerance that allows the host to withstand pathogen infection. Future experiments are required to functionally characterize the roles of these bermudagrass candidate genes in the host-pathogen interaction, which suggest a symbiotic relationship. The results presented will serve as valuable genomic resources for future studies in these plant-pathogen interactions and population genetics in the spring dead spot of bermudagrass pathosystem. Moreover, this will enhance traditional breeding efforts to incorporate better host plant tolerance to the SDS fungi in bermudagrass cultivars.

TABLE OF CONTENTS

Chapter Page

LIST OF TABLES

Table Page

Table Page

Table	Page

LIST OF FIGURES

Figure Page

Figure Page

Figure Page

CHAPTER I

INTRODUCTION AND OBJECTIVES

Bermudagrass is a perennial warm-season grass cultivated successfully in the southern United States [294]. There are two predominant bermudagrass turfgrass types: common bermudagrass (*Cynodon dactylon* (L.) Pers.) and interspecific hybrids of common bermudagrass and African bermudagrass (*C. dactylon x C. transvaalensis* Burt-Davy) [54,295]. Areas planted with improved bermudagrass varieties include residential lawns, commercial landscapes, sports fields, and golf courses [213]. Maintaining healthy, problem-free bermudagrass in this region is challenging because of diverse environmental conditions, diseases, and insects pests [53,54,279,295].

In areas of the southern United States, where bermudagrass enters cold-temperature induced dormancy, spring dead spot (SDS) is considered the most destructive disease of these grasses. The pathogens, *Ophiosphaerella herpotricha* (Fries) J. Walker, *O. korrae* (J. Walker & A. M. Smith) R. A. Shoemaker & C. E. Babcock and *O. narmari* (J. Walker & A. M. Smith) Wetzel, Hubert & Tisserat, colonize and cause necrotic lesions in belowground organs. Symptoms associated with SDS appear in the spring season when dead patches with well-defined margins and variable diameters can be observed [321]. Despite being an important bermudagrass disease, little is known about the host-pathogen interactions between the fungi that cause SDS and their hosts.

The colonization of various bermudagrass cultivars by transgenic isolates of *O. korrae* [37] and *O. herpotricha* [95] has been studied. Infected roots of interspecific bermudagrass hybrid 'Tifway' (susceptible to SDS) had the entire cortex colonized with extensive discoloration [95]. Infected roots of common bermudagrass 'U3' biotype (tolerant) had vascular colonization and absent or delayed of root discoloration. The colonization of vasculature in this 'U3' biotype resembled a symbiotic plant-fungal relationship [95,269]. Production of reactive oxygen species associated with the fungal mycelium increased when fungus colonized the vasculature, supporting that this is similar to a symbiotic association [97].

These studies suggest that the same *Ophiosphaerella* species can use different strategies to colonize roots of a susceptible or tolerant cultivar of bermudagrass. However, the genetics underlying colonization of bermudagrass cultivars by these pathogens has not been fully elucidated. Therefore, the goal of this research was to use a bioinformatic approach to elucidate the genes expressed by *Ophiosphaerella* spp. during colonization, and to identify gene(s) from bermudagrasses that determine host susceptibility and tolerance. Such information will enhance traditional breeding efforts to incorporate better host plant tolerance to the fungi that cause SDS in bermudagrass cultivars. Through the release of improved bermudagrass cultivars, stakeholders such as sod producers, homeowners, and golf course superintendents will have reduced costs repairing damaged stands of bermudagrass and associated weed removal in the damaged areas. The specific objectives of this research were:

1. To generate a genome resource and perform comparative genomic analysis of the eleven isolates of *Ophiosphaerella*.
2. To elucidate the mechanisms of pathogenesis with transcriptional profiling of infected bermudagrass roots.
3. To elucidate gene expression during susceptible and tolerant responses of infected bermudagrass roots with transcriptional profiling.

CHAPTER II

REVIEW OF LITERATURE

1. TURFGRASSES AND THE TURFGRASS INDUSTRY

Species of plants in the family Poaceae (formely Gramineae) can be managed as turfgrasses and were reported to be used by ancient civilizations in pastures and lawn gardens thousands of years ago. Species in the subfamily Festucoideae are classified as C_3 grasses, and denominated as cool-season grasses due to their intolerance to prolonged high temperatures and dry conditions. Genera belonging to this subfamily include *Agrostis*, *Lolium,* and *Poa*. Species in the subfamilies Eragrostoideae and Panicoideae are classified as C_4 grasses, and commonly referred to as warm-season grasses because of their intolerance to extensive periods of cold temperatures. These subfamilies include the genera *Buchlöe*, *Cynodon,* and *Zoysia* [279].

In the United States, turfgrasses cover an estimated area of 202,000 km^2 and turfgrass maintenance and establishment is estimated to be a $40 billion annual industry [219]. In Oklahoma, the turfgrass industry is estimated to be valued at $300 million [213]. The estimated area dedicated to turfgrasses in Oklahoma is approximately 2,600 km^2. This area accounts for residential lawns, commercial landscapes, landscapes, sports fields, and golf courses [213].

2. BERMUDAGRASS

Bermudagrass is a perennial warm-season grass cultivated successfully in latitudes between 45°N and 45°S because of its intolerance to cold temperatures [53,294]. Although best adapted to warm and humid climates, bermudagrasses tend to be drought and salt tolerant, allowing for broader adaptation to warmer and drier climates [353].

There are two predominant bermudagrass turfgrass types cultivated currently in the United States. The first, common bermudagrass (*Cynodon dactylon* (L.) Pers.) consists of seeded varieties and tends to have a coarse leaf texture [53]. The second includes interspecific hybrids of common bermudagrass and African bermudagrass (*C. transvaalensis* Burt-Davy) that have better quality for commercial use. These hybrids are typically sterile triploids, as common bermudagrass is tetraploid and African bermudagrass is diploid [295]. Consequently, reproduction and establishment of these hybrid varieties is done vegetatively with sod or sprigs [53]. Hybrid varieties have more desirable traits, such as finer leaf texture, good density, and fast growth, which make these suitable for high maintenance sports fields and golf courses [53,295].

In the United States, bermudagrasses are cultivated in the south and into the turfgrass transition zones. The transition zone is the zone where both warm-season and the cool-season grasses can be grown, but not without challenges due to temperatures at the extremes of their growth ranges. Oklahoma is located in the transition zone and maintaining healthy, injury-free, bermudagrass can be challenging because of environmental conditions, diseases, and insect pests.

In the turfgrass transition zone, air and soil temperatures go below 10°C in the fall and winter, inducing bermudagrass to enter winter-dormancy. During winter-dormancy, bermudagrass growth ceases and foliar tissues die, resulting in tan colored stands of turf. In the spring, when soil temperature approaches 16°C, bermudagrass resumes root, stolon, and rhizome growth. Optimal growth occurs when soil temperatures are between 21° and 30°C [53,54,295].

Stolons and rhizomes provide an abundance of meristematic tissues for new growth in the spring. Bermudagrass can produce an extensive root system and have the highest growth rates compared with other warm-season grasses such as zoysiagrass (*Zoysia* spp. Willd.) and buffalograss (*Bouteloua dactyloides* [Nutt.] Engelm.) [35,53,353]. An extensive root system and high growth rates promote quick establishment of bermudagrass, which makes it a very versatile plant for soil cover and stabilization [53,295,353]. Additionally, stolons and rhizomes promote rapid rebound from injury, wear, or dormancy [295].

Insect pests and diseases can severely damage bermudagrass. In the transition zone, one of the most important diseases of bermudagrass is spring dead spot (SDS) a disease caused by three soilborne fungi in the genus *Ophiosphaerella* spp. [279].

3. SPRING DEAD SPOT

The first published report of SDS of bermudagrass was by Wadsworth and Young [321]. They reported SDS in common bermudagrass fields in Stillwater, OK in 1954, and within three years found SDS around the state [321]. In less than a decade after the report published in 1954, SDS was reported in Kansas, Nebraska, Arkansas, Missouri, and Pennsylvania [61,278,321]. Subsequently, SDS was reported in Australia and New Zealand [323].

Above ground symptom of SDS is observed after turf type bermudagrass resumes growth from winter-dormancy [165,321] and is most important in the transition zone [202,321]. This disease has been frequently observed in high maintenance and in lower maintenance bermudagrass [73,165,321]. The disease has been reported in several different environmental conditions, soil textures, and fertility levels, all of which did not affect disease severity [61,86]. Since the first disease report, the pathogens causing the disease were determined, and taxonomic placement of these fungi has changed throughout the decades.

3.1. PATHOGENS, HOST RANGE, AND DISTRIBUTION

Three distinct species of fungi in the genus *Ophiosphaerella* cause SDS: *Ophiosphaerella herpotricha* (Fries) J. Walker, *O. korrae* (J. Walker & A. M. Smith) R. A. Shoemaker & C. E. Babcock and *O. narmari* (J. Walker & A. M. Smith) Wetzel, Hubert & Tisserat. The taxonomic classification is as follows [248]

Kingdom: Fungi,

Phylum: Ascomycota,

Class: Dothideomycetes,

Subclass: Pleosporomycetidae,

Order: Pleosporales,

Family: Phaeosphaeriaceae

Initially, Wadsworth and Young [321] described the causal agent of SDS as an unknown species of *Helminthosporium*. In another study, species of *Helminthosporium*, *Fusarium*, *Curvularia,* and *Pythium* were isolated from bermudagrass roots, but attempts to reproduce SDS symptoms and were unsuccessful [165]. Then, Smith [280], in Australia, isolated a fungus from common bermudagrass ('couch grass') and obtained confirmation of pathogenicity by Koch's postulates. The SDS pathogen was first identified as *Ophiobolus herpotrichus* (Fr.) Sacc. based on morphology of perithecia, asci and ascospores [280]. After that, the fungus was repositioned into the genus *Leptosphaeria* and named *Leptosphaeria korrae* [281]. Later Walker and Smith [323] identified another fungus causing SDS in common bermudagrass and named it *Leptosphaeria narmari*. The species designations by Walker and Smith '*korrae*' and '*narmari*' are based on Australian aboriginal words for grasses. Further examinations of *L. korrae* and *L. narmari* resulted in the reclassification of both species into the genus *Ophiosphaerella* [248,277].

Ophiosphaerella korrae was first reported in Australia [280], but it is currently present in other countries. In Italy, it was isolated from a bermudagrass hybrid [89,121].

In the United States, *O. korrae* has been found in several states including Alabama, Kentucky, Mississippi, South Carolina, Tennessee, West Virginia, Virginia [89,141], California [86], Oklahoma, and Kansas [89,336,337] associated with both common and hybrid bermudagrasses. Besides bermudagrass, *O. korrae* has been associated with zoysiagrass *(Zoysia japonica)* in North Carolina, and with red fescue (*Festuca rubra* subsp. *rubra)* in Maryland [53,303].

Ophiosphaerella korrae is also the causal agent of necrotic ring spot disease of the cool-season turf Kentucky bluegrass (*Poa pratensis* L.). This disease has been reported in Michigan [336], New York [39], Rhode Island [60], and Wisconsin [336] in the US, and in Canada [341].

Ophiosphaerella narmari is reported to be more prevalent in Australia and New Zealand and was isolated from several grasses such as common bermudagrass, African bermudagrass, barley (*Hordeum vulgare* L.), rice (*Oryza sativa* L.), and wheat (*Triticum aestivum* L.) [39,89,143,323]. In the United States, *O. narmari* has been found in California, Oklahoma, Kansas [89,336,337], and in North Carolina [89,141].

Based on sexual structures formed in roots and stolons, an isolate collected from diseased bermudagrass in Kansas was identified as *O. herpotricha* [298]. The fungal name is synonymous with the former *Ophiobolus herpotrichus* [298,323]. While named *Ophiobolus herpotrichus*, this fungus was isolated from several grass species in the North America [10,89,113], Europe [72,89,221,309], Asia [89,184,332] and Africa [80,89]. After reclassified to *Ophiosphaerella herpotricha*, this species has been reported in Europe [89,186,312] and in the United States from infected bermudagrass [298], buffalograss [229], zoysiagrass [118], vertivergrass (*Vetiveria zizanioides* (L.) Nash) [89,322], and maize [89,271].

3.2. MORPHOLOGY AND IDENTIFICATION

The three SDS-causing species of *Ophiosphaerella* spp. are slow growing, mostly sterile fungi in media culture *in vitro* and there is no evidence of conidial stages [335]. Differentiation among species is difficult in the initial stages of colony growth because all three fungi start growing as generic white mycelium. Colony morphology changes in color after a few days of incubation. On potato dextrose agar, mycelium of *O. korrae* starts to darken from the center of the colony in shade of dark gray [280], *O. narmari* darkens to buff [323], and mycelium of *O. herpotricha* becomes tan to dark brown after several days of incubation [335]. However, colony morphology is highly variable among species [304].

Classification of *Ophiosphaerella* spp. fungi was done according to characteristics of pseudothecia, asci, and ascospores [298,323]. Production of pseudothecia is rare, although Smith [281], Wadsworth and Young [321], and Tisserat et al. [298] reported pseudothecia production in *O. narmari*, *O. korrae,* and *O. herpotricha*. Production of pseudothecia have been reported in field conditions, but seldom observed in the United States [143,323].

Identification of *Ophiospharella* species causing SDS must be conducted in the laboratory because fruiting bodies of these species are rarely found under field conditions [143]. Reliable identification can be done using primers that amplify the ribosomal DNA small subunit, rDNA large subunit and rDNA internal transcribed spacer regions, translation elongation factor 1-α, and RNA polymerase II second largest subunit [96], and then compared to reference sequences available at the National Center for Biotechnology information (https://www.ncbi.nlm.nih.gov).

4. BERMUDAGRASS AND SPRING DEAD SPOT PATHOSYSTEM

Ophiosphaerella spp. are soilborne fungi that infect and colonize roots, stolons, and rhizomes of bermudagrass [279]. The optimal growth rate of infection and colonization occurs during wet periods in the fall and early winter, when soil temperature is between 15 and 25°C [60,281,323]. The optimal temperature for infection is approximately 20°C [325]. The infection and colonization of bermudagrass by *O. korrae* and *O. herpotricha* are very similar. Both infect directly, do not form any specialized structures, and usually occurs within four days post inoculation [37,95].

After inoculation, the hyphae of *O. narmari* were observed to accumulate and form an infection cushion on the epidermis surface, which resembles a sclerotia-like structure [323]. Hyphae of *O. korrae* can accumulate in strands or form dark sclerotia of variable diameters, which is not always observed in the plant [60,95,323], and can also colonize the surface of stolons by forming a mycelium aggregate [95].

These pathogens can survive as hyphal aggregates or inside the infected tissue [37]. Consequently, dispersal of SDS to disease-free areas is more likely to occur by movement of infested soil or infected plant parts [175].

The injury caused by *Ophiosphaerella* spp. is necrosis of belowground organs that can be observed during fall through early winter. Symptoms associated with SDS in bermudagrass are more prominent above ground in the spring season, when dead patches are observed [321]. The affected areas appear as dead patches with distinct margins and variable diameters. Dead patches are perennial and generally increase in diameter every year. Sudden bermudagrass mortality in the spring is strictly associated with very cold temperature-induced injury [86,280,298]. The death of bermudagrass during dormancy due to SDS is likely caused by necrosis that weakens rhizomes and stolons by means of nutrient depletion and reduced function of rotten roots, which enhance cold temperature sensitivity [37,95,324,325].

Stolons and rhizomes of bermudagrass resume growth in the spring and can regrow into the inside of a dead patch. However, if a dead patch is large, recolonization might take longer than one season. Often, proliferation of weeds occurs inside of a dead patch that can easily overgrow bermudagrass. Consequently, herbicide applications are necessary to promote bermudagrass colonization [61,304,321].

For turfgrass type bermudagrasses, there are no symptoms of disease prior to dormancy and symptoms are only evident in the spring. When examined in the spring, roots, stolons and rhizomes are necrotic and black in color as result of *Ophiosphaerella* spp. colonization. Occasionally, dark hyphae can be observed around necrotic lesions [143,280].

Caasi et al. [37] and Flores et al. [95] studied the response of bermudagrass cultivars to *Ophiosphaerella* infection. A contrasting response among bermudagrass cultivars 'Tifway' (hybrid of *Cynodon dactylon* x *C. transvaalensis,* and susceptible to SDS) and one more resistant common bermudagrass, 'U3' biotype, were reported in both studies. Infected roots of 'Tifway' had the entire cortex colonized by the fungi with prominent necrosis. Colonization stopped at endodermis and cortical necrosis was observed as early as two days post inoculation. Infected roots of the resistant biotype showed vascular colonization without necrotic lesions 14 days after inoculation [37,95].

The absence of necrosis and colonization of vasculature in this common ‘U3’ biotype resembled an endosymbiotic fungal-plant relationship [37,95]. Production of reactive oxygen species associated with the fungal mycelium increased when the fungus colonized the vasculature of the ‘U3’ biotype, which has been reported in symbiotic associations [97].

The mechanism by which SDS fungi induce necrosis in the bermudagrass root is not well understood. Additionally, the genetics underlying colonization of bermudagrass cultivars by these pathogens has not been fully elucidated.

5. ROOT DEFENSE STRATEGIES

5.1. ROOT DEFENSE STRUCTURES

In a transverse section of a mature root, the epidermis, the cortex and the vascular cylinder are the primary tissue systems. The epidermis is the outer layer of tissue that is in contact with the soil. Epidermal cells are covered with a thin layer of mucigel that allows the roots to have better contact with soil particles, and provides protection from desiccation. The function of the epidermis is to absorb water and nutrients, which is facilitated by extensions of epidermal cells, known as roots hairs. The cortex occupies the area between the epidermis and the vascular tissue. The thin outermost layer of the cortex is called exodermis. The cells of the cortex often serve as storage of starch, and these cells are connected by plasmodesmata that aid the transport of water and nutrients to the vasculature. The cortex layer is characterized by intercellular spaces for aeration of cells. The innermost layer of the cortex is the endodermis, in which cells are more compactly arranged without intercellular spaces. The vascular cylinder is a complex of vascular tissues (phloem, protoxylem and metaxylem) and pericycle cells. The pericycle cells contribute to formation of lateral roots and to the vascular cambium [88,259].

There are two main preformed physical barriers in the roots: the exodermis and the endodermis. Both layers of tissue feature ‘Casparian strips' that are impregnation of the primary cell walls of adjacent cells [44,110,111]. The Casparian strips are composed mainly of lignin-like polymers and, because of their hydrophobic nature, they form a barrier to water and ions being transported from the epidermis to the vasculature. Exo- and endodermal tissue might also deposit suberin, which is also hydrophobic and known to be highly resistant to enzymatic degradation. The Casparian strips and the suberized cell walls of the exodermis reduce water loss from the root to the soil, and also provide protection against penetration by plant pathogens [88,110,111,259].

5.2. ROOT DEFENSE PROTEINS

Root exudates play an important role between roots and soilborne pathogenic and non-pathogenic microorganisms [70]. Plants can produce pathogenesis-related (PR) proteins constitutively present in roots and leaves, but many PR proteins accumulate in certain organs or during specific developmental stages [64,69,316]. For instance, β-glucanases (PR-2) and chitinases (PR-3) are produced in the roots but not in the leaves of healthy tobacco plants [34]. In healthy and stress-free *Arabidopsis thaliana*, β-glucanase, chitinases, thaumatin-like protein, peroxidases and osmotin were found in root exudates. The expression of these PR proteins varied during plant development, and most up-regulation of these PR proteins occurred during flowering [69].

The functions of these PR proteins secreted in the rhizosphere are yet to be fully understood. Previous studies indicated that chitinases and β-glucanases might play a role in the plant development, i.e. flowering stage, and in further development of floral organs [69,201,228]. Another study provided evidence that PR proteins were secreted depending on the organism, because these proteins were involved in recognition of a pathogenic and a non-pathogenic microorganism [70]. Lectin, a class of protein involved in plant recognition of microorganisms [28], was found in roots exudates of *A. thaliana* and *Medicago sativa* challenged by *Pseudomonas syringae* and *Sinorhizobium meliloti* [69]. Two lectin proteins were secreted in greater quantity when the non-pathogenic bacterium *S. meliloti* was present, which suggested that *S. meliloti* was recognized by the plant when *P. syringae* was not [70]. Another role of PR proteins is in changing the microbial community in the rhizosphere by favoring beneficial organisms over pathogenic organisms [81].

5.3. PLANT INNATE IMMUNITY

There are two types of plant innate immunity: basal or horizontal resistance, and vertical resistance [68,146]. Pathogen-associated molecular patterns (PAMPs) trigger a basal mechanism of resistance in which the plant recognizes conserved molecules, or molecular patterns, of a microorganism [77,146]. Co-evolution of plants with pathogens has resulted in pathogenic microorganisms being able to suppress plant basal defenses.

Successful pathogens produce molecules known as effectors that mask PAMPs, resulting in effector-triggered susceptibility [65,146]. Plants have developed strategies to circumvent effector-triggered susceptibility by recognizing pathogen effectors, a process mediated by host receptor genes that leads to effector-triggered immunity [63,77].

5.3.1. BASAL RESISTANCE

Pathogen-associated molecular patterns (PAMPs) are recognized by pattern recognition receptors (PRRs) on the surface of host cell. Plants can also recognize signals of damage caused during pathogen penetration, such as fragments of their own cell wall components, which are called danger-associated molecular patterns (DAMPs). The first line of plant immunity is known as PAMP-triggered immunity (PTI), which results in race-non-specific hypersensitive response (HR) or non-host resistance [26,30,64,146,172,206,231,275,308].

Bacterial flagellin (flg22) is a classic example of PAMP [30,91,127,146,231,357]. Flagellin is the main protein in the bacterium flagellum, which is a whip-like appendage that serves many purposes such as mobility, and adhesion to the host. The transmembrane FLS2 PRR recognizes flagellin. The FLS2 is a leucine-rich repeat receptor kinase that has been identified in rice, tomato, *Arabidopsis* and *Nicotiana* [30,52,114,146,357]. It has been shown that FLS2 forms a complex with BAK1, which is considered an immune co-receptor as it can also bind to flg22 when associated with FLS2. The BAK1 co-receptor has also been shown to serve as signal in the phosphorylation pathway to induce PTI [26,267,273,291,357].

Fungal chitin is another example of PAMP [26,92,149,231]. Chitin is a major component of the cell wall of fungi, and is perceived by PRRs in host plants. However, the perception might be different in monocots versus dicots. There are three receptors identified in *Arabidopsis* so far: LYK1/CERK1, LYK4, and LYK5 [87,216,231,328,346]. Recognition of chitin by CERK1 triggered internalization and phosphorylation of LYK5 inside the cell, which is believed to serve as signal transduction of PTI. LYK4 is also involved in signaling of PTI [87,231,328]. In rice, two receptors were identified as well: OsCEBiP and OsCERK1, which is similar to the one in *Arabidopsis*. In rice, however, the perception of chitin is done by OsCEBiP, and subsequent signal transduction is conducted by OsCERK1. Since CEBiP has not been found yet in *Arabidopsis*, it is believed that chitin perception might be different between these two plant species [149,216,231,276].

5.3.2. EFFECTOR-TRIGGERED SUSCEPTIBILITY

Successful pathogens produce inducers of plant susceptibility, also known as effectors. Effectors are a common name of products of avirulence genes (AVR) that are secreted into host cells to promote disease. Virulence factors include phytotoxins, enzymes, and other molecules that quantitatively enhance disease severity. Pathogen-derived decoys function to protect or to mimic PAMPs and effectors to divert host recognition and thus promoting effector-triggered susceptibility (ETS) [26,172,241].

There are two types of decoys: receptor and bodyguard [241]. A receptor decoy function to mimic the recognition molecules of the host in order to prevent the recognition response of the host. An example is the Ecp6 (extracellular protein-6) produced by *C. fulvum.* Ecp6 binds to chitin in the same capacity as LYK1/CERK1 as described in the previous section. By capturing chitin, Epc6 prevents chitin from binding to the tomato receptor CERK1 to deviate PTI [66,241,268]. A bodyguard decoy is an inactive version of an effector or a virulence factor that serves to shield the active elicitor. An example is PsXLP1, which is an inactive form of the virulence factor PsXEG1 of *Phytophthora sojae.* PsXEG1 is a crucial virulence factor in promoting infection in soybean, but the soybean host produces GIP1 to inhibit PsXEG1 and counteract the attack. To bypass inhibition of PsXEG1, *P. sojae* co-secretes PsXLP1 that strongly binds to GIP1, thus shielding the virulence factor and enhancing disease [205,241].

Necrotrophic fungi characteristically produce phytotoxic peptides that are necessary for disease to occur (host selective toxins) or that aid disease infection and colonization (non-host selective toxins). An example of fungal non-host selective toxins is the group of hydrophobin proteins. Hydrophobins are secreted by many species of filamentous fungi and are characterized by high hydrophobicity, self-assembly in the aqueous environment, small size peptides, and eight highly conversed cysteine amino acid residues [23,333,342]. Hydrophobins have many roles in virulence, adhesion, and protection, by forming a mucilaginous layer on hyphae and conidia [5,23,157,180,317]. It was shown that *M. grisea* possesses the *MHP1* gene that encodes magnaporin, a type of hydrophobin that is required for fungal development and pathogenicity of rice [157].

Host selective toxins (HSTs) have been characterized in a few fungal genera such as *Cochliobolus*, *Parastagonospora*, and *Pyrenophora*. A single species can produce many of these phytotoxic peptides that act like an AVR, and interact with a host receptor gene to trigger effector-triggered immunity (ETI). The interactions of necrotrophs' HSTs and plant host receptors are referred to as "inverse gene-for-gene" because they enhance disease susceptibility [100,101,340].

T-toxin produced by *Cochliobolus heterostrophus*, the causal agent of Southern corn leaf blight is a HST that belongs to the class of linear polyketides. Its biosynthesis is complex, controlled by a total of nine Tox1 genes that are located in two different loci (Tox1A and Tox1B) in separate chromosomes. Two polyketide synthase genes (PKS1 and PKS2) and one decarboxylase (DEC1) are required for T-toxin synthesis. The other genes include dehydrogenases and an unknown protein [140,222,253,266,289,344]. T-toxin promotes hypervirulence of the pathogen on corn that harbor the Texas male sterile cytoplasm (Tcms). The toxin directly binds to the Tcms gene product, T-urf13, which is located in the mitochondrial membrane. Upon binding, the protein changes in conformation, and induces detrimental effects to the host mitochondria, such as pore formation, leakage, and swelling that lead to cell death [253,289].

Parastagonospora nodorum (Berk.) Castellani & E. G. Germano, causal agent of Stagonospora nodorum blotch of wheat, secretes multiple HSTs. One of them is SnTox3, encoded by the SnTox3 gene [100,198]. SnTox3 was shown to induce ETS in the form of HR in wheat leaves of varieties that carried the toxin sensitivity gene Snn3 [198].

5.3.3. EFFECTOR-TRIGGERED IMMUNITY

Plants developed strategies to circumvent ETS by recognizing pathogen elicitors, particularly effectors, intracellularly. Recognition of an AVR is mediated by host receptor protein. The host receptor proteins consist of two domains: an intracellular nucleotide-binding (NB) site and a leucine-rich repeat (LRR). These receptors were referred to as R genes in older literature, but are denominated NLRs (NB-LRR receptors) in recent literature. Many plant NLR also contain an N-terminal Toll, interleukin-1 receptor, resistance protein (TIR) domain, or a coiled-coil domain (CC) [62,77,109,146,313]. Recognition of pathogen derived AVR by host NLR results in effector-triggered immunity (ETI) [63,77].

Plant NLRs can interact by direct physical association with an AVR, which fits the gene-for-gene relationship [64,99]. Flor's classical gene-for-gene hypothesis stated that "for each gene that conditions reaction in the host there is a corresponding gene in the parasite that conditions pathogenicity" [93]. Direct interaction of the NLR and the AVR can be demonstrated by yeast two-hybrid assays. These assays were used to demonstrate that the rice NLR Pi-ta bonded to the AvrPita effector of *M. grisea* [77,145], and that the flax TIR-NLR receptors L and M bonded to effectors AvrL567 and AvrM of the flax rust pathogen, *Melampsora lini*, respectively [45,78,79].

Many plant NLRs did not fit the classical gene-for-gene interaction model. In the last decade, two additional models were put forward to explain indirect interactions of effectors and NLRs. The guard [62] and the decoy models [314] rationalized that the effector interacted with an intermediate surveillance protein, which was then recognized/perceived by an NLR to activate ETI. More recently, the decoy model expanded further into two mechanisms of action [241]. In addition, the integrated sensors model (or integrated decoy) [46,147] was proposed because of newly discovered NLR domains [111], and evidence that pairs of NLRs act as decoy and are necessary for ETI [46-48].

The guard model hypothesized that an AVR was perceived by an accessory guardee (guard) protein and the cognate NLR. The guard model suggested that more than one AVR could be detected by one guardee. The guardee protein was required for cognate NLR to function in host defense. In the absence of the cognate NLR, AVR-guardee interaction would result in host susceptibility (or pathogen virulence) [62,313,314]. An example is *A. thaliana* plasma membrane guardee RIN4 and NLRs RPM1 and RPS2. RPM1 recognizes the presence of *P. syringae* effectors, i.e. AvrB and AvrRPM1, upon phosphorylation and/or cleavage of RIN4 [2,62,207,345]. Besides these, other *P. syringae* effectors target RIN4 as well [15,339]. When the guard model was proposed, it was not known if RIN4 had a role in enhancing disease [62]. Recently, it was confirmed that modification of RIN4 by *P. syringae* effectors enhances disease in *A. thaliana* genotypes that lack NLRs RPM1 and RPS2 [147,183].

The decoy model was initially proposed to explain evidence of accessory proteins that did not have a function in defense or enhancing susceptibility in the absence of the cognate NLR [241,314]. That initial model expanded over the years to accommodate three different types of decoy proteins (receptor, bodyguard and sensing). Both receptor and bodyguard decoys are pathogen-derived and were described previously. Sensing decoys are host-derived and act as baits for pathogen effectors [214].

Sensing decoys mimic the recognition of the cognate NLR to perceive pathogen effectors. The classic example is the decoy Pto and the cognate NLR Prf. Pto is a Ser/Thr receptor kinase decoy that is needed for tomato resistance against *P. syringae* harboring AvrPto and AvrPtoB. Pto mimics receptor-like kinases that are the targets of these AVRs. Prf is the cognate NLR that triggers ETI [241,314,355].

The integrated sensors model [46,168,208,343] has been suggested because of (i) newly discovered NLR domains, referred to as sensor domains [168,208], and (ii) pairs of NLRs that can form complexes, are necessary to confer ETI in host plants, and can recognize AVR gene targets from fungal and bacterial pathogens [46-48,208]. The *Arabidopsis* pair of TIR-NLRs RPS4 and RRS1 is required for recognition of AvrRps4 of *Ralstonia solanacearum,* and for recognition of *Colletotrichum higginsianum* [27,46,225]. Additionally, an NLR can recognize more than one Avr gene. The rice CC-NLR pair, RGA5-A and RGA4, interact to recognize two effectors of *M. grisea*, Avr-Pia and Avr-CO39 [48]. Furthermore, RGA4 was shown to be an active HR-inducer in rice and *Nicotiana benthamiana* independently of effector recognition. RGA5-A acts as a repressor of RGA4 in the absence of effector recognition. Upon recognition of Avr-Pia by RGA5-A, the repression is relieved and HR as result of ETI was observed [47].

6. PLANT DEFENSE SIGNALING AND RESPONSES

Defense responses downstream of PTI and ETI are a cascade of cellular events triggered by signaling molecules [77,286]. Important signaling molecules are calcium, reactive oxygen species, nitric oxide, and phytohormones. Mitogen-activated protein kinases are important proteins involved in the signaling pathway from cell receptors into the cytoplasm. The defense signaling pathway leads to changes in gene expression such as up-regulation of WRKY transcription factors, PR proteins, and defense-related genes. Other cellular events that are hallmark of defense responses include callose deposition and HR [26,30,77,146,286,296].

6.1. CALCIUM

Changes in calcium (Ca^{2+}) in the cytosol is referred to as Ca^{2+} signature. Ca^{2+} signatures are associated with transduction of signals due to biotic and abiotic events in plants [4,148]. Ca^{2+} signatures are stimulus-specific and are recognized by proteins that bind to Ca^{2+} (Ca^{2+} sensors), such as calcium-dependent protein kinases (CDPKs), and calmodulin (CaM) proteins [170,261,282].

Influx of Ca^{2+} from the extracellular through the plasma membrane is one of the earliest events in plant defense signaling. Cells of tobacco showed Ca^{2+} influx within 30 minutes of treatment with a PAMP [182]. Ca^{2+} signature due to a PAMP stimulus is perceived by Ca^{2+} sensors like CaM. Expression of CaM genes occurs during pathogenesis, and CaM proteins are activated upon binding with Ca^{2+}. In soybean inoculated with *P. syringae* pv. *glycinea*, CaM gene was expressed quickly (30 minutes) upon contact with that pathogen [239]. Furthermore, CaM binds to other signaling molecules and proteins involved in the pathway of defense, such as Mitogen-activated protein kinases and transcription factors, among others [50,238].

6.2. REACTIVE OXYGEN SPECIES

Oxidative burst is the rapid production of reactive oxygen species (ROS), which is another signal observed in early plant defense. Early Ca^{2+} influx due to PAMP recognition activate NADPH oxidases in the plasma membrane to produce ROS. Reactive oxygen species can also be produced by peroxisomes, mitochondria, chloroplasts [12,14,117,300], and include: hydrogen peroxidase, superoxide, singlet oxygen, and hydroxyl radical. Oxidative burst is biphasic: first an unspecific phase that can last minutes followed by a later specific phase. Prolonged ROS accumulation on the second phase correlates with defense [6,19].

Reactive oxygen species and Ca^{2+} are intimately associated in defense signaling. Ca^{2+} influx activates CaM genes, which increases the production of ROS [251]. But also, ROS production increased influx of Ca^{2+} as demonstrated by presence of hydrogen peroxide in tobacco cells [153,188]. Hydrogen peroxide has been shown to activate expression of transcription factors that regulate defense genes [128], and of PR proteins that have antimicrobial activity such as PR-1 and PR-5 in tobacco [75,230]. Additionally, hydrogen peroxide and other ROS can induce nitric oxide (NO) synthesis [229] and phytohormone signaling [75,76,90,123,128,300,318,320].

Arabidopsis mutants deficient in ROS production showed increased susceptibility to *Rhizoctonia solani* and to *Peronospora parasitica* [98,178]. When challenged with *P. parasitica*, *Arabidopsis* developed ETI in leaves, whereas roots failed to produce ROS and trigger ETI [132], this could indicate that defense responses in the roots cannot be extrapolated from research on leaves [64].

6.3. NITRIC OXIDE

Nitric oxide (NO) is a gaseous signaling molecule associated with early defense responses. High Ca^{2+} signature, CaM activation, and ROS production lead to production of NO [25]. Nitric oxide is synthesized through different pathways in plants, but primarily by the NO synthase-like pathway [174,358]. Production of NO is also associated with phytohormones and the expression of defense-related genes in several plant systems [159,194].

Tobacco cells showed a rapid increase in NO upon being elicited by a PAMP [174]. In *Arabidopsis,* genes NIA1 and NIA2 were involved in NO synthesis [242]. Double mutants of these genes resulted in greater susceptibility to the soilborne fungus *Sclerotinia sclerotiorum,* and activation of defense-related genes was delayed or not activated [242]. In contrast, *Arabidopsis* roots infected by *Verticillium longisporum*, another soilborne fungus, did not show an increase in NO production [297]. This supports the statement that defense responses in the roots cannot be extrapolated from research on leaves [64].

6.4. MITOGEN-ACTIVATED PROTEIN KINASE AND WRKY TRANSCRIPTION FACTORS

Mitogen-activated protein kinases (MAPKs) form a signal transduction pathway, directly or indirectly, from PRRs to defense responses inside the cell such as activation of transcription factors. The signal transduction is a cascade of events that consists of phosphorylation (loss of phosphorus, K) from one kinase to another. The MAPK cascade consists of phosphorylation of a MAPK kinase kinase (MAPKKK) that phosphorylates a MAPKK that phosphorylates a MAPK [77,133,212].

In the *Arabidopsis* genome, 90 MAPKs have been identified [139]. This suggests redundancy and deeper network signaling among MAPKs [258]. However, only three MAPKs have been extensively studied, MPK3, MPK4 and MPK6. These MAPKs are involved in the PTI cascade [13,106,246]. MPK3 was shown to be associated with PTI against the fungal pathogen *Botrytis cinerea* [106]. *Pseudomonas syringae* effector HopF2 inactivates that MAPK cascade and lead to PTI against nonpathogenic strains of *P. syringae*. [195,250,331]. It was also shown that MPK3 and MPK6 are involved in PTI by activation of the transcription factors WRKY22, WRKY29, and PR-1 gene [272]. MPK4 has been shown to negatively regulate the SA levels and PTI [246]. The *Arabidospsis mpk4* mutant constitutively activated PR genes and resulted in a plant with a dwarf phenotype compared to a wild type [246]. In soybean, a MPK4 homolog negatively regulated the levels of salicylic acid (SA) and hydrogen peroxide production [195].

Defense responses, particularly ETI, are strong immune responses that involve transcriptional reprogramming. Transcriptional reprogramming means that signaling molecules activate transcription factors and defense-related genes like PR genes and NLR downstream of pathogen recognition [258]. WRKY transcription factors bind to a conserved sequence of certain genes involved in defense and induce transcription. Interestingly, when a pathogen is not present, MPK4 forms a complex with another protein (MKS1) and the transcription factor WRKY33. Upon recognition of a PAMP, the complex dissociates and WRKY33 activates defense-related genes. These activated genes include PR genes and PAD genes in *Arabidopsis*, which encodes the antimicrobial compound camalexin [254,255,258]. Additionally, mutants lacking WRKY33 showed susceptibility to *B. cinerea* [354].

6.5. PHYTOHORMONES

Three phytohormones, salicylic acid (SA), jasmonic acid (JA) and ethylene (ET), have roles in plant defense signaling to a broad range of pathogens and to herbivores. Salicylic acid is associated with defense signaling to biotrophic and hemibiotrophic pathogens, whereas JA and ET are associated with necrotrophic pathogens and herbivores [22,117]. There is evidence that SA and JA/ET work antagonistically and synergistically, based on studies that focus on challenging the plant with one pathogen at a time, which is uncommon in natural settings [36,67,158]. It was suggested that the cross talk between these phytohormones is more dependent on the lifestyle of the pathogen [1,22]. Accumulation of SA due to pathogen infection was linked to EDS1, PAD4 and NDR1 coding genes that were shown to regulate PTI to biotrophic pathogens [59,102,161]. Salicylic acid acts as activator of PR genes such as the NPR1, which has a role in SA-JA balance, and WRKY transcription factors, which are involved in activation of defense-related genes [158].

Another role of SA is in systemic acquired resistance (SAR). SAR occurs when non-inoculated parts of the plants develop activation of defense-related genes and become resistant to future inoculations. SAR occurs because of the SA signal, induced by a pathogen infection/recognition, which spreads to other, non-inoculated, parts of the plant through the vasculature. These non-inoculated parts of the plant are referred to as being “primed” [58,215].

6.6. DOWNSTREAM DEFENSE RESPONSES

Callose deposition is one of the downstream responses of defense [115] and to wounding [263]. Callose is a β-glucan polymer that is synthesized by callose synthase genes such as PMR4 [232]. Callose is deposited at the plant cell wall near the infection site and serves as a physical barrier, along with antimicrobial compounds delivered to inhibit further colonization. In seedling roots of *Arabidopsis*, PTI were evidenced by callose deposition after challenged with chitin, peptidoglycan and flagellin [214]. Besides chitin, flagellin and elongation factor Tu of bacteria were also shown to induce callose deposition [114,142,171]. Callose deposition has been shown to be preceded by accumulation of ROS, particularly accumulation of hydrogen peroxide [30,203].

An important hallmark of host defense is the HR, which is rapid induction of programmed cell death (PCD) at the infection site. Programmed cell death in plants is regulated by autophagy, which is a natural mechanism to eliminate unwanted cells and also include unwanted microorganisms [211,290]. Localized PCD is a mechanism that inhibits biotrophic pathogens from colonizing the host, but can enhance colonization by necrotrophic pathogens [55,100]. Programmed cell death in plants is classified in autolytic and non-autolytic [315]. Autolytic-PCD is a localized death caused by release of hydrolases from vacuoles and clearing of cytoplasm. However, the HR in plants is believed to be non-autolytic-PCD. Non-autolytic-PCD is cell death activated by receptor recognition followed by fusion of the central vacuolar membrane to the plasma membrane of the cell [130,223,315]. Development of HR in plants is triggered by recognition of pathogens via PTI or ETI, and is controlled by signaling molecules that include ROS, NO, SA, and JA, and also by light [103,144], and defense-related genes.

For example, HR via ETI in *Arabidopsis* was triggered rapidly after recognition of NLR RPM1. Additionally, HR was shown to be controlled by genes such as ATG3, ATG6, ATG12, and ATG16L [197,240,257,301].

Additional evidence of HR, either by effector-induced or phytotoxin-induced HR, is internucleosomal DNA fragmentation [330]. More specifically in roots, the phenomenon is referred to as root cortical cell death. Root cortical cell death can happen naturally [24,131,191], be induced by abiotic factors [179], or induced by pathogens [192]. The prehelminthosporol phytotoxin of *Bipolaris sorokiniana* was shown to stimulate nuclear DNA fragmentation in root cortical cells [193]. DNA fragmentation and cell death in tomato caused by HSTs secreted by *Alternaria alternata* f. sp. *lycopersici* has also been reported [330].

High levels of ROS are lethal to cells, therefore, HR is usually preceded by ROS production [290]. The root apex zone is very active in cell division, elongation, tissue differentiation, and also during ROS production [108,305,306]. High levels of ROS can also be produced by roots under abiotic stresses, such as growth under phosphate deficiency [307]. The HR caused by root pathogens has not been widely studied [237]. There is one report of HR in soybean roots of a recessive mutant that developed spontaneous necrotic lesions [163]. However, evidence of a HR caused by soilborne bacteria or fungal pathogens in plant roots, and reports of occurrence of a HR in roots are poorly examined [64,237].

The differences between HR observed in leaves and in roots could be related to the different genes being expressed in the roots due of organ specialization [237]. Another reason could be the complex interaction with microorganisms in the rhizosphere.

Roots are constantly exposed and interacting with high densities of microbes in the soil including a high number of beneficial microorganisms/symbionts, therefore a less stringent molecular defense might occur [70,164]. Hence, defense responses in the roots cannot be extrapolated from research on leaves [64].

CHAPTER III

THE DRAFT GENOMES OF THREE *OPHIOSPHAERELLA* SPP. REVEAL INSIGHTS INTO THE PATHOGENESIS OF THE SPRING DEAD SPOT OF BERMUDAGRASS

ABSTRACT

Ophiosphaerella herpotricha, O. korrae and *O. narmari* are the causal agents of spring dead spot of bermudagrass. These pathogens colonize roots of susceptible bermudagrass causing necrosis and death of plants. Although categorized as necrotrophs, the strategy of pathogenesis and genetic information of these pathogens remained unknown. This research presents the first report of genomes of 11 isolates of *Ophiosphaerella* from different hosts and geographical locations. The genomes of 11 isolates were sequenced using short- and long-read sequencing technologies. The transcriptomes of 6 of these isolates were sequenced to assist with prediction of gene models. The predicted proteome of one isolate of *O. herpotricha* was validated by protein mass spectrometry. Genome assembly sizes ranged from 45 Mb to 70 Mb. The number of predicted protein coding genes varied from twelve to fourteen thousand across the three

species. A phylogenomic analysis of placed *Ophiosphaerella* spp. close to *Parastagonospora nodorum*, a plant pathogen of wheat. The functions of protein databases. These analyses indicate *Ophiosphaerella* utilizes multiple strategies during pathogenesis with evidence of predicted secreted proteins, necrotrophic effectors, plant cell wall degrading enzymes, and secondary metabolites. These genomes and putative gene functions are the first genomic resources of these pathogens, and will be important for subsequent studies to understand the host-pathogen interactions in this pathosystem.

1. INTRODUCTION

Bermudagrass (*Cynodon* spp.) is a perennial warm-season grass cultivated as turfgrass in in the southern United States. This region comprises both the warm-season and the transition zone of turfgrass cultivation [53]. In Oklahoma, located in the transition zone, common bermudagrass (*C. dactylon* (L.) Pers.) and bermudagrass hybrids (*C. dacytlon* x *C. transvaalensis*) are the predominant turfgrass types on golf courses and athletic fields. Maintaining healthy, injury-free bermudagrass in the transition zone is challenging. The two main limitations are unpredictable winter weather that can cause winter-kill and a disease called spring dead spot (SDS) [279].

Spring dead spot is the most devastating disease of bermudagrass where low temperature induces dormancy (Figure III-1) [279]. This is a disease caused by three fungal species in the genus *Ophiosphaerella* (Figure III-1C), namely *Ophiosphaerella herpotricha* (Fries) J. Walker, *O. korrae* (J. Walker & A. M. Smith) R. A. Shoemaker & C. E. Babcock and *O. narmari* (J. Walker & A. M. Smith) Wetzel, Hubert & Tisserat. Taxonomic placement of these fungi is in the Class Dothideomycetes, Order

Pleosporales, and Family Phaeosphaericeae [63]. All three species are present in the US, but *O. herpotricha* and *O. korrae* are more commonly found and can be associated with other warm-season grasses such as zoysiagrass (*Zoysia* spp.) [118,298,303]. Among the three species, only *O. korrae* is known to cause disease of another cool-season grass, known as necrotic ring spot disease of Kentucky bluegrass (*Poa pratensis* L.) [336]. The same pathogen was recently found to cause a root rot in barley (*Hordeum vulgare* L.) [135].

The pathogens that cause SDS are soilborne and colonize roots, stolons, and rhizomes. Infection occurs in the pre-dormancy period, which is fall and early winter. During the pre-dormancy period there are no symptoms of the disease aboveground, but necrosis can be observed in belowground plant parts (Figure III-1B). Symptoms associated with SDS are prominent in the spring season (post-dormancy)), when healthy plants resume growth., as dead patches. The dead patches are unsightly and sunken, with variable diameters and distinct margins (Figure III-1A). Bermudagrass death caused by SDS is likely due to depletion of water and nutrients in belowground organs that enhance sensitivity to cold temperature [37,95,324,325]. Spring dead spot negatively interferes with sports activities and scheduling of tournaments in golf courses, which are important sources of revenue for these establishments. Once symptoms appear, recolonization of dead patches occurs by stolons and rhizomes and can require the entire growing season to restore turfgrass coverage to the damaged areas. Often weed proliferation occurs inside the dead patch and additional herbicide applications are necessary to maintain weed-free stands.

Ophiosphaerella spp. are classified as necrotrophic pathogens. Caasi et al. [37] and Flores et al. [95] showed that colonization of a susceptible cultivar of bermudagrass occurred in the entire root cortex with strong necrosis as early as two days post inoculation. Flores [94] attempted to isolate a potential phytotoxin involved in root discoloration/necrosis, but had inconsistent results. Necrotrophic fungi can deploy plant cell wall degrading enzymes, phytotoxin, and/or necrotrophic effectors as strategies of pathogenesis. However, it is not known how these strategies play a role in *Ophiosphaerella*-induced necrosis because a genomic resourced for *Ophiosphaerella* species are lacking.

Since the early 2000s, the cost of whole-genome sequencing has dropped significantly due to high-throughput sequencing technologies [210,334]. The genome of many organisms were sequenced through big initiatives such as the 5,000 Insect Genomes Project [264], and the 1,000 Fungal Genomes Project [120], or by private initiatives, where individual research groups paid for sequencing services. To date, at least 191 genomes of fungal plant pathogens are publicly available [16]. The majority of these genomes are from pathogens of grains and fruit crops and gymnosperms [16]. Some of these species have been sequenced extensively to obtain reference genomes such as *Parastagonospora nodorum* [262], *Magnaporthe grisea* [129]. These publicly available genomes are valuable resources of genetic information for studies of pathogen lifestyles, comparative genomics, and plant-pathogen interactions [234,235,292,349].

To address the lack of genomic resource for SDS pathogens, the objectives of this study were (i) to sequence the genomes of *Ophiosphaerella* spp. isolates with differing host range and from different geographical location, and (ii) to provide insights of candidate genes involved in pathogenesis and *Ophiosphaerella*-induced necrosis.

2. METHODS

2.1. GENOME AND TRANSCRIPTOME SEQUENCING

A total of 11 isolates of *Ophiosphaerella* spp. were selected for genome and transcriptome sequencing (Table III-1). Isolates were selected based on place of origin and host. Total genomic DNA was extracted according to Möller et al. [217] with modifications for exopolysaccharide producing-fungi. Mycelia were cultured in potato dextrose broth in the dark without agitation. After seven to ten days, mycelia were harvested using vacuum filtration, squeezed in sterile cheesecloth, and rinsed with sterile nanopure water. Mycelia were freeze dried overnight, and stored at -20°C. For DNA extraction, approximately but no more than, 50 mg of freeze-dried mycelium was ground to a fine powder. Cell lysis occurred in 500 µl warm TES Buffer (100 mM Tris-HCl, pH 8.0, 10 mM EDTA, 2% SDS, 1% PVP and 0.2% 2-mercaptoethanol) amended with 2 µl Proteinase K (0.01 g/ml) for 45 minutes to one hour at 50°C with slight agitation. Acidic polysaccharides were bound together by addition of 1.4 M NaCl and 0.1 volume of 10% CTAB at 80°C for 15 min with slight agitation. DNA was separated from CTAB-bound polysaccharides with an equal volume of chloroform:isoamyl alcohol (24:1) followed by centrifugation at 14,000 rpm for 10 minutes at 4°C. The upper aqueous phase (80%) was carefully transferred to a new tube. An adequate volume of 5 M ammonium acetate was added to final concentration of 2.5M. The tube was stored at 4°C for 30 min before centrifugation at 14,000 rpm for 10 minutes at 4ºC. The supernatant was carefully transferred to a new tube without disturbing the pellet. DNA was precipitated with an equal volume of isopropanol and centrifuged for three minutes at 13,000 rpm. DNA pellet was washed with 70% ethanol and air-dried. The pellet was resuspended in warm 1X TE buffer and incubated at 60°C until dissolved. The resuspended DNA sample was stored at -80°C until submitted to sequencing.

Quality and quantity of genomic DNA was assessed by agarose gel, NanoDrop™ (Thermo Fisher Scientific, Waltham, MA, USA) and Qubit® (Thermo Fisher Scientific, Waltham, MA, USA) techniques. In agarose gel, one intact band representing the genomic DNA without degradation was used for further analysis. For the NanoDrop™, the cutoff for the 260/280 nm absorbance ratio was 1.8, and for 260/230 nm absorbance ratio was 1.8-2.2. For the Qubit®, total yield of double stranded DNA was assessed. The quantity of double stranded DNA was adjusted according to sequencing platform requirements. Additionally, the internal transcriber spacer (ITS) and the elongation factor 1-alpha (ef1-α) regions of each genomic DNA sample were amplified by PCR. These fragments were sequenced to confirm fungal identity and to assess contamination with other microorganisms.

A total of six isolates of *Ophiosphaerella* spp. were selected for RNA sequencing (Table III-1). Total RNA was extracted from actively growing mycelium. Mycelium was cultured in potato dextrose broth or over a cellophane sheet on potato dextrose agar for seven to ten days, vacuum filtered and washed with distilled autoclaved water. Recovered mycelia were flash frozen in liquid nitrogen, placed in a 2 mL sterile tube with

RNAlater®-ICE (Ambion, Inc., Austin, TX) and incubated at -20°C until used. Approximately, 50 mg of each mycelium was used for extraction. Excess RNAlate*r*®-ICE was removed by squeezing the mycelium with a forceps. Total RNA was isolated using RNase Plant Mini Kit (Qiagen, Inc., Valencia, CA) following the manufacturer recommendations. Eluted RNA sample was stored at -80°C until submitted for sequencing.

Quality and quantity of total RNA was assessed by agarose gel, NanoDrop™ and Agilent Bioanalyzer 2100 (Agilent Technologies Inc., Santa Clara, CA). In agarose gel, two intact bands representing the 28S and 18S without degradation were required. For the NanoDrop™, the cutoff for the 260/280 nm absorbance ratio was 2.0, and for the 260/230 nm absorbance ratio was 2.0-2.2. For the Agilent Bioanalyzer, RNA integrity number greater than 6.5 was acceptable, but greater than 7.0 was desirable.

The genomes and transcriptomes of *Ophiosphaerella* spp. were sequenced using two platforms (Table III-1): Illumina HiSeq System and Pacific Biosciences (PacBio). High molecular weight genomic DNA and highly pure total RNA that passed quality control were sequenced. Library preparation of 11 DNA and 6 RNA samples was performed by Novogene Bioinformatics Technology Co., Ltd. (Shatin, Hong Kong). These libraries were sequenced on an Illumina HiSeq System (Illumina Inc., San Diego, CA, USA) to produce 150bp pair-ended libraries. Library preparation of two DNA samples was performed by Research and Testing Laboratory (Lubbock, Texas, USA) and sequenced on a PacBio SMRT Sequencing System (Pacific Biosciences, Menlo Park, CA, USA). Each library was sequenced on one SMRT cell.

2.2. GENOME ASSEMBLY AND ANNOTATION

Raw Illumina reads were assessed for quality using FastQC [9] and filtered for low quality or adaptor trimming using Trimmomatic [29]. Clean reads were *de novo* assembled in SPAdes [21] using short-reads only, and using hybrid mode making use of long-reads for scaffolding [21,233]. PacBio reads in fasta format were error corrected, trimmed and *de novo* assembled in Canu [162]. Genome assembly was also carried out in hybrid mode in SPAdes. All *Ophiosphaerella* spp. genome assemblies were filtered to a minimum contig length cutoff of 500 bp. A comparative qualitative assessment of the assemblies was done in QUAST [124]. A quantitative assessment was done using sets of Benchmarking Universal Single-Copy Orthologs (BUSCO) [167]. Genome coverage was determined by mapping reads to the finished assemblies using HiSAT2 [156] for Illumina reads and Blasr [49] for PacBio reads, and subsequently by using BEDtools [256] coupled with custom Python scripts to determine coverage. Coverage is given as number of sequencing read bases that contribute to each base of the genome.

Gene models for each isolate were created using PASA (Program to Assemble Spliced Alignments) [126], and protein-coding genes predicted with Augustus *ab initio* [288]. The mitochondrial genome (mtDNA) of *Ophiosphaerella* species was identified by homology search using BLAST against the mitochondrial genome of *Parastagonospora nodorum* [33,129]. The isolate of which the mtDNA was contained in one contig was functionally annotated with MFannot [176,177], and plotted with OGDRAW [199]. Functional annotation of the predicted protein-coding genes was done using the eggNOG-mapper server [138] using Diamond as mapping mode and Ascomycota as taxonomic Scope. Genes involved in meiosis were obtained based on pathway mapping of the Kyoto Encyclopedia of Genes and Genomes (KEGG) [151] orthologs produced by eggNOG-mapper to the yeast meiosis pathway (ko04113) in the online KEGG Network reconstruction tool. Mating type genes of *Ophiosphaerella* were obtained through BLAST search of partial coding sequences of genes of *O. korrae* previously reported [136]. Genes coding for enzymes that assemble, modify and breakdown carbohydrate substrates were annotated using dbCAN2 server [205] and database for the Carbohydrate-Active enZymes (CAZymes) [41]. Secondary metabolite gene clusters were predicted through online batch search against the Secondary Metabolite Unique Regions Finder (SMURF) [154]. Predicted proteases were predicted through BLAST search against the MEROPS database [260]. Genes involved in plant-pathogen interaction were predicted through BLAST search of proteins against the PHI-base (Pathogen-Host Interactions database) [310] using e-value threshold 1e-10, minimum query coverage 60%, and minimum percent identity 50%. Secretome was predicted using SignalP [247]. Secreted fungal effectors were predicted by EffectorP [285], LOCALIZER [283], and ApoplastP [284].

2.3. VALIDATION OF GENES MODELS

The gene models of *O. herpotricha* isolate ISCC16F were validated as follows. Mycelium was grown in potato dextrose broth for at least 15 days until harvested using vacuum filtration. Mycelia was rinsed with sterile nanopure water and squeezed in sterile cheesecloth. Protein extraction of mycelia was done using Extraction 1 of the ReadyPrep Sequential Extraction kit (Bio-Rad Laboratories, Berkeley, California). Briefly, one gram of fungal mycelia was grounded to a powder in the presence of liquid nitrogen. The powder was homogenized in 500 µl of Reagent1 buffer (ReadyPrep Sequential Extraction kit) by sonication on ice. The homogenized solution was centrifuged at 13,000rpm for five minutes at room temperature. The supernatant was transferred to a new sterile centrifuge tube, and an aliquot was used to assess quality and quantity of proteins. Quality was assessed by running a 1:10 dilution of the sample in an SDS-PAGE gel. Quantity of proteins was determined by Bradford assay [32].

Samples were sent to the Oklahoma State University Biochemistry and Molecular Biology Recombinant DNA and Protein Core Facility in Stillwater, OK, for preparation and scanning. Peptide samples were scanned in the Thermo Scientific™ Orbitrap Fusion™ Tribrid™ mass spectrometer (Thermo Fisher Scientific, Inc., San Jose, CA) coupled to an electrospray ion source. A customized peptide mass database of the predicted proteome of *Ophiosphaerella herpotricha* ISCC16F was done using Mascot (Matrix Science, Inc. Boston, MA). Sample peptide masses were searched against the customized database to infer peptide sequences using Perseus software (Max Planck Institute of Biochemistry, Germany). Predicted proteins with two or more peptide hits were considered validated.

2.4. COMPARATIVE GENOMICS AND PHYLOGENETIC ANALYSIS

The genomic resources of selected ascomycete fungi (Table III-2) were downloaded from the JGI [119,120]. A phylogenomic tree was constructed for all *Ophiosphaerella* species and related ascomycetes. Single copy ortholog gene clusters were obtained by ProteinOrtho [181]. Alignments were done using MUSCLE [84] and trimmed using trimAl [42] with the -automated1 option. The alignments of 500 ortholog groups were randomly selected and concatenated using FASconCAT [169]. The concatenated alignment in PHYLIP format was used to build a maximum likelihood tree by RAxML-NG [166] using the --all option, which constructs a tree based on 1,000 bootstraps.

3. RESULTS

3.1. GENOME SEQUENCING, ASSEMBLY, AND GENE MODELS

All *Ophiosphaerella* genomes were sequenced with Illumina and two genomes (*O. narmari* BCGC-C2, and *O. korrae* HCW2) were sequenced with PacBio (Table III-1) platforms. Illumina sequencing (150 bp pair-ended) yielded a total of 55,180,407 reads on average (minimum, *O. narmari* AUS58: 44,728,426, and maximum, *O. korrae* OW11: 64,468,206). PacBio sequencing yielded 90,696 reads for *O. narmari* BCGC-C2 and 163,261 reads for *O. korrae* HCW2. After correction and trimming in Canu [162], 75,022 reads for *O. narmari* BCGC-C2 and 117,736 reads for *O. korrae* HCW2 were used for the assembly. The longest read lengths were 31,392 bp and 41,540 bp, respectively (Figure III-2). The majority of PacBio read representation (75th percentile) was below 12,000 bp for both isolates with median read length of 6,281 bp and 6,803 bp, respectively.

Initially, *Ophiosphaerella* genomes were assembled using Illumina reads and PacBio reads separately (Table III-3). The genome assemblies of Illumina reads were, on average 58 million base pairs (Mbp) for *O. herpotricha*, 65 Mbp for *O. korrae*, and 45

Mbp for *O. narmari*. The assemblies of PacBio reads yielded smaller genome sizes. For *O. narmari* BCGC-C2, genome size was approximately 38 Mbp, and for *O. korrae* HCW2, 43 Mbp. Genome coverage, the number of sequencing read bases that contributed to each base of the genome, (Figure III-3) for Illumina assemblies were at least 108X, whereas PacBio assemblies were 13X. BUSCO assessment of genome completeness (Figure III-4) showed that all Illumina assemblies had a higher percentage of complete and single-copy BUSCO genes. Illumina assemblies of *O. narmari* BCGC-C2 and *O. korrae* HCW2 had 93.2% and 92.5% of complete and single-copy genes, respectively. In contrast, their PacBio counterpart had 72.1% and 85.9% complete genes, respectively. PacBio assembly of *O. narmari* BCGC-C2 had the poorest quality assessment since almost 27% of BUSCO genes were fragmented or missing.

Subsequently, draft genomes were produced by hybrid assembly approach incorporating Illumina and PacBio reads (Table III-4). The genome sizes were, in average 60 Mbp for *O. herpotricha*, 66 Mbp for *O. korrae*, and 45.9 Mbp for *O. narmari*. Average genome coverage (Figure III-5) of assemblies produced by Illumina reads were at least 112X, whereas PacBio reads contributed at maximum 16X. Hybrid assemblies had improved BUSCO scores of complete genes (Figure III-6). All genomes had improvements in the number of single-copy genes, besides *O. korrae* HCW2 and *O. narmari* AUS58 that stayed the same. *O. herpotricha* KS28 has the highest improvement with 33 new single-copy genes represented in the hybrid assembly. All 11 *de novo* assemblies of *Ophiosphaerella* spp. can be considered nearly complete because each genome has more than 92% of complete and single-copy BUSCO genes.

Gene models were predicted on the genomes obtained by hybrid assemblies. Sequencing of RNA of *in vitro* culture from six isolates (Table III-1) were used to assist with gene prediction. Illumina sequencing (150 bp pair-ended) yielded a total of 43,922,482 reads in average (minimum, *O. narmari* AUS58: 40,690,894, and maximum, *O. herpotricha* ISCC16F: 52,133,180). Across all three *Ophiosphaerella* species, there were 13,220 complete genes (with start and stop annotations) and 13,509 predicted proteins (Figure III-5). Gene length was 1,560 bp in average. Additionally, there were 1.7 introns and 2.7 exons per gene. Average intron and exon length were 135 bp and 1,421 bp, respectively.

BUSCO scores of complete protein-coding genes were comparable to the scores of the genomes; however, with slightly higher percentage of fragmented (3.8%, average) and duplicated single-copy (55 genes, in average) BUSCO genes (Figure III-8). The variation of genome size of *Ophiosphaerella* species was attributed to an expansion of intergenic bases (Figure III-9). In *O. herpotricha* isolates at least 64% of genome bases were intergenic. In *O. korrae*, intergenic sequences represented in average 68% of the genome.

Validation of proteins of *O. herpotricha* ISCC16F was carried out with mass spectrometry. Peptide masses obtained from the mass spectrometer were compared to a custom database of peptide masses of the predicted proteome of *O. herpotricha* ISCC16F. The resulting matrix was parsed using Python scripts. Proteins with two or more peptide matches were considered validated. Using this threshold, there were 2,883 proteins validated.

The mitochondrial genome (mtDNA) of *Ophiosphaerella* was searched against the *P. nodorum* mtDNA [33,129]. The mtDNAs of all *Ophiosphaerella* assemblies consisted of two or more contigs. The exception was *Ophiosphaerella herpotricha* KS28, which consisted of a single contig of 67,256 bp in length (Figure III-9). A total of 65 genes were predicted in the *O. herpotricha* KS28 mtDNA, of which 12 are known fungal mitichondrial genes: one ATP synthase (atp6), seven NADH dehydrogenase subunits (nad1 - nad4, nad4L, nad5, and nad6), and four subunits of respiratory chain complex (cob, cox1, cox2 and cox3) [3]. Additionally, 29 were transferRNAs, 21 ORFs, 1 ribosomal protein S3 (rps3), and 2 ribosomal DNAs (rnl, and rns) [3]. The *O. herpotricha* KS28 mtDNA had 17 introns, which comprised a total of 22,031 bp and an average of 1,295.9 bp in length. The mtDNA of *O. herpotricha* KS28 is larger than the *P. nodorum* (49,761 bp) [33,129] and the *E. nidulans* (33,227 bp) [11,104] mtDNAs, but shorter than other fungal species, such as *Bipolaris cookei* (135,790 bp) [349].

3.2. ORTHOLOG ANALYSIS AND PHYLOGENOMIC ANALYSIS

The protein-coding genes of a total of 16 proteomes (11 *Ophiosphaerella*, 5 other fungi - Table III-2) were submitted to ProteinOrtho analysis. A total of 1,336 single-copy orthologous gene groups were obtained. For the phylogenomic analysis, 500 single-copy orthologous gene groups were selected randomly. The concatenated alignment consisted of 250,281 bases. A maximum likelihood tree (Figure III-10) was built in RAxML-NG with 1,000 bootstrap replicates. Isolates of each *Ophiosphaerella* species clustered as one monophyletic group with strong branch support (>84) in which *O. herpotricha* and *O. narmari* form a sister group with *O. korrae*. *Ophiosphaerella* species clade formed a sister group with *Parastagonospora nodorum*. These results are consistent with previous multilocus phylogeny of *Ophiosphaerella* species [96]. Flores et al. [95] reported that at the family and species level, *Ophiosphaerella* species formed a monophyletic group, but *O. korrae* TX1.4 placed as a monotypic branch. In the current phylogenomic analysis, the placement of *O. korrae* TX1.4 has been resolved. This isolate is now grouped within the *O. korrae* clade, which maintains this species as a sister group with the other two species.

3.3. PREDICTED FUNCTIONAL ANNOTATION OF GENES

3.3.1. POTENTIAL EFFECTORS

Effectors were predicted on the secretome. The secretome was subjected to EffectorP prediction of effectors. Subsequently, effectors were subjected to ApoplastP and LOCALIZER to predict their location inside the host cell (Table III-7). Secreted effectors that had at least one predicted location were considered to be potential effectors. On average, there were 167 potential effectors predicted in *Ophiosphaerella.* The *O. herpotricha* TX2.5A had the highest number of potential effectors (n=203), and *O. korrae* TX14 the second highest (n=184). With the exception of TX14, *O. korrae* had the lowest number of predicted effectors compared to the other *Ophiosphaerella* species.

3.3.2. CARBOHYDRATE-ACTIVE ENZYMES

The CAZyme database consists of five classes of enzymes that act in carbohydrates: GT (glycosyltransferase), GH (glycoside hydrolase), CE (carbohydrate esterases), PL (polysaccharide lyase) and AA (auxiliary activity), and one associated modules of enzymes: CBM (carbohydrate-binding module).

Ophiosphaerella species shared approximately the same number of CAZymes in each class (Table III-8). On average, these fungi produced 576 CAZymes, of which 234 are predicted to be secreted. The average CAZymes of *Ophiosphaerella* species were compared to other Ascomycete fungi (Table III-9), and an expansion of the number of genes in the AA and CE classes was observed. The five most populated CAZyme classes were AA7 with 42 genes on average, CE10 with 40 genes, AA9 with 32 genes, AA3 with 31 genes, and CE1 with 17 genes (Figure III-11). The CE1 and CE10 families include many esterases that act in hemicellulose and pectin found in plant cell walls. The CE1 family predominantly targets hemicellulose. The enzymes in the AA9 families are lytic polysaccharide monooxigenases that aid the degradation of cellulose and hemicellulose. AA3 involved in lignin degradation, and found in many wood-degrading fungi [8,41,187,200,204].

Plant cell wall degradation is not the only role CAZymes play in plant-pathogen interaction. Based on predictions of CAZymes, PHI-base, SignalP, EffectorP, and eggNOG-mapper, a homolog of *M. grisea* MoCDIP4 was found in all *Ophiosphaerella* genomes. The functional prediction of these homologs is consistent with the information of Chen *et al.* [51] as being a secreted AA9 CAZyme with cellulose binding domain. Although the *Ophiosphaerella* homologs were predicted to be effectors by EffectorP, they were not predicted to be located in the mitochondria by LOCALIZER.

Based on predictions of CAZymes, PHI-base, SignalP, and eggNOG-mapper, a homolog of *P. sojae* PsXEG1 was found in all genomes of *Ophiosphaerella* sequenced in this study. The functional prediction of these homologs is consistent with Ma *et al.* [205] as being a secreted GH12 CAZyme. These homologous proteins were predicted to be secreted by SignalP, but were not predicted to be effectors by EffectorP. When subjecting the PsXEG1-homologous protein sequences of *Ophiosphaerella* species to LOCALIZER, the protein was not predicted to be localized in the apoplast by ApoplastP tool.

3.3.3. SECONDARY METABOLITE PREDICTION

Genes involved in the biosynthesis of secondary metabolites (SMs) were predicted using SMURF. The prediction takes into consideration protein families and genomic location of the protein in the genome. The biosynthesis of a SM involves many enzymes. The genes encoding these enzymes are often located in clusters in the genome, and are referred to as backbone genes. SMURF predicts six types of enzymes: demethylallyl tryptophan synthase (DMAT), nonribosomal peptide synthatase (NRPS), polyketide synthases (PKS), PKS-like, terpene cyclase (TC), and NRPS-PKS hybrid (hybrid) [154].

Ophiosphaerella isolates showed a consistent number of backbone genes observed in each enzyme category (Table III-10). On average, there were a total of 51 backbone genes. *O. herpotricha* TX2.5A has the lowest number of backbone genes (43), whereas *O. korrae* ISCC14B had the highest (67). Overall, there were more representatives of NRPS and PKS enzymes. On average, there were 27 PKS and 10 NRPS predicted across *Ophiosphaerella*. There was no TC enzymes predicted from any genome.

Some *Ophiosphaerella* isolates had a homolog to the *Magnaporthe grisea ACE1* avirulence gene, which produces a hybrid backbone enzyme [56,196]. Based on predictions obtained by SMURF, PHI-base, and eggNOG-mapper, *O. narmari* ATCC201719 and *O. korrae* HCW2 had the homolog. In these isolates, the ACE1 was predicted in a cluster of ten and nine genes, respectively. In both clusters, there were the ACE1 homolog and another PKS gene present, which is consistent with information in the literature [56]. However, the predicted function of the other genes in those clusters were inconsistent among the isolates, and are not the same genes observed in *M. grisea* [56].

3.3.4. PROTEASES

Proteases are essential for living organisms and serve multiple purposes such as degradation of proteins, recycling of amino acids, and in plant-pathogen interactions. The classification of these enzymes in the MEROPS database are based on their catalytic mechanism. Currently, there are nine classes of proteases in MEROPS, but the most represented classes are cysteine (C), serine (S), threonine (T), aspartic (A) (named after the residue catalyzed by the proteases), and metalloproteases (M). Proteases are classified further into families, i.e. T1, and subfamilies, i.e. T1A [260]. In *Ophiosphaerella* species, the total number of proteases varied from 33 to 50, with the most populated protease category being T01A, which is a constitutive proteasome subunit (Table III-12) [260]. Homologs to *Fusarium oxysporum* fungalysin (M36) were found in the genomes of *Ophiosphaerella* species. Fungalysin was shown to cleave plant host chitinases and thus is a virulence factor [226]. Besides *F. oxysporum*, fungalysin has been reported in the plant pathogen species *F. verticillioides* [226] and *Ustilago maydis* [236]. Trypsin (S01A) is another protease that plays a role in plant-pathogen interactions, and homologs to trypsin were found in *Ophiosphaerella* species. It has been demonstrated that *Parastagonospora nodorum* secretes trypsin named SNP1 during the early stages of infection that promotes cell wall degradation during infection [43].

3.3.5. SEXUAL REPRODUCTION

Ophiosphaerella species are considered sterile in artificial media culture. There is no evidence of asexual reproduction and sexual reproduction is seldom observed in *vivo* or in *vitro* [143,323,335]. However, pseudothecia, asci and ascospores were used for species identification and taxonomy placing [298,323]. In another *Ophiosphaerella* species, *O. agrostis*, production of pseudothecia has been reported in the field and in laboratory conditions [150]. Sexual reproduction in fungi is governed by mating type (MAT) genes. In ascomycete fungi, two idiomorphs of MAT genes can exist, the MAT1-1 and MAT1-2 [338]. In *O. korrae*, these MAT genes have been identified [136]. The evidence of MAT genes in *O. korrae* [136] support that these fungi are homothallic fungi, which means that an isolate has one of each of the two MAT idiomorphs.

The partial sequence of *O. korrae* MAT genes (MAT1-1: AF486624.1, MAT1-2: AF486625.1) [136] were retrieved from the National Center for Biotechnology Information (NCBI) nucleotide database and used to mine the genomes of *Ophiosphaerella* using BLAST search tool. All three species of *Ophiosphaerella* species sequenced in this study had at least one copy of the MAT idiomorphs (Table III-13). Two isolates of *O. korrae*, HCW2 and KY162, had two MAT genes in their genome, which suggests that these fungi are heterothallic. Using the KEGG ortholog (KO) entries obtained from eggNOG-mapper, protein coding genes of *Ophiosphaerella* species were mapped to the yeast meiosis pathway (ko:04113) (Figure III-12). A total of 65 KO entries of *Ophiosphaerella* were mapped to this pathway. The presence of MAT genes and of genes involved in meiosis suggest that these pathogens reproduce sexually. Future studies are necessary to investigate if these isolates can cross under natural conditions and what are the necessary stimuli, conditions, or gene expression levels for sexual reproduction .

4. DISCUSSION

Spring dead spot, caused by three fungal species in the genus *Ophiosphaerella*, is a destructive soilborne disease of turf type bermudagrass in the southern US. These pathogens colonize roots of susceptible bermudagrass causing necrosis and death of plants. The underlying genetics involved in colonization of the susceptible host by *Ophiosphaerella* species remained unknown for many decades, which posed a great challenge to bermudagrass breeding programs. To address the lack of genomic resource for SDS pathogens and provide insights into the strategies of *Ophiosphaerella* pathogenesis, the draft genomes of 11 isolates were assembled, analyzed, and compared to other model fungal plant pathogens. Putative function of genes involved in pathogenesis and necrosis were identified and assessed comparatively. The draft genomes of *Ophiosphaerella* species provide insights into the strategies of pathogenesis of these pathogens, and will allow many more research studies in the future to improve the understanding of this pathosystem.

Accessibility and efficacy of whole genome sequencing revolutionized biology, and the genomes of many organisms across all kingdoms of life have been sequenced, including multiple plant pathogens. At least, 191 genomes of fungal plant pathogens are publicly available [16] and constitute an important resource for plant-pathogen interaction studies. However, a few challenges still remain. Modern algorithms used in genome assembly share the difficulty of resolving complex genomic regions to produce chromosome length assemblies (reference assemblies). Hybrid assembly of Illumina paired-end short reads and PacBio long reads are highly desired to overcome challenges of closing gaps of complex genomes [270,292]. Additionally, many sequencing runs are necessary to obtain a reference genome. In *Parastagonospora nodorum*, many sequencing efforts were necessary to obtain a refined genome assembly [262,76]. In research efforts by Richards et al. [262], nine PacBio SMRT cells were used to sequence the isolate Sn4, and the resolution of this genome improved significantly. The sequencing of nine PacBio SMRT cells resulted in more than 485,000 reads with average read length of 11,000 [67]. Although the price of sequencing has become more accessible in general, PacBio sequencing remains very expensive, which makes this technology less accessible than Illumina, considering the number of sequencing runs that are necessary to obtain thousands of sequencing reads to resolve genome complexities.

Quality of input DNA is another limitation for a successful sequencing run, especially for PacBio sequencing. In this research project, great challenges were encountered with DNA extraction from *Ophiosphaerella* isolates, particularly *O. herpotricha* isolates. PacBio sequencing of *O. herpotricha* ISCC16F was attempted four times, and in all occasions, it failed due to poor quality of isolated DNA. Many conventional DNA extraction protocols were tested, but high-quality high-molecular weight DNA was never achieved.

Similar challenges were faced in the DNA extraction of the other species, *O. korrae* and *O. narmari*, although less severe. After testing different mycelia preparation (data not shown) and protocol modifications (Appendix I), two isolates, *O. korrae* HCW2 and *O. narmari* BCGC-C2, could be sequenced. However, the PacBio sequencing of these isolates did not yield the expected number of reads or the desired length of reads; therefore, the inclusion of PacBio reads in the hybrid assemblies did not significantly improve the assembly statistics.

A qualitative assessment of the hybrid assemblies was done by analyzing mainly the number of contigs, the N50 value, and the size of the largest contig. The assembly of *O. narmari* isolates yielded the best quality scores with the largest contig of 1,8 Mbp (AUS58), the largest N50 of 305 Kbp (BCGC-C2), and the assembly with the least number of contigs (2,271, BCGC-C2) (Table III-4). The higher the number of intergenic bases (Figure III-9) present in the assembled genomes, the lower the quality of those assemblies. The assembly of *O. korrae* TX1.4 has the highest percentage of intergenic bases (50.8%). Consequently, this assembly yielded one of the lowest N50 (46.5Kb), and the highest number of contigs (10,568).

The addition of PacBio reads in the assembly of *O. korrae* HCW2 and *O. narmari* BCGC-C2 genomes did not increase assembly quality metrics nor did the long-read assembly by itself represent the genomes fully. The low resolution of these genome assemblies did not reflect their completeness or a comparable number of protein coding genes (Figure III-9). Nonetheless, the genomes generated can be considered reliable enough for the purpose of this research.

The CAZyme database consists of five classes of enzymes that act in carbohydrates [41]. The enzymes in the GT class are involved in synthesis of glycosidic bonds between two carbohydrates. The CBM includes modules that can be found in the peptide of other CAZymes peptides, and function to aid the activity of that enzyme. The CBM can co-occur in CAZymes in the GH and PL classes [31]. The GH class comprises enzymes that hydrolase glycosidic bonds of carbohydrates. The CE are enzymes that hydrolase esters. The PL class includes enzymes that cleave the glycosidic bonds of acid polysaccharides and result in unsaturated oligosaccharides. Many of GH, CE and PL substrates are components of plant cell walls such as cellulose, and lignin. The AA class comprises enzymes that facilitate the action of GH, CE and PL enzymes in their polysaccharide substrates. Therefore, AA enzymes are considered to aid the role of GH, CE and PL enzymes in plant cell wall degradation [31,41,187,200].

Fungi are known to have a diverse arsenal of enzymes to aid breakdown of plant cell wall. A saprobe of interest is the inky cap mushroom *Coprinopsis cinerea*, which is known to degrade dead plant biomass [187]. Currently in the JGI, the annotation of the genome of *C. cinerea* strain ‘Okayama 7’ shows a total of 114 AA genes [287]. The AA and CE families are attractive to the biotechnology and biofuel industries because these enzymes convert dead plant biomass into energy [311]. The expansion in the number of enzymes in the AA and CE families (Table III-9) is promising to the potential use of *Ophiosphaerella* enzymes in those industries. Plant pathogens can utilize CAZymes to promote disease by means other than plant cell wall degradation [41,51]. The

Magnaporthe grisea MoCDIP4-homolog (AA9) and the *Phytophthora sojae* PsXEG1-homolog (GH12) have been demonstrated to function as PAMPs.

It has been shown that *Magnaporthe grisea* produces an AA9 CAZyme called MoCDIP4 that has a cellulose binding domain, which has been shown to be a type of PAMP. It has been demonstrated that *in planta* expression of MoCDIP4 induced cell death (PTI) in rice [51]. Furthermore, the mechanism of MoCDIP4-triggered PTI was to suppress an anti-apoptotic protein, BCL-2 in the mitochondria [51].

Phytophthora sojae, is an oomycete phytopathogen responsible for causing stem and root rot of soybeans. This pathogen secretes the endoglucanase PsXEG1 (GH12) in the apoplast and is recognized as PAMP [205]. It has been shown that soybeans recognize PsXEG1 through direct binding to GmGIP1, which is an glucanase inhibitor protein, to induce PTI [205]. Because this PsXEG1 is an essential virulence factor, *P. sojae* developed a way to protect PsXEG1 and cause disease. Ma *et al.* [205] showed that this pathogen secretes a decoy protein to protect PsXEG1 and avoid host inhibitor. The decoy protein is PsXLP1, an inactive version of PsXEG1; thus a paralogous protein. The decoy PsXLP1 is recognized by GmGIP1, and consequently frees PsXEG1 to infect the host cell.

The presence of these genes in *Ophiosphaerella* suggests that the necrosis observed in the susceptible bermudagrass cultivars is HR as the result of PTI. The presence of the *M. grisea* ACE1-homolog, which is involved in ETI, supports that statement. Further studies are necessary to characterize these genes, and to evaluate their expression in infected plants.

The current phylogenomic analysis (Figure III-10) is consistent with previous multilocus phylogeny of *Ophiosphaerella* species [96] that showed *Ophiosphaerella* species formed a monophyletic group. In the current phylogenomic analysis, the placement of *O. korrae* TX1.4 has been resolved within the *O. korrae* clade. The *Ophiosphaerella* clade is a sister group with *Parastagonospora nodorum*. *P. nodorum* together with *Pyrenophora tritici-repentis* have emerged as model necrotroph phytopathogens since the discovery that these pathogens deploy necrotrophic effector proteins (previously referred to as host-selective toxins) to trigger plant cell death and disease enhancement [101,198]. The placement of *Ophiosphaerella* as a sister group with *P. nodorum* and the discovery of homolog genes found to be involved in plant cell death strengthen the evidence that *Ophiosphaerella* deploys necrotrophic effectors to induce plant cell death and promote disease in bermudagrass.

The three *Ophiosphaerella* species are sterile in culture and there is no evidence of conidial stages [335]. Additionally, these pathogens do not produce any specialized structures during plant infection [37,95]. Taxonomical classification of *Ophiosphaerella* spp. was done according to characteristics of pseudothecia, asci, and ascospores [298,323]. Production of pseudothecia have been reported in field conditions but seldom observed in the United States [35,82]. These pathogens can survive as hyphal aggregates or inside the infected tissue [37]. Consequently, dispersal of SDS to disease-free areas is more likely to occur by movement of infested soil or infected plant parts [175]. The evidence of MAT genes and genes involved in meiosis in *Ophiosphaerella* species indicate movement of these pathogens can occur by dispersal of ascospores or pseudothecia. Additionally, evidence of sexual reproduction has implications in the persistence, variability of isolates, and development of fungicide resistance in the field [220].

In a preliminary study (data not shown), *Ophiosphaerella* isolates harboring one or both MAT idiomorphs were isolated from the edge of spring dead spot patches from bermudagrass on a golf course fairway in Broken Arrow, OK in 2017 (Figure III-1A), which supports the evidence that sexual reproduction might be occurring in the field. However, evidence of pseudothecia remains to be found.

5. CONCLUSION

This is the first report of draft genomes of eleven isolates of three *Ophiosphaerella* species, the causal agents of spring dead spot of bermudagrass. The results presented will serve as valuable genomic resources for future studies of plant-pathogen interaction and population genetics in this pathosystem. The discovery of candidate necrotrophic effector genes lends support to the hypothesis that *Ophiosphaerella*-induced necrosis is the result of a plant basal defense mechanism known as PTI. Future experiments are required to determine gene expression levels in infected bermudagrass roots, and to functionally characterize these candidate genes to more conclusively reveal the strategy of pathogenesis.

FIGURES:

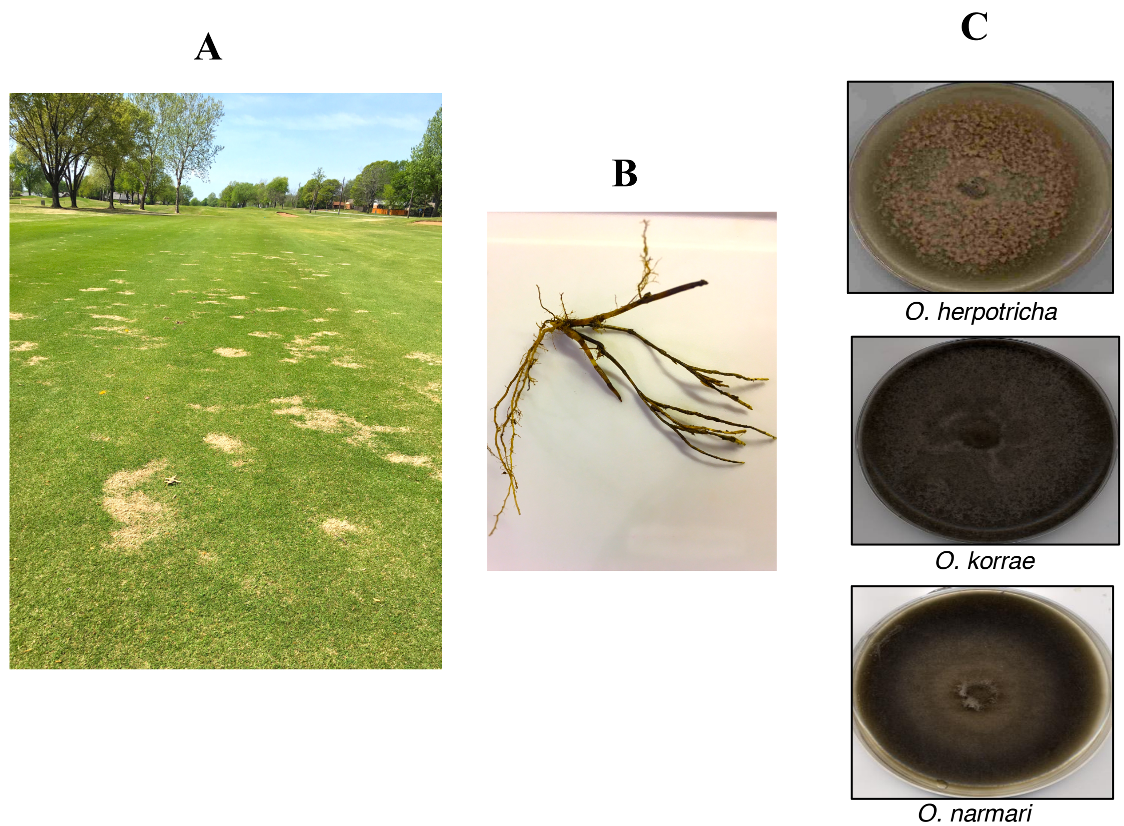

Figure III-1. Spring dead spot (SDS) of bermudagrass. (A) Bermudagrass in a golf course fairway with SDS symptoms. Picture was taken in Broken Arrow, OK, April, 2017. (B) Necrotic lesions on infected bermudagrass stolons and roots. (C) Difference in melanization of Ophiosphaerella species. growing in potato dextrose agar medium.

Ophiosphaerella korrae HCW2

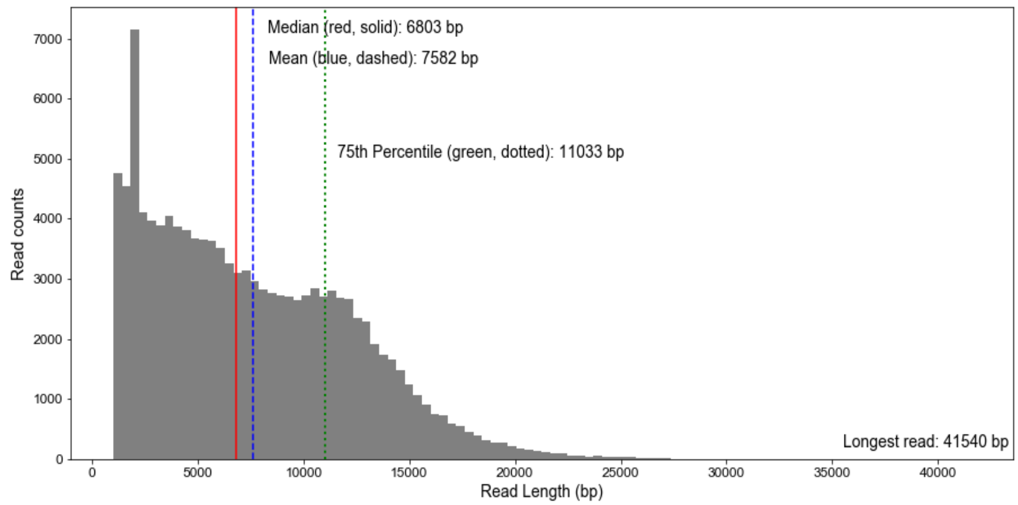

Ophiosphaerella narmari BCGC-C2

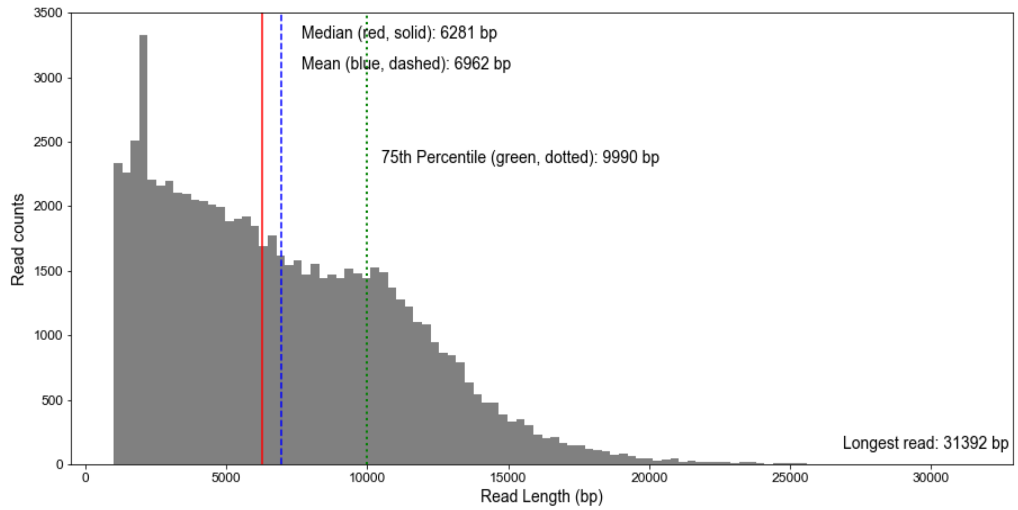

Figure III-2. Read length (in base pairs, bp) distribution of PacBio reads of *Ophiosphaerella korrae* HCW2 and *O. narmari* BCGC-C2. Reads were corrected and trimmed, which resulted in 17,736 reads of *O. korrae* HCW2 and 75,022 reads of *O. narmari* BCGC-C2 used for genome assembly.

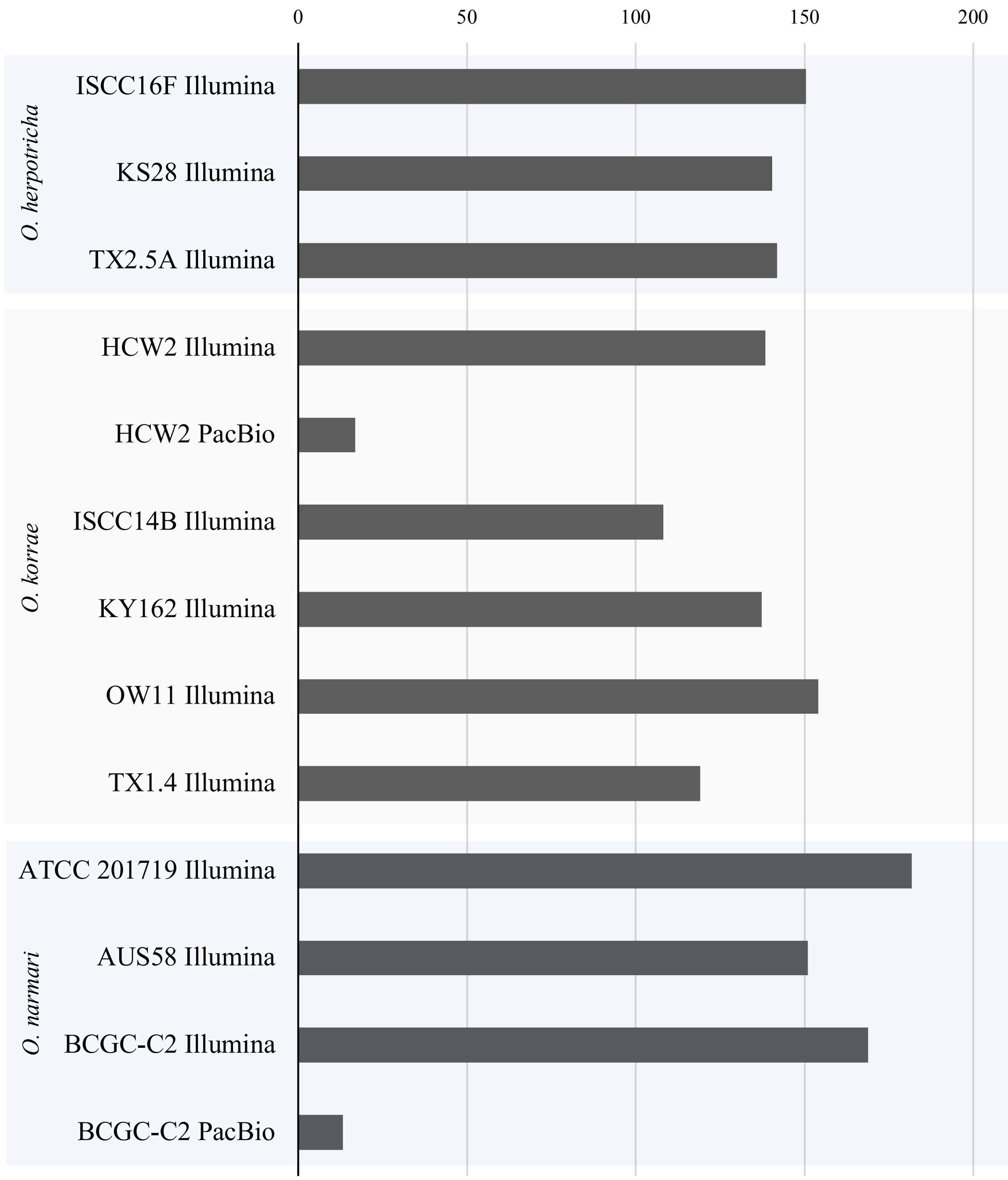

Figure III-3. Comparison of average genome coverage of *Ophiosphaerella* species using assemblies of Illumina and PacBio reads separately. Genome coverage is given as 'X', number of sequencing read bases that contribute to each base of the genome.

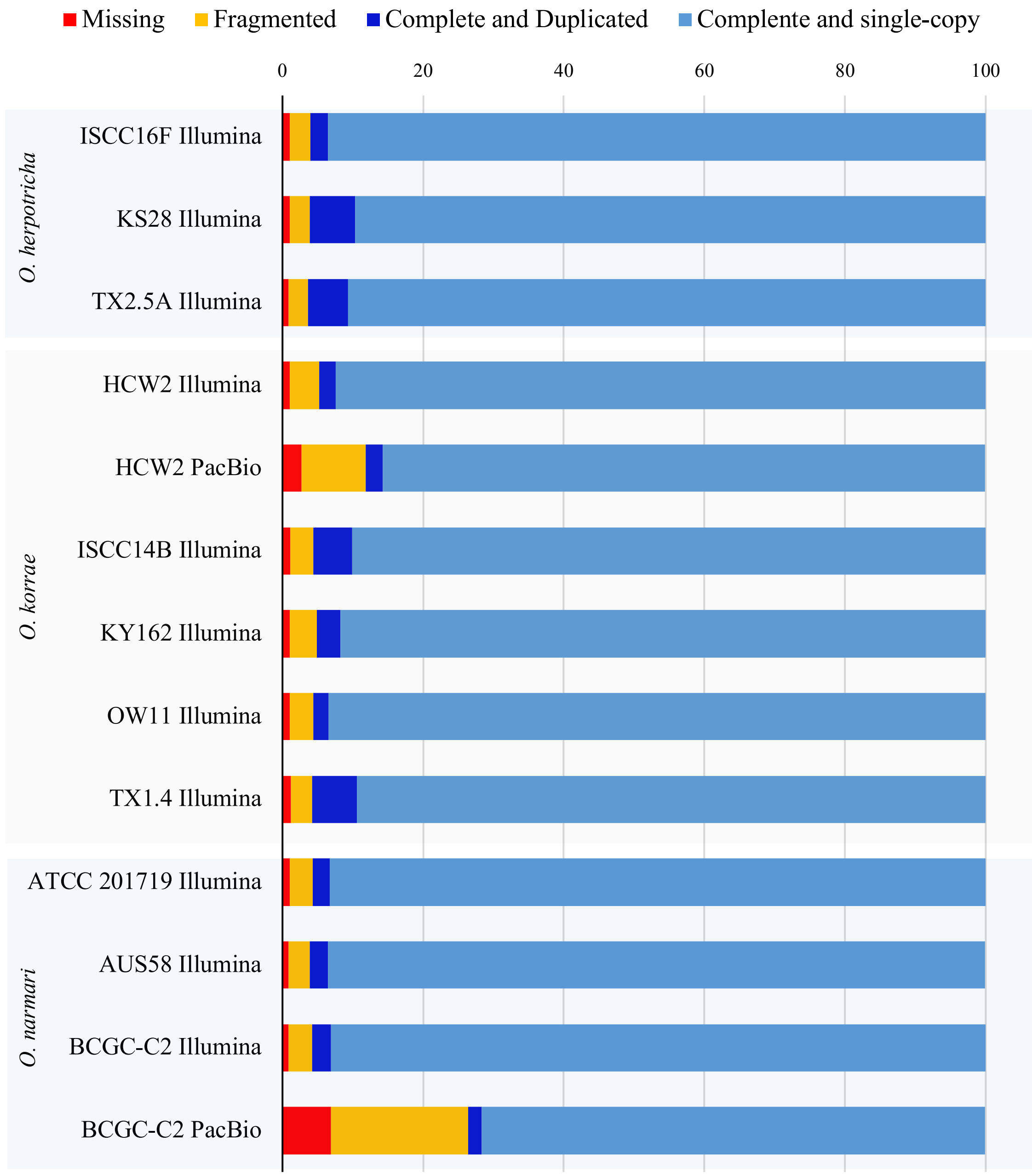

Figure III-4. BUSCO assessment of the genomes of *Ophiosphaerella* spp. using Illumina and PacBio reads separately.

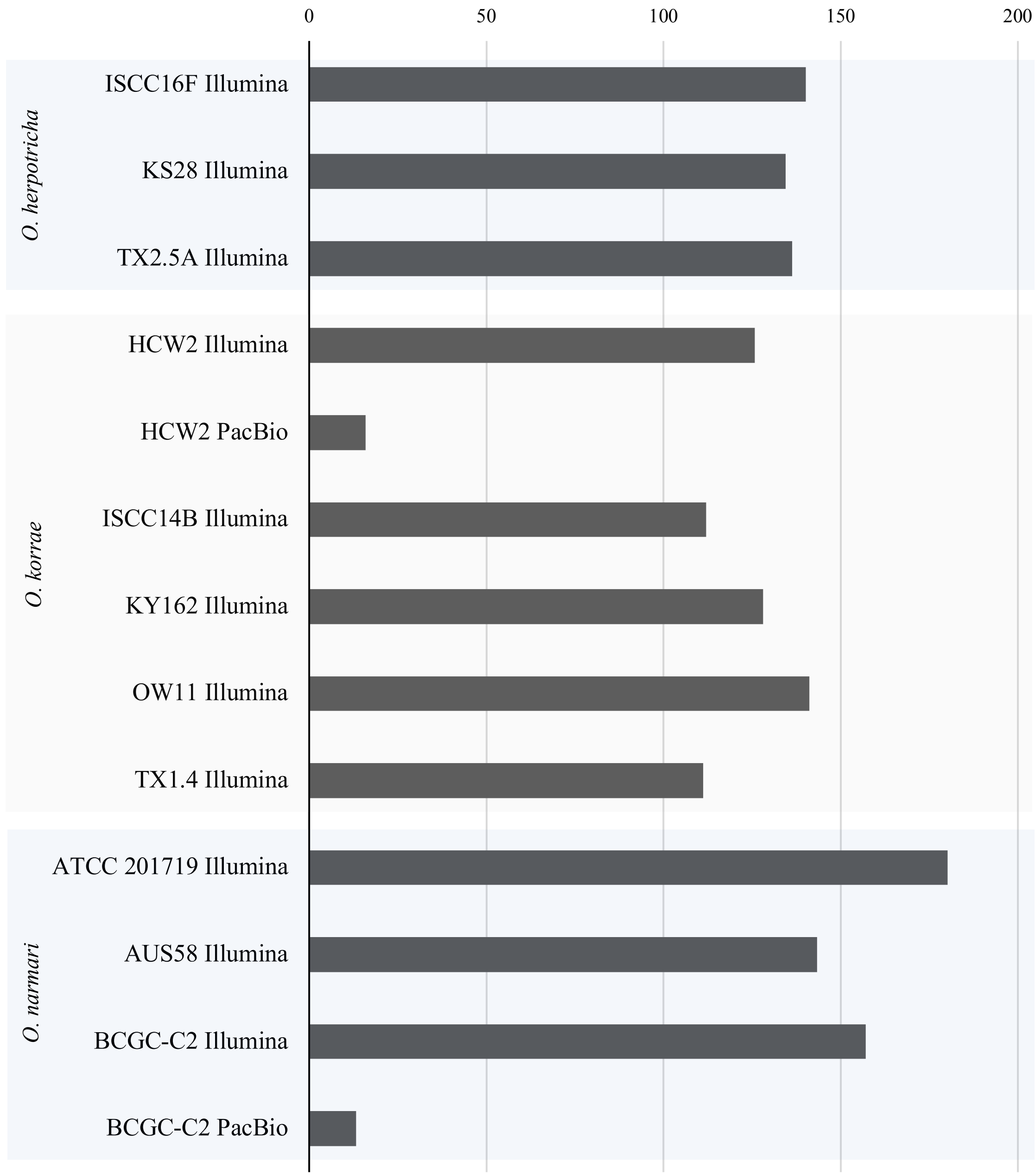

Figure III-5. Comparison of average genome coverage of *Ophiosphaerella* spp. hybrid assembly approach. Genome coverage is given as 'X' number of sequencing read bases that contribute to each base of the genome. Values are based on the contribution of Illumina and/or PacBio read bases to the hybrid genome assembly.

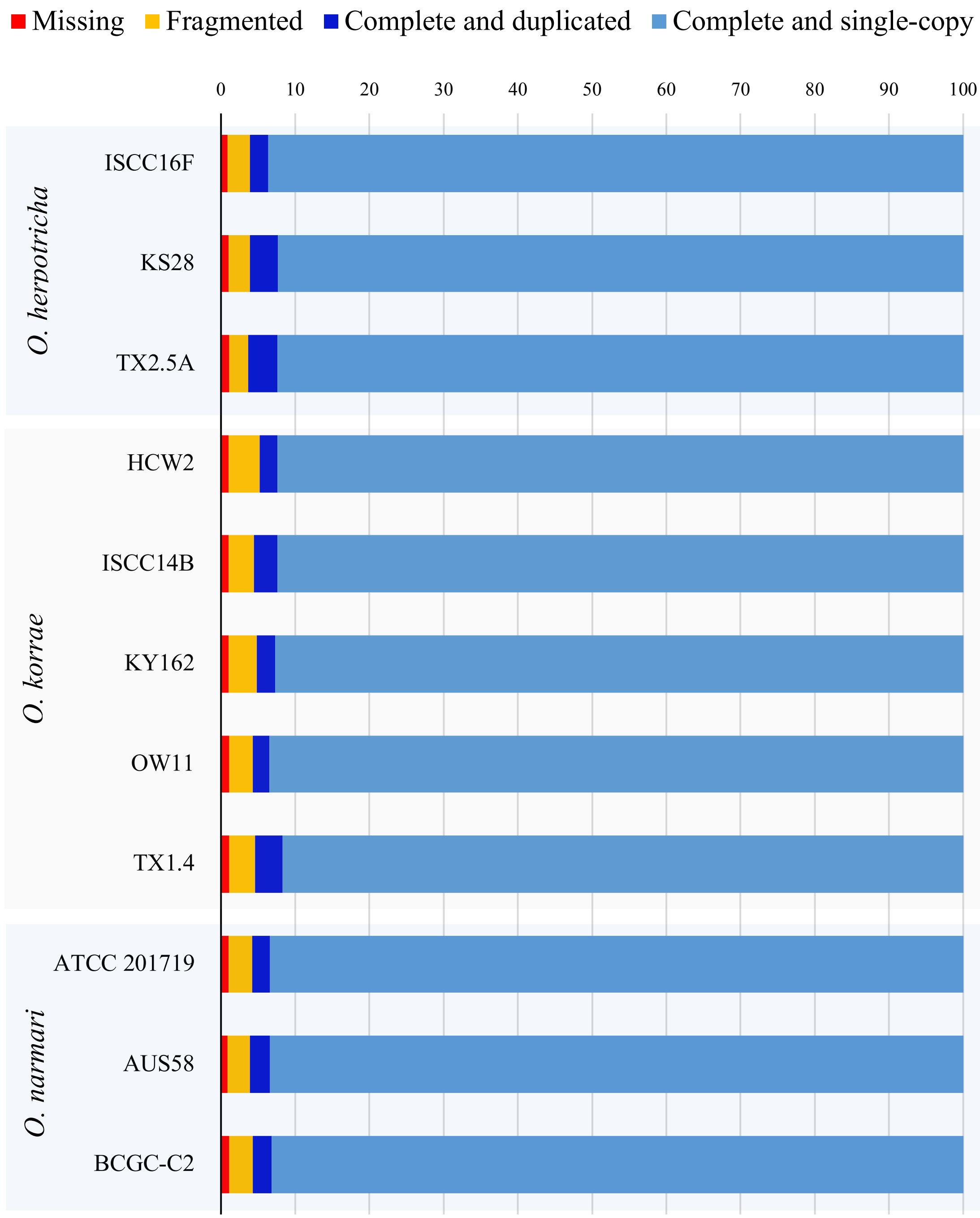

Figure III-6. BUSCO assessment of the genomes of *Ophiosphaerella* spp. in hybrid assembly.

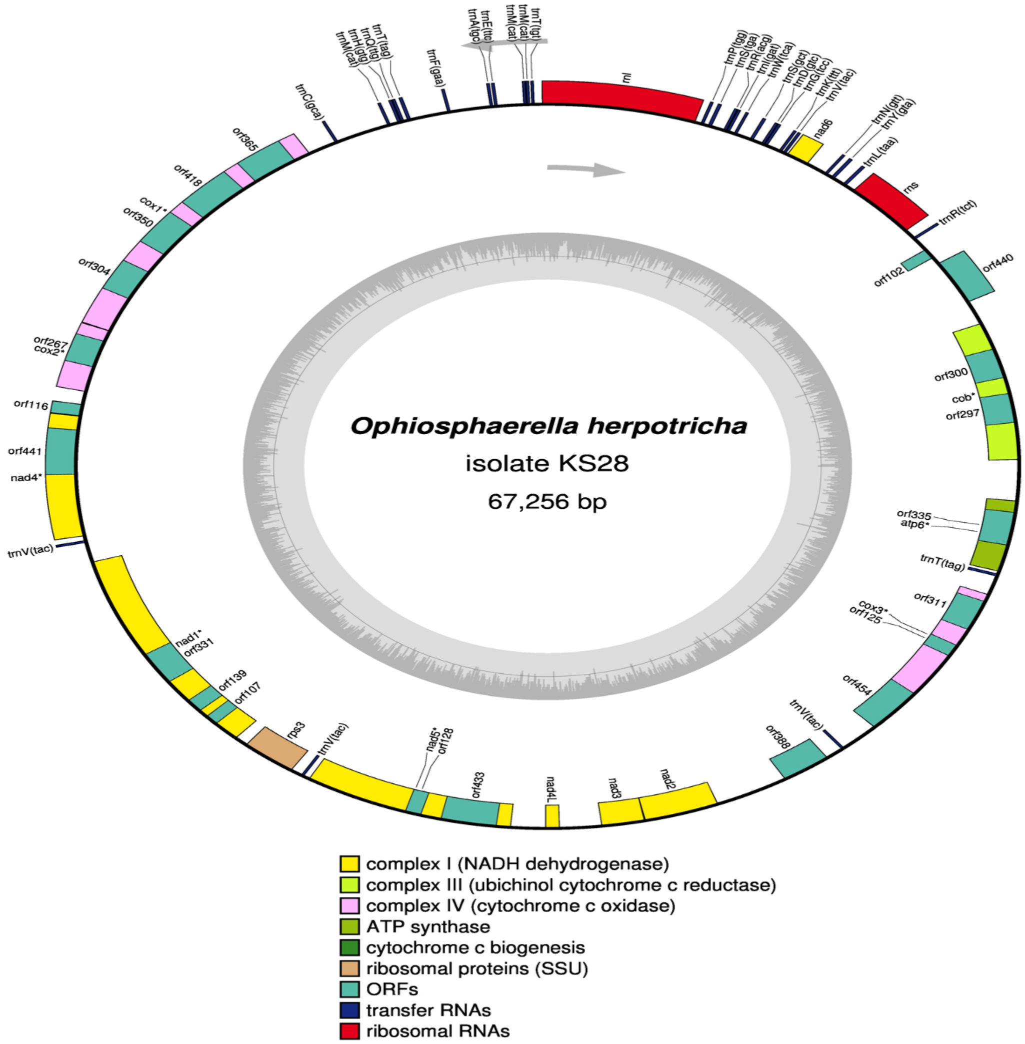

Figure III-7. Circular representation of the *Ophiosphaerella herpotricha* KS28 mitochondrial genome. Mitochondrial genes are represented as colored rectangles on the outermost circle. The grey arrows indicate the direction of transcription. Genes on the reverse strand are drawn inward. The innermost grey circle is the representation of GC content along the length of the mitochondrial genome. The gray line represents 50% GC content.

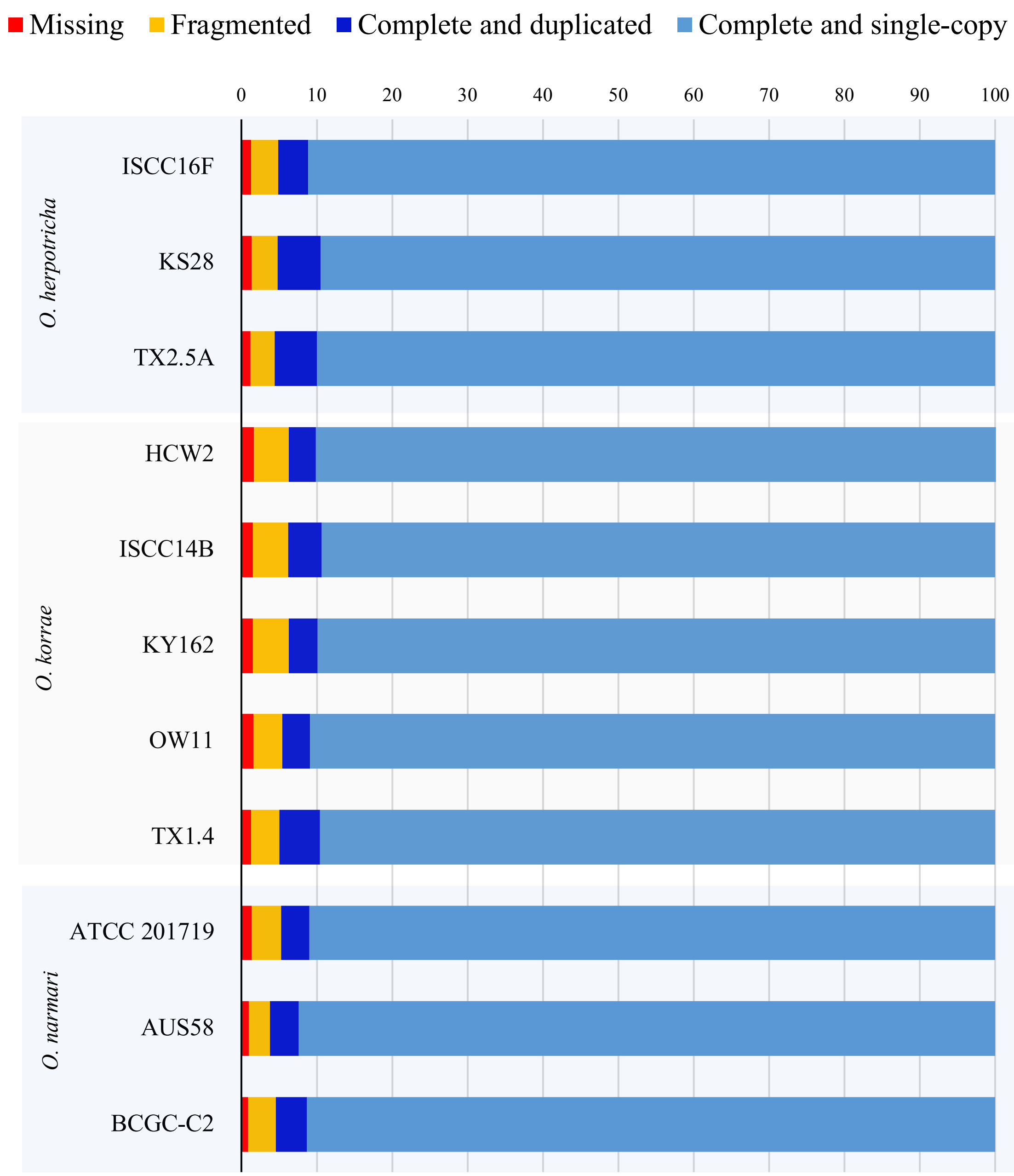

Figure III-8. BUSCO assessment of protein-coding genes models predicted from *Ophiosphaerella* spp. in hybrid assemblies.

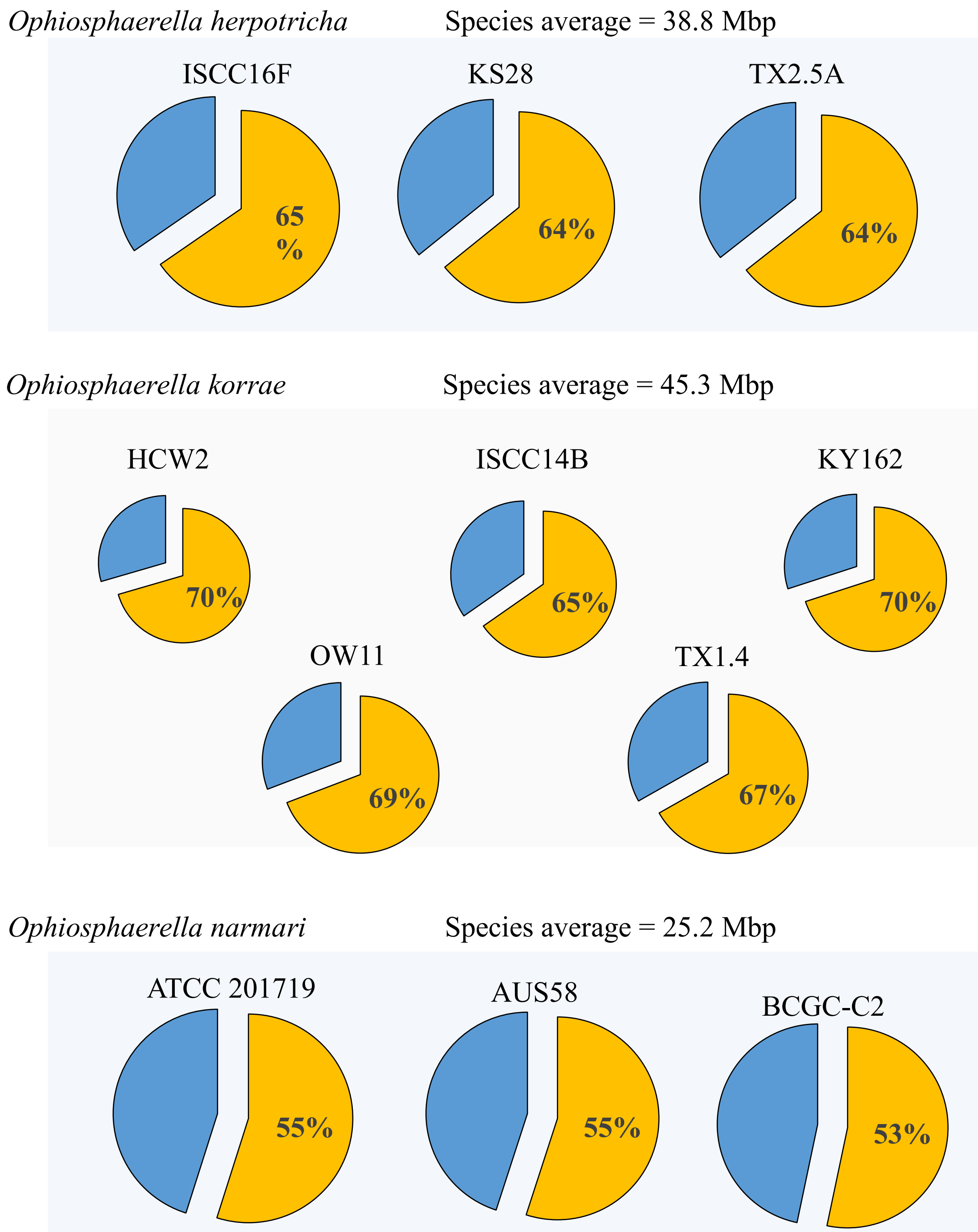

Figure III-9. Comparison of the percentage of intergenic regions (yellow) of the genomes *Ophiosphaerella* spp.

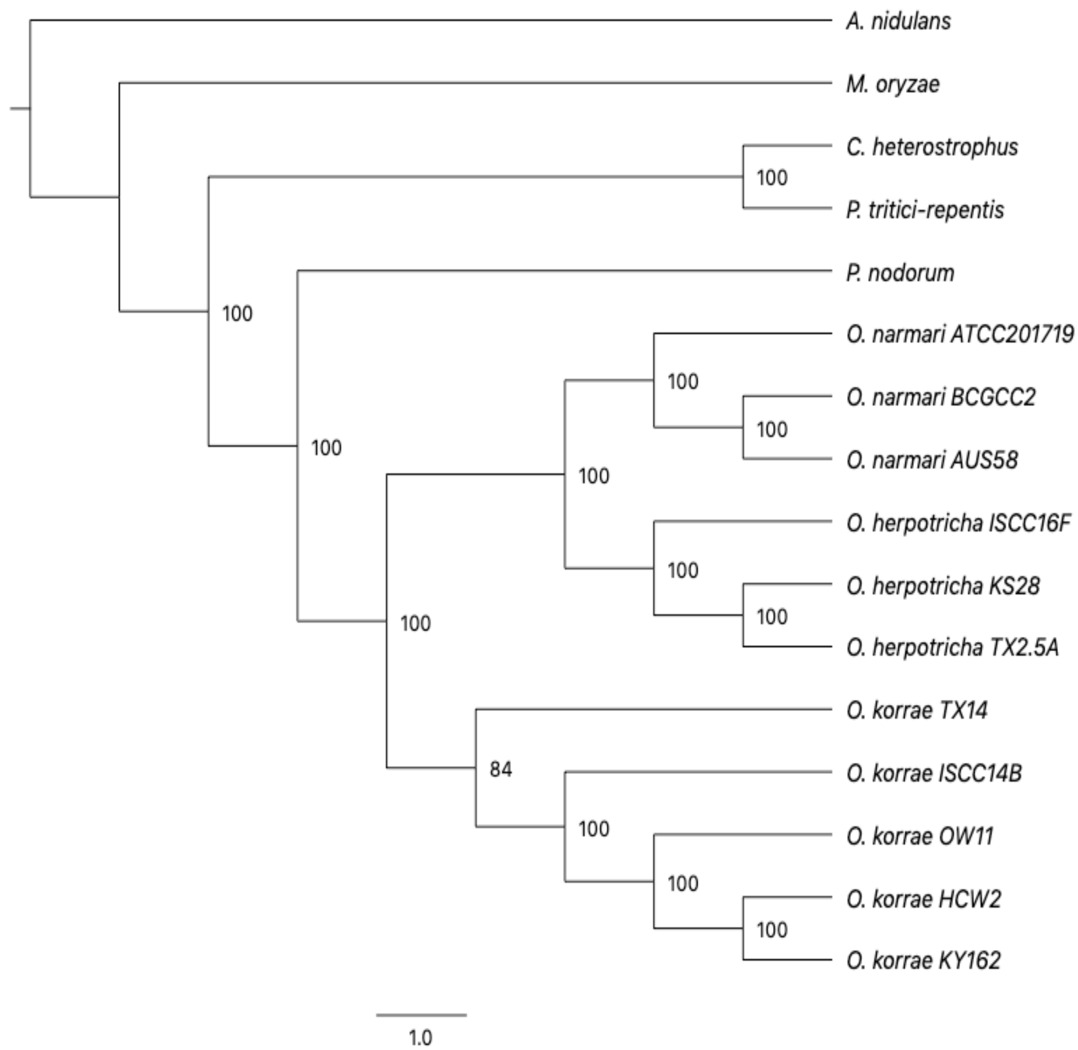

Figure III-10. Maximum likelihood tree of *Ophiosphaerella* spp. and other ascomycete fungi (retrieved from the JGI Genome Portal, Table III-2). A total of 500 single-copy ortholog protein coding genes were used. Bootstrap values (1000 replicates) were obtained at the nodes. The tree was rooted at *A. nidulans*.

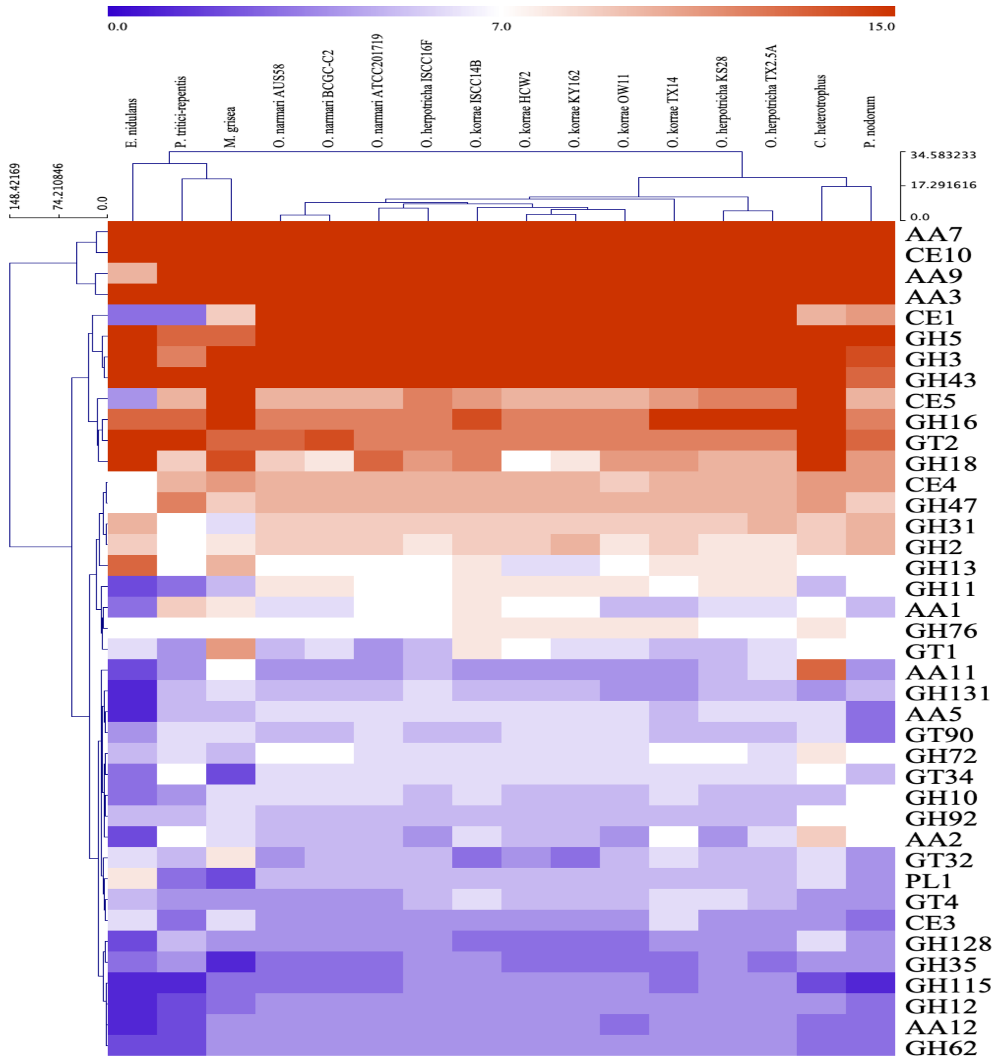

Figure III-11. Hierarchical clustering of carbohydrate-active enzymes (CAZymes) of *Ophiosphaerella* species and selected Ascomycete fungi (Table III-2). The forty most populated CAZyme families observed in *Ophiosphaerella* were selected for this heatmap. CAZymes were predicted using the CAZy database in the dbCAN2 server. Secreted CAZymes were predicted with SignalP. Heatmap was produced in MeV with Euclidean distance are distance metric and complete linkage clustering as linkage method. GH: glycoside hydrolases, GT: glycosyltransferases, CE: carbohydrate esterases, CBM: carbohydrate-binding modules, AA: auxiliary activities, and PL: polysaccharide lyases.

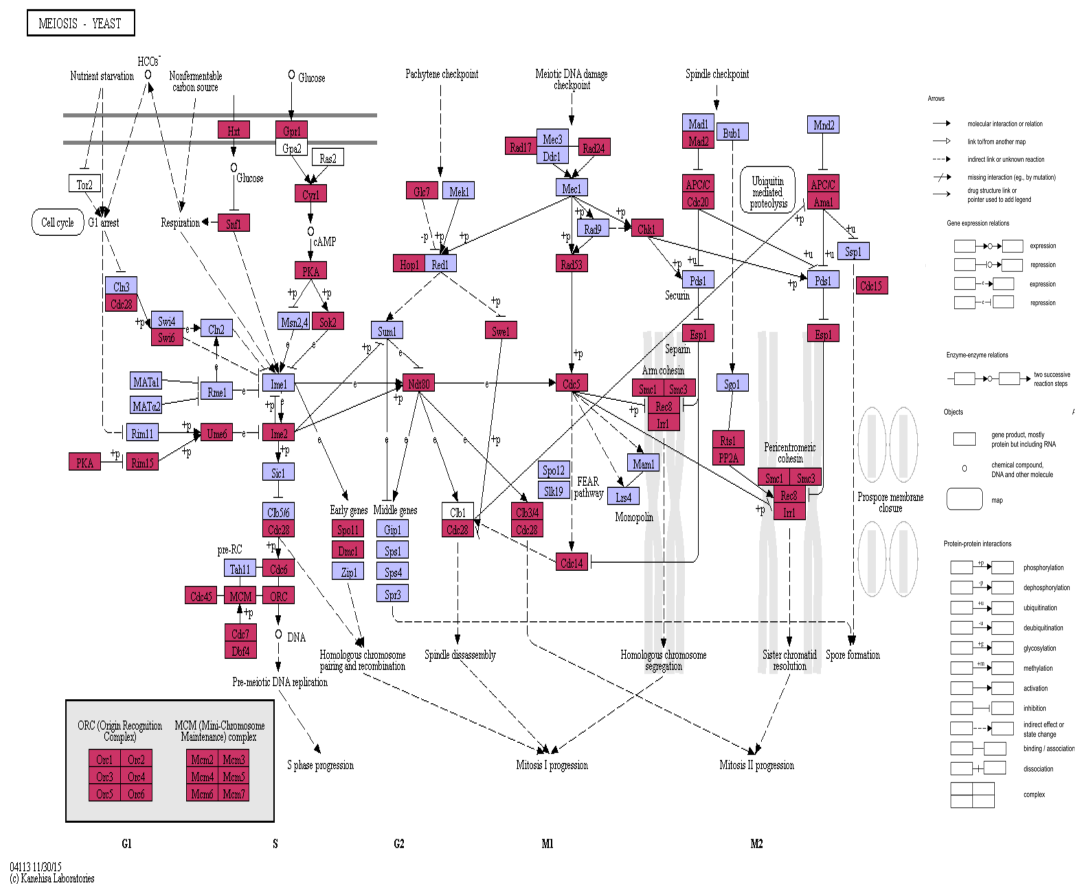

Figure III-12. KEGG orthologs (KO) of meiosis pathway (ko:04113) found in *Ophiosphaerella*. The meiosis pathway KOs found in all *Ophiosphaerella* species were mapped. The boxes filled with light blue color are genes/entries present in this pathway. The boxes filled with dark red color are genes of *Ophiosphaerella* species that were mapped to this pathway.

TABLES:

Table III-1. List of species and isolates of *Ophiosphaerella* selected for genome and transcriptome sequencing. Isolates were selected based on place of origin and host.

Species	Isolate	Location	Host	Short-read	Long-read	Transcriptome
O. herpotricha	ISCC16F	Tulsa, OK	Bermudagrass	✓	-	✓
O. herpotricha	KS28	Kansas	Bermudagrass	✓	-	✓
O. herpotricha	TX2.5A	Amarilllo, TX	Bermudagrass	✓	-	-
O. korrae	HCW2	Post Falls, ID	Kentucky Bluegrass	✓	✓	-
O. korrae	ISCC14B	Tulsa, OK	Bermudagrass	✓	-	✓
O. korrae	KY162	Kentucky	Kentucky Bluegrass	✓	-	-
O. korrae	OW11	Mississippi	Bermudagrass	✓	-	-
O. korrae	TX1.4	Amarillo, TX	Bermudagrass	✓	-	✓
O. narmari	ATCC 201719	Afton, OK	Bermudagrass	✓	-	-
O. narmari	AUS58	Australia	Unknown	✓	-	✓
O. narmari	BCGC-C2	San Diego, CA	Bermudagrass	✓	✓	✓

Table III-2. List of genetic resources of ascomycete fungi retrieved from the JGI Genome Portal used for comparative genomic and phylogenomic analyses.

Organism	Strain	Version	Host	Pathogen lifestyle	References
Emericella nidulans	FGSC A4	-	-	-	[11,104]
Cochliobolus heterotrophus	C5	2.0	corn	necrotrophic	[57,235]
Magnaporthe grisea	70-15 (MG8)	-	rice	hemibiotrophic	[71]
Parastagonospora nodorum	SN15	2.0	wheat	necrotrophic	[33,129]
Pyrenophora tritici-repentis	Pt-1C-BFP race 1	-	wheat	necrotrophic	[209]

Table III-3. Comparison of genome assembly statistics *Ophiosphaerella* species. using Illumina and PacBio reads separately.

Species	Isolate	Read type	Assembly size (bp)	N50 (bp)	L50 (contigs)	GC content (%)	Number of contigs	Largest contig (bp)
O. herpotricha	ISCC16F	Illumina	55,893,274	109,734	108	42.0	6,466	1,027,658
O. herpotricha	KS28	Illumina	58,836,657	72,900	152	42.4	10,047	921,607
O. herpotricha	TX2.5A	Illumina	59,694,109	74,247	152	42.2	11,150	1,136,638
O. korrae	HCW2	Illumina	67,582,958	75,120	234	39.2	3,953	588,543
		PacBio	43,601,651	298,786	43	47.0	310	922,984
O. korrae	ISCC14B	Illumina	64,383,715	46,877	273	42.9	9,031	574,816
O. korrae	KY162	Illumina	68,052,665	53,043	275	39.3	6,223	493,864
O. korrae	OW11	Illumina	63,287,114	72,319	185	39.1	4.443	526,753
O. korrae	TX1.4	Illumina	63,490,026	50,600	241	42.5	11,871	507,790
O. narmari	ATCC 201719	Illumina	46,299,996	253,116	54	46.3	1,792	1,245,331
O. narmari	AUS58	Illumina	44,838,570	264,035	44	46.9	2,306	1,500,792
O. narmari	BCGC-C2	Illumina	44,844,703	266,272	48	47.0	2,280	893,710
		PacBio	38,247,245	344,496	36	47.0	193	1,249,990

Table III-4. Comparison of genome assembly statistics *Ophiosphaerella* species in hybrid mode.

Species	Isolate	Assembly size (bp)	N50 (bp)	L50 (contigs)	GC content (%)	Number of contigs	Largest contig (bp)
O. herpotricha	ISCC16F	60,599,105	63,812	165	40.5	8,744	686,546
O. herpotricha	KS28	59,336,677	79,146	144	41.5	7,178	914,685
O. herpotricha	TX2.5A	60,119,832	71,323	161	41.2	7,531	1,067,401
O. korrae	HCW2	69,184,385	48,572	335	38.8	5,282	479,782
O. korrae	ISCC14B	62,722,361	45,608	298	42.7	6,527	456,646
O. korrae	KY162	68,384,830	54,432	307	39.0	4,391	484,841
O. korrae	OW11	65,998,299	45,531	287	38.3	6,897	516,330
O. korrae	TX1.4	64,713,409	46,516	263	41.7	10,568	423,522
O. narmari	ATCC 201719	46,899,196	153,863	81	45.9	2,239	1,378,950
O. narmari	AUS58	45,506,787	227,361	54	46.5	2,381	1,885,537
O. narmari	BCGC-C2	45,574,816	305,039	41	46.6	2.271	1,060,906

Table III-5. Predicted gene statistics of the genomes of *Ophiosphaerella* species.

Species	Isolate	Predicted Proteome	Complete Genes	Average of: Gene length (bp)	Introns per gene	Intron length (bp)	Exons per gene	Exon length (bp)
O. herpotricha	ISCC16F	13,316	13,206	1,573	1.79	140	2.78	1,429
O. herpotricha	KS28	13,971	13,526	1,521	1.70	133	2.69	1,384
O. herpotricha	TX2.5A	14,051	13,555	1,524	1.65	141	2.63	1,379
O. korrae	HCW2	12,681	12,525	1,609	1.68	134	2.67	1,472
O. korrae	ISCC14B	13,698	12,992	1,588	1.63	140	2.61	1,444
O. korrae	KY162	12,647	12,395	1,621	1.66	143	2.65	1,475
O. korrae	OW11	12,679	12,467	1,602	1.66	124	2.65	1,474
O. korrae	TX1.4	13,996	13,537	1,536	1.67	132	2.66	1,400
O. narmari	ATCC 201719	13,442	13,318	1,573	1.72	137	2.71	1,433
O. narmari	AUS58	14,123	14,005	1,495	1.68	126	2.68	1,366
O. narmari	BCGC-C2	13,998	13,891	1,521	1.75	139	2.75	1,378

Table III-6. Comparison of annotated gene features of *Ophiosphaerella* species. Gene ontology (GO) terms and Kyoto Encyclopedia of Genes and Genomes (KEGG) orthology were obtained by EggNog-Mapper. The secretome was predicted by SignalP. Homologs of pathogenesis-related genes were predicted by BLAST search against PHI-base.

Species	Isolate	GO terms	KEGG	Predicted Secretome	Homologs in PHI-base
O. herpotricha	ISCC16F	7108	7443	1215	746
O. herpotricha	KS28	7702	8049	1240	798
O. herpotricha	TX2.5A	7770	8108	1259	834
O. korrae	HCW2	7227	7559	1150	739
O. korrae	ISCC14B	8115	8443	1200	823
O. korrae	KY162	7214	7554	1150	736
O. korrae	OW11	7197	7553	1146	751
O. korrae	TX1.4	7957	8296	1273	808
O. narmari	ATCC 201719	7378	7737	1211	747
O. narmari	AUS58	7554	7910	1230	764
O. narmari	BCGC-C2	7396	7744	1216	759

Table III-7. Prediction of secreted effectors and their location in the host cell. The secretome of *Ophiosphaerella* species were subjected to EffectorP. Subsequently, effectors were subjected to ApoplastP and LOCALIZER to predict their location inside the host cell. Secreted effectors that had at least one predicted location were considered to be potential effectors.

Species	**Isolate**	**Predicted Effectors**	**Predicted location of the effector in the host cell**				**Potential Effectors**
			Apoplast	**Chloroplast**	**Mitochondria**	**Nucleous**	
O. herpotricha	ISCC16F	253	158	23	5	21	179
O. herpotricha	KS28	256	160	21	6	20	177
O. herpotricha	TX2.5A	271	183	21	7	21	203
O. korrae	HCW2	218	131	13	4	22	149
O. korrae	ISCC14B	235	143	15	6	20	158
O. korrae	KY162	211	129	13	5	22	148
O. korrae	OW11	213	129	17	4	19	150
O. korrae	TX1.4	262	161	18	6	23	184
O. narmari	ATCC 201719	230	142	20	6	26	161
O. narmari	AUS58	236	139	19	1	21	164
O. narmari	BCGC-C2	325	139	21	2	24	164

Table III-8. Comparison of carbohydrate-active enzymes (CAZymes) families of all *Ophiosphaerella* species. Secreted CAZymes were predicted with SignalP. GH: glycoside hydrolases, GT: glycosyltransferases, CE: carbohydrate esterases, CBM: carbohydrate-binding modules, AA: auxiliary activities, and PL: polysaccharide lyases.

Species	**Isolate**	**GH**	**GT**	**CE**	**CBM**	**AA**	**PL**	**Total**	**Secreted CAZymes**
O. herpotricha	ISCC16F	250	75	94	10	141	12	574	239
O. herpotricha	KS28	253	82	89	10	138	12	576	229
O. herpotricha	TX2.5A	254	80	92	10	139	12	579	241
O. korrae	HCW2	250	78	94	11	136	12	570	226
O. korrae	ISCC14B	260	82	94	11	139	12	587	246
O. korrae	KY162	253	79	92	10	136	12	572	224
O. korrae	OW11	248	78	92	10	132	12	563	238
O. korrae	TX1.4	258	82	100	10	141	12	595	243
O. narmari	ATCC 201719	249	77	91	10	139	12	569	233
O. narmari	AUS58	250	79	96	11	132	12	572	233
O. narmari	BCGC-C2	249	81	97	10	134	12	575	230

Table III-9. Comparison of carbohydrate-active enzymes (CAZymes) families of *Ophiosphaerella* species and selected Ascomycete fungi (Table III-2). CAZymes are represented by average per species of *Ophiosphaerella*. CAZymes were predicted using the CAZy database in the dbCAN2 server. Secreted CAZymes were predicted with SignalP. GH: glycoside hydrolases, GT: glycosyltransferases, CE: carbohydrate esterases, CBM: carbohydrate-binding modules, AA: auxiliary activities, and PL: polysaccharide lyases.

Species	GH	GT	CE	CBM	AA	PL	Total
O. herpotricha	252	79	92	10	139	12	584
O. korrae	254	80	94	10	137	12	587
O. narmari	249	79	95	10	135	12	580
E. nidulans FGSC A4	275	97	29	90	57	37	585
C. heterotrophus C5	276	104	49	102	89	15	635
M. grisea 70-15 (MG8)	261	102	52	117	91	6	629
P. nodorum SN15	257	90	49	61	99	10	566
P. tritici-repentis Pt-1C-BFP of race 1	245	91	39	45	119	10	549

Table III-10. Comparison of secondary metabolite backbone genes predicted across all *Ophiosphaerella* species. Secondary metabolites backbone genes of *Ophiosphaerella* species was predicted using SMURF. DMAT: demethylallyl tryptophan synthase, NRPS: nonribosomal peptide synthatases, PKS: polyketide synthases, and Hybrid: NRPS-PKS enzymes.

Species	**Isolate**	**DMAT**	**Hybrid**	**NRPS**	**NRPS-Like**	**PKS**	**PKS-Like**	**Total**
O. herpotricha	ISCC16F	0	1	11	4	27	5	48
O. herpotricha	KS28	0	1	9	4	27	5	46
O. herpotricha	TX2.5A	0	1	8	3	27	4	43
O. korrae	HCW2	1	2	10	7	27	5	52
O. korrae	ISCC14B	0	7	17	15	23	5	67
O. korrae	KY162	1	2	9	7	25	7	51
O. korrae	OW11	0	2	10	6	24	8	50
O. korrae	TX1.4	1	4	11	5	26	7	54
O. narmari	ATCC 201719	2	2	6	8	31	7	56
O. narmari	AUS58	0	3	6	7	30	2	48
O. narmari	BCGC-C2	0	3	7	4	29	2	45

Table III-11. Comparison of secondary metabolite backbone genes of *Ophiosphaerella* species and selected Ascomycete fungi (Table III-2). Secondary metabolites backbone genes and clusters were predicted using SMURF. The backbone genes of selected fungi was obtained from the JGI. DMAT: demethylallyl tryptophan synthase, NRPS: nonribosomal peptide synthatases, PKS: polyketide synthases, and Hybrid: NRPS-PKS enzymes.

Species	**DMAT**	**Hybrid**	**NRPS**	**NRPS-Like**	**PKS**	**PKS-Like**	**Total**
O. herpotricha	0	1	9	4	27	5	0
O. korrae	1	3	11	8	25	6	0
O. narmari	1	3	6	6	30	4	0
E. nidulans FGSC A4	5	1	9	13	22	5	1
C. heterotrophus C5	3	0	9	19	19	3	6
M. grisea 70-15 (MG8)	2	5	7	5	23	3	6
P. nodorum SN15	2	1	9	6	13	1	2
P. tritici-repentis Pt-1C-BFP of race 1	0	1	10	10	14	3	1

Table III-12. Comparison of proteases predicted across all *Ophiosphaerella* species. Genes encoding proteases were predicted using BLAST search against the MEROPS database. Seven most populated MEROPS families, and total proteases per isolates are shown. T: threonine, M: metalloproteases, S: serine, and A: aspartic.

Species	Isolate	T01A	M24A	S10	S01A	A01A	M67A	M28E	Total
O. herpotricha	ISCC16F	8	3	2	2	2	2	2	33
O. herpotricha	KS28	8	3	3	2	4	2	2	48
O. herpotricha	TX2.5A	8	3	3	2	4	2	2	50
O. korrae	HCW2	8	3	2	2	2	2	3	33
O. korrae	ISCC14B	7	2	4	2	2	2	3	50
O. korrae	KY162	8	3	2	2	3	2	3	39
O. korrae	OW11	8	3	2	2	2	1	3	36
O. korrae	TX1.4	9	3	4	3	2	3	3	50
O. narmari	ATCC 201719	9	3	2	2	2	2	2	34
O. narmari	AUS58	9	3	2	2	2	2	2	37
O. narmari	BCGC-C2	9	3	2	2	2	2	1	33

Table III-13. Mating type genes found in *Ophiosphaerella* species. Mating type idiomorphs were mined from the genome using BLAST search against partial sequence of *O. korrae* MAT genes (MAT1-1: AF486624.1, MAT1-2: AF486625.1).

Species	**Isolate**	**MAT1-1**	**MAT1-2**
O. herpotricha	ISCC16F	✓	-
O. herpotricha	KS28	-	✓
O. herpotricha	TX2.5A	✓	-
O. korrae	HCW2	✓	✓
O. korrae	ISCC14B	-	✓
O. korrae	KY162	✓	✓
O. korrae	OW11	-	✓
O. korrae	TX1.4	-	✓
O. narmari	ATCC 201719	-	✓
O. narmari	AUS58	✓	-
O. narmari	BCGC-C2	✓	-

CHAPTER IV

EXPRESSION PROFILING OF *OPHIOSPHAERELLA HERPOTRICHA* DURING BERMUDAGRASS INFECTION

ABSTRACT

Spring dead spot (SDS) is a devastating disease of bermudagrass in golf courses, athletic fields, and in the landscape. This disease is caused by the fungi: *Ophiosphaerella herpotricha, O. korrae,* and *O. narmari* that colonize roots, stolons, and rhizomes of bermudagrass. While the colonization of a susceptible cultivar results in necrosis of belowground plant organs, the same isolate is able to colonize the vasculature of a tolerant cultivar with no root discoloration, which resembles an endophytic association. The underlying genetics by which these fungi colonize bermudagrass roots is not fully elucidated. Therefore, the objective of this study was to identify differentially expressed genes of *O. herpotricha* during early stages of bermudagrass infection. Transcriptomes of *O. herpotricha* ISCC16F in artificial culture and in association with two bermudagrass hosts (one tolerant, and one susceptible to SDS) were sequenced in an Illumina Hi-Seq platform. Differentially expressed genes were determined in a genome-guided approach, and were evaluated based on the following comparisons: *in vitro* vs. *in planta, in vitro* vs. *in planta*-susceptible cultivar, *in vitro* vs. *in planta*-tolerant cultivar, and between *in planta* susceptible vs. tolerant. The functions of differentially expressed genes and enrichment analyses were predicted using functional annotation tools and databases. The results revealed an up-regulation enrichment of genes involved in plant biomass degradation *in planta*. Among these genes, 16 had effector signal, including three candidate genes associated with pathogen-associated molecular patterns. One of these proteins was also annotated as a carbohydrate-active enzyme that act on acts on plant cell wall components. Many genes lacked convergent annotations. No significant enrichment was observed in the comparison of the two *in planta* conditions. This is the first report of the molecular basis of *O. herpotricha* colonization of bermudagrass roots. Future experiments are required to functionally characterize these candidate genes.

1. INTRODUCTION

Bermudagrass (*Cynodon* spp.) is a perennial warm-season grass with three main types: common bermudagrass (*C. dactylon* (L.) Pers.), African bermudagrass (*C. transvaalensis* Burt-Davy) and interspecific hybrids (*C. dacytlon* x *C. transvaalensis*) [54]. In the United States, bermudagrass can be successfully cultivated in the southern region where common and hybrid bermudagrass are the predominant types used on athletic fields and golf courses [53]. Common bermudagrass consists of seeded varieties with coarse leaf texture. Bermudagrass interspecific hybrids often have improved agronomic traits such as fine leaf texture, fast growth, density and drought resistance, which make these very suitable for high maintenance sports fields [53,295]. The two mains limitations to bermudagrass cultivation in the southern region are unpredictable winter weather that can cause cold induced winter-kill, and a disease called spring dead spot (SDS).

Spring dead spot is the most devastating disease of bermudagrass in the southern US where the grass enters cold temperature-induced dormancy [279]. The disease is caused by three fungal species namely *Ophiosphaerella herpotricha* (Fries) J. Walker, *O. korrae* (J. Walker & A. M. Smith) R. A. Shoemaker & C. E. Babcock and *O. narmari* (J. Walker & A. M. Smith) Wetzel, Hubert & Tisserat. These pathogens colonize root, stolons and rhizomes of bermudagrass when soil temperatures are below 22ºC. Symptoms associated with SDS are prominent in the spring season (post bermudagrass dormancy) as dead patches appear as healthy grass resumes growth. The injury caused by SDS-pathogens is likely due to depletion of water and nutrients in belowground organs, which enhances sensitivity to cold temperature [37,95,324,325].

Ophiosphaerella species are categorized as necrotrophic soilborne pathogens. The host-pathogen interaction at the tissue level has been described for both *O. herpotricha* and *O. korrae*, and the strategies of colonization of both species were shown to be very similar [37,95]. Both species penetrated roots directly without any specialized structures [37]. After penetration, the fungi grew longitudinally along the root and inside the root inter- and intracellularly. Colonization of a susceptible cultivar of bermudagrass was limited to the root cortex with strong necrosis as early as two days post inoculation, with strong necrosis as early as two days post inoculation. In contrast, colonization of a tolerant cultivar, by the same isolate, showed cortex and vascular colonization and absence or delay of necrosis [37,85,95].

Necrotrophic pathogens kill host cells by means of secretion of necrotrophic effectors (formerly, host selective toxins and avirulence genes) that trigger host programmed cell death (PCD) to enhance disease [134]. *Parastagonospora nodorum*, the causal agent of *Stagonospora nodorum* blotch in wheat, is an example of a necrotrophic phytopathogen that deploys necrotrophic effectors. The fungus can encode at least three known necrotrophic effectors, one of them being SnTox3 [101,198]. The SnTox3 phytotoxin was shown to induce PCD in wheat leaves of varieties that carried the toxin sensitivity gene Snn3 [101,198]. This interaction resulted in spread of pathogen colonization and susceptibility, which is also referred to as inverse gene-for-gene relationship [101,198].

Ophiosphaerella herpotricha was suspected to produce phytotoxic compounds [94]. Culture filtrates of *O. herpotricha* caused discoloration on bermudagrass roots, but without differentiation in the reaction of a susceptible and tolerant cultivar [94]. In a tolerant cultivar, the colonization by SDS-fungi resembled an endophytic interaction [95,97]. Root-generated reactive oxygen species (ROS) was significantly higher in the tolerant cultivar, which supports the endophytic interaction [83,97,269]. The evidence of higher levels of ROS in the tolerant cultivar suggested that the mechanism by which *Ophiosphaerella* induced necrotic PCD on bermudagrass roots was not due to an oxidative burst [94].

The underlying genetics of root colonization by SDS-pathogens remained unknown. Therefore, the objective of this study was to elucidate the genetic basis of *Ophiosphaerella* colonization of bermudagrass roots with differential gene expression-based analysis. The hypothesis of this study was that *Ophiosphaerella* up-regulates gene(s) encoding phytotoxic peptides that cause plant cell necrosis in a susceptible cultivar, but not in a tolerant cultivar.

2. METHODS

2.1. BIOLOGICAL MATERIALS

Two bermudagrass cultivars were grown in a greenhouse: 'Tifway (419)' (hybrid, susceptible to SDS) and a common bermudagrass biotype called 'U3' (tolerant). Plants were cultivated in plastic pots with a sterile mixture of sand and growing mix (Sunshine® Redi-Earth Plug & Seedling, Sun Gro® Horticulture, Agawam, MA) (sand:growing mix 9:1). The pots were watered twice a day for 15 minutes through an automatic sprinkle irrigation system and fertilized with a nutrient solution containing 1 tbs/gal of 24-8-26 N-P-K plus micronutrients (Miracle-Gro®, Scotts Miracle-Gro Products, Inc., Marysville, OH) every seven days. Stolons were cut and placed in plastic trays containing sterile sand to root for approximately five to eight days. Single-node rooted stolons were carefully washed with reverse osmosis water to remove soil particles, and were subsequently surface sterilized with 5.3% hypochlorite solution for four minutes. Injury- and blemish-free rooted nodes were transferred to petri dishes. The roots were placed in between sterile filter paper. Approximately, 2 ml of sterile nanopore water was added to moisten filter papers. Seven to ten day-old cultures of *O. herpotricha* isolate ISCC16F on agar plugs covered with fungal mycelium were used as inoculum. Agar plugs were placed directly onto roots one centimeter below the node. Petri dishes were wrapped with aluminum foil and incubated vertically in a growth chamber set at approximately 16 to 18°C and 12-hour photoperiod for five days. Additionally, fungal mycelium was cultured over a cellophane sheet in potato dextrose agar. The experiment was conducted in a completely randomized design on one shelf inside the growth chamber with three replicates.

2.2. TRANSCRIPTOME SEQUENCING

Total RNA was extracted from roots and from actively grown mycelium five days after inoculation. Mycelium was scrapped from cellophane sheet, and roots were harvested by cutting and detaching the root from the node. Agar plugs were removed from inoculated roots, and roots were harvested. Samples were immediately flash frozen in liquid nitrogen, placed in a 2 mL sterile tube with RNAlater®-ICE (Ambion, Inc., Austin, TX) and incubated at -20°C until used. Approximately, less than 50 mg of mycelium and 30 mg of roots were used for extraction. Excess RNAlater®-ICE was removed from samples by squeezing with forceps. Total RNA was isolated using RNase Plant Mini Kit (Qiagen, Inc., Valencia, CA) following manufacturer recommendations. Eluted RNA samples were stored at -80°C until submitted to sequencing. Quality and quantity of total RNA was assessed by agarose gel, NanoDrop™ and Agilent Bioanalyzer 2100 (Agilent Technologies Inc., Santa Clara, CA). In agarose gel, two intact bands representing the 28S and 18S without degradation was required. For the NanoDrop™, the cutoff for the 260/280 nm absorbance ratio was 1.8, and for 260/230 nm absorbance ratio was 1.8-2.2. For the Agilent Bioanalyzer, RNA integrity number greater than 6.5 was acceptable, but greater than 7.0 was desirable.

Sequencing library preparation of RNA samples was performed by Novogene Bioinformatics Technology Co., Ltd. (Shatin, Hong Kong). The libraries were sequenced on an Illumina HiSeq System (Illumina Inc., San Diego, CA, USA) to produce 150bp pair-ended libraries.

2.3. GENOME-GUIDED TRANSCRIPTOME ANALYSIS

Reads obtained from *in vitro* (culture media) and *in planta* ('Tifway' and 'U3' biotype) libraries were used in this study. Raw Illumina reads were assessed for quality using FastQC [9] and filtered for low quality or adaptor trimming using Trimmomatic [29]. Reads were mapped to the genome of the *O. herpotricha* ISCC16F (referred to as reference genome for the purpose of this chapter, see chapter III for details) using HISAT2 [156]. Reads that mapped to the reference genome were used for the genome-guided transcriptome profilling analysis [243]. In this analysis, the reads were mapped to the reference genome using HISAT2 [156] again, and transcript abundances were estimated with StringTie [244]. Gene count matrix was obtained using the prepDE.py script from StringTie [244].

Differential expression analysis was performed using edgeR package [265] in R. Read count data was filtered allowing more than one read in three or more samples, and normalized using the trimmed mean of M-values method. Differential expression was computed between condition pairs using the exactTest function. The pairs were: in culture vs. *in planta*-'Tifway', (ii) in culture vs. *in planta*-'U3' biotype, and (iii) *in planta*-'Tifway' vs. *in planta*-'U3' biotype. Genes were considered differentially expressed based on 5% false discoverey rate (FDR, P value < 0.05) and log fold change of two.

2.4. FUNCTIONAL ANNOTATION

Hypothetical protein sequences of newly predicted transcripts were obtained using TransDecoder [82]. Functional annotation of the predicted proteins was done using dbCAN2 online meta server [49] and database for the Carbohydrate-Active enZymes (CAZy) [41]. Secondary metabolite gene clusters were predicted through online batch search against the Secondary Metabolite Unique Regions Finder (SMURF) [154]. Predicted proteases were predicted through BLAST search of proteins against the MEROPS database [260] using e-value threshold 1e-5, minimum percent identity of 50%, an minimum query coverage of 50%. Proteins involved in plant-pathogen interaction were predicted through BLAST search of proteins against the PHI-base (Pathogen-Host Interactions database) [310] using e-value threshold 1e-5, minimum percent identity of 50%, an minimum query coverage of 50%. Secretome was predicted using SignalP [247]. Secreted fungal effectors were predicted by EffectorP [285], LOCALIZER [283], and ApoplastP [284]. For enrichment analysis, BLAST search of proteins against the UniProt/SwissProt database of fungi was done using using e-value threshold 1e-5, minimum percent identity of 50%, an minimum query coverage of 50%. Subsequently, enrichment analysis for Gene Ontologies (GO), Kyoto Encyclopedia of Genes and Genomes (KEGG), Protein Family (Pfam) were performed in STRING v.11 [293] using FDR threshold of 1%. For this analysis, predicted proteins were subjected to BLAST search of proteins against the *Magnaporthe oryzae* (rice blast pathogen) proteome downloaded from the UniProtKB database using e-value threshold 1e-5, minimum percent identity of 50%, an minimum query coverage of 50%.

3. RESULTS

3.1. TRANSCRIPTOME SEQUENCING

Illumina sequencing of 150 bp pair-ended libraries yielded, in average across three replicates, 75,266,986 raw reads *in vitro* (culture media), 74,927,238 raw reads for *in planta*-‘Tifway’ (susceptible), and 76,278,322 raw reads for *in planta*-‘U3’ biotype (tolerant). After quality check and trimming, raw reads were mapped to the reference genome. At least 55,890,982 of the filtered *in vitro* reads mapped to the isolate’s genome. The average across three replicates was 61,334,551. The mapping of *in planta*-‘Tifway’ varied from 28,663,882 to 34,770,760 reads. The mapping of *in planta*-‘U3’ biotype varied from 15,770,782 to 23,991,118 reads. Mapped reads were used for differential gene expression analysis using a genome-guided approach [243].

3.2. GENOME-GUIDED TRANSCRIPTOME PROFILLING ANALYSIS

Sequencing reads were aligned to the reference genome using HISAT2 [156], and transcript abundances were estimated by StringTie [244]. There were a total of 27,929 transcripts and 13,930 genes, and the average transcript per gene was 2.12 (Figure IV-1A). The majority of transcripts were less than 5,000 bp (Figure IV-1B), and the longest transcript was 32,855 bp long.

These data were pre-processed and analyzed using edgeR [265] package in R. Diagnostic plots of exploratory data quality were obtained (Figure IV-2 and Figure IV-3). Total read count (Figure IV-2A) showed variation in sample-read size, which was due to mixed transcriptome of bermudagrass and spring dead spot fungus. After filtering and normalization of expression values (log-cpm) (Figure IV-2B) variation among samples and replicates was very small. Quality and normalization of count data were performed by a principal component analysis (PCA) (Figure IV-3A), and the correlation distances between all replicates (Figure IV-3B). As demonstrated by the PCA, the largest variability (84.2%) in the dataset corresponded to the different conditions used in this study (*in vitro* and *in planta*) (Figure IV-3A). The *in planta* ('Tifway' and 'U3' biotype) replicates had higher distance correlation values with one another compared to the distance values with *in vitro* (culture media) replicates (Figure IV-3B). A similar trend was observed when the 500 most expressed genes were clustered hierarchically with a heatmap (Figure IV-4). Two main clusters were formed: *in vitro* (culture) and *in planta*. Within the *in planta* cluster, there were three further clusters. One corresponded to *in planta*-'Tifway, another cluster corresponded to *in planta* 'U3 biotype', and a third cluster included one replicate of the *in planta*-'Tifway' and the *in planta*-'U3' biotype. These results indicate changes in gene expression profile when *O. herpotricha* is associated with bermudagrass roots.

Differential expression of transcripts and genes were computed based on 5% FDR (P value < 0.05) and log-fold change of 2. Comparisons of differentially expressed genes and transcripts were done between conditions pairs: (i) *in planta*-'Tifway' vs. in culture, (ii) *in planta*-'U3' biotype vs. in culture, and (iii) *in planta*-'U3' biotype vs. *in planta*-

‘Tifway’ (Table IV-1). Subsequently, differentially expressed transcripts and genes were annotated using tools and databases, and enrichment analyses performed. Candidate pathogenicity genes up-regulated in each *in planta* conditions were obtained.

3.3. CANDIDATE PATHOGENICITY GENES

In the comparison *in planta*-‘Tifway’ vs. in culture, there were 2,153 differentially expressed genes (DEGs), of which 1,522 were up-regulated in ‘Tifway’ (Table IV-1). In the comparison of *in planta*-‘U3’ biotype vs. in culture had 2,663 differentially expressed genes, of which 1,718 were significantly up-regulated (Table IV-1). Enrichment analyses of ‘Tifway’ and ‘U3’ up-regulated DEGs for Gene Ontologies (GO) Biological Process showed significant enrichment of metabolic and catabolic processes of carbohydrates and polyssacharides in ‘Tifway’ (Table IV-2 and Table IV-3). The GO Molecular functions showed enrichment of enzymes with hydrolase activity (break of chemical bonds, degradation). Enrichment analysis for Pfam domain showed an agreement with GO, as cellulose binding and glycosyl hydrolase domains were enriched (Table IV-4 and Table IV-5). Using the gene function obtained from UniProt/SwissProt and the annotations from other tools and databases, the enriched *O. herpotricha* candidate genes were categorized as candidate plant cell wall degradating enzymes (PCWDEs), and candidate effectors genes (Table A-2 to Table A-5, for a list of all candidate effector genes predicted on the secretome by EffectorP, ApoplastP and LOCALIZER).

3.3.1. ‘TIFWAY’ VS. CULTURE

There were 89 unique genes retrieved from enrichment analyses. Twelve candidate PCWDEs were categorized according to Uniprot/ SwissProt function (Table IV-6). These candidate genes had roles in degradation of cellulose (endo-/beta-glucosidases, enzyme class 3.2.1.21, and glucanase, EC 3.2.1.4), xylan (xylanase, EC 3.2.1.8), mannan (mannanases, EC 3.2.1.78) and cutin (cutinase, EC 3.1.1.74). These genes had varying logFC from +2.24 up to +7.20. Enzymes with plant biomass degradation function that also had effector signal and PHI-base annotations, were categorized as potential necrotrophic effectors (Table IV-7). An up-regulation of genes with role in virulence (n=57), and three necrotrophic effectors were found in ‘Tifway’. Seven genes with effector signal, and eight genes with role in pathogenicity were retrieved from the enrichment analyses (Table IV-8). One of these candidate effectors (g8845.t1, logFC +5.01), was not obtained from the enrichment analyses, but was included in this category because of effector signal and PHI-base annotation. A MAP kinase gene (g7402.t1, logFC +4.88) was up-regulated in this condition, which indicates a change in the extracellular environment caused a signalling pathway in the fungus cell. The candidate necrotrophic effector genes had varying logFC from +2.71 up to 17.19.

3.3.2. ‘U3’ BIOTYPE VS. CULTURE

There were 102 unique genes retrieved from enrichment analyses. The trend observed in ‘U3’ biotype was very similar to the one observed in ‘Tifway’. Fourteen candidate PCWDEs that were categorized according to Uniprot/SwissProt function

(Table IV-9). These candidate genes had roles in degradation of cellulose (endo-/beta-glucosidases, EC 3.2.1.21, and glucanase, EC 3.2.1.4), xylan (xylanase, EC 3.2.1.8), mannan (mannanase, EC 3.2.1.78). These genes had varying logFC from +2.35 up to +9.69. Virulence and effector genes were mined using the annotations obtained from search against PHI-base (Table IV-10). An up-regulation of genes with role in virulence (n=63), and three necrotrophic effectors were also found in 'U3' biotype. Seven genes with effector signal, and eleven genes with role in pathogenicity were retrieved from the enrichment analyses (Table IV-11). One of these candidate effectors (g8845.t1, logFC +5.92), was not obtained from the enrichment analyses. The MAP kinase (HOG1) was not enriched in this comparison. Three genes were only up-regulated in the 'U3' biotype. A neutral trelase (EC 3.2.1.28, logFC +6.43) gene, predicted to be involved in host colonization by fungal hyphae, was only up-regulated in this condition. Two genes (MSTRG.8692, logFC +4.33, and g9656.t1, logFC +3.42) encoding the same transcription factor (StuA), which was predicted to have a role in pathogenicity and to regulate the biosynthesis of necrotrophic effector Tox3. The third gene was a chromatin remodeling gene (g659.t1, logFC +7.65) (Table IV-12).

3.3.3. 'U3' BIOTYPE'TIFWAY' VS. 'TIFWAY'

In the comparison between the two *in planta* conditions, there were 104 genes DEGs in 'U3' biotype, and 230 in 'Tifway' (Table IV-1). Due to low number of DEGs, and low annotation rate, there was no enrichment for GO or Pfam domain for these DEGs.

4. DISCUSSION

Spring dead spot is a damaging disease of bermudagrass in the southern US. The three fungal pathogens, *Ophiosphaerella herpotricha, O. korrae* and *O. narmari*, colonize roots, stolons and rhizomes of bermudagrass resulting in necrosis of belowground plant organs. The colonization of a susceptible cultivar was limited to the root cortex with strong necrosis. Whereas colonization of a tolerant cultivar, by the same isolate, showed cortex and vascular colonization and absence or delay of necrosis [37,85,95]. The molecular basis of the *Ophiosphaerella*-bermudagrass interaction needs to be understood in order to develop new cultivars with resistance to this disease. To elucidate the underlying genetics of colonization, this study presented differential gene expression-based analyses during early infection of bermudagrass roots by *O. herpotricha* ISCC16F. The hypothesis formulated was that *Ophiosphaerella* up-regulates genes encoding phytotoxic peptides that cause necrotic PCD in the susceptible cultivar, but not in the tolerant cultivar. The results provided insight into candidate genes involved in pathogenesis, and candidate genes associated with vasculature colonization that will serve as important genetic resources for future studies of plant-pathogen interaction.

The results showed that *O. herpotricha* up-regulates PCWDEs of substrates such as cellulose, and xylan. However, these enzymes could have other roles besides degradation of plant cell wall such as to trigger pathogen-associated molecular patterns (PAMP)-triggered immunity (PTI) [51]. The *M. oryzae* necrotrophic effector MoCDIP4 is an AA9 CAZy that acts as PAMP and induces rice cell death by suppressing an anti-apoptotic protein in the mitochondria [51]. A homolog to the MoCDIP4 was found to be up-regulated by *O. herpotricha* under *in planta* conditions. This candidate gene also had predicted CAZy AA9 assignment, and was positive for SignalP, EffectorP and ApoplastP, which are consistent with functional characterization of the effector [51]. Another CAZy characterized as PAMPs is the glucanase PsXEG1 of *Phytophthora sojae* that acts on the apoplast. The results obtained in this study showed that *O. herpotricha* had a PsXEG1-homologous gene. This candidate gene also had CAZy GH12 assignment, and was positive for SignalP and ApoplastP, which was consistent with the reports by Ma *et al.* [205].

Another necrotrophic effector, a homolog to *M. oryzae* MoCDIP1, was found to be up-regulated by *O. herpotricha* under *in planta* conditions. This gene was reported to lack sequence similarity to other well studied fungal necrotrophic effectors that induce PCD, but was characterized to be involved in PTI [51]. The mechanisms of PCD was shared among MoCDIP4, MoCDIP1 and other genes in the MoCDIP family. Besides suppression anti-apoptotic protein, MoCDIP genes were shown to inhibit calcium channels on the host as means to trigger cell death [51]. The candidate *O. herpotricha* homolog was only found in the search against PHI-base, and was positive for SignalP, EffectorP, and ApoplastP, which were consistent with the reports by Chen *et al.* [51].

Previous studies reported weak evidence of phytotoxic peptides produced by *Ophiosphaerella* being involved in causing root necrosis [94,319]. Culture filtrates of *O. herpotricha* grown in different induction media caused discoloration on bermudagrass roots. However, there was no differentiation in the reaction of a susceptible and tolerant cultivar [94]. Another study identified that phytotoxic metabolites in *O. herpotricha* [319]. Those compounds were only tested on bermudagrass leaves on which were found to cause leaf toxicity, but root responses were not assessed and potential gene clusters involved in the biosynthesis of those metabolites were not provided [319]. This present study did not show enrichment of candidate genes involved in the biosynthesis of secondary metabolites. However, candidate genes with SMURF assignment were observed but not enriched. These could consist of uncharacterized or novel secondary metabolites. The role these candidate metabolites play in the *Ophiosphaerella*-bermudagrass interaction remains unclear. Further studies are necessary to functionally characterize these candidate secondary metabolite gene clusters to more conclusively reveal the strategy of pathogenesis.

Collectively, the results of this study showed that *O. herpotricha* secreted plant cell wall degrading enzymes and candidate necrotrophic effectors in both *in planta* conditions. Two of these necrotrophic effectors were reported as PAMP because triggered basal plant resistance by means of suppression of anti-apoptotic protein and of inhibiting calcium channels [51]. Predicted secondary metabolites were up-regulated *in planta* in both tolerant and susceptible cultivars. Many of these candidate genes lacked convergent annotations, they were considered novel and will be subject of future studies to clarify their role in bermudagrass colonization. The initial hypothesis of this study was that *Ophiosphaerella* up-regulates genes encoding phytotoxic peptides that cause plant cell necrosis in a susceptible cultivar, but not in a tolerant cultivar. This hypothesis cannot be completely refuted as the role of phytotoxic metabolites in bermudagrass colonization remain unclear. The evidence of secretion of necrotrophic effectors give rise to another hypothesis, which is that the bermudagrass host can modulate the outcome of *O. herpotricha* colonization.

5. CONCLUSION

This is the first report of the molecular basis of *Ophiosphaerella herpotricha* colonization of bermudagrass roots. The results presented will serve as valuable genomic resources for future studies in plant-pathogen interaction in this pathosystem. The evidence of three candidate necrotrophic-effector genes (MoCDIP4, MoCDIP1, and PsXEG1) indicate that *Ophiosphaerella*-induced necrosis is the result of a plant basal defense mechanism known as PTI. Future experiments are required to functionally characterize these candidate genes in infected bermudagrass roots.

FIGURES:

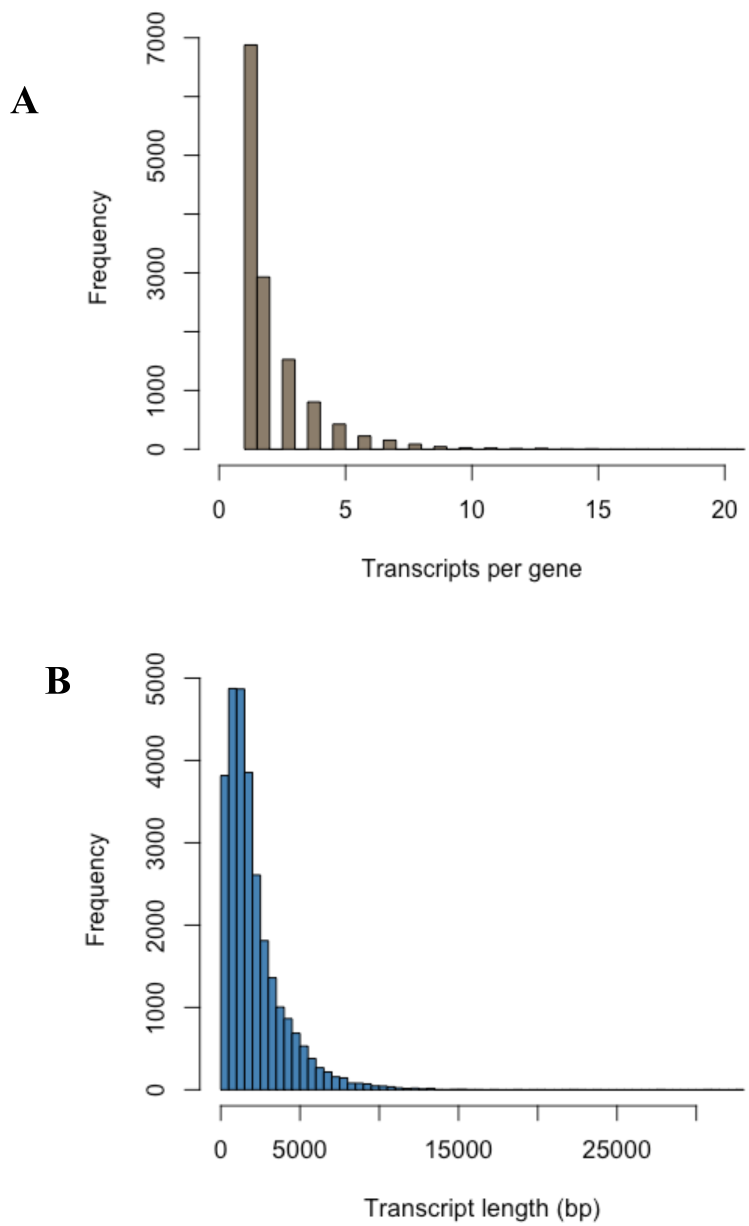

Figure IV-1. (A) Distribution of number of transcripts per gene. (B) Distribution of transcript length in base pairs, bp.

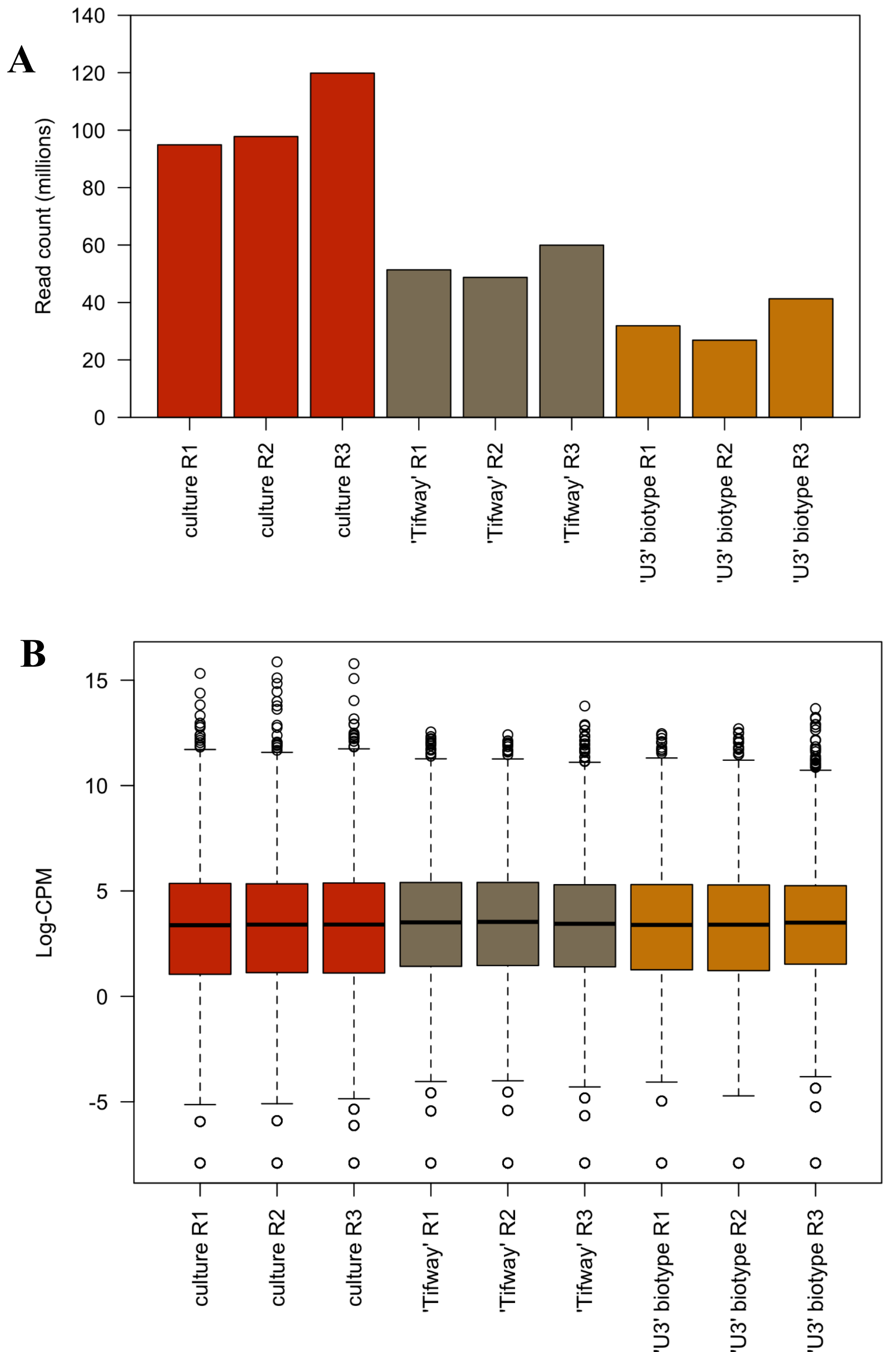

Figure IV-2. Diagnostic plots of data filtering and normalization. (A) Total transcript read counts, in millions. (B) Distribution of transformed expression values (log-counts per million, CPM).

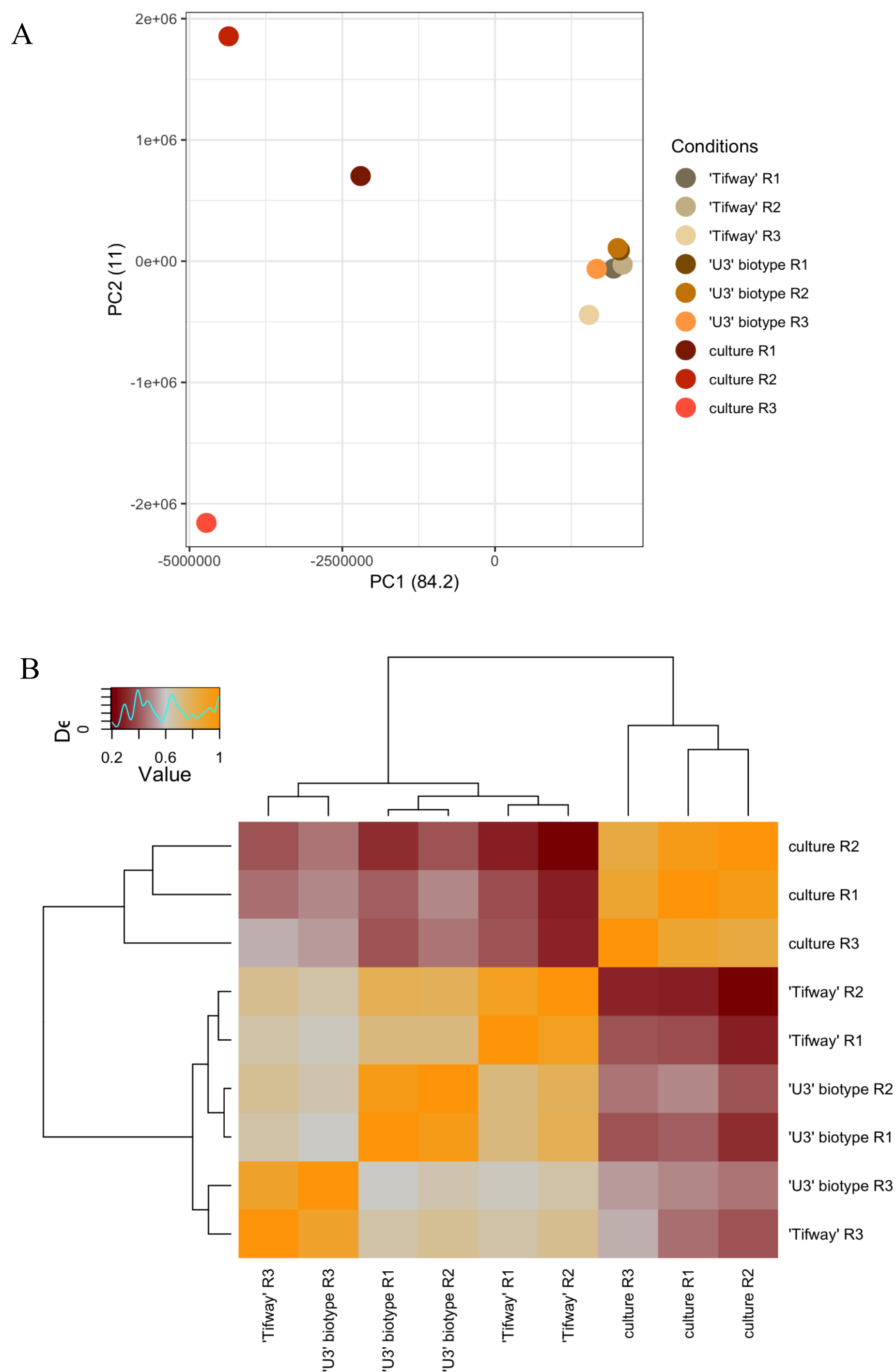

Figure IV-3. Diagnostic plots of data set variance. (A) Principal component analysis of filtered data. (B) Distance correlation of the normalized data of all samples and replicates.

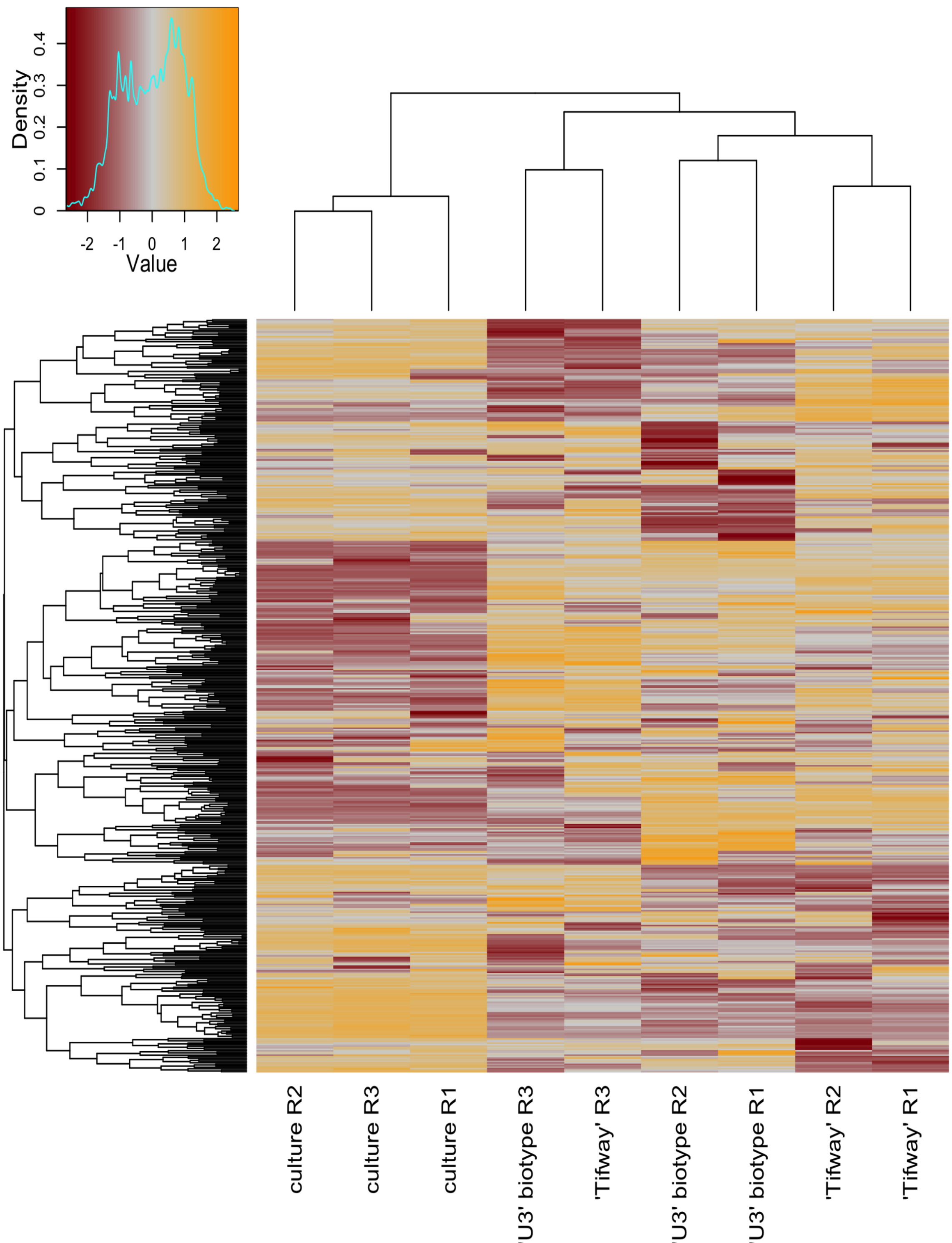

Figure IV-4. Heatmap of the most differentially expressed genes.

TABLES:

Table IV-1. Comparisons of the number of differentially expressed transcripts and genes between three conditions. Transcripts and genes were considered differentially expressed at false discovery rate of 5% (P value < 0.05) and log-fold change (logFC) of two. In these comparisons, the condition listed first was the baseline for the comparision ('Tifway', 'U3' biotype, and 'U3' biotype, respectively). Transcripts or genes with logFC greater than or equal to +2 were considered to be up-regulated in the baseline condition (and vice-versa with transcripts with logFC less than or equal to -2).

Comparisons	**Total**	**Up-regulated (logFC > +2)**	**Down-regulated (logFC < -2)**
Transcripts:			
'Tifway'vs in culture	2,284	1,600	638
'U3' biotype vs in culture	2,821	1,795	955
'U3' biotype vs 'Tifway'	342	106	236
Genes:			
'Tifway'vs in culture	2,153	1,522	605
'U3' biotype vs in culture	2,663	1,718	904
'U3' biotype vs 'Tifway'	330	104	230

Table IV-2. Comparison: in 'Tifway' vs in culture. Enrichment analysis for Gene Ontologies up-regulated in 'Tifway'.

GO term	Term description	Transcript count	False discovery rate
Biological Process			
GO:0044262	cellular carbohydrate metabolic process	8	7.86e-05
GO:0000272	polysaccharide catabolic process	7	0.00015
GO:0044264	cellular polysaccharide metabolic process	7	0.00015
GO:0030243	cellulose metabolic process	5	0.00052
GO:0030245	cellulose catabolic process	5	0.00052
GO:0043170	macromolecule metabolic process	14	0.009
Cellular Component			
GO:0005576	extracellular region	12	2.59e-08
Molecular Function			
GO:0003824	catalytic activity	17	0.00022
GO:0004553	hydrolyzing O-glycosyl compounds	7	0.00022
GO:0016787	hydrolase activity	13	0.00022
GO:0140096	catalytic activity, acting on a protein	6	0.0057

Table IV-3. Comparison: in 'U3' biotype vs in culture. Enrichment analysis for Gene Ontologies up-regulated in 'U3' biotype.

GO term	Term description	Transcript count	False discovery rate
Biological Process			
GO:0044262	cellular carbohydrate metabolic process	9	2.6e-05
GO:0016052	carbohydrate catabolic process	8	8.86e-05
GO:0000272	polysaccharide catabolic process	7	0.00022
GO:0044264	cellular polysaccharide metabolic process	7	0.00022
GO:0044275	cellular carbohydrate catabolic process	6	0.00022
GO:0030243	cellulose metabolic process	5	0.0011
GO:0030245	cellulose catabolic process	5	0.0011
GO:0044238	primary metabolic process	18	0.0041
GO:0043170	macromolecule metabolic process	16	0.005
GO:0071704	organic substance metabolic process	18	0.0063
GO:0048468	cell development	3	0.0092
GO:0008152	metabolic process	19	0.0093

Cellular Component			
GO:0005576	extracellular region	12	1.3e-07
Molecular Function			
GO:0016787	hydrolase activity	16	1.38e-05
GO:0004553	hydrolyzing O-glycosyl compounds	8	3.06e-05
GO:0003824	catalytic activity	18	0.00015

Table IV-4. Comparison: in 'Tifway' vs in culture. Enrichment analysis for Pfam domains up-regulated in 'Tifway'.

Pfam	Term description	Transcript count	False discovery rate
PF00734	Fungal cellulose binding domain	11	7.85e-07
PF00933	Glycosyl hydrolase family 3 N terminal domain	8	0.00013
PF01915	Glycosyl hydrolase family 3 C-terminal domain	8	0.00013
PF07690	Major Facilitator Superfamily	25	0.00017
PF00083	Sugar (and other) transporter	16	0.00027
PF14310	Fibronectin type III-like domain	7	0.00027
PF03443	Glycosyl hydrolase family 61	7	0.0015
PF04616	Glycosyl hydrolases family 43	6	0.003
PF00150	Cellulase (glycosyl hydrolase family 5)	5	0.0083

Table IV-5. Comparison: in 'U3' biotype vs in culture. Enrichment analysis for Pfam domains up-regulated in 'U3' biotype.

Pfam	Term description	Transcript count	False discovery rate
PF00734	Fungal cellulose binding domain	11	3.3e-06
PF07690	Major Facilitator Superfamily	30	1.42e-05
PF01915	Glycosyl hydrolase family 3 C-terminal domain	9	2.46e-05
PF00933	Glycosyl hydrolase family 3 N terminal domain	9	2.68e-05
PF14310	Fibronectin type III-like domain	8	7.01e-05
PF00083	Sugar (and other) transporter	18	0.0001
PF04616	Glycosyl hydrolases family 43	7	0.00094
PF00150	Cellulase (glycosyl hydrolase family 5)	6	0.0021
PF03443	Glycosyl hydrolase family 61	7	0.0028

Table IV-6. Candidate genes and transcripts up-regulated in 'Tifway' (comparison: 'Tifway' vs culture) that are involved in plant biomass degradation.

Gene/Transcript ID	logFC	logCPM	PValue	FDR	Gene name	Function (UniProt/SwissProt)
MSTRG.11526 / MSTRG.11526.1	7.20	6.56	2.6e-03	2.6e-02	Probable beta-glucosidase A (EC 3.2.1.21)	Cellulose degradation
MSTRG.2089	6.96	1.86	3.4e-06	1.1e-04	Probable beta-glucosidase M (EC 3.2.1.21)	Cellulose degradation
g12516.t1	6.45	6.61	1.7e-04	2.9e-03	Probable beta-glucosidase A (EC 3.2.1.21)	Cellulose degradation
g5968.t1	6.19	6.32	4.0e-05	8.5e-04	Probable endo-beta-1,4-glucanase B (EC 3.2.1.4)	Degradation of complex natural cellulosic substrates
MSTRG.11526 / MSTRG.11526.2	5.95	5.54	1.0e-03	1.2e-02	Probable beta-glucosidase A (EC 3.2.1.21)	Cellulose degradation
g12708.t1	5.82	5.31	2.2e-09	1.6e-07	Probable beta-glucosidase C (EC 3.2.1.21)	Cellulose degradation
g8009.t1	5.80	7.60	3.9e-07	1.6e-05	Probable 1,4-beta-D-glucan cellobiohydrolase C (EC 3.2.1.91)	Involved in the conversion of cellulose to glucose
g7739.t1	5.35	0.01	4.5e-04	6.3e-03	Cutinase (EC 3.1.1.74)	Degradation of plant cuticle

g11877.t1	4.58	5.41	3.5e-04	5.2e-03	Probable endo-beta-1,4-mannanase C (EC 3.2.1.78)	Depolymerization of galactomannans and galactoglucomannans
g9518.t1	4.23	6.11	1.4e-05	3.6e-04	Endo-1,4-beta-xylanase I (EC 3.2.1.8)	Major xylan-degrading enzyme
MSTRG.900	3.93	6.42	1.2e-03	1.4e-02	Probable beta-glucosidase G (EC 3.2.1.21)	Cellulose degradation
g11240.t1	3.39	7.67	3.9e-05	8.3e-04	Endo-beta-1,4-mannanase A (Man5A) (EC 3.2.1.78)	Hydrolase activity
g1499.t1	2.75	7.80	5.4e-05	1.1e-03	Probable beta-glucosidase F (EC 3.2.1.21)	Cellulose degradation
MSTRG.4953	2.24	5.86	5.8e-03	4.9e-02	Beta-glucosidase cel3A (EC 3.2.1.21)	Cellulose degradation

Table IV-7. Comparison: in 'Tifway' vs in culture. Number of transcripts with predicted function in plant-pathogen interaction. Annotations were based on predicted protein search against the PHI-base.

	Number of up-regulated transcripts						
	Reduced virulence	**Unaffected pathogenicity**	**Loss of pathogenicity**	**Lethal**	**Effector**	**Mixed**	**Total**
In culture	18	21	6	2	0	3	50
In 'Tifway'	57	47	8	6	3	17	138

Table IV-8. Candidate pathogenicity genes up-regulated in 'Tifway' (comparison: 'Tifway' vs culture).

Gene/Transcript ID	logFC	logCPM	PValue	FDR	Gene name	Function (UniProt/SwissProt)	PHI-base assignment	Effector signal
g12955.t1	17.19	7.20	9.8e-24	9.4e-21	Neutral protease 2 homolog (EC 3.4.24.39)	Secreted metalloproteinase that allows assimilation of proteinaceous substrates	-	-
MSTRG.2827	10.26	7.10	1.7e-12	2.7e-10	-	-	Unaffected pathogenicity	✓
MSTRG.4365	7.84	-0.52	1.8e-03	2.0e-02	Major facilitator superfamily multidrug transporter mfsB	Major facilitator superfamily transporter	Reduced virulence	-
g5806.t1	7.58	2.85	2.4e-04	3.8e-03	Endoglucanase cel12B (EC 3.2.1.4)	Hydrolyze 1,3-1,4-beta-glucan during infection and spore formation	Unaffected pathogenicity	✓
g12843.t1	7.53	6.63	9.0e-06	2.5e-04	Endo-1,4-beta-xylanase F3 (EC 3.2.1.8)	Xylan degradation	Reduced virulence	✓
g1817.t1	7.03	3.14	1.1e-04	2.0e-03	Probable xyloglucan-specific endo-beta-1,4-glucanase A (EC 3.2.1.151)	Degradation of xyloglucan	PAMP, homolog to *P. sojae* Psxeg1	✓

g6814.t1	6.44	5.29	2.1e-12	3.2e-10	Cutinase (EC 3.1.1.74)	Degradation of plant cuticle	Unaffected pathogenicity	✓
MSTRG.4067	5.80	6.39	4.9e-04	6.8e-03	Endo-1,4-beta-xylanase G (EC 3.2.1.8)	Xylan degradation	Unaffected pathogenicity	✓
g9420.t1	5.39	4.31	1.0e-06	3.7e-05	Isocitrate lyase (ICL) (Isocitratase) (EC 4.1.3.1)	Key step of the glyoxylate cycle. Plays an important role in plant pathogenicity	Reduced virulence	-
g8845.t1	5.01	6.81	8.0e-09	5.3e-07	-	-	PAMP, homolog to *M. oryzae* Mocdip1	✓
g12710.t1	4.99	10.47	1.09e-06	3.99e-05	Extracellular metalloproteinase 2 (EC 3.4.24.-) (Fungalysin MEP2)	Secreted metalloproteinase that allows assimilation of proteinaceous substrates	Reduced virulence	-
g8981.t1	4.97	0.07	2.2e-04	3.5e-03	Chitin synthase D (EC 2.4.1.16)	Plays a major role in cell wall biogenesis.	Reduced virulence	-
g7402.t1	4.88	0.26	1.9e-03	2.0e-02	Mitogen-activated protein kinase HOG1 (MAP kinase HOG1) (EC 2.7.11.24)	Signal transduction pathway that is activated by changes in the osmolarity of the extracellular environment	Unaffected pathogenicity	-
g936.t1	3.46	4.09	7.2e-04	9.3e-03	Endoglucanase cel12A (EC 3.2.1.4)	Hydrolyze 1,3-1,4-beta-glucan during infection and spore formation	-	✓

g8219.t1	3.35	9.31	5.5e-05	1.1e-03	Leucine aminopeptidase 1 (EC 3.4.11.-)	Extracellular aminopeptidase that allows assimilation of proteinaceous substrates	-	-
g12803.t1	2.71	5.72	1.8e-04	3.0e-03	-	-	PAMP, homolog to *M. oryzae* Mocdip4	✓

Table IV-9. Candidate genes and transcripts up-regulated in 'U3' biotype (comparison: 'U3' vs culture) that are involved in plant biomass degradation.

Gene/Transcript ID	logFC	logCPM	PValue	FDR	Gene name	Function (UniProt/SwissProt)
g4125.t1	9.69	4.90	1.1e-06	3.7e-05	Beta-glucosidase cel3A (EC 3.2.1.21)	Cellulose degradation
g5968.t1	7.52	6.32	2.5e-06	7.4e-05	Probable endo-beta-1,4-glucanase B (EC 3.2.1.4)	Degradation of complex natural cellulosic substrates
MSTRG.11526.2	6.99	5.54	2.2e-04	3.2e-03	Probable beta-glucosidase A (EC 3.2.1.21)	Cellulose degradation
g12708.t1	6.59	5.31	6.0e-11	6.4e-09	Probable beta-glucosidase C (EC 3.2.1.21)	Cellulose degradation
g8009.t1	6.56	7.60	3.0e-08	1.6e-06	Probable 1,4-beta-D-glucan cellobiohydrolase C (EC 3.2.1.91)	Involved in the conversion of cellulose to glucose
MSTRG.2089	6.35	1.86	1.6e-05	3.5e-04	Probable beta-glucosidase M (EC 3.2.1.21)	Cellulose degradation
g9518.t1	5.96	6.11	1.7e-08	9.4e-07	Endo-1,4-beta-xylanase I (EC 3.2.1.8)	Major xylan-degrading enzyme

g11877.t1	5.93	5.41	1.3e-05	3.1e-04	Probable endo-beta-1,4-mannanase C (EC 3.2.1.78)	Depolymerization of galactomannans and galactoglucomannans
MSTRG.900	4.45	6.42	3.3e-04	4.4e-03	Probable beta-glucosidase G (EC 3.2.1.21)	Cellulose degradation
MSTRG.11526.1	4.35	5.75	9.8e-05	1.7e-03	Probable beta-glucosidase A (EC 3.2.1.21)	Cellulose degradation
g11240.t1	3.95	7.67	2.9e-06	8.4e-05	Endo-beta-1,4-mannanase A (Man5A) (EC 3.2.1.78)	Hydrolase activity
g11177.t1	3.19	1.20	3.7e-03	2.9e-02	Probable beta-glucosidase E (EC 3.2.1.21)	Cellulose degradation
g1499.t1	2.78	7.80	4.4e-05	8.3e-04	Probable beta-glucosidase F (EC 3.2.1.21)	Cellulose degradation
g10056.t1	2.36	8.67	3.3e-03	2.7e-02	Probable beta-glucosidase G (EC 3.2.1.21)	Cellulose degradation
MSTRG.4953	2.35	5.86	3.9e-03	3.0e-02	Beta-glucosidase cel3A (EC 3.2.1.21)	Cellulose degradation

Table IV-10. Comparison: in 'U3' biotype vs in culture. Number of transcripts with predicted function in plant-pathogen interaction. Annotations were based on predicted protein search against the PHI-base.

	Number of up-regulated transcripts						
	Reduced virulence	**Unaffected pathogenicity**	**Loss of pathogenicity**	**Lethal**	**Effector**	**Mixed**	**Total**
In culture	29	22	10	4	0	7	72
In 'U3' biotype	63	58	10	8	3	17	159

Table IV-11. Candidate effector genes up-regulated in 'U3' biotype (comparison: 'U3' biotype vs culture).

Gene/Transcript ID	logFC	logCPM	PValue	FDR	Gene name	Function (UniProt/SwissProt)	PHI-base assignment	Effector signal
g12955.t1	16.43	7.20	3.8e-22	2.5e-19	Neutral protease 2 homolog SNOG_02177 (EC 3.4.24.39)	Secreted metalloproteinase that allows assimilation of proteinaceous substrates	-	-
g5806.t1	9.84	2.85	1.7e-05	3.8e-04	Endoglucanase cel12B (EC 3.2.1.4)	Hhydrolyze 1,3-1,4-beta-glucan during infection and spore formation	Unaffected pathogenicity	✓
g12843.t1	9.20	6.63	3.8e-07	1.4e-05	Endo-1,4-beta-xylanase F3 (EC 3.2.1.8)	Xylan degradation	Reduced virulence	✓
g1817.t1	8.41	3.14	1.3e-05	3.0e-04	Probable xyloglucan-specific endo-beta-1,4-glucanase A (EC 3.2.1.151)	Degradation of xyloglucan	PAMP, homolog to *P. sojae* Psxeg1	-
MSTRG.4365	6.85	-0.52	6.9e-03	4.8e-02	Major facilitator superfamily multidrug transporter mfsB	Major facilitator superfamily transporter	Reduced virulence	-
g6814.t1	6.63	5.29	7.3e-13	1.1e-10	Cutinase (EC 3.1.1.74)	Degradation of plant cuticle.	Unaffected pathogenicity	✓
g11152.t1	6.43	2.29	1.3e-04	2.1e-03	Neutral trehalase (EC 3.2.1.28)	Plays a role in pathogenicity, specifically in proliferation of invasive hyphae	Unaffected pathogenicity	-

g936.t1	5.98	4.09	1.9e-07	7.8e-06	Endoglucanase cel12A (EC 3.2.1.4)	Hydrolyze 1,3-1,4-beta-glucan during infection and spore formation	-	✓
g8845.t1	5.92	6.81	6.4e-11	6.8e-09	-	-	PAMP, homolog to *M. oryzae* Mocdip1	✓
g9420.t1	5.82	4.31	2.3e-07	9.1e-06	Isocitrate lyase (ICL) (Isocitratase) (EC 4.1.3.1)	Key step of the glyoxylate cycle. Plays an important role in plant pathogenicity	Reduced virulence	-
g8981.t1	5.20	0.07	1.3e-04	2.1e-03	Chitin synthase D (EC 2.4.1.16)	Plays a major role in cell wall biogenesis.	Reduced virulence	-
MSTRG.4067	5.06	6.39	1.6e-03	1.6e-02	Endo-1,4-beta-xylanase G (EC 3.2.1.8)	Xylan degradation	Unaffected pathogenicity	✓
g7739.t1	5.03	0.01	8.1e-04	9.0e-03	Cutinase (EC 3.1.1.74)	Degradation of plant cuticle	Unaffected pathogenicity	-
g12710.t1	4.73	10.47	2.8e-06	8.3e-05	Extracellular metalloproteinase 2 (EC 3.4.24.-) (Fungalysin MEP2)	Secreted metalloproteinase that allows assimilation of proteinaceous substrates	Reduced virulence	-
g12803.t1	4.57	5.72	6.7e-09	4.2e-07	-	-	PAMP, homolog to *M. oryzae* Mocdip4	✓
MSTRG.8692	4.33	4.82	3.9e-04	5.1e-03	Cell pattern formation-associated protein StuA (Stunted protein A)	Transcription factor that regulates asexual reproduction, required for pathogenicity, and positively regulates the synthesis of the mycotoxins.	Reduce virulence	-

g9656.t1	3.42	-0.02	4.1e-03	3.2e-02	Cell pattern formation-associated protein StuA (Stunted protein A)	Transcription factor that regulates asexual reproduction, required for pathogenicity, and positively regulates the synthesis of the mycotoxins.	Reduce virulence	-
MSTRG.4805	2.91	8.15	5.8e-03	4.2e-02	-	-	Loss of pathogenicity	-

CHAPTER V

EXPRESSION PROFILING OF BERMUDAGRASS ROOTS DURING *OPHIOSPHAERELLA HEPOTRICHA* COLONIZATION

ABSTRACT

Spring dead spot (SDS) is a devastating disease of bermudagrass in golf courses, athletic fields, and in the landscape. This disease is caused by the fungi *Ophiosphaerella herpotricha, O. korrae,* and *O. narmari* that colonize roots, stolons, and rhizomes of bermudagrass. The underlying genetics by which bermudagrass roots respond to *Ophiosphaerella* infection is not fully elucidated. Results of the previous studies, indicated that *O. herpotricha* ISCC16F might deploy three candidate necrotrophic-effector genes that trigger the plant basal defense known as pathogen-associated molecular pattern-trigger immunity. With that, the objective of this study was to identify differentially expressed genes of bermudagrass roots during *O. herpotricha* colonization. Differentially expressed genes were determined in a *de novo* approach from root transcriptomes of a susceptible and a resistant bermudagrass cultivar that were inoculated with *O. herpotricha*, compared to the transcriptome of the non-inoculated cultivars. The

results of this study showed that infected roots of a susceptible and a tolerant bermudagrass cultivars up-regulated genes involved in response to biotic stresses and defense responses. Candidate plant immunity genes of the susceptible cultivar 'Tifway' included transcription factor WRKY 33, cis-jasmone-related genes such as lipoxygenase (LOX2), and pathogenesis-related proteins, which have been shown to cooperate with WRKY33- and jasmonate-mediated signaling pathway in the regulation of basal plant defense and hypersensitive response. In the tolerant common bermudagrass biotype 'U3', up-regulated candidate plant immunity genes included transcription factors, non-expressor of PR-1 (NPR1), and others indicate a network of defense responses potentially mediated by salicylic acid hormone. The tolerant 'U3' biotype also showed activation of defense response, but how it can potentially modulate *O. herpotricha* morphology/physiology to establish a potentially symbiotic relationship remains to be elucidated. Future experiments are required to functionally characterize these candidate genes.

1. INTRODUCTION

Bermudagrass (*Cynodon* spp.) is a perennial grass of three main types: common bermudagrass (*C. dactylon* (L.) Pers.), African bermudagrass (*C. transvaalensis* Burt-Davy) and interspecific hybrids (*C. dacytlon* x *C. transvaalensis*). Bermudagrass is adapted to warm climates, and has a broader adaptation range as improved cultivars tend to be drought and salt tolerant as well. Bermudagrass has a high growth rate and extensive root system through development from meristematic tissue in stolons and rhizomes. This makes bermudagrass a versatile grass for soil cover and stabilization

[53,295,353]. In the United States, bermudagrass is successfully cultivated as turf in the southern region where common bermudagrass and interspecific hybrids are the two main types [53]. Interspecific hybrids often have improved agronomic traits such as fine leaf texture and fast growth, which make these very suitable for high maintenance sports fields and golf courses [53,295].

An important limitation to bermudagrass cultivation in the colder north portion of the southern region is soilborne disease called spring dead spot (SDS). The disease is caused by *Ophiosphaerella herpotricha* (Fries) J. Walker, *O. korrae* (J. Walker & A. M. Smith) R. A. Shoemaker & C. E. Babcock and *O. narmari* (J. Walker & A. M. Smith) Wetzel, Hubert & Tisserat. These *Ophiosphaerella* species colonize roots, stolons and rhizomes of bermudagrass causing root discoloration and necrosis in susceptible cultivars. Symptoms of SDS are prominent in the spring season as dead patches, which are the result of root injury that depletes belowground organs of water and nutrients and thus enhances cold sensitivity [37,95,324,325].

Limited information is available regarding host-pathogen interaction in this pathosystem. The host-pathogen interaction at the cellular level has been described [37,95]. In a susceptible cultivar, colonization was limited to the root cortex with strong root discoloration within 48 hours of inoculation. Root discoloration and necrosis have been hypothesized to be due to potential fungal phytotoxic compounds [94,319] but strong evidence to support that remains to be reported. In contrast, colonization of a resistant cultivar by the same isolate showed vascular colonization, delay or absence of necrosis [37,85,95], and production of reactive oxygen species (ROS) that suggested an endophytic interaction [83,97,269]. The evidence of higher levels of ROS in the resistant cultivar suggested that the mechanism by which the pathogen induced root necrosis was other than oxidative burst [94].

The underlying genetics of root colonization by SDS-pathogens remained unknown. The results of the previous chapter indicated that the fungus can secrete potential necrotrophic effectors that were characterized to trigger pathogen-associated molecular pattern-triggered immunity. Additionally, there were no significant differences in the up-regulation of genes between a resistant and a susceptible host (genes with assigned function), which indicated that the host could modulate the outcome of *O. herpotricha* colonization. Therefore, the objective of this study was to elucidate the molecular basis of bermudagrass root-*Ophiosphaerella* colonization with differential gene expression-based analysis. The hypothesis of this study was that a susceptible cultivar up-regulates genes involved in disease response, particularly basal resistance, which are distinct in the resistant cultivar response.

2. METHODS

2.1. BIOLOGICAL MATERIALS

Two bermudagrass cultivars were grown in a greenhouse: ‘Tifway (419)’ (hybrid, susceptible to SDS) and a common bermudagrass biotype called ‘U3’ (resistant). Plants were cultivated in plastic pots with a sterile mixture of sand and growing mix (Sunshine® Redi-Earth Plug & Seedling, Sun Gro® Horticulture, Agawam, MA) (sand:growing mix 9:1). The pots were watered twice a day for 15 minutes through an automatic sprinkle irrigation system and fertilized with a nutrient solution containing 1 tbs/gal of 24-8-26 N-P-K plus micronutrients (Miracle-Gro®, Scotts Miracle-Gro Products, Inc., Marysville, OH) every seven days. Stolons were cut and placed in plastic trays containing sterile sand to root for approximately five to eight days. Single-node rooted stolons were carefully washed with reverse osmosis water to remove soil particles, and were subsequently surface sterilized with 5.3% hypochlorite solution for four minutes. Injury- and blemish-free rooted nodes were transferred to petri dishes. The roots were placed in between sterile filter paper. Approximately, 2 ml of sterile nanopore water was added to moisten filter papers. Seven to ten days old cultures of *O. herpotricha* isolate ISCC16F on agar plugs covered with fungal mycelium were used as inoculum. Culture plugs were placed directly onto roots one centimeter below the node, mycelium touching the surface of the root. Petri dishes were wrapped with aluminum foil and incubated vertically in a growth chamber set at approximately 16 to 18°C and 12-hour photoperiod, for five days. Additionally, fungal mycelium was cultured over a cellophane sheet on potato dextrose agar. The experiment was conducted in a completely randomized design, on one shelf inside the growth chamber, with three replicates.

2.2 TRANSCRIPTOME SEQUENCING

Total RNA was extracted from roots five days after inoculation. Roots were cut and immediately flash frozen in liquid nitrogen, placed in a 2 mL sterile tube with RNAlater®-ICE (Ambion, Inc., Austin, TX) and incubated at -20°C until used. Approximately, 30 mg of roots was used for extraction. Excess RNAlate*r*®-ICE was removed from samples by squeezing with forceps. Total RNA was isolated using RNase

Plant Mini Kit (Qiagen, Inc., Valencia, CA) following manufacturer recommendations. Eluted RNA sample was stored at -80°C until submitted for sequencing. Quality and quantity of total RNA was assessed by agarose gel, NanoDrop™ and Agilent Bioanalyzer 2100 (Agilent Technologies Inc., Santa Clara, CA). In agarose gel, two intact bands representing the 28S and 18S without degradation was required. For the NanoDrop™, the cutoff for the 260/280 nm absorbance ratio was 1.8, and for 260/230 nm absorbance ratio was 1.8-2.2. For the Agilent Bioanalyzer, RNA integrity number greater than 6.5 was acceptable, but greater than 7.0 was desirable. Sequencing library preparation of RNA samples was performed by Novogene Bioinformatics Technology Co., Ltd. (Shatin, Hong Kong). The libraries were sequenced on an Illumina HiSeq System (Illumina Inc., San Diego, CA, USA) to produce 150bp pair-ended libraries.

2.3. *DE NOVO* TRANSCRIPTOME PROFILING ANALYSIS

Raw Illumina reads from *in planta*-'Tifway' and 'U3' biotype libraries were assessed for quality using FastQC [9] and filtered for low quality or adaptor trimming using Trimmomatic [29]. Reads of inoculated libraries were paired to the reference genome of the *O. herpotricha* isolate ISCC16F (see chapter III for details) using HISAT2 [156] to mine fungal transcripts. Reads of inoculated libraries, which did not pair with the *O. herpotricha* genome, and reads of non-inoculated libraries were used for the *de novo* transcriptome assembly. The 'Tifway' and 'U3' biotype transcriptomes were assembled *de novo* using Trinity [116,125], transcript abundance was estimated by RSEM [189], and differential gene expression analysis was done using edgeR [265] in R. For differential gene expression analysis, read count data was filtered to allow at least one count in three or more samples, and normalized using the trimmed mean of M-values method. Genes were considered differentially expressed based on 5% false discovery rate (FDR, P value < 0.05) and log fold change of two.

2.4. FUNCTIONAL ANNOTATION

Hypothetical protein sequences of predicted differentially expressed transcripts were obtained using TransDecoder [82]. Functional classification and annotation of predicted proteins was done using BLAST search of proteins against the UniProtKB/SwissProt *Arabidopsis thaliana* proteome database using an e-value threshold of 1e-5, minimum percent identity of 50%, and minimum query coverage of 50%. Hits from BLAST search were parsed to allow the highest scoring pair (based on e-value) per gene. For enrichment term and protein network analyses of Gene Ontology (GO), Protein families (Pfam), and Kyoto Encyclopedia of Genes and Genomes (KEGG) pathways were obtained in STRING v.11 [293] with FDR cutoff of 0.001.

3. RESULTS AND DISCUSSION

3.1. TRANSCRIPTOME SEQUENCING

Illumina sequencing of 150 bp pair-ended libraries yielded, in average across three replicates, 74,927,238 raw reads for inoculated 'Tifway' (susceptible), 62,664,507 raw reads for non-inoculated 'Tifway', 76,278,322 raw reads for inoculated 'U3' biotype (resistant), and 72,017,921 raw reads for non-inoculated 'U3' biotype. After quality check and trimming, reads of inoculated libraries were mapped to the reference genome of *O. herpotricha*, and unpaired reads were further used. The average across three replicates of inoculated 'Tifway' varied from 36,880,152 to 44,571,518 reads, and of inoculated 'U3' biotype varied from 40,018,866 to 62,122,286 reads. Raw reads of non-inoculated libraries were checked for quality and trimmed, and used without mapping.

3.2. *DE NOVO* TRANSCRIPTOME PROFILING ANALYSIS

In the 'Tifway' assembly obtained *de novo* by Trinity, there were a total of 216,788 genes identified, with an average of 2.3 transcripts per gene (Figure V-1A). The majority of transcript length (75th percentile) was 261 base pairs (bp), with the longest transcript length being 4471 bp (Figure V-1B). In the 'U3' biotype assembly, there were 228,021 genes identified, with an average of 2 transcripts per gene (Figure V-2A). The majority of transcript length (75th percentile) was 299 bp, and the longest transcript was 5,136 bp (Figure V-2B).

These data were pre-processed and analyzed using edgeR [265] in R. Diagnostic plots of exploratory data quality were obtained. Total read count of 'Tifway' (Figure V-3A) and 'U3' biotypes (Figure V-4A) showed variation in sample-read size, which was due to mixed transcriptome of bermudagrass and *O. herpotricha* (see Chapter IV). After filtering and normalization of expression values (log-cpm), the variation among replicates was very small (Figure V-3B and Figure V-4B). Quality and normalization of count data was performed by a principal component analysis (PCA) (Figure V-5A and Figure V-6A), and the correlation distances between replicates was computed and plotted as a heatmap (Figure V-5B and Figure V-6B). In the case of 'Tifway' replicates, the two groups of inoculated and non-inoculated (except ‘n-inoc r3’) showed a very slow variability (PC2 = 8.6%) (Figure V-5A). low variability (PC2 = 8.6%) (Figure V-5A). A similar trend was also observed by the distance correlation values between inoculated and non-inoculated replicates did not vary much (Figure V-6A). In the case of ‘U3’ biotype, the PCA (Figure V-6A) showed the inoculated and non-inoculated replicates grouped along the horizontal axis that explained almost 95% of the variation observed among sample. The same was observed in the distance correlation heatmap (Figure V-6B). The replicate ‘inoc R3’ showed a higher correlation with non-inoculated replicates. The 500 most differentially expressed genes of ‘Tifway’ (Figure V-7) and of ‘U3’ biotype (Figure V-8) were clustered hierarchically with a heatmap.

Differential gene expression was computed based on 5% FDR and log-fold change of two (Table V-1). In the bermudagrass hybrid ‘Tifway’, there was a total of 4,224 genes differentially expressed of which 2,849 were up-regulated and 1,080 down-regulated in the inoculated condition. In the common bermudagrass ‘U3’ biotype transcriptome, there was a total of 14,046 genes differentially expressed of which 3,118 were up-regulated and 5,897 down-regulated in the inoculated condition. The BLAST searches against the UniProt/SwissProt *A. thaliana* proteome database were parsed to retain the best scoring (lowest e-value) transcript per gene. In the ‘Tifway’ transcriptome, there were a total of 1,106 matches (873 up-regulated, and 233 down-regulated). In the ‘U3’ biotype, there were 3,238 matches (1,067 up-regulated, 2,171 down-regulated) These *Arabidopsis*-homologous gene identifiers were used to obtain GO, PFAM, and KEGG pathway enrichments in STRING v11 [293] to explore potential functions/roles in plant immunity.

Diagnostic plots of exploratory data quality were obtained by edgeR [265]. Total read count of 'Tifway' (Figure V-3A) and 'U3' biotypes (Figure V-4A) showed variation in sample-read size, which was due to mixed transcriptome of bermudagrass and *O. herpotricha* (see Chapter IV). After filtering and normalization of expression values (log-cpm), the variation among replicates was not significant (Figure V-3B and Figure V-4B). Quality and normalization of count data was performed by a principal component analysis (PCA) (Figure V-5A and Figure V-6A), and the correlation distances between replicates was computed and plotted as a heatmap (Figure V-5B and Figure V-6B). PCA demonstrated that, in the case of 'Tifway' replicates, the two groups of inoculated and non-inoculated (except 'n-inoc r3') showed a very slow variability (PC2 = 8.6%) (Figure V-5A). A similar trend was also observed by the distance correlation values between inoculated and non-inoculated replicates did not vary much (Figure V-6A). In the case of 'U3' biotype, the PCA (Figure V-6A) showed the inoculated and non-inoculated replicates grouped along the horizontal axis, which explained almost 95% of the variation observed among sample. The same was observed in the distance correlation heatmap (Figure V-6B). The replicate 'inoc R3' showed a higher correlation with non-inoculated replicates. The 500 most differentially expressed genes of 'Tifway' (Figure V-7) and of 'U3' biotype (Figure V-8) were clustered hierarchically in the heatmap.

Differential gene expression was computed based on 5% FDR and log-fold change of two (Table V-1). In the bermudagrass hybrid 'Tifway', there was a total of 4,224 genes differentially expressed of which 2,849 were up-regulated and 1,080 down-regulated in the inoculated condition. In the common bermudagrass 'U3' biotype transcriptome, there was a total of 14,046 genes differentially expressed of which 3,118 were up-regulated and 5,897 down-regulated in the inoculated condition. The BLAST searches against the UniProt/SwissProt *A. thaliana* proteome database were parsed to retain the best scoring (lowest e-value) transcript per gene. In the 'Tifway' transcriptome, there were a total of 1,106 matches (873 up-regulated, and 233 down-regulated). In the 'U3' biotype, there were 3,238 matches (1,067 up-regulated, 2,171 down-regulated). These *Arabidopsis*-homologous gene identifiers were used to obtain GO, PFAM, and KEGG pathway enrichments in STRING v11 [293] to explore potential functions/roles in plant immunity.

3.3. ENRICHMENT ANALYSES OF DIFFERENTIALLY EXPRESSED GENES

There were 13 PFAM domains enriched in 'Tifway' (Table V-2). Protein domains observed in the up-regulated conditon included: ABC transporter (PF00005), cupin domain (PF07883, PF00190), and proteasome (PF00227). In 'U3' biotype there were 45 PFAM domains enriched. In addition to ABC transporters, protein kinase domains (PF00069, PF07714, PF12398), PAN-like domains (PF08276), and cell-wall associated receptor kinases (PF13947) domains were enriched (Table V-3). It was possible to observe a greater number of PFAM domains in the down-regulated conditions of both cultivars. There were a total of 29 KEGG pathways enriched in 'Tifway' (Table V-4). Among these, 102 genes in 'biosynthesis of secondary metabolites' (ath:01110), 14 genes in 'phenylpropanoid metabolism' (ath:00360), 13 genes in ' plant-pathogen interaction' (ath:04626), and 8 genes in 'fatty acid metabolism' (ath:04016) were observed. In the 'U3' biotype there were 21 enriched KEGG pathways (Table V-5). The 'plant-pathogen interaction' pathway was not significally enriched (FDR = 0.0133).

There were a total of 327 GO Biological Process (BP) terms enriched in ‘Tifway’, with 252 terms enriched in the up-regulated condition (Figure V-9 and Figure V-10). Terms related to plant immunity included: 30 genes in ‘defense response to bacterium’ (GO:0009617), 46 genes in ‘defense response to other organism’ (GO:0098542), and 56 genes in ‘defense response’ (GO:0006952). In ‘U3’ biotype, there were 433 GO BP terms enriched, and 154 were enriched in the up-regulated condition (Figure V-11 and Figure V-12). Terms related to plant immunity included: 23 genes in ‘innate immune response’ (GO:0045087), 32 genes in ‘defense response to bacterium’ (GO:0009617), 51 genes in ‘defense response to other organism’ (GO:0098542), and 65 genes in ‘defense response’ (GO:0006952).

The broad GO BP ‘response to biotic stimulus’ (GO:0009607) was used to explore candidate genes in plant immunity. There were 64 unique up-regulated *A. thaliana*-homologous genes enriched in ‘Tifway’, and a total of 80 unique up-regulated *A. thaliana*-homologous genes enriched in ‘U3’ biotype. The enriched gene annotations were compared, and candidate plant immunity genes were presented in the following manner: (i) shared between ‘Tifway’ and ‘U3’ biotype, (ii) unique to ‘Tifway’, and (iii) unique to ‘U3’ biotype (Table V-6 and Table V-7). These candidate genes were subjected to protein network analysis in STRING v11 [63].

3.4. CANDIDATE GENES INVOLVED IN PLANT IMMUNITY

Basal resistance is the first layer of the plant immune system. The basal resistance mechanism of defense is recognizing conserved molecules of the pathogen, referred to as pathogen-associated molecular pattern (PAMP) [146]. Fungal chitin is a PAMP that is perceived by host plants by pattern recognition receptors (PRRs), such as the *Arabidopsis* CERK1 [149] and OsCEBiP [276], and will trigger host defenses. The results of this study did not demonstrate up-regulation of PRRs-homologs in either 'Tifway' or 'U3' biotype. However, there was up-regulation of chitinases and β-glucanases, which are pathogenesis-related (PR) proteins, PR3 and PR2, respectively, induced upon *O. herpotricha* infection. In both hosts, an up-regulation of PR2, *Arabidopsis thaliana* (At)-homolog BG3 EC 3.2.1.39 (candidate 'Tifway' gene TRINITY_DN246405_c3_g1 logFC+3.98, and candidate 'U3' gene TRINITY_DN246405_c3_g1 logFC+5.27). Each host also up-regulated endochitinases (PR3). In 'Tifway' there were two PR3 candidate genes: AtCHI5 endochitinase EP3 EC 3.2.1.14 (candidate TRINITY_DN150924_c0_g1 gene: logFC+4.43), and AtCHIB basic endochitinase EC 3.2.1.14 (candidate TRINITY_DN154152_c0_g1 gene logFC+5.13). Two copies of a candidate PR3 were also up-regulated in 'U3' biotype: AtCHIA acidic endochitinase EC 3.2.1.14 (candidate genes: TRINITY_DN246596_c0_g2 logFC+2.44, and TRINITY_DN246596_c0_g2 logFC+3.84). These PR proteins have been shown to have antimicrobial properties, and to have functions beyond plant innate immunity such as plant development [69]. In addition, the expression of these PR proteins have been shown to be tissue dependent. In tobacco, PR2 and PR3 were shown to be produced in roots and not in leaves [34].

The Mediator complex (MED) is conserved in eukaryotes. Its function is in the transcriptional machinery in serving as a bridge to link transcription factors to RNA polymerase II [348]. The MED complex was shown to play a role in plant innate immunity defense against pathogens [38,252]. In *Arabidopsis*, subunits of the MED were shown to be involved in response to biotrophic and necrotrophic pathogens [38,252,352].

For example, MED33 was shown to contribute to expression of necrotrophic fungus-induced basal defense genes [329]. These basal defense induced genes were a PDF1.2 defensin protein, Hevein-like protein (PR4), and basic chitinase, which were shown to be required for full basal resistance to *Botrytis cinerea* [329]. In this study, subunits of the MED were enriched in both bermudagrass cultivars. Candidate MED37E genes were up-regulated in ‘Tifway’ (TRINITY_DN144547_c5_g3 logFC+5.13) and in ‘U3’ biotype (TRINITY_DN265881_c6_g4 logFC+12.59). Unique units of MED were up-regulated in each host as well. In ‘Tifway’, candidate MD37C was enriched (TRINITY_DN155817_c1_g6 logFC+8.34). In ‘U3’ biotype, two candidate MED 37D subunit genes were enriched (TRINITY_DN267363_c3_g1 log FC+5.06, and TRINITY_DN265380_c1_g4 logFC+6.81). In addition, a candidade Hevein-like gene was enriched in both hosts (HEVL genes: candidate ‘Tifway’ TRINITY_DN151060_c0_g1 logFC+3.40, and ‘U3’ candidate TRINITY_DN247869_c0_g1 logFC+4.10). A homolog of the Arabidopsis PDF1.2 was not found in either bermudagrass host.

Similarly to what has been demonstrated for *B. cinerea* [329], ‘Tifway’ up-regulated a candidate basic chitinase (AtCHIB basic endochitinase EC 3.2.1.14; candidate TRINITY_DN154152_c0_g1 gene logFC+5.13) upon *O. herpotricha* infection. In addition, in the previous chapter, three candidate *O. herpotricha* necrotrophic effectors were predicted to serve as PAMP. One of them, the glucanase XEG1 homologous to *Phytophthora sojae* [205], that was predicted to act on the apoplast. The PsXEG1 is a PAMP that is perceived by a host PR2 protein (endoglucanase GIP1) to inhibit PsXEG1 and counteract the attack [205]. A PR2 protein was found to be up-regulated and enriched in 'Tifway', the At-homolog BG3 EC 3.2.1.39 (candidate gene TRINITY_DN246405_c3_g1 logFC+3.98). This indicated the bermudagrass cultivar 'Tifway' might activate basal disease resistance mechanisms against *O. herpotricha* infection.

Upon pathogen perception by the host plant, a cascade of events take place inside the cell that can ultimately lead to defense. This cascade of events is triggered by signaling molecules such as phytohormones, reactive oxygen species (ROS, mainly hydrogen peroxide), and mitogen-activated protein (MAP) kinases that are implicated in a network of defense responses inside the cell. The defense signaling pathway leads to changes in gene expression such as up-regulation of transcription factors, PR proteins, and defense-related genes (R genes) [146]. Candidate transcription factors, phytohormones and MAP kinases were up-regulated and enriched in the bermudagrass hosts in this study (Table V-6 and Table V-7).

Infected roots of bermudagrass cultivar 'Tifway' showed the entire cortex colonized by *Ophiosphaerella* with prominent necrosis. Colonization was limited to the root cortex, and root discoloration could be observed as early as two days post inoculation [37,95]. The protein network analysis of 'Tifway' (Figure V-13) indicated that of *O. herpotricha* (chitin) triggered the activation of PR proteins (PR1, PR2/BG3, PR3/HCHIB, PR4) and of two candidate transcription factor AtWRKY33 (TRINITY_DN165204_c1_g1 logFC+2.34, and TRINITY_DN152416_c0_g1 logFC+2.94). Activation of WRKY33 is considered one of the hallmarks of systemic acquired resistance against necrtrophic pathogens [173], and taking together the strong evidence for interaction with [7], and up-regulation of, AtATG18a (AT18A)

(TRINITY_DN156208_c5_g3 logFC+7.25) supported that the phenotype of necrosis observed in ‘Tifway’-infected roots might be a result of cell death. In addition, AtWRKY33 was shown to interact with MAP kinases MPK4 and MPK3, which were shown to negatively regulate salicylic acid and induce hypersensitive response [246,258]. Candidates MPK3 (TRINITY_DN158728_c0_g1 logFC+2.53) and MPK4 (TRINITY_DN152183_c3_g1 logFC+9.06) were uniquely up-regulated by ‘Tifway’, as well as candidates AtWRK33 and AtATG18a. The network analysis also demonstrated that up-regulated candidate gene AT1G49050/APCB1 (TRINITY_DN168665_c1_g1 logFC+3.31), which was downstream of MPK3, is a protease involved in proteolytic activity (cleavage) of BAG6 [152,190]. The cleavage of BAG6 was induced by pathogen infection/PAMP, and resulted in cell death [152,190]. Therefore, it was concluded that APCB1-BAG6 is involved in basal plant resistance [152,190]. A homolog of At-BAG6 was not differentially expressed in ‘Tifway’. However, up-regulation of jasmonic acid biosynthesis (LOX2, ACX1, and AOS/CP74A) and salicylic acid catabolism (DMR6, and AT4G10490/DLO2) related genes supported the claim that *O. herpotricha*-‘Tifway’ interaction might result in systemic acquired resistance mediated by the jasmonic acid and activation of transcription factors involved in cell death/hypersensitive response [40,107]. The possibility of hypersensitive response-induced genes in the susceptible cultivar infected by *O. herpotricha* was raised in a previous study [353].

Besides hypersensitive response, another cellular event that is considered a hallmark of defense responses is callose deposition [203]. The results of the protein network analysis showed the enrichement of three candidate genes involved in callose deposition: CYP79B2/C79B2 (TRINITY_DN158778_c0_g3 logFC+5.48), CYP79B3/C79B3 (TRINITY_DN158778_c0_g2 logFC+3.28), and TSA2/TRPA2 (TRINITY_DN153587_c0_g2 logFC+9.50), which could limit the colonization of the root cortex by *O. herpotricha* [37,95]. The results of this study showed that at least 13 candidate genes were involved in the pathogen recognition cascade by the susceptible bermudagrass cultivar 'Tifway' and activation of basal disease resistance resulting in callose deposition and hypersensitive response. Further studies will be necessary to confirm the function of the reported candidate genes.The regulatory NPR1 protein is involved in systemic acquired resistance (SAR)-mediated by salicyclic acid [17]. The activation of SAR by NPR1 is accomplished by a tranlational cascade with TGA transcription factors and PR proteins [17]. The protein network analysis of 'U3' biotype (Figure V-14) demonstrated that candidate NPR1 protein interacts with high confidence with candidates TGA transcription factors. In the case of interaction with TGA1 and TGA3, subsquently downstream interaction with PR proteins was demonstrated in the network analysis. Two candidate genes were identifed to play a role in salicylic acid metabolism: AtDLO2 [350] (TRINITY_DN246730_c3_g1 logFC+3.16) and AtDMR6 [73] (TRINITY_DN246730_c4_g1 logFC+3.81). In support of development of SAR, NPR1 [17], WKR53 [137], and another candidate transcription factor, EFR [356] (TRINITY_DN252762_c0_g2 logFC+3.14) that were shown to be involved in hypersensitive response/cell death activation. There were other enriched candidate genes involved in cell death as a result of defense mechanisms. These genes were: two candidate BCS1/HSR4 [227] (TRINITY_DN258901_c2_g3 logFC+2.67, and TRINITY_DN258901_c2_g3 logFC+5.35), and SAG12 [6] (TRINITY_DN259644_c1_g1 logFC+5.54).

The reaction of the tolerant ‘U3’ biotype to *Ophiosphaerella* infection was different than of the susceptible cultivar [37,95]. Infected roots of the tolerant ‘U3’biotype showed colonization of the entire root cortex and of the vascular bundle without necrotic lesions or with delayed necrosis 14 days after inoculation [37,95].The colonization of vasculature in the tolerant ‘U3’ biotype resembled a symbiotic plant-fungal relationship [37,95]. Production of reactive oxygen species associated with the fungal mycelium increased when the fungus colonized the vasculature of the ‘U3’ biotype, supporting the hypothesis that this is similar to a symbiotic association [97]. The up-regulated candidate genes of ‘U3’ biotype indicated that recognition of *O. herpotricha* chitin triggered the activation of PR proteins (PR1, PR1-like/PRB1, PR2/BG3, PR4 and CHIA), candidate regulatory protein NPR1 (TRINITY_DN268959_c1_g3 logFC+2.43), two candidate WRKY53 transcription factors (TRINITY_DN267640_c2_g1 logFC+3.35, and TRINITY_DN255329_c1_g2 logFC+3.47), and candidate TGA transcription factors (TGA1 TRINITY_DN264416_c1_g1 logFC+2.37, TGA3 TRINITY_DN269605_c3_g2 logFC+2.63, and TGA9 TRINITY_DN269154_c2_g2 logFC+2.45). The regulatory NPR1 protein was involved in systemic acquired resistance (SAR)-mediated by salicyclic acid [17]. The activation of SAR by NPR1 was accomplished by a translational cascade with TGA transcription factors and PR proteins [17]. The protein network analysis of ‘U3’ biotype (Figure V-14) demonstrated that a candidate NPR1 protein interacted with high confidence with candidate TGA transcription factors. In the case of interaction with TGA1 and TGA3, subsquent downstream interaction with PR proteins was demonstrated in the network analysis. Two candidate genes were identifed to play a role in salicylic acid metabolism: AtDLO2 [73] (TRINITY_DN246730_c3_g1 logFC+3.16) and AtDMR6 [350] (TRINITY_DN246730_c4_g1 logFC+3.81). The observation of NPR1 [17], WKR53 [350], and another candidate transcription factor, EFR [356] (TRINITY_DN252762_c0_g2 logFC+3.14), that were shown to be involved in hypersensitive response/cell death activation, support the development of SAR. There were other enriched candidate genes involved in cell death as a result of defense mechanisms. These genes were: two candidate BCS1/HSR4 [227] (TRINITY_DN258901_c2_g3 logFC+2.67, and TRINITY_DN258901_c2_g3 logFC+5.35), and SAG12 [20] (TRINITY_DN259644_c1_g1 logFC+5.54).

The basidiomycete *Piriformospora indica* is a symbiont fungus [245] with various plant host species, such as barley [327] and soybean [18]. When associated with barley, *P. indica* had endophytic development and increased biomass and grain yield [327]. Even thought *P. indica* is a non-pathogenic fungus, it required host cell death for proliferation and establishment of mutualism in barley [74]. Furthermore, *P. indica* induced systemic resistance to other fungal pathogens and to abiotic stresses [18,327]. The results of enriched differentially expressed genes in 'U3' biotype suggested activation of SAR and genes involved with cell death/hypersensitive response, which agree with the association outcome of *P. indica*-barley. Besides a potential activation of resistance mediated by salicylic acid, a candidate protein (TRINITY_DN263448_c1_g1 logFC+4.14) involved in local systemic resistance (induced systemic resistance, ISR) [249] was found to be uniquely enriched in 'U3' biotype. This *Arabidopsis*-homologous gene was shown to be a PR5, and it was activated on the vascular bundle of roots upon rhizobacteria colonization

[185]. This candidate gene could be implicated in colonization of vasculature by *O. herpotricha*.

The injury caused by *Ophiosphaerella* infection includes necrosis of belowground organs that can be observed during fall through early winter. Symptoms, however, are most prominent above ground in the spring when bermudagrass mortality results in dead patches. Bermudagrass mortality due to spring dead spot is likely due to weakened rhizomes and stolons by means of nutrient depletion and reduced function of rotted roots that enhance cold temperature sensitivity [321,325]. In the tolerant bermudagrass biotype 'U3', symptoms associated with spring dead spot are rarely seen in field conditions. The interest in this biotype was to explore candidate activated pathways that could be involved in biotic and abiotic stress tolerance.

Salicylic acid is a phytohormone that improves abiotic stress tolerance in crops [112,122,155]. Application of salicylic acid to corn plants showed increased salinity tolerance, and promoted accumulation of nutrients such as nitrogen and magnesium [122]. In addition, salicylic acid improveimprovedIn addition, salicylic acid was shown to improve cold temperature tolarence in barley [224] and banana [152]. The results of this study demonstrated enrichment of genes involved in salicylic acid regulation in 'U3' biotype. These findings suggest that tolerance of this biotype could be result of the activation of salicylic acid and enhancement of nutrient uptake by bermudagrass in the spring when bermudagrass resumes root, stolon and rhizome growth. when bermudagrass resumes root, stolon and rhizome growth.

Spring dead spot is a devastating disease of bermudagrass in the southern US. The causal agents, *O. herpotricha, O. korrae* and *O. narmari*, colonize roots, stolons and rhizomes of bermudagrass resulting in necrosis of belowground plant organs. In contrast, colonization of a tolerant common bermudagrass biotype, by the same isolate, showed cortex and vascular colonization and absence or delay of necrosis [37,85,95]. To elucidate the underlying genetics of bermudagrass response to *Ophiosphaerella* colonization, this study presented an expression profiling analysis during early infection of roots of two bermudagrass cultivars by *O. herpotricha* ISCC16F. The hypothesis of this study was that a susceptible cultivar up-regulates genes involved in innate immunity responses, particularly basal resistance, that are distinct of the resistant cultivar response. This hypothesis did not hold entirely true. Up-regulated candidate genes involved in defense were related to ‘response to biotic stress’. Candidate genes involved in innate immunity response, signaling, and hypersensitive response/cell death were observed in both cultivars. Candidate genes unique to the susceptible cultivar ‘Tifway’ indicated the development of programed cell death and systemic acquired resistance, which agrees with the activation of defense against necrotrophic fungal pathogens [40]. Candidate genes unique to the tolerant ‘U3’ biotype indicated a network of salicylic acid-signaling, and potential priming, that might implicate the recognition of this fungus differently to allow vasculature colonization [185]. In addition, salicylic acid might be implicated in priming for improved tolerance to abiotic stress [112,122,155] in ‘U3’. The results of this study provided insight into bermudagrass candidate genes involved in root disease response against *O. herpotricha*. These candidate genes will serve as important genetic resources for future studies of plant-pathogen interactions in this pathosystem.

4. CONCLUSION

The results of this study indicated that necrosis observed on roots of susceptible bermudagrass cultivar ‘Tifway’ infected with *O. herpotricha* could be the result of hypersensitive response through activation of jasmonic acid-mediated systemic acquired resistance. The tolerant ‘U3’ biotype also showed activation of basal defense responses, such as pathogenesis-related proteins and salicylic acid-mediated signaling. Salicylic acid-mediated signaling could be involved in enhanced tolerance of nutrient starvation and cold temperatures. The results presented will serve as valuable genomic resources for future studies in plant-pathogen interaction in this pathosystem. Future experiments are required to functionally characterize these bermudagrass candidate genes, and to confirm the establishment of a symbiotic relationship in a tolerant cultivar.

FIGURES:

A

B

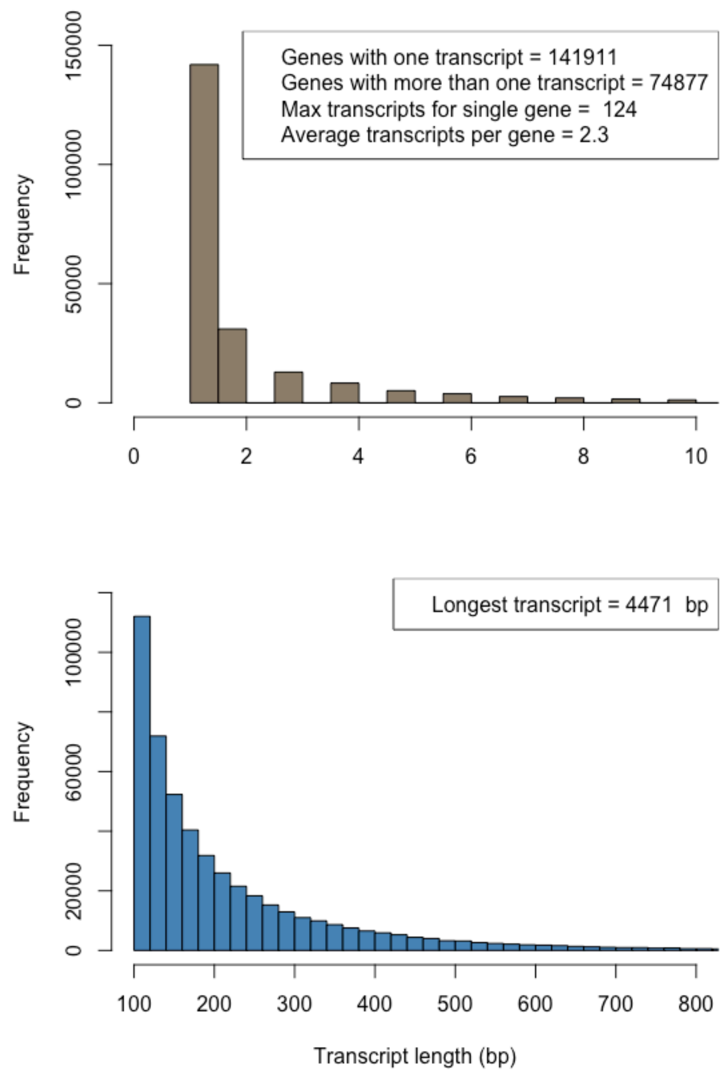

Figure V-1. (A) Distribution of number of transcripts per gene and (B) distribution of transcript length in base pairs (bp) of 'Tifway' transcriptome assembly.

A

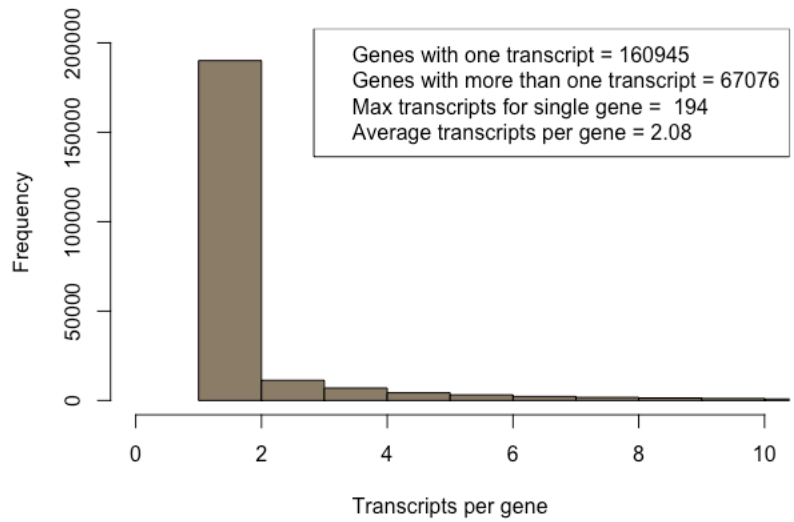

B

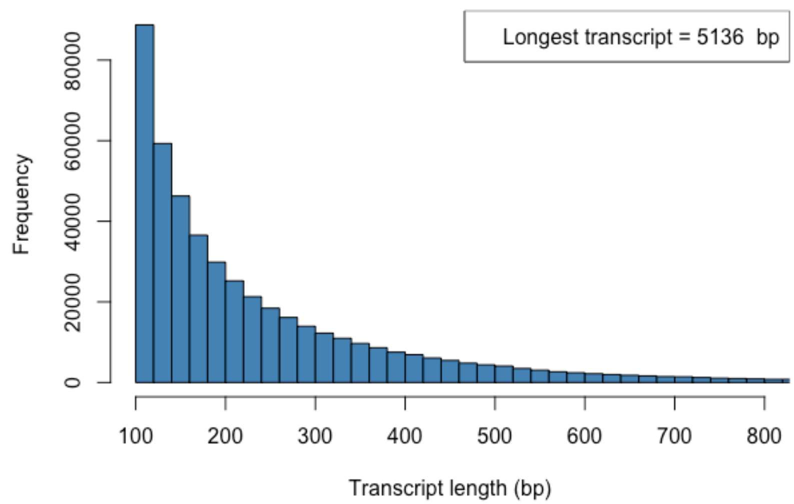

Figure V-2. (A) Distribution of number of transcripts per gene and (B) distribution of transcript length in base pairs (bp) of 'U3' biotype transcriptome assembly.

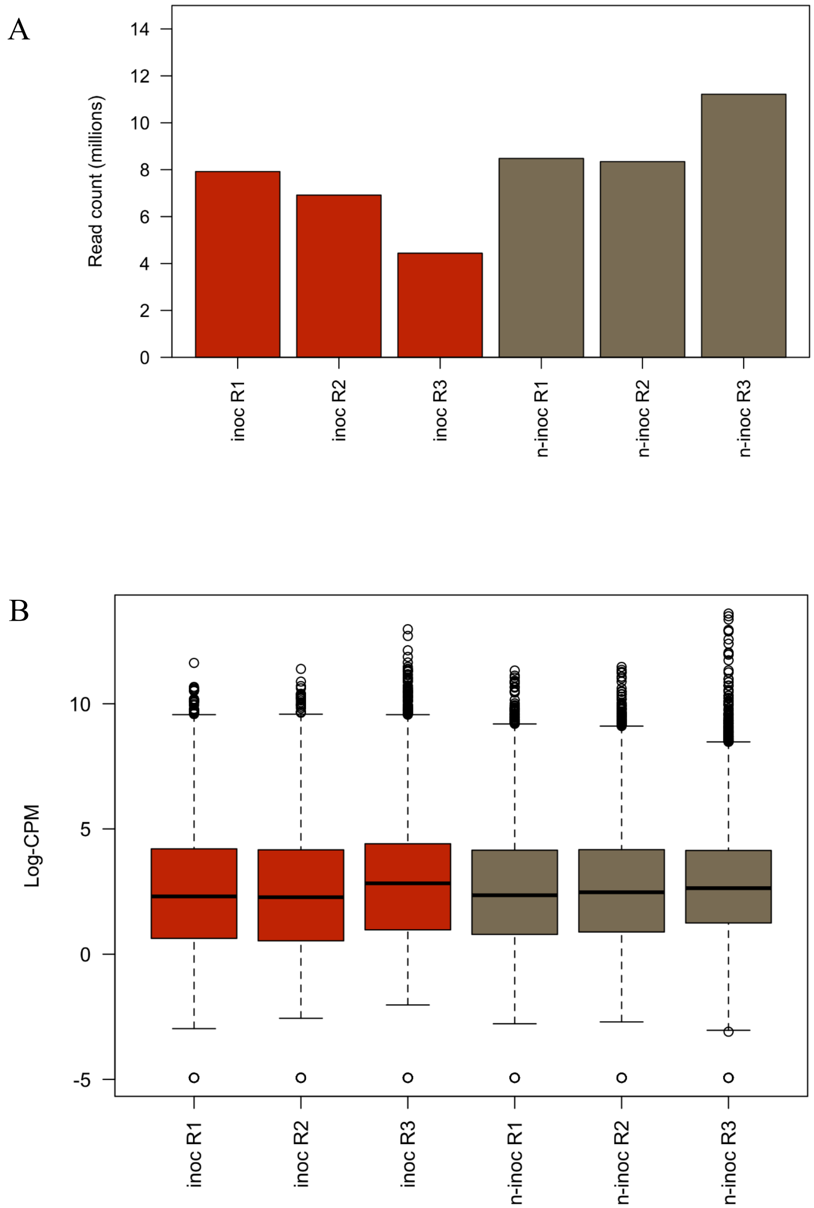

Figure V-3. Diagnostic plots of data filtering and normalization of 'Tifway'. (A) Total transcript read counts, in millions. (B) Distribution of transformed expression values (log-counts per million, CPM).

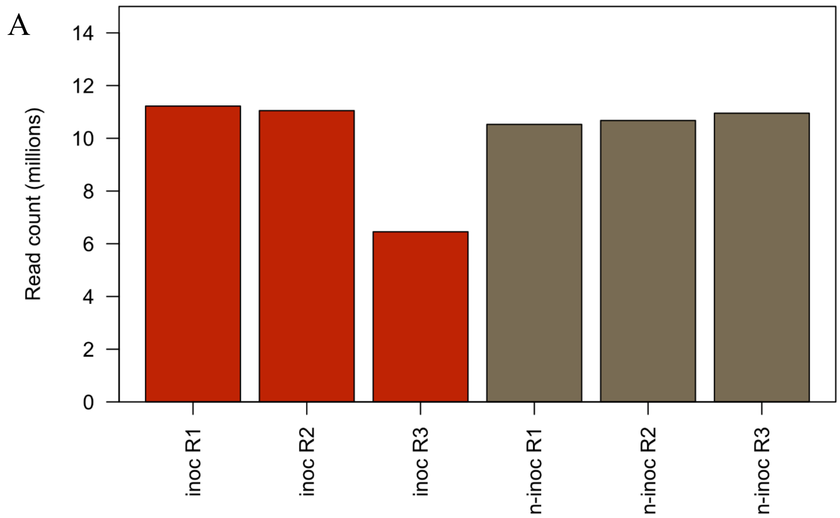

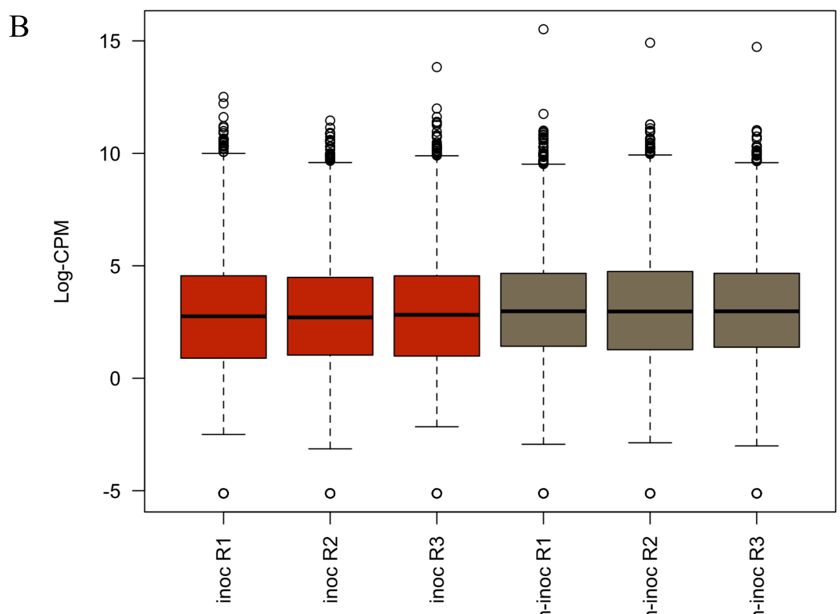

Figure V-4. Diagnostic plots of data filtering and normalization of 'U3' biotype. (A) Total transcript read counts, in millions. (B) Distribution of transformed expression values (log-counts per million, CPM).

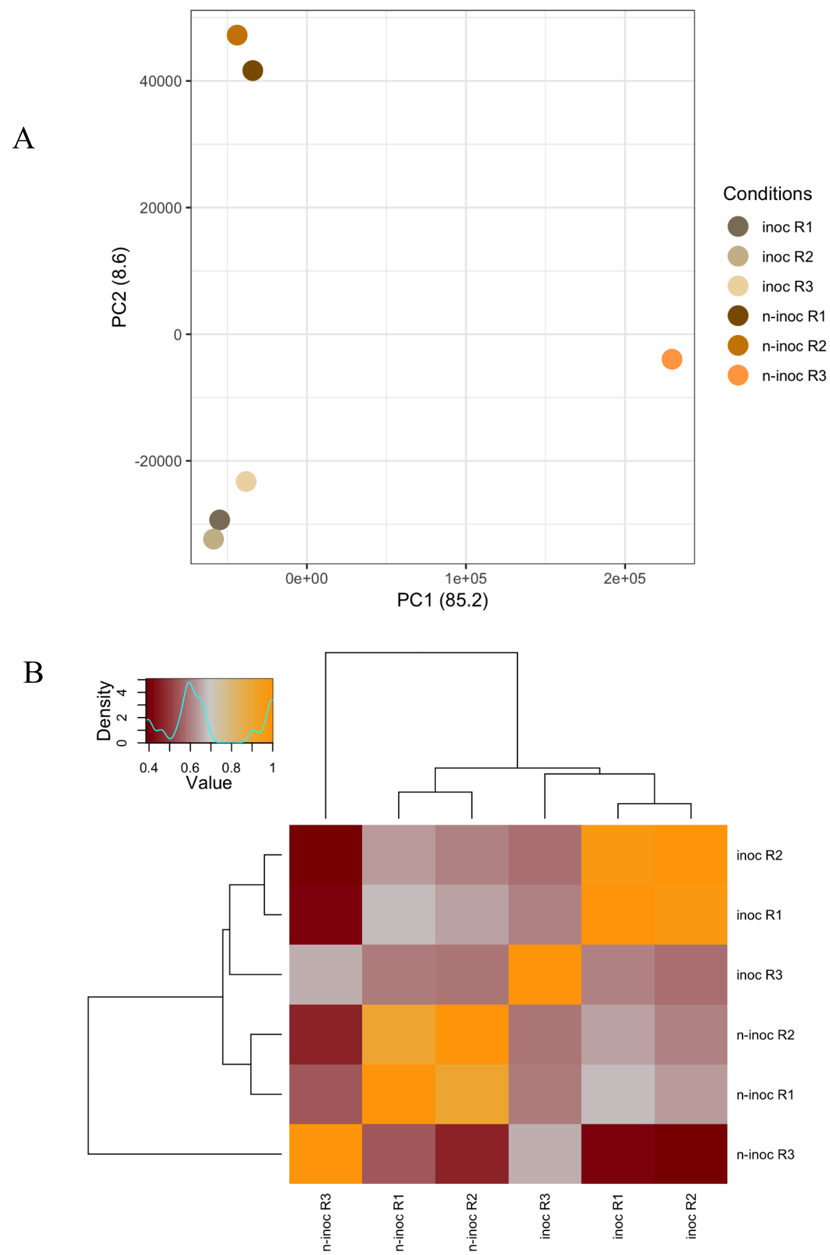

Figure V-5. Diagnostic plots of data set variance of 'Tifway'. (A) Principal component analysis of filtered data. (B) Distance correlation of the normalized data of all samples and replicates.

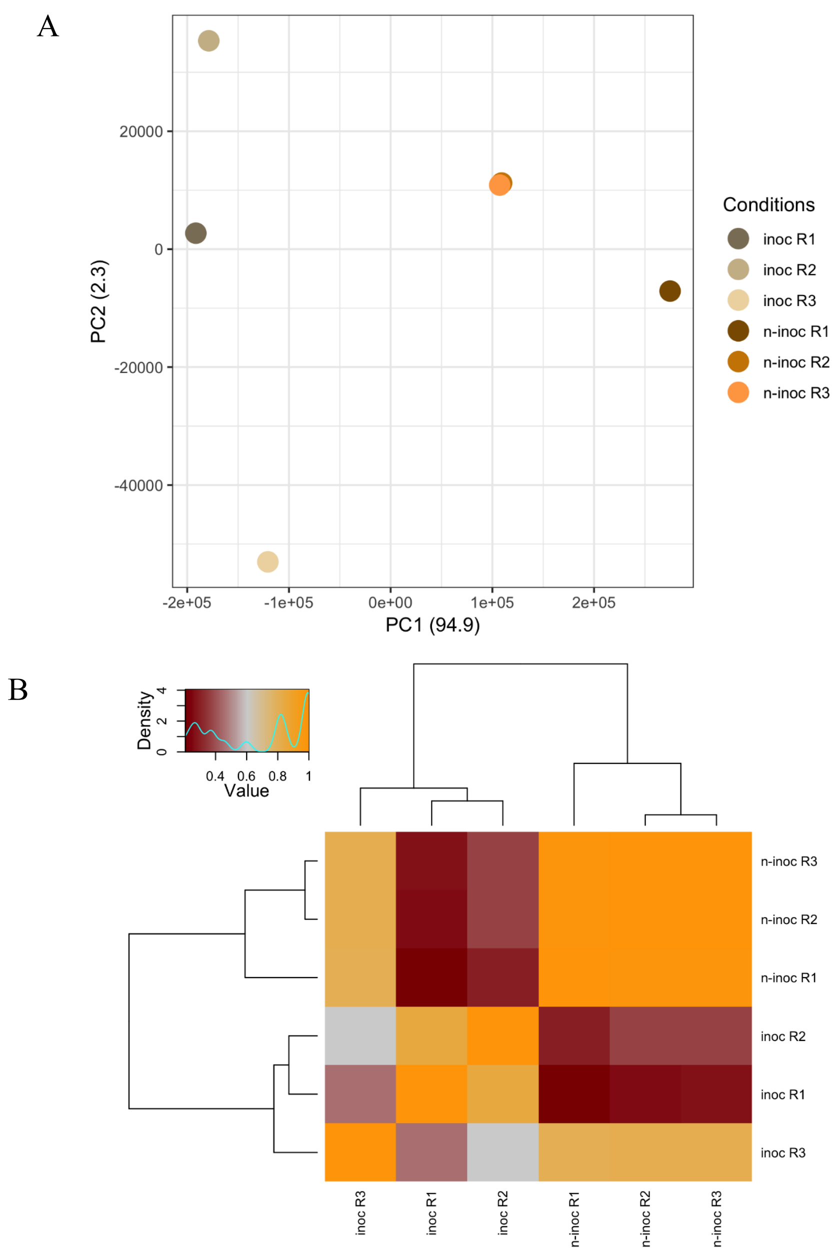

Figure V-6. Diagnostic plots of data set variance of 'U3' biotype. (A) Principal component analysis of filtered data. (B) Distance correlation of the normalized data of all samples and replicates.

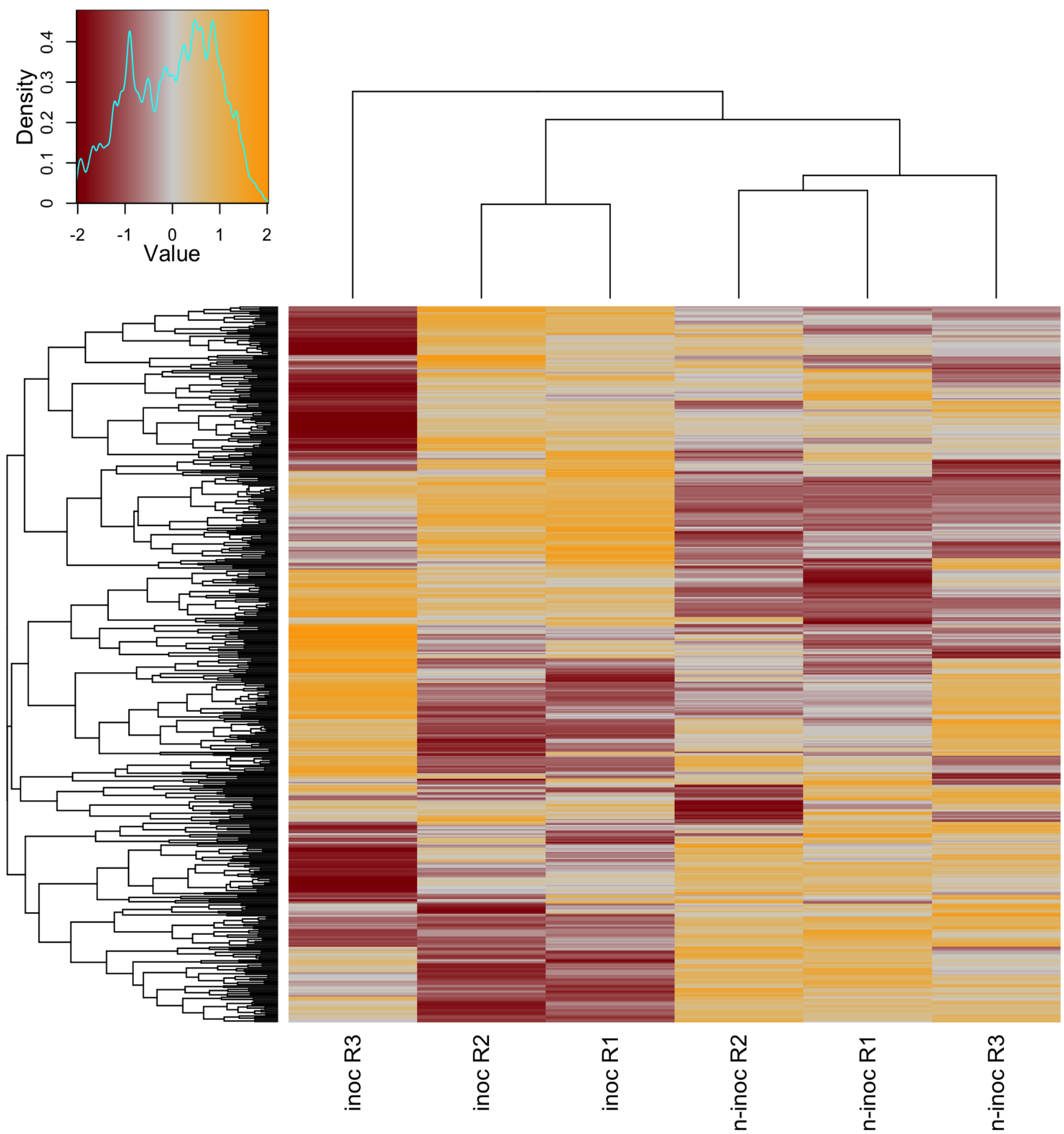

Figure V-7. Heatmap of the most differentially expressed genes of 'Tifway'

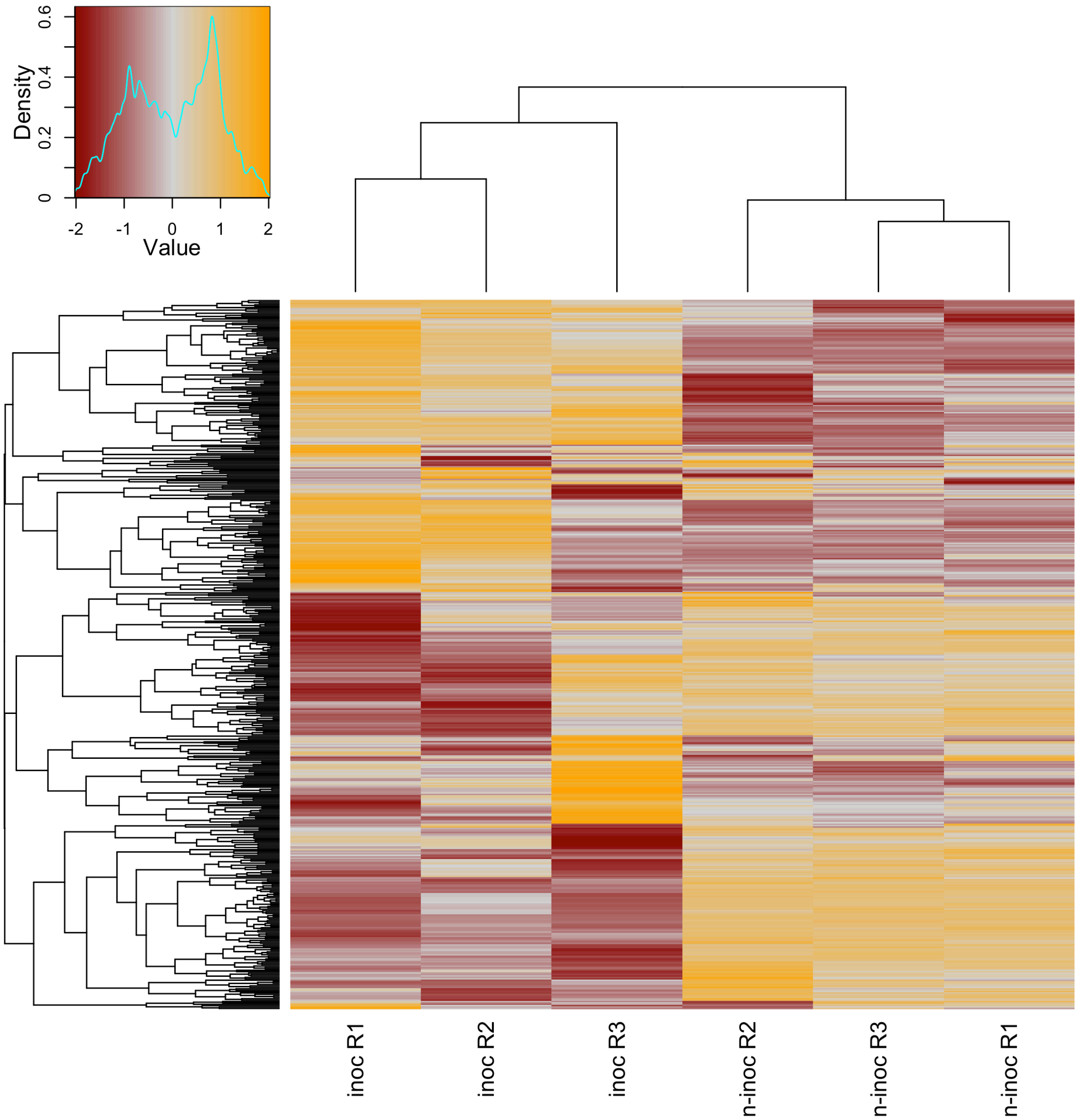

Figure V-8. Heatmap of the most differentially expressed genes of 'U3' biotype.

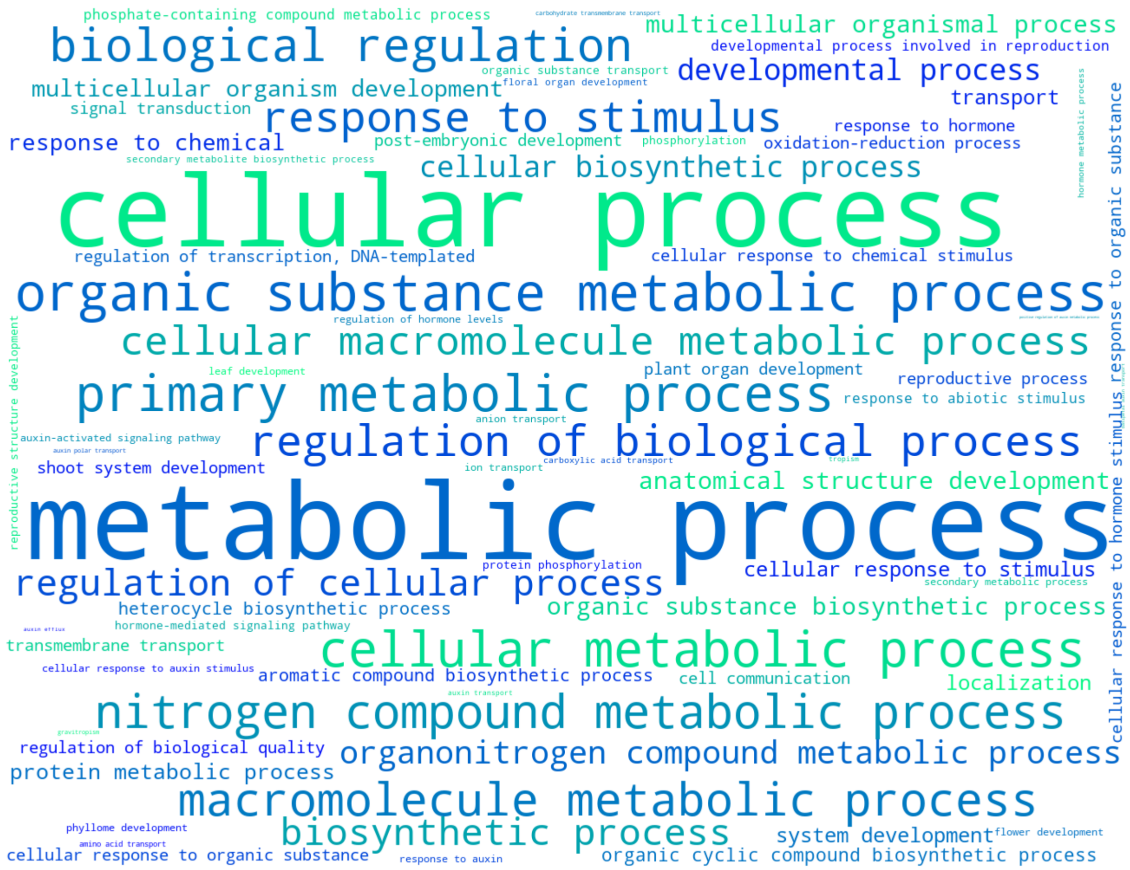

Figure V-9. Word cloud representing all enriched Gene Ontology Biological Process terms down-regulated in 'Tifway'. Font size represent the number of genes observed in each term.

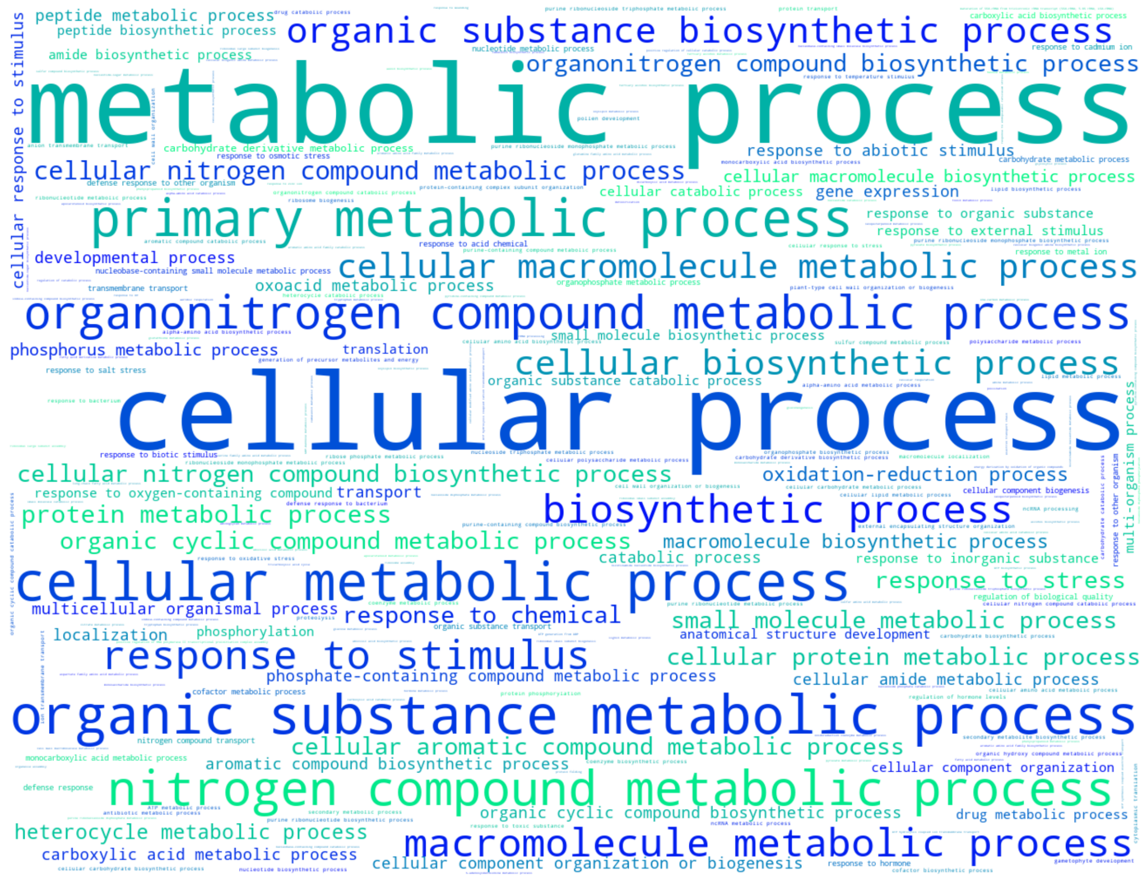

Figure V-10. Word cloud representing all enriched Gene Ontology Biological Process terms up-regulated in ‘Tifway’. Font size represent the number of genes observed in each term.

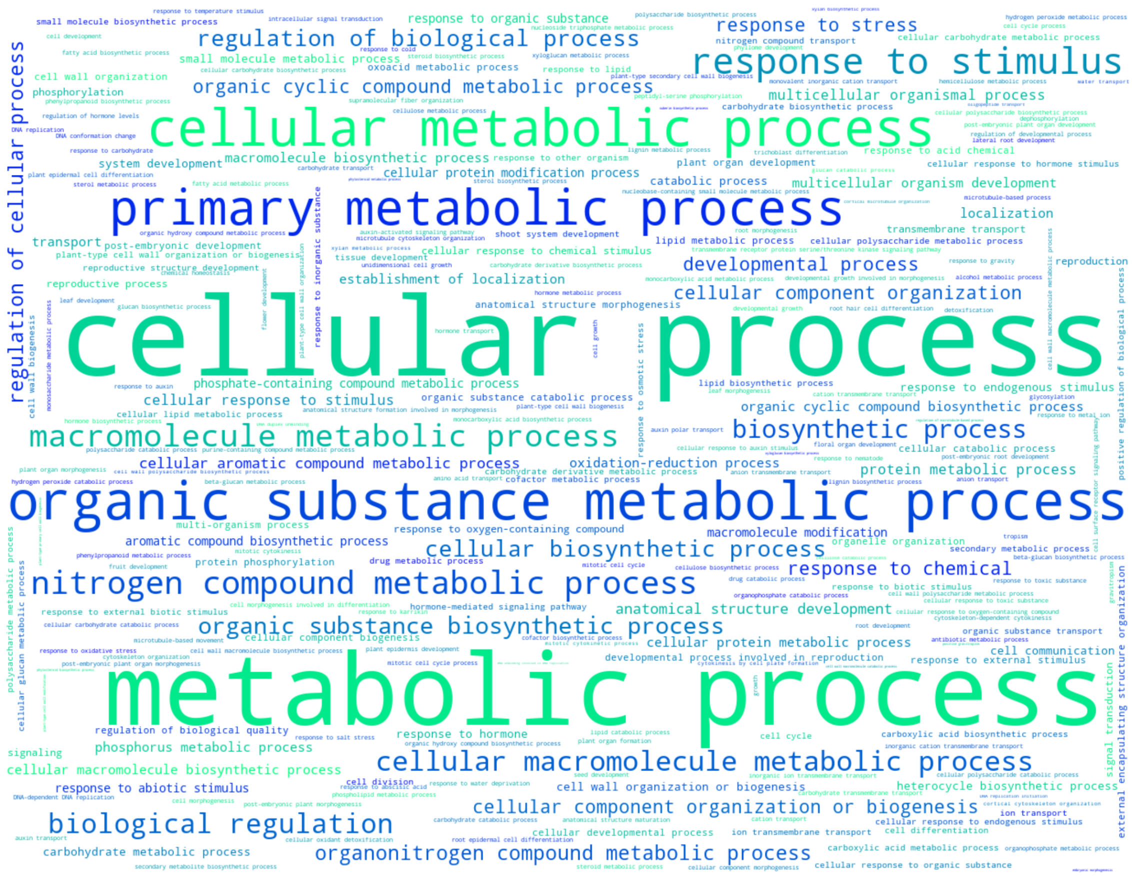

Figure V-11. Word cloud representing all enriched Gene Ontology Biological Process terms down-regulated in ‘U3’ biotype. Font size represent the number of genes observed in each term.

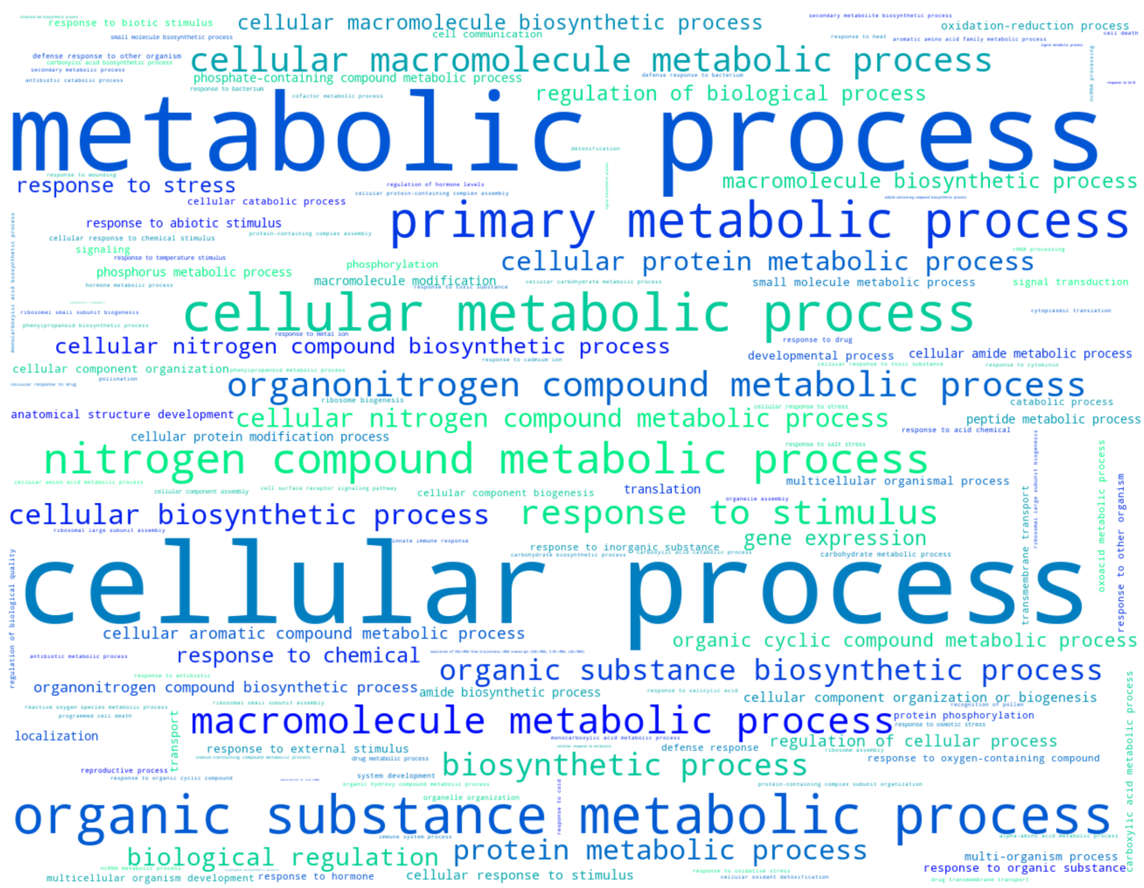

Figure V-12. Word cloud representing all enriched Gene Ontology Biological Process terms up-regulated in 'U3' biotype. Font size represent the number of genes observed in each term.

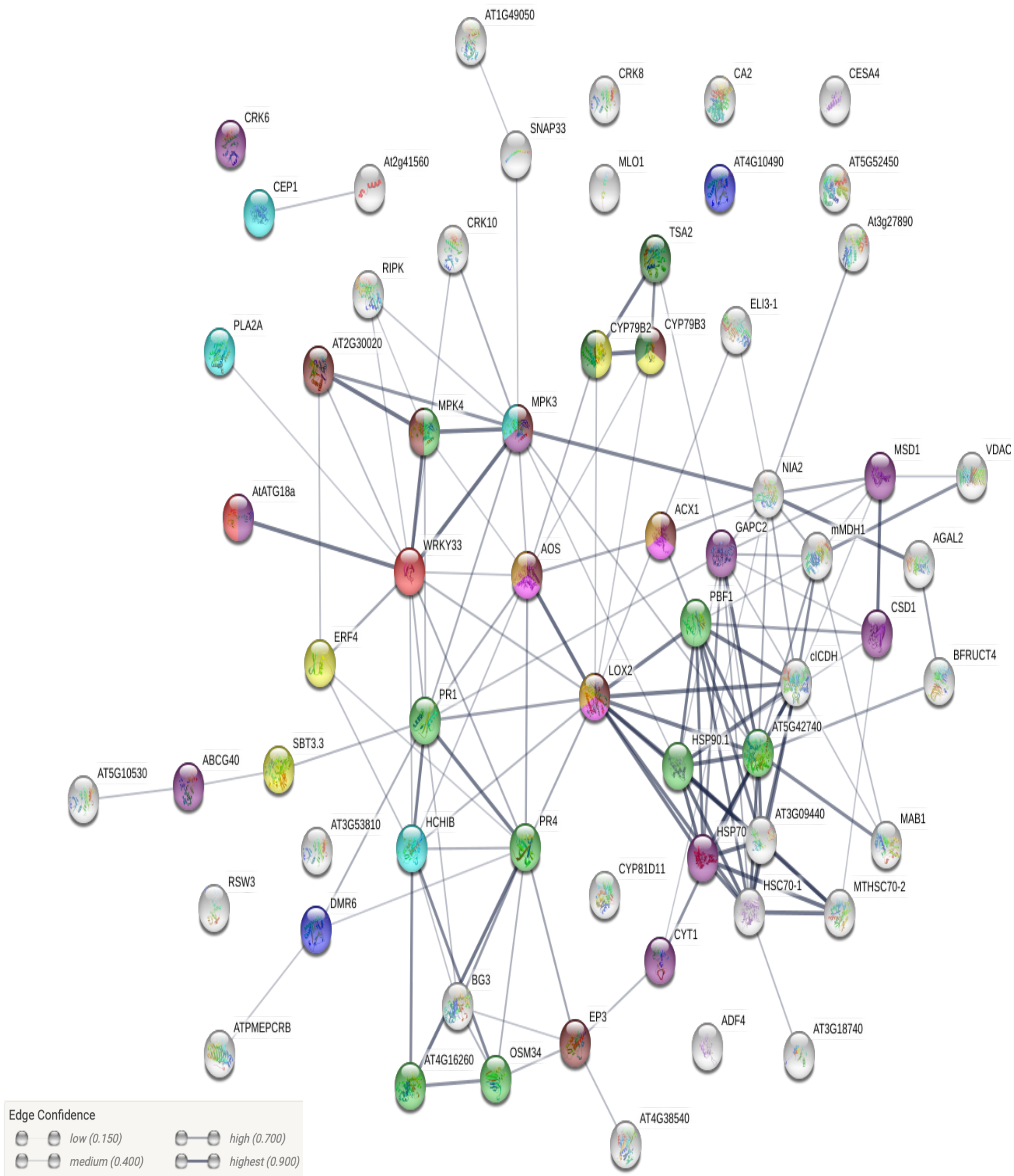

Figure V-13. Protein network analysis on candidate plant immunity genes of 'Tifway'. Nodes (circles) represent proteins, edges (gray lines) represent protein-protein associations, and do not necessarily mean they are physically binding to each other. Empty nodes represent unknown protein structure, and filled nodes represent some 3D structure is known. Node colors represent enriched Gene Ontology Biological Process terms: light green - GO:0009814 (defense response, incompatible reaction), brown - GO:0009611 (response to wounding), dark purple – GO:0006979 (response to oxidative stress), yellow - GO:0009682 (induced systemic resistance), dark green - GO:0052544 (defense response by callose deposition in cell wall), pink - GO:0009695 (jasmonic acid biosynthetic process), tan - GO:0009694 (jasmonic acid metabolic process), cian - GO:0009626 (plant-type hypersensitive response), dark blue - GO:0046244 (salicylic acid catabolic process), red - GO:0010508 (positive regulation of authophagy).

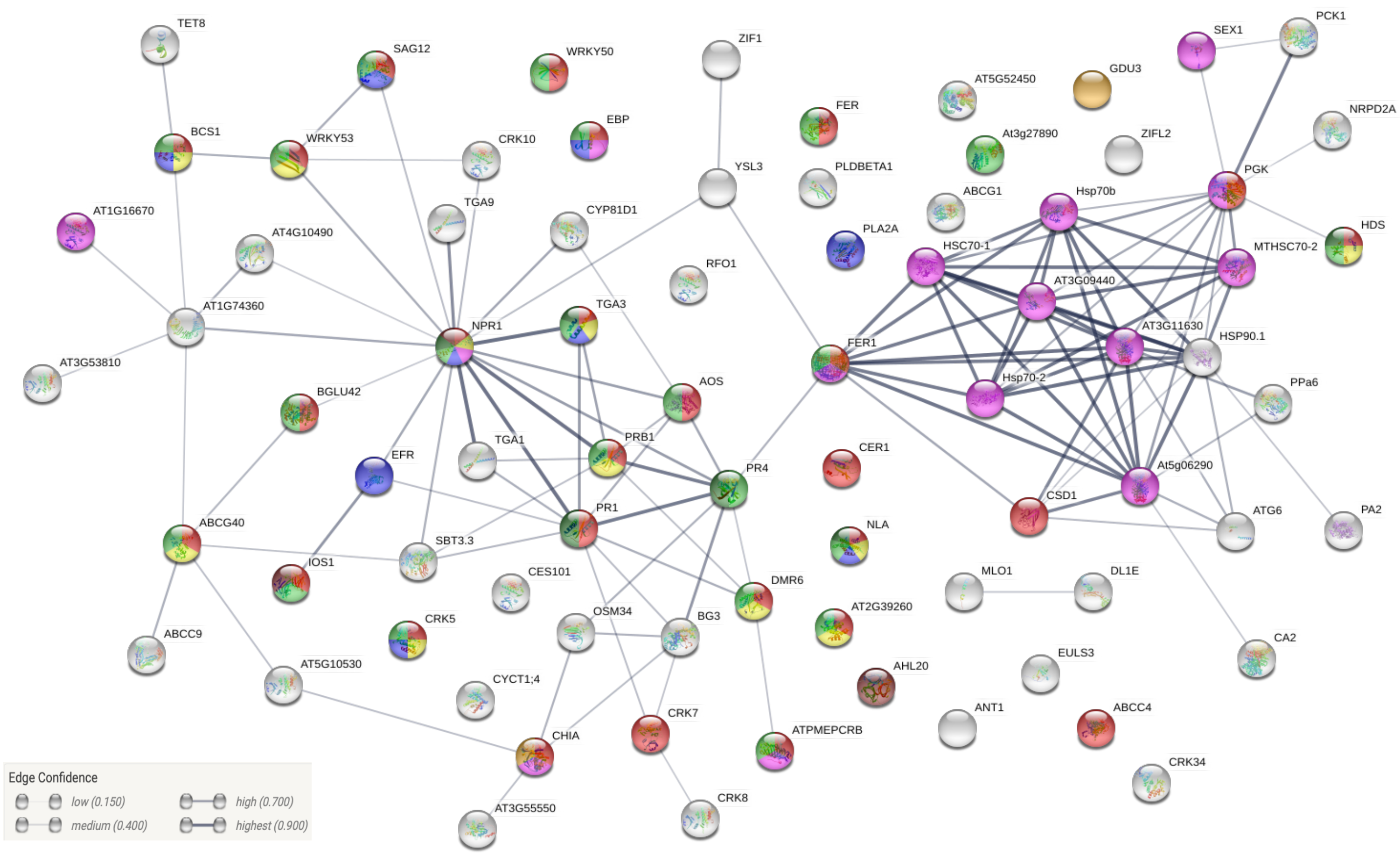

Figure V-14. Protein network analysis on candidate plant immunity genes of 'Tifway'. Nodes (circles) represent proteins, edges (gray lines) represent protein-protein associations, and do not necessarily mean they are physically binding to each other. Empty nodes represent unknown protein structure, and filled nodes represent some 3D structure is known. Node colors represent enriched Gene Ontology Biological Process terms: red - GO:1901700 (response to oxygen-containing compound), yellow - GO:0009751 (response to salicylic acid), pink - GO:0009666 (response to temperature stimulus), dark blue - GO:0008219 (cell death), light green - GO:0009725 (response to hormone), dark green - GO:0009627 (systemic acquired resistance), tan - GO:0044003 (modification by symbiont of host morphology or physiology, FDR = 0.0171, not enriched).

TABLES:

Table V-1. Comparisons of the number of differentially expressed genes in 'Tifway' and 'U3' biotype conditions. Genes were considered differentially expressed at false discovery rate of 5% (P value < 0.05) and log-fold change (logFC) of two. In these comparisons, the condition listed first was the baseline for the comparision (inoculated 'Tifway', and inoculated 'U3' biotype, respectively). Genes with logFC greater than or equal to +2 were considered to be up-regulated in the baseline condition (and vice-versa with transcripts with logFC less than or equal to -2).

Comparisons	Total	Up-regulated (logFC > +2)	Down-regulated (logFC < -2)
'Tifway' Inoculated vs non-inoculated	4,224	2,849	1,080
'U3' biotype Inoculated vs non-inoculated	14,046	3,118	5,897

Table V-2. Enrichment analysis for Pfam domains in 'Tifway'.

Pfam term ID	Term Description	Gene Count	FDR	*Arabidopsis* homologous-genes
down-regulated				
PF00067	Cytochrome P450	12	7.91e-05	BAS1 CYP71A22 CYP71B34 CYP735A2 CYP76C1 CYP76C4 CYP78A5 CYP78A6 CYP78A9 CYP86A1 CYP89A2 KAO2
PF08263	Leucine rich repeat N-terminal domain	11	7.91e-05	AT1G34110 AT1G60630 AT2G01210 AT2G36570 AT3G24480 AT3G28040 AT4G26540 AT5G48940 At1g28440 At3g49670 MPA24.5
PF00560	Leucine Rich Repeat	10	0.00023	AT1G13230 AT1G34110 AT2G01210 AT3G24240 AT3G28040 AT5G48940 At1g28440 At3g49670 MEE62 MPA24.5
PF00069	Protein kinase domain	22	0.00025	AT1G34110 AT1G60630 AT2G01210 AT2G19130 AT2G23450 AT2G36350 AT2G36570 AT3G24240 AT3G28040 AT4G26540 AT5G48940 At1g28440 At3g49670 CIPK19 CPK29 D6PKL1 IBS1 MEE62 MPA24.5 OST1 PID UCNL
PF07714	Protein tyrosine kinase	22	0.00025	AT1G34110 AT1G60630 AT2G01210 AT2G19130 AT2G23450 AT2G36350 AT2G36570 AT3G24240 AT3G28040 AT4G26540 AT5G48940 At1g28440 At3g49670 CIPK19 CPK29 D6PKL1 IBS1 MEE62 MPA24.5 OST1 PID UCNL
PF03083	Sugar efflux transporter for intercellular exchange	4	0.00047	SAG29 SWEET1 SWEET3 SWEET9

PF00664	ABC transporter transmembrane region	5	0.00075	ABCB1 ABCB11 ABCB15 ABCB19 ABCB21
PF00005	ABC transporter	7	0.00086	ABCB1 ABCB11 ABCB15 ABCB19 ABCB21 ABCG10 ABCG23
PF13855	Leucine rich repeat	10	0.00094	AT1G13230 AT1G34110 AT3G24240 AT3G24480 AT3G28040 AT4G26540 AT5G48940 At1g28440 At3g49670 MEE62
up-regulated				
PF07883	Cupin domain	10	4.28e-05	AT1G18980 AT3G05950 AT5G38940 AT5G38960 AT5G39110 AT5G39130 AT5G39150 AT5G39160 GLP4 GLP9
PF00005	ABC transporter	15	7.15e-05	ABCA1 ABCA7 ABCB15 ABCB16 ABCB22 ABCC14 ABCC8 ABCE2 ABCG28 ABCG34 ABCG37 ABCG39 ABCG40 ABCG42 NAP12
PF00190	Cupin	10	7.15e-05	AT1G18980 AT3G05950 AT5G38940 AT5G38960 AT5G39110 AT5G39130 AT5G39150 AT5G39160 GLP4 GLP9
PF00227	Proteasome subunit	8	7.15e-05	At5g35590 PAE1 PAE2 PAG1 PBB2 PBE1 PBF1 PRC3

Table V-3. Enrichment analysis for Pfam domains in 'U3' biotype.

Pfam term ID	Term Description	Gene Count	FDR	*Arabidopsis* homologous-genes
down-regulated				
PF00225	Kinesin motor domain	30	5.01e-15	ARK2 ARK3 AT1G18550 AT1G63640 AT1G72250 AT2G21300 AT2G22610 AT2G28620 AT2G36200 AT2G37420 AT2G47500 AT3G20150 AT3G44050 AT3G45850 AT3G49650 AT3G51150 AT4G14330 AT4G39050 AT5G27550 AT5G60930 ATK5 HIK KIN12B KIN13A KP1 MRH2 POK1 POK2 ZCF125 ZWI
PF16796	Microtubule binding	30	5.01e-15	ARK2 ARK3 AT1G18550 AT1G63640 AT1G72250 AT2G21300 AT2G22610 AT2G28620 AT2G36200 AT2G37420 AT2G47500 AT3G20150 AT3G44050 AT3G45850 AT3G49650 AT3G51150 AT4G14330 AT4G39050 AT5G27550 AT5G60930 ATK5 HIK KIN12B KIN13A KP1 MRH2 POK1 POK2 ZCF125 ZWI
PF00069	Protein kinase domain	117	2.53e-13	AGC1.5 ALE2 AT1G01540 AT1G08590 AT1G09600 AT1G12460 AT1G24030 AT1G33260 AT1G34110 AT1G34300 AT1G51820 AT1G54610 AT1G56130 AT1G60630 AT1G61590 AT1G68400 AT1G72180 AT1G76370 AT1G78530 AT1G80640 AT2G01210 AT2G16250 AT2G26730 AT2G36570 AT2G41970 AT2G42960 AT2G43850 AT3G03770 AT3G07070 AT3G08680 AT3G24240 AT3G28040 AT3G51990 AT3G53380 AT3G56370 AT3G59350 AT4G03230 AT4G10390 AT4G26540 AT4G28650 AT4G31250 AT4G34500 AT4G36180 AT4G37250 AT5G01020 AT5G01890 AT5G10530 AT5G18610 AT5G35370 AT5G48940 AT5G49770 AT5G55830 AT5G57670 AT5G58300 AT5G61350 AT5G65600 AUR3 At3g49670 B120 BAM3 BRL2 BSK2 BSK5 CCR4 CDKB1;2 CDKB2;1 CIPK10 CIPK12 CIPK19 CIPK20 CIPK22 CPK13 CPK5 CPK6 CRK1 CaMK4 D6PKL2 FEI1 FU GHR1 GSO1 HERK2 IBS1 IMK2 IRE Kin3 LYK3 MEE62 MPA24.5 MRH1 NCRK NEK6 NP3 PERK8 PERK9 PID PID2 PK1B PR5K PRK5 PSY1R PTI1-4 RBK2 RHS3 RHS6 RKL1 RUK SIP3 SNRK2-8 SOS2 SRF6 SRF7 SRF8 WAG1 WEE1 ckl4 ckl8
PF07714	Protein tyrosine kinase	117	2.53e-13	AGC1.5 ALE2 AT1G01540 AT1G08590 AT1G09600 AT1G12460 AT1G24030 AT1G33260 AT1G34110 AT1G34300 AT1G51820 AT1G54610 AT1G56130 AT1G60630 AT1G61590 AT1G68400 AT1G72180 AT1G76370 AT1G78530 AT1G80640 AT2G01210 AT2G16250 AT2G26730 AT2G36570 AT2G41970 AT2G42960 AT2G43850 AT3G03770 AT3G07070 AT3G08680 AT3G24240 AT3G28040 AT3G51990 AT3G53380 AT3G56370 AT3G59350 AT4G03230 AT4G10390 AT4G26540 AT4G28650 AT4G31250 AT4G34500 AT4G36180 AT4G37250 AT5G01020 AT5G01890 AT5G10530 AT5G18610 AT5G35370 AT5G48940 AT5G49770 AT5G55830 AT5G57670 AT5G58300 AT5G61350 AT5G65600 AUR3 At3g49670 B120 BAM3 BRL2 BSK2 BSK5 CCR4 CDKB1;2 CDKB2;1 CIPK10 CIPK12 CIPK19 CIPK20 CIPK22 CPK13 CPK5 CPK6 CRK1 CaMK4 D6PKL2 FEI1 FU GHR1 GSO1 HERK2 IBS1 IMK2 IRE Kin3 LYK3 MEE62 MPA24.5 MRH1 NCRK NEK6 NP3 PERK8 PERK9 PID PID2 PK1B PR5K PRK5 PSY1R PTI1-4 RBK2 RHS3 RHS6 RKL1 RUK SIP3 SNRK2-8 SOS2 SRF6 SRF7 SRF8 WAG1 WEE1 ckl4 ckl8
PF00141	Peroxidase	29	3.52e-12	AT1G44970 AT1G68850 AT1G71695 AT2G18980 AT2G24800 AT2G39040 AT2G41480 AT3G01190 AT3G21770 AT3G49960 AT4G11290 AT4G25980 AT4G33420 AT4G36430 AT4G37520 AT5G06730 AT5G14130 AT5G15180 AT5G19890 AT5G39580 AT5G51890 AT5G58390 AT5G58400 AT5G66390 PA2 PER64 PRX52 RCI3 RHS19
PF08263	Leucine rich repeat N-terminal domain	41	4.53e-10	AT1G08590 AT1G12460 AT1G34110 AT1G60630 AT1G68400 AT1G72180 AT2G01210 AT2G26730 AT2G36570 AT3G08680 AT3G22800 AT3G24480 AT3G28040 AT3G56370 AT4G26540 AT4G28650 AT4G31250 AT4G36180 AT4G37250 AT5G01890 AT5G48940 AT5G49770 AT5G58300 At3g49670 BAM3 BRL2 DRT100 FEI1 GHR1 GSO1 IMK2 LRX1 LRX2 MPA24.5 MRH1 PRK5 PSY1R RKL1 SRF6 SRF7 SRF8
PF00722	Glycosyl hydrolases family 16	15	3.12e-07	EXGT-A3 TCH4 XTH1 XTH12 XTH13 XTH15 XTH16 XTH24 XTH25 XTH26 XTH31 XTH32 XTH5 XTH8 XTH9

PF06955	Xyloglucan endo-transglycosylase (XET) C-terminus	15	3.12e-07	EXGT-A3 TCH4 XTH1 XTH12 XTH13 XTH15 XTH16 XTH24 XTH25 XTH26 XTH31 XTH32 XTH5 XTH8 XTH9
PF03552	Cellulose synthase	12	8.30e-06	CESA1 CESA2 CESA4 CESA6 CESA9 CEV1 CSLB04 CSLD3 CSLD5 CSLD6 IRX1 IRX3
PF00854	POT family	15	3.66e-05	AT1G22540 AT1G22570 AT1G33440 AT1G59740 AT1G68570 AT1G72140 AT2G26690 AT5G46040 GTR2 NRT1.1 NRT1.9 PTR2 PTR3 PTR4 PTR6
PF13632	Glycosyl transferase family group 2	12	4.07e-05	CESA1 CESA2 CESA4 CESA6 CESA9 CEV1 CSLA02 CSLC5 CSLD5 CSLD6 IRX1 IRX3
PF14569	Zinc-binding RING-finger	8	4.36e-05	CESA1 CESA2 CESA4 CESA6 CESA9 CEV1 IRX1 IRX3
PF01061	ABC-2 type transporter	13	7.06e-05	ABCG1 ABCG10 ABCG11 ABCG15 ABCG16 ABCG2 ABCG20 ABCG23 ABCG32 ABCG40 ABCG5 ABCG6 ABCG8
PF01357	Pollen allergen	12	7.06e-05	EXLA1 EXPA1 EXPA11 EXPA13 EXPA15 EXPA17 EXPA20 EXPA7 EXPB2 EXPB3 EXPB4 EXPB6
PF00493	MCM2/3/5 family	7	0.00011	MCM2 MCM3 MCM4 MCM5 MCM6 MCM9 PRL
PF03330	Lytic transglycolase	12	0.00011	EXLA1 EXPA1 EXPA11 EXPA13 EXPA15 EXPA17 EXPA20 EXPA7 EXPB2 EXPB3 EXPB4 EXPB6
PF17207	MCM OB domain	7	0.00011	MCM2 MCM3 MCM4 MCM5 MCM6 MCM9 PRL
PF02469	Fasciclin domain	9	0.00015	FLA1 FLA10 FLA11 FLA16 FLA17 FLA2 FLA7 FLA8 SOS5
PF13855	Leucine rich repeat	34	0.00019	AT1G08590 AT1G34110 AT1G51820 AT1G56130 AT1G72180 AT2G16250 AT2G26730 AT3G03770 AT3G22800 AT3G24240 AT3G24480 AT3G28040 AT3G56370 AT4G26540 AT4G28650 AT4G36180 AT5G01890 AT5G48940 AT5G58300 At3g49670 BRL2 DRT100 GHR1 GSO1 IMK2 LRX2 MEE62 PRK5 RKL1 RLP4 SRF6 SRF7 SRF8 TMM
PF00005	ABC transporter	20	0.0003	ABCB1 ABCB15 ABCB19 ABCB2 ABCB7 ABCC10 ABCG1 ABCG10 ABCG11 ABCG15 ABCG16 ABCG2 ABCG20 ABCG23 ABCG32 ABCG40 ABCG5 ABCG6 ABCG8 ABCI17
PF14551	MCM N-terminal domain	6	0.0003	MCM2 MCM3 MCM4 MCM5 MCM6 PRL
PF01078	Magnesium chelatase, subunit ChlI	7	0.00036	MCM2 MCM3 MCM4 MCM5 MCM6 MCM9 PRL
PF14416	PMR5 N terminal Domain	12	0.00045	ESK1 PMR5 TBL19 TBL21 TBL27 TBL28 TBL3 TBL33 TBL34 TBL37 TBL38 TBL6
PF08541	3-Oxoacyl-[acyl-carrier-protein (ACP)] synthase III C terminal	9	0.00049	KCS1 KCS11 KCS12 KCS2 KCS20 KCS4 KCS6 T3P18.20 TT4
PF13839	GDSL/SGNH-like Acyl-Esterase family found in Pmr5 and Cas1p	12	0.0005	ESK1 PMR5 TBL19 TBL21 TBL27 TBL28 TBL3 TBL33 TBL34 TBL37 TBL38 TBL6
PF00067	Cytochrome P450	30	0.00068	AOS BAS1 CPD CYP51G1 CYP707A1 CYP708A2 CYP709B2 CYP710A1 CYP710A2 CYP711A1 CYP71B14 CYP71B2 CYP71B23 CYP72A15 CYP735A1 CYP735A2 CYP76C2 CYP76C4 CYP78A5 CYP78A7 CYP79B2 CYP81D1 CYP81D11 CYP86A4 CYP86A8 CYP86B1 CYP89A2 CYP94C1 DWF4 TT7
PF05637	galactosyl transferase GMA12/MNN10 family	6	0.00068	AT2G22900 XT1 XT2 XXT3 XXT4 XXT5

PF00759	Glycosyl hydrolase family 9	9	0.00071	CEL3 GH9A1 GH9B1 GH9B13 GH9B5 GH9B6 GH9B8 GH9C2 KOR2
PF00560	Leucine Rich Repeat	26	0.00097	AT1G34110 AT1G72180 AT2G01210 AT2G16250 AT3G03770 AT3G24240 AT3G28040 AT3G56370 AT4G28650 AT4G36180 AT5G01890 AT5G48940 AT5G58300 At3g49670 BAM3 BRL2 DRT100 GHR1 GSO1 IMK2 MEE62 MPA24.5 MRH1 PSY1R RLP4 TMM
up-regulated				
PF00069	Protein kinase domain	73	1.48e-12	AT1G06840 AT1G07650 AT1G11330 AT1G11340 AT1G16670 AT1G26970 AT1G53430 AT1G56130 AT1G56140 AT1G61360 AT1G61420 AT1G66910 AT1G69730 AT1G74360 AT2G19130 AT2G24130 AT2G45910 AT3G09830 AT3G15890 AT3G21340 AT3G25490 AT3G47570 AT3G53810 AT3G55550 AT3G59350 AT4G00960 AT4G27290 AT4G27300 AT4G31100 AT5G01020 AT5G02070 AT5G10530 AT5G38250 AT5G38260 AT5G39020 AT5G49770 B120 BRL1 BRL3 CDC2 CES101 CIPK17 CIPK19 CIPK7 CKI6 CRCK1 CRK10 CRK20 CRK34 CRK5 CRK7 CRK8 CST EFR FER IOS1 LRK1 MPK1 MPK9 PR5K PTI1-4 RFO1 RK1 RK2 RK3 SD2-5 SERK1 SNC4 SOBIR1 WAK2 WAK3 WAK5 WNK9
PF07714	Protein tyrosine kinase	73	1.48e-12	AT1G06840 AT1G07650 AT1G11330 AT1G11340 AT1G16670 AT1G26970 AT1G53430 AT1G56130 AT1G56140 AT1G61360 AT1G61420 AT1G66910 AT1G69730 AT1G74360 AT2G19130 AT2G24130 AT2G45910 AT3G09830 AT3G15890 AT3G21340 AT3G25490 AT3G47570 AT3G53810 AT3G55550 AT3G59350 AT4G00960 AT4G27290 AT4G27300 AT4G31100 AT5G01020 AT5G02070 AT5G10530 AT5G38250 AT5G38260 AT5G39020 AT5G49770 B120 BRL1 BRL3 CDC2 CES101 CIPK17 CIPK19 CIPK7 CKI6 CRCK1 CRK10 CRK20 CRK34 CRK5 CRK7 CRK8 CST EFR FER IOS1 LRK1 MPK1 MPK9 PR5K PTI1-4 RFO1 RK1 RK2 RK3 SD2-5 SERK1 SNC4 SOBIR1 WAK2 WAK3 WAK5 WNK9
PF00005	ABC transporter	21	4.30e-09	ABCB15 ABCB22 ABCB4 ABCB5 ABCB7 ABCB9 ABCC15 ABCC3 ABCC4 ABCC8 ABCC9 ABCE2 ABCF1 ABCG1 ABCG11 ABCG16 ABCG20 ABCG28 ABCG40 NAP12 PGP10
PF08276	PAN-like domain	12	8.78e-08	AT1G11330 AT1G11340 AT1G61360 AT1G61420 AT2G19130 AT4G27290 AT4G27300 B120 CES101 RK1 RK2 RK3
PF01453	D-mannose binding lectin	13	1.64e-07	AT1G11330 AT1G11340 AT1G61360 AT1G61420 AT2G19130 AT4G27290 AT4G27300 B120 CES101 RK1 RK2 RK3 SD2-5
PF00664	ABC transporter transmembrane region	12	6.75e-07	ABCB15 ABCB22 ABCB4 ABCB5 ABCB7 ABCB9 ABCC15 ABCC3 ABCC4 ABCC8 ABCC9 PGP10
PF00954	S-locus glycoprotein domain	11	7.19e-07	AT1G11330 AT1G11340 AT1G61360 AT1G61420 AT2G19130 AT4G27290 AT4G27300 B120 RK1 RK2 RK3
PF13947	Wall-associated receptor kinase galacturonan-binding	8	0.00076	AT1G69730 AT4G31100 AT5G02070 AT5G38250 RFO1 WAK2 WAK3 WAK5

Table V-4. Enrichment analysis for KEGG pathways in 'Tifway'.

KEGG term ID	Term Description	Gene Count	FDR	*Arabidopsis* homologous-genes
down-regulated				
ath02010	ABC transporters	5	0.00011	ABCB1 ABCB11 ABCB15 ABCB19 ABCB21
up-regulated				
ath01100	Metabolic pathways	161	9.11e-45	4CL2 AAE14 AAO3 AAS ACLA-1 ACLB-2 ACO3 ACX1 ADK2 ADT6 AGK2 AK2 ALDH2B4 ALDH6B2 ALN AO AOS ASA2 ASB1 ASP1 ASP3 AT1G09400 AT1G54220 AT1G55090 AT1G71695 AT1G74320 AT2G04400 AT2G18620 AT2G26800 AT2G43590 AT2G45290 AT2G47550 AT3G02360 AT3G03980 AT3G04000 AT3G29320 AT4G02610 AT4G13720 AT5G06730 AT5G08680 AT5G08690 AT5G09300 AT5G15180 AT5G42740 AT5G57655 AT5G58980 ATCS ATMS1 ATP1 ATP6-2 ATPMEPCRB ATTPPA BFRUCT4 BGLU46 C4H CAD6 CADG CI51 CYT1 CYTB CYTC-1 DHS1 DIN9 EDA9 ELI3-1 EMB1467 EMB1873 EP3 FAC1 FBA5 FBA6 FBP FDH FUM1 GA2 GAPC1 GAPC2 GAPCP-1 GDH2 GGPS1 GLDP2 GLN1-1 GLN1;4 GMD1 GSH2 GSR2 HCHIB HEMA1 HMGS HMT-1 HOG1 ICDH ICL KCR1 LACS1 LACS3 LACS4 LOS2 LOX2 MAB1 MCCB MEE25 MEE31 MEE32 MIPS3 MTHFR2 NAD7 NADP-ME4 NAGK NCED3 NCED5 NCED9 NDPK2 NDPK3 NRPB2 OPR1 OPR2 PAI3 PAL1 PAL4 PFK3 PGM2 PKT4 PLDBETA2 PRX52 PUR7 PYR6 Prx37 RCI3 RNR2A RSW3 SAHH2 SAM-2 SBH2 SDH1-1 SDH2-2 SERAT2;1 SHM1 SHM4 SMT1 STT3B THFS TIM TPK1 TPPG TPPJ TSA2 TSB2 TT4 TYRDC UDG4 UGD3 UGE5 USP UXS6 VAB2 VHA-A c-NAD-MDH2 cICDH mMDH1 mtLPD1
ath03010	Ribosome	68	5.60e-39	AT1G29965 AT1G67430 AT1G70600 AT1G74050 AT2G01250 AT2G09990 AT2G31610 AT2G36160 AT2G39390 AT2G39590 AT2G44120 AT2G47610 AT3G02080 AT3G05560 AT3G09630 AT3G10610 AT3G16780 AT3G18740 AT3G23390.1 AT3G24830 AT3G28900 AT3G45030 AT3G47370 AT3G56340 AT3G58700 AT3G60770 AT4G00810 AT4G15000 AT4G16720 AT4G17390 AT4G18100 AT4G30800 AT4G34555 AT4G34670 AT4G36130 AT5G02870 AT5G02960 AT5G04800 AT5G07090 AT5G15200 AT5G18380 AT5G23900 AT5G27700 AT5G28060 AT5G48760 AT5G56710 AT5G58420 AT5G59240 AT5G60670 AT5G67510 BBC1 EMB2296 P40 PGY1 RPL10B RPL16A RPL18 RPL23AB RPL27AB RPL3B RPL5B RPS18C RPS5A RPS6A RPSAb RPSL2 SAG24 emb2171
ath01110	Biosynthesis of secondary metabolites	102	1.91e-31	4CL2 AAE14 AAO3 AAS ACLA-1 ACLB-2 ACO3 ACX1 ADT6 AK2 ALDH2B4 AOS ASA2 ASB1 ASP1 ASP3 AT1G09400 AT1G54220 AT1G71695 AT2G04400 AT2G18620 AT2G24190 AT2G45290 AT3G02360 AT3G29320 AT4G02610 AT4G27270 AT5G06730 AT5G09300 AT5G15180 AT5G42740 ATCS ATMS1 BGLU46 C4H CAD6 CADG CHAT CYP79B2 CYP79B3 CYT1 DHS1 DIN9 ELI3-1 FAC1 FBA5 FBA6 FBP FUM1 GA2 GAPC1 GAPC2 GAPCP-1 GGPS1 GLDP2 HEMA1 HMGS HMT-1 ICDH ICL KCR1 LOS2 LOX2 LPP2 MAB1 MEE31 MEE32

				NAGK NCED3 NCED5 NCED9 NDPK2 NDPK3 OPR1 OPR2 PAI3 PAL1 PAL4 PFK3 PGM2 PKT4 PLDBETA2 PRX52 PUR7 Prx37 RCI3 SAM-2 SDH1-1 SDH2-2 SERAT2;1 SHM1 SHM4 SMT1 TIM TSA2 TSB2 TT4 TYRDC c-NAD-MDH2 cICDH mMDH1 mtLPD1
ath01200	Carbon metabolism	38	1.19e-16	ACO3 ALDH6B2 ASP1 ASP3 AT1G54220 AT2G45290 AT3G02360 AT5G42740 ATCS EDA9 FBA5 FBA6 FBP FDH FUM1 GAPC1 GAPC2 GAPCP-1 GDH2 GLDP2 ICDH ICL LOS2 MAB1 MTHFR2 NADP-ME4 PFK3 SDH1-1 SDH2-2 SERAT2;1 SHM1 SHM4 THFS TIM c-NAD-MDH2 cICDH mMDH1 mtLPD1
ath01230	Biosynthesis of amino acids	36	4.99e-16	ACO3 ADT6 AK2 ASA2 ASB1 ASP1 ASP3 AT2G04400 AT2G45290 AT4G02610 ATCS ATMS1 DHS1 EDA9 FBA5 FBA6 GAPC1 GAPC2 GAPCP-1 GLN1-1 GLN1;4 GSR2 ICDH LOS2 MEE32 NAGK PAI3 PFK3 SAM-2 SERAT2;1 SHM1 SHM4 TIM TSA2 TSB2 cICDH
ath03050	Proteasome	15	1.05e-09	AT1G04810 AT5G23540 At5g35590 PAE1 PAE2 PAG1 PBB2 PBE1 PBF1 PRC3 RPT1A RPT2b RPT3 RPT4A RPT5A
ath00020	Citrate cycle (TCA cycle)	14	1.80e-08	ACLA-1 ACLB-2 ACO3 AT1G54220 ATCS FUM1 ICDH MAB1 SDH1-1 SDH2-2 c-NAD-MDH2 cICDH mMDH1 mtLPD1
ath00520	Amino sugar and nucleotide sugar metabolism	18	8.51e-08	AT2G43590 AT5G42740 CBR CYT1 DIN9 EP3 GMD1 HCHIB MEE25 MEE31 PGM2 RGP3 RHM1 UDG4 UGD3 UGE5 USP UXS6
ath00400	Phenylalanine, tyrosine and tryptophan biosynthesis	12	2.09e-07	ADT6 ASA2 ASB1 ASP1 ASP3 AT2G04400 AT4G02610 DHS1 MEE32 PAI3 TSA2 TSB2
ath00710	Carbon fixation in photosynthetic organisms	13	3.27e-07	ASP1 ASP3 AT2G45290 FBA5 FBA6 FBP GAPC1 GAPC2 GAPCP-1 NADP-ME4 TIM c-NAD-MDH2 mMDH1
ath00630	Glyoxylate and dicarboxylate metabolism	13	7.08e-07	ACO3 ATCS FDH GLDP2 GLN1-1 GLN1;4 GSR2 ICL SHM1 SHM4 c-NAD-MDH2 mMDH1 mtLPD1
ath00010	Glycolysis / Gluconeogenesis	15	1.89e-06	ALDH2B4 AT1G54220 AT5G42740 FBA5 FBA6 FBP GAPC1 GAPC2 GAPCP-1 LOS2 MAB1 PFK3 PGM2 TIM mtLPD1
ath00051	Fructose and mannose metabolism	11	6.49e-06	AT5G57655 CYT1 DIN9 FBA5 FBA6 FBP GMD1 MAN7 MEE31 PFK3 TIM
ath00480	Glutathione metabolism	13	8.72e-06	AT3G02360 ERD9 GSH2 GSTL3 GSTU1 GSTU16 GSTU18 GSTU22 GSTU23 GSTU8 ICDH RNR2A cICDH
ath04146	Peroxisome	12	1.45e-05	ACX1 AT2G26800 CER4 CSD1 CSD2 ICDH LACS1 LACS3 LACS4 MSD1 PKT4 cICDH
ath04141	Protein processing in endoplasmic reticulum	18	1.90e-05	AT3G09440 AtCDC48C BIP2 CDC48 CNX1 CRT1a CRT1b ERO1 HSC70-1 HSP70 HSP90.1 Hsp81.4 PDIL2-2 RSW3 SAR1B SK11 STT3B UBC11
ath00592	alpha-Linolenic acid metabolism	8	7.04e-05	ACX1 AOS AT1G09400 CHAT LOX2 OPR1 OPR2 PKT4
ath01210	2-Oxocarboxylic acid metabolism	10	8.97e-05	ACO3 AK2 ASP1 ASP3 ATCS CYP79B2 CYP79B3 ICDH NAGK cICDH
ath00190	Oxidative phosphorylation	14	9.90e-05	AT5G08680 AT5G08690 ATP1 ATP6-2 AVP1 CI51 CYTB EMB1467 NAD7 PPa4 SDH1-1 SDH2-2 VAB2 VHA-A

ath00270	Cysteine and methionine metabolism	12	0.00013	AK2 ASP1 ASP3 ATMS1 GSH2 HMT-1 HOG1 SAHH2 SAM-2 SERAT2;1 c-NAD-MDH2 mMDH1
ath00280	Valine, leucine and isoleucine degradation	8	0.00013	ALDH2B4 ALDH6B2 AT2G26800 AT5G09300 HMGS MCCB PKT4 mtLPD1
ath00220	Arginine biosynthesis	7	0.0002	ASP1 ASP3 GDH2 GLN1-1 GLN1;4 GSR2 NAGK
ath00940	Phenylpropanoid biosynthesis	14	0.00026	4CL2 AT1G71695 AT5G06730 AT5G15180 BGLU46 C4H CAD6 CADG ELI3-1 PAL1 PAL4 PRX52 Prx37 RCI3
ath00260	Glycine, serine and threonine metabolism	9	0.00028	AK2 AT4G02610 EDA9 GLDP2 SHM1 SHM4 TSA2 TSB2 mtLPD1
ath00360	Phenylalanine metabolism	7	0.00041	4CL2 AAS ASP1 ASP3 C4H PAL1 PAL4
ath00030	Pentose phosphate pathway	8	0.00042	AT2G45290 AT3G02360 AT5G42740 FBA5 FBA6 FBP PFK3 PGM2
ath04626	Plant-pathogen interaction	13	0.00072	AT1G18530 AT1G76640 AT3G59350 CAM8 CEN1 CPK2 CPK30 HSP90.1 Hsp81.4 MPK3 MPK4 PR1 WRKY33
ath00250	Alanine, aspartate and glutamate metabolism	7	0.00087	AO ASP1 ASP3 GDH2 GLN1-1 GLN1;4 GSR2
ath01212	Fatty acid metabolism	8	0.00093	ACX1 AT3G03980 AT3G04000 KCR1 LACS1 LACS3 LACS4 PKT4

Table V-5. Enrichment analysis for KEGG pathways in 'U3' biotype.

KEGG term ID	Term Description	Gene Count	FDR	*Arabidopsis* homologous-genes
down-regulated				
ath01110	Biosynthesis of secondary metabolites	166	1.52e-33	4CL2 4CL3 AAS ABA2 ACLA-3 ACLB-1 ACS7 ACS8 ACX4 ALDH3F1 AOC3 AOS APL2 ASE2 ASN1 AT1G11860 AT1G15710 AT1G28580 AT1G28590 AT1G31670 AT1G32780 AT1G44000 AT1G44970 AT1G68850 AT1G71695 AT1G73050 AT1G74470 AT1G76550 AT1G77330 AT2G18980 AT2G24190 AT2G24800 AT2G39040 AT2G41480 AT3G01190 AT3G21770 AT3G49960 AT4G11290 AT4G25980 AT4G27270 AT4G33420 AT4G36430 AT4G36750 AT4G37520 AT5G06730 AT5G14130 AT5G15180 AT5G19890 AT5G36160 AT5G39580 AT5G42250 AT5G51890 AT5G58390 AT5G58400 AT5G66390 ATCAD4 ATCS At1g80820 At3g01180 At4g25700 BGLU12 BGLU16 BGLU17 BGLU27 BGLU31 BGLU42 BGLU43 BGLU44 BGLU46 CAD5 CAD6 CAD9 CAS1 CCoAOMT1 CHAT CHIL CHLM CLA1 CPD CPT CYP51G1 CYP710A1 CYP710A2 CYP735A1 CYP735A2 CYP79B2 DWF1 DWF4 EFE ELI3-1 EMB3003 FBA2 FK FLS1 FPS1 G-TMT G6PD1 GA20OX2 GA2OX8 GAD5 GAPC1 GOX1 GPAT1 GPAT5 GPAT6 GPAT7 GPDHC1 HMG1 HPR3 HXK1 HYD1 IDH1 IPP2 IRX4 KCR1 KCS1 KCS11 KCS12 KCS2 KCS20 KCS4 KCS6 LDOX LPP3 LTA2 MEE31 MTO3 NCED3 NCED4 NDPK1 NIT4 NPC2 NPC6 OMT1 OPR1 OPR2 PA2 PANB2 PER64 PGM2 PHS2 PKP-ALPHA PLA2-ALPHA PLDALPHA1 PLDALPHA2 PLDALPHA3 PLDDELTA PRX52 PSY RCI3 RHS19 SMO1-1 SMT2 SOT16 SOT17 SQS1 STE1 TAT7 TPI TT4 TT5 TT7 VTC4 dl3510w mMDH1 mtLPD1
ath01100	Metabolic pathways	211	1.04e-24	4CL2 4CL3 AAS ABA2 ACLA-3 ACLB-1 ACS7 ACS8 ACX4 ALDH3F1 AMY1 AOC3 AOS APL2 ASE2 ASN1 AT1G11860 AT1G15710 AT1G24360 AT1G31670 AT1G32780 AT1G44970 AT1G51650 AT1G62660 AT1G68850 AT1G71695 AT1G74470 AT1G76550 AT1G77330 AT2G02050 AT2G18980 AT2G24580 AT2G24800 AT2G39040 AT2G41480 AT3G01190 AT3G03980 AT3G05620 AT3G19620 AT3G21770 AT3G49960 AT4G11290 AT4G25980 AT4G33420 AT4G36430 AT4G37520 AT5G06730 AT5G08680 AT5G14130 AT5G15180 AT5G19730 AT5G19890 AT5G36160 AT5G39580 AT5G40810 AT5G42250 AT5G51890 AT5G58390 AT5G58400 AT5G66390 ATCAD4 ATCS ATPQ AUD1 AXS2 At1g73010 At1g80820 At3g01180 At4g25700 BGAL2 BGLU12 BGLU16 BGLU17 BGLU27 BGLU31 BGLU42 BGLU43 BGLU44 BGLU46 CAB1 CAD5 CAD6 CAD9 CAS1 CCoAOMT1 CHIA CHIL CHLM CIB22 CLA1 CMT2 CSLD5 CYP51G1 CYP710A1 CYP710A2 CYP735A1 CYP735A2 CYP86A4 CYP86A8 CYTC-1 DPB2 DUT1 DWF1 DWF4 EFE ELI3-1 EMB2813 EMB3003 FATB FBA2 FK FLS1 FOLB1 FPS1 G-TMT G6PD1 GA20OX2 GAD5 GAE4 GAPB GAPC1 GOX1 GPAT1 GPAT5 GPAT6 GPAT7 GS2 GSH2 GSR2 GSTZ1 GlcNA.1UT2 HCHIB HEXO3 HMG1 HPR3 HXK1 HYD1 ICU2 IDH1 IPP2 IRX4 KASI KCR1 LDOX LHCB5 LTA2 MEE31 MET1 MET3-1 MOD1 MTACP-1 MTHFR2 MTO3 NAD4 NCED3 NCED4 NDPK1 NIT4 NPC2 NPC6 OMT1 OPR1 OPR2 PA2 PANB2 PAO1 PER64 PGM2 PHS2 PIP5K1 PKP-ALPHA PLA2-ALPHA PLDALPHA1 PLDALPHA2 PLDALPHA3 PLDDELTA PME2 PPC1 PPC2 PRX52 PSAD-2 PSY RBCS1A RCI3 RHS19 RNR1 SAMDC SBH2 SMO1-1 SPS3F SQS1 STE1 T3P18.20 TAR2 TAT7 TIL1 TPI TT4 TT5 TT7 UGD2 UGE2 UGP2 UXS5 VTC4 XYL4 YUC11 YUC5 dl3510w mMDH1 mtLPD1
ath00940	Phenylpropanoid biosynthesis	50	1.38e-19	4CL2 4CL3 ALDH2C4 AT1G44970 AT1G68850 AT1G71695 AT2G18980 AT2G24800 AT2G39040 AT2G41480 AT3G01190 AT3G21770 AT3G49960 AT4G11290 AT4G25980 AT4G33420 AT4G36430 AT4G37520 AT5G06730 AT5G14130 AT5G15180 AT5G19890 AT5G39580 AT5G51890 AT5G58390 AT5G58400 AT5G66390 ATCAD4 At1g80820 BGLU12 BGLU16 BGLU17 BGLU27 BGLU31 BGLU42

				BGLU43 BGLU44 BGLU46 CAD5 CAD6 CAD9 CCoAOMT1 ELI3-1 IRX4 OMT1 PA2 PER64 PRX52 RCI3 RHS19
ath00520	Amino sugar and nucleotide sugar metabolism	22	8.24e-05	APL2 AT3G19620 AUD1 AXS2 CHIA CSLD5 GAE4 GlcNA.1UT2 HCHIB HEXO3 HXK1 MEE31 NRS/ER PGM2 QUA1 RGP3 RHM3 UGD2 UGE2 UGP2 UXS5 XYL4
ath00100	Steroid biosynthesis	11	0.00011	CAS1 CYP51G1 CYP710A1 CYP710A2 DWF1 FK HYD1 SMO1-1 SMT2 SQS1 STE1
ath00500	Starch and sucrose metabolism	23	0.00011	AMY1 APL2 AT1G11820 AT1G62660 AT2G01630 AT4G31140 AT5G58090 At3g01180 BGLU12 BGLU16 BGLU17 BGLU27 BGLU31 BGLU42 BGLU43 BGLU44 BGLU46 HXK1 PGM2 PHS2 SPS3F TRBAMY UGP2
ath03030	DNA replication	12	0.00043	AT3G52630 DPB2 EMB2813 ICU2 MCM2 MCM3 MCM4 MCM5 MCM6 PRL RPA70B TIL1
ath00564	Glycerophospholipid metabolism	16	0.0007	GDPD6 GPAT1 GPAT5 GPAT6 GPAT7 GPDHC1 LPP3 NPC2 NPC6 PLA2-ALPHA PLDALPHA1 PLDALPHA2 PLDALPHA3 PLDDELTA PMEAMT XPL1
up-regulated				
ath03010	Ribosome	96	2.77e-64	AT1G07070 AT1G08360 AT1G23410 AT1G41880 AT1G48830 AT1G52300 AT1G67430 AT1G70600 AT1G74050 AT1G74060 AT1G74270 AT1G77940 AT2G01250 AT2G09990 AT2G21580 AT2G31610 AT2G34480 AT2G37190 AT2G37600 AT2G39590 AT2G41840 AT2G47610 AT3G02080 AT3G04840 AT3G05560 AT3G09200 AT3G09630 AT3G10610 AT3G11250 AT3G11510 AT3G16780 AT3G23390.1 AT3G24830 AT3G28900 AT3G44590 AT3G45030 AT3G52580 AT3G53870 AT3G55170 AT3G56340 AT3G57490 AT3G58700 AT3G60245 AT3G62870 AT4G00810 AT4G10450 AT4G13170 AT4G15000 AT4G16720 AT4G17390 AT4G18100 AT4G26230 AT4G30800 AT4G34555 AT4G34670 AT4G36130 AT5G02870 AT5G02960 AT5G04800 AT5G07090 AT5G09500 AT5G15200 AT5G18380 AT5G22440 AT5G23900 AT5G28060 AT5G35530 AT5G52650 AT5G58420 AT5G59240 AT5G59850 AT5G60670 AT5G67510 AtCg00380 EMB2207 EMB2296 EMB3010 P40 RPL10B RPL16A RPL18 RPL23AB RPL27AB RPL34 RPL3B RPL5B RPS10B RPS13A RPS18C RPS30A RPS5A RPS5B RPS6A RPSAb SAG24 emb2171
ath01110	Biosynthesis of secondary metabolites	76	3.26e-14	4CL2 AAO3 AAS ABA2 ACX4 ALDH2B4 ALDH2B7 AOS ASA2 ASP3 AT1G02190 AT1G71695 AT1G76550 AT1G79870 AT2G04400 AT2G24190 AT4G02610 AT4G33070 AT4G33420 AT5G06730 AT5G08300 AT5G09300 AT5G14130 AT5G19890 AT5G35170 AT5G47720 AT5G57890 AT5G58400 ATGA2OX1 At5g17990 BCAT-2 BCE2 BGLU11 BGLU42 BGLU45 BGLU46 CADG CAT CCoAOMT1 CER1 CYP98A3 FBP GAPC1 GAPCP-1 GGPS1 HCD1 HDS ICDH KAO2 KCS11 LCAT3 MAT3 MLS NCED9 NDPK1 OASB OPR2 PA2 PAL2 PCK1 PFK6 PGK PKT3 PLDBETA1 PLDGAMMA1 PRX52 RCI3 SAM-2 SBE2.2 SUR1 TAT7 THA1 TSB2 c-NAD-MDH2 cPT4 dl3510w
ath01100	Metabolic pathways	105	6.14e-13	4CL2 AAO3 AAS ABA2 ACX4 ADSS ALDH2B4 ALDH2B7 ALDH6B2 AOS ARA1 ASA2 ASP3 AT1G71695 AT1G76550 AT1G79870 AT2G04400 AT2G47550 AT3G04000 AT4G02610 AT4G33070 AT4G33420 AT5G06730 AT5G08300 AT5G08690 AT5G09300 AT5G14130 AT5G19890 AT5G35170 AT5G47720 AT5G57890 AT5G58400 ATP1 ATP9 ATPMEPCRB ATSPS4F ATTPPA At1g60140 At5g17990 BCAT-2 BCE2 BGLU11 BGLU42 BGLU45 BGLU46 CADG CCoAOMT1 CHIA CI51 CLPC1 CYP98A3 DGD1 EMB1467 FBP GALT1 GAPC1 GAPCP-1 GDH2 GDH3 GGPS1 GLN1.3 HDS HOG1 ICDH KAO2 LACS3 LACS4 LAP1 LCAT3 LCB2 MAT3 MLS MST1 NAD-ME2 NAD7 NADK2 NADP-ME1 NCED9 NDPK1 OASB OPR2 PA2 PAL2 PCK1 PFK6 PGK PKT3 PLDBETA1 PLDGAMMA1 PPDK PRX52 RCI3 SAM-2 SBE2.2 SOX TAG1 TAT7 THA1 TPPI TRE1 TSB2 UGP2 VHA-A c-NAD-MDH2 dl3510w
ath00940	Phenylpropanoid biosynthesis	18	1.28e-05	4CL2 AT1G71695 AT4G33420 AT5G06730 AT5G14130 AT5G19890 AT5G58400 BGLU11 BGLU42 BGLU45 BGLU46 CADG CCoAOMT1 CYP98A3 PA2 PAL2 PRX52 RCI3

ath01200	Carbon metabolism	21	9.48e-05	ALDH6B2 ASP3 AT1G79870 AT5G08300 AT5G47720 CAT FBP GAPC1 GAPCP-1 GDH2 GDH3 ICDH MLS NAD-ME2 NADP-ME1 OASB PCK1 PFK6 PGK PPDK c-NAD-MDH2
ath02010	ABC transporters	7	0.00017	ABCB15 ABCB22 ABCB4 ABCB5 ABCB7 ABCB9 PGP10
ath00710	Carbon fixation in photosynthetic organisms	10	0.00025	ASP3 FBP GAPC1 GAPCP-1 NAD-ME2 NADP-ME1 PCK1 PGK PPDK c-NAD-MDH2
ath01230	Biosynthesis of amino acids	19	0.00025	ASA2 ASP3 AT2G04400 AT4G02610 AT5G57890 At5g17990 BCAT-2 GAPC1 GAPCP-1 GLN1.3 ICDH MAT3 OASB PFK6 PGK SAM-2 TAT7 THA1 TSB2
ath00280	Valine, leucine and isoleucine degradation	8	0.00042	ALDH2B4 ALDH2B7 ALDH6B2 AT5G09300 AT5G47720 BCAT-2 BCE2 PKT3
ath00380	Tryptophan metabolism	8	0.00093	AAS ALDH2B4 ALDH2B7 AO4 AT5G47720 CAT CYP71A13 SUR1
ath00400	Phenylalanine, tyrosine and tryptophan biosynthesis	8	0.00093	ASA2 ASP3 AT2G04400 AT4G02610 AT5G57890 At5g17990 TAT7 TSB2
ath04146	Peroxisome	10	0.00093	ACX4 At5g22500 CAT CSD1 CSD2 FAR2 ICDH LACS3 LACS4 PKT3
ath00071	Fatty acid degradation	7	0.00099	ACX4 ALDH2B4 ALDH2B7 AT5G47720 LACS3 LACS4 PKT3

Table V-6. Up-regulated candidade genes of 'Tifway' with role in plant immunity, which were obtained in the Gene Ontology Biological Process 'response to biotic stress'. Candidade genes in common with 'U3' biotype, and 'unique' to 'Tifway', and *Arabidopsis thaliana* homologous gene name and function obtained from UniProt/SwissProt.

Candidade gene/loci	logFC	Arabidopsis gene name	*Arabidopsis* gene function
in common			
TRINITY_DN170938_c6_g1	2.96	AB40G	FUNCTION: May be a general defense protein (By similarity)
TRINITY_DN149514_c3_g1	7.31	BCA2	FUNCTION: Reversible hydration of carbon dioxide. This isoform ensures the supply of bicarbonate for pep carboxylase
TRINITY_DN165689_c1_g1	3.98	BG3	FUNCTION: May play a role in plant defense against pathogens
TRINITY_DN159764_c0_g1	2.55	CP74A	Allene oxide synthase, chloroplastic (EC 4.2.1.92) (Cytochrome P450 74A) (Hydroperoxide dehydrase)
TRINITY_DN155029_c0_g1	2.62	CP74A	
TRINITY_DN155029_c0_g2	2.64	CP74A	
TRINITY_DN159344_c0_g2	2.31	CRK10	Cysteine-rich receptor-like protein kinase 10 (Cysteine-rich RLK10) (EC 2.7.11.-) (Receptor-like protein kinase 4)
TRINITY_DN171270_c1_g1	3.32	CRK8	Cysteine-rich receptor-like protein kinase 8 (Cysteine-rich RLK8) (EC 2.7.11.-)
TRINITY_DN151770_c0_g1	4.37	DLO2	FUNCTION: Converts salicylic acid (SA) to 2,3-dihydroxybenzoic acid (2,3-DHBA) (By similarity)
TRINITY_DN169631_c2_g1	3.89	DMR6	
TRINITY_DN152606_c1_g1	2.85	DTX16	Protein DETOXIFICATION 16 (AtDTX16) (Multidrug and toxic compound extrusion protein 16) (MATE protein 16)
TRINITY_DN151060_c0_g1	3.40	HEVL	FUNCTION: Fungal growth inhibitors
TRINITY_DN167046_c0_g9	5.63	HS901	FUNCTION: Molecular chaperone involved in R gene-mediated disease resistance
TRINITY_DN167893_c3_g1	4.72	HSP7C	FUNCTION: In cooperation with other chaperones, Hsp70s are key components that facilitate folding of de novo synthesized proteins, assist translocation of precursor proteins into organelles, and are responsible for degradation of damaged protein under stress conditions
TRINITY_DN144547_c5_g2	5.12	HSP7J	FUNCTION: Chaperone involved in the maturation of iron-sulfur [Fe-S] cluster-containing proteins. Has a low intrinsic ATPase activity which is markedly stimulated by HSCB and ISU1 (By similarity). In cooperation with other chaperones, Hsp70s are key components that facilitate folding of de novo synthesized proteins, assist translocation of precursor proteins into organelles, and are responsible for degradation of damaged protein under stress conditions (Probable)
TRINITY_DN162387_c0_g2	2.23	LRK42	FUNCTION: Required during pollen development. FUNCTION: Involved in resistance response to the pathogenic bacteria.
TRINITY_DN156138_c0_g2	2.63	LRK42	
TRINITY_DN153448_c1_g1	3.70	LRK42	
TRINITY_DN162566_c0_g1	5.65	LRK91	

TRINITY_DN154452_c2_g1	6.43	LRK91	FUNCTION: Promotes hydrogen peroxide production and cell death. FUNCTION: Involved in resistance response to the pathogenic oomycetes
TRINITY_DN144547_c5_g3	5.13	MD37E	FUNCTION: Component of the Mediator complex, a coactivator involved in the regulated transcription of nearly all RNA polymerase II-dependent genes. FUNCTION: Heat shock protein probably involved in defense response. Chaperone involved in protein targeting to chloroplasts. May cooperate with SGT1 and HSP90 in R gene-mediated resistance towards oomycete
TRINITY_DN167406_c2_g1	2.27	MLO1	FUNCTION: May be involved in modulation of pathogen defense and leaf cell death. Activity seems to be regulated by calcium-dependent calmodulin binding and seems not to require heterotrimeric G proteins (By similarity)
TRINITY_DN169870_c2_g2	2.99	MLO1	
TRINITY_DN167406_c2_g2	4.51	MLO1	
TRINITY_DN145613_c2_g1	2.49	NQR	FUNCTION: The enzyme apparently serves as a quinone reductase in connection with conjugation reactions of hydroquinones involved in detoxification pathways
TRINITY_DN164020_c0_g1	2.27	OSL3	Osmotin-like protein OSM34
TRINITY_DN159383_c1_g1	6.82	OSL3	
TRINITY_DN156463_c1_g5	9.17	OSL3	
TRINITY_DN150058_c2_g1	3.14	PLP2	FUNCTION: Possesses non-specific lipolytic acyl hydrolase (LAH) activity. Negatively affects disease resistance to the necrotic fungal pathogen and the avirulent bacteria by promoting cell death and reducing the efficiency of the hypersensitive response, respectively.
TRINITY_DN152664_c1_g5	4.97	PLP2	
TRINITY_DN170039_c2_g2	6.02	PLP2	
TRINITY_DN152664_c1_g1	6.10	PLP2	
TRINITY_DN170039_c2_g4	6.75	PLP2	
TRINITY_DN163264_c1_g2	6.86	PLP2	
TRINITY_DN163259_c1_g1	4.68	PME41	FUNCTION: Acts in the modification of cell walls via demethylesterification of cell wall pectin
TRINITY_DN154581_c2_g6	8.35	PR1	FUNCTION: Partially responsible for acquired pathogen resistance.
TRINITY_DN144994_c4_g1	3.76	SBT33	FUNCTION: Serine protease that plays a role in the control of the establishment of immune priming and systemic induced resistance
TRINITY_DN168978_c3_g3	7.51	SBT33	
TRINITY_DN169046_c2_g2	8.12	SBT33	
TRINITY_DN149945_c2_g1	10.24	SBT33	
TRINITY_DN165680_c0_g2	2.18	SODC1	FUNCTION: Destroys radicals which are normally produced within the cells and which are toxic to biological systems
TRINITY_DN160228_c3_g1	6.90	SODC1	
unique			
TRINITY_DN171309_c1_g1	7.35	ACA4	FUNCTION: This magnesium-dependent enzyme catalyzes the hydrolysis of ATP coupled with the translocation of calcium from the cytosol into small vacuoles
TRINITY_DN151569_c2_g2	7.66	ACOX1	FUNCTION: Catalyzes the desaturation of both long- and medium-chain acyl-CoAs to 2-trans-enoyl-CoAs. Most active with C14-CoA. Activity on long-chain mono-unsaturated substrates is 40% higher than with the corresponding saturated substrates. Seems to be an important factor in the general metabolism of root tips. May be involved in the biosynthesis of jasmonic acid
TRINITY_DN145473_c0_g1	2.79	ADF4	FUNCTION: Actin-depolymerizing protein. May modulate defense signal transduction pathway.
TRINITY_DN169155_c0_g3	9.49	AGAL2	FUNCTION: May regulate leaf (and possibly other organ) development by functioning in cell wall loosening and cell wall expansion

TRINITY_DN168665_c1_g1	3.31	APCB1	FUNCTION: Involved in proteolytic processing of BAG6 and plant basal immunity
TRINITY_DN156208_c5_g3	7.25	AT18A	FUNCTION: The PI(3,5)P2 regulatory complex regulates both the synthesis and turnover of phosphatidylinositol 3,5-bisphosphate (PtdIns(3,5)P2). Required for autophagy by autophagosome formation during nutrient deprivation, senescence and under abiotic stresses, including oxidative, high salt and osmotic stress conditions. Cooperates with jasmonate- and WRKY33-mediated signaling pathways in the regulation of plant defense responses to necrotrophic pathogens
TRINITY_DN164851_c3_g2	5.34	BGNEM	FUNCTION: May be involved in plant defense against cyst nematode pathogens
TRINITY_DN158778_c0_g3	5.48	C79B2	FUNCTION: Converts tryptophan to indole-3-acetaldoxime, a precursor for tryptophan-derived glucosinolates and indole-3-acetic acid (IAA). Involved in the biosynthetic pathway to 4-a cyanogenic metabolite required for inducible pathogen defense.
TRINITY_DN158778_c0_g2	3.28	C79B3	
TRINITY_DN158630_c0_g2	6.62	C8D11	FUNCTION: May play a role in cis-jasmone-activated defense response
TRINITY_DN149031_c1_g3	4.85	CADH7	FUNCTION: Involved in lignin biosynthesis
TRINITY_DN169797_c0_g1	2.64	CEP1	FUNCTION: Possesses protease activity in vitro. Involved in the final stage of developmental programmed cell death and in intercalation of new cells.
TRINITY_DN151303_c0_g1	2.08	CESA4	FUNCTION: Catalytic subunit of cellulose synthase terminal complexes ('rosettes'), required for beta-1,4-glucan microfibril crystallization, a major mechanism of the cell wall formation. Involved in the secondary cell wall formation. Required for the xylem cell wall thickening
TRINITY_DN150924_c0_g1	4.43	CHI5	FUNCTION: Probably involved in hypersensitive reaction
TRINITY_DN154152_c0_g1	5.13	CHIB	FUNCTION: Defense against chitin-containing fungal pathogens. Seems particularly implicated in resistance to jasmonate-inducing pathogens. In vitro antifungal activity.
TRINITY_DN155475_c1_g1	2.01	CRK6	Cysteine-rich receptor-like protein kinase 6 (Cysteine-rich RLK6) (EC 2.7.11.-) (Receptor-like protein kinase 5)
TRINITY_DN160002_c2_g1	2.66	ERF78	FUNCTION: Acts as a transcriptional repressor. Binds to the GCC-box pathogenesis-related promoter element. Involved in the regulation of gene expression by stress factors and by components of stress signal transduction pathways
TRINITY_DN156313_c3_g5	2.66	G3PC2	FUNCTION: Key enzyme in glycolysis that catalyzes the first step of the pathway by converting D-glyceraldehyde 3-phosphate (G3P) into 3-phospho-D-glyceroyl phosphate. Essential for the maintenance of cellular ATP levels and carbohydrate metabolism
TRINITY_DN169839_c3_g2	3.47	G3PC2	
TRINITY_DN169839_c2_g1	8.33	G3PC2	
TRINITY_DN106752_c0_g1	7.79	G6PI	Glucose-6-phosphate isomerase, cytosolic (GPI) (EC 5.3.1.9) (Phosphoglucose isomerase) (PGI) (Phosphohexose isomerase) (PHI)
TRINITY_DN152046_c3_g3	8.97	GMPP1	FUNCTION: Catalyzes a reaction of the Smirnoff-Wheeler pathway, the major route to ascorbate biosynthesis in plants. Plays an essential role in plant growth and development and cell-wall architecture
TRINITY_DN167712_c3_g2	4.88	ICDHC	FUNCTION: May supply 2-oxoglutarate for amino acid biosynthesis and ammonia assimilation via the glutamine synthetase/glutamate synthase (GS/GOGAT) pathway. May be involved in the production of NADPH to promote redox signaling or homeostasis in response to oxidative stress
TRINITY_DN156594_c0_g7	8.46	ICDHC	
TRINITY_DN143053_c0_g1	2.20	INVA4	FUNCTION: Possible role in the continued mobilization of sucrose to sink organs. Regulates root elongation
TRINITY_DN160631_c0_g2	5.29	INVA4	
TRINITY_DN167505_c1_g1	3.09	LOX2	FUNCTION: 13S-lipoxygenase that can use linolenic acid as substrates. Plant lipoxygenases may be involved in a number of diverse aspects of plant physiology including growth and development, pest resistance, and senescence or responses to wounding. Required for the wound-induced synthesis of jasmonic acid in leaves
TRINITY_DN167505_c1_g2	3.25	LOX2	

TRINITY_DN155817_c1_g6	8.34	MD37C	FUNCTION: Component of the Mediator complex, a coactivator involved in the regulated transcription of nearly all RNA polymerase II-dependent genes. FUNCTION: ATP-dependent molecular chaperone that assists folding of unfolded or misfolded proteins under stress conditions. Mediates plastid precursor degradation to prevent cytosolic precursor accumulation, together with the E3 ubiquitin-protein ligase CHIP. Recognizes specific sequence motifs in transit peptides and thereby led to precursor degradation through the ubiquitin-proteasome system. Plays a critical role in embryogenesis. FUNCTION: In cooperation with other chaperones, Hsp70s are key components that facilitate folding of de novo synthesized proteins, assist translocation of precursor proteins into organelles, and are responsible for degradation of damaged protein under stress conditions.
TRINITY_DN165071_c1_g1	7.95	MDHM1	FUNCTION: Catalyzes a reversible NAD-dependent dehydrogenase reaction involved in central metabolism and redox homeostasis between organelle compartments (Probable).
TRINITY_DN156898_c0_g1	3.65	MO2	Monooxygenase 2 (AtMO2) (EC 1.14.13.-)
TRINITY_DN158728_c0_g1	2.53	MPK3	FUNCTION: Involved in oxidative stress-mediated signaling cascade. Involved in the innate immune MAP kinase signaling cascade (MEKK1, MKK4/MKK5 and MPK3/MPK6). May be involved in hypersensitive response (HR)-mediated signaling cascade by modulating LIP5 phosphorylation and subsequent multivesicular bodies (MVBs) trafficking. May phosphorylate regulators of WRKY transcription factors. MKK9-MPK3/MPK6 module phosphorylates and activates EIN3, leading to the promotion of EIN3-mediated transcription in ethylene signaling. MPK3/MPK6 cascade regulates camalexin synthesis through transcriptional regulation of the biosynthetic genes after pathogen infection
TRINITY_DN152183_c3_g1	9.06	MPK4	FUNCTION: The ANPs-MKK6-MPK4 module is involved in the regulation of plant cytokinesis during meiosis and mitosis. Essential to promote the progression of cytokinesis and for cellularization (formation of the cell plate). Involved in root hair development process. Negative regulator of systemic acquired resistance (SAR) and salicylic acid- (SA) mediated defense response. Required for jasmonic acid- (JA) mediated defense gene expression. May regulate activity of transcription factor controlling pathogenesis-related (PR) gene expression. Seems to act independently of the SAR regulatory protein NPR1 (Nonexpresser of PR1)
TRINITY_DN148056_c1_g1	3.73	NIA2	FUNCTION: Nitrate reductase is a key enzyme involved in the first step of nitrate assimilation in plants, fungi and bacteria.
TRINITY_DN150184_c2_g2	3.28	ODPB1	FUNCTION: The pyruvate dehydrogenase complex catalyzes the overall conversion of pyruvate to acetyl-CoA and CO(2).
TRINITY_DN160887_c1_g1	8.50	P2C25	FUNCTION: Protein phosphatase that negatively regulates defense responses. Inactivates MPK4 and MPK6 MAP kinases involved in stress and defense signaling
TRINITY_DN126620_c0_g1	7.85	PSB1	FUNCTION: The proteasome is a multicatalytic proteinase complex which is characterized by its ability to cleave peptides with Arg, Phe, Tyr, Leu, and Glu adjacent to the leaving group at neutral or slightly basic pH. The proteasome has an ATP-dependent proteolytic activity.
TRINITY_DN169516_c0_g3	6.07	PSL5	FUNCTION: Cleaves glucose residues from the oligosaccharide precursor of immature glycoproteins (By similarity). Essential for stable accumulation of the receptor EFR that determines the specific perception of bacterial elongation factor Tu (EF-Tu), a potent elicitor of the defense response to pathogen-associated molecular patterns (PAMPs). Required for sustained activation of EFR-mediated signaling
TRINITY_DN170358_c1_g1	7.35	PSL5	
TRINITY_DN144755_c0_g1	4.06	RIPK	FUNCTION: Serine/threonine-protein kinase involved in disease resistance. Seems to act as negative regulator of plant basal defense responses and may play a role in pathogen-associated molecular pattern (PAMP)-triggered immunity (PTI)
TRINITY_DN167480_c0_g8	6.11	RL303	60S ribosomal protein L30-3
TRINITY_DN157500_c2_g1	2.46	SNP33	FUNCTION: t-SNARE involved in diverse vesicle trafficking and membrane fusion processes, including cell plate formation. May function in the secretory pathway.

TRINITY_DN139043_c15_g1	8.18	SODM1	FUNCTION: Destroys superoxide anion radicals which are normally produced within the cells and which are toxic to biological systems.
TRINITY_DN153587_c0_g2	9.50	TRPA2	FUNCTION: The alpha subunit is responsible for the aldol cleavage of indoleglycerol phosphate to indole and glyceraldehyde 3-phosphate. Required for tryptophan biosynthesis. Contributes to the tryptophan-independent indole biosynthesis, and possibly to auxin production
TRINITY_DN149526_c2_g1	2.08	VDAC1	FUNCTION: Forms a channel through the mitochondrial outer membrane that allows diffusion of small hydrophilic molecules (By similarity). Involved in plant development at reproductive stage, is important for pollen development and may regulate hydrogen peroxide generation during disease resistance
TRINITY_DN165204_c1_g1	2.34	WRK33	FUNCTION: Transcription factor, a frequently occurring elicitor-responsive cis-acting element. Involved in defense responses. Required for resistance to the necrotrophic fungal pathogen. Required for the phytoalexin camalexin synthesis following infection. Acts as positive regulator of the camalexin biosynthetic genes PAD3 (CYP71B15) and CYP71A13 by binding to their promoters. Acts downstream of MPK3 and MPK6 in reprogramming the expression of camalexin biosynthetic genes, which drives the metabolic flow to camalexin production
TRINITY_DN152416_c0_g1	2.94	WRK33	FUNCTION: Transcription factor, a frequently occurring elicitor-responsive cis-acting element. Involved in defense responses. Required for resistance to the necrotrophic fungal pathogen. Required for the phytoalexin camalexin synthesis following infection. Acts as positive regulator of the camalexin biosynthetic genes PAD3 (CYP71B15) and CYP71A13 by binding to their promoters. Acts downstream of MPK3 and MPK6 in reprogramming the expression of camalexin biosynthetic genes, which drives the metabolic flow to camalexin production

Table V-7. Up-regulated candidade genes of 'U3' biotype with role in plant immunity, which were obtained in the Gene Ontology Biological Process 'response to biotic stress'. Candidade genes in common with 'Tifway', and 'unique' to 'U3', and *Arabidopsis thaliana* homologous gene name and function obtained from UniProt/SwissProt.

Candidade gene/loci	logFC	Arabidopsis gene name	Arabidopsis gene function
in common			
TRINITY_DN256164_c0_g1	5.02	AB40G	FUNCTION: May be a general defense protein (By similarity)
TRINITY_DN258739_c0_g3	5.66	AB40G	FUNCTION: May be a general defense protein (By similarity)
TRINITY_DN242096_c0_g2	4.19	BCA2	FUNCTION: Reversible hydration of carbon dioxide. This isoform ensures the supply of bicarbonate for pep carboxylase.
TRINITY_DN246405_c3_g1	5.27	BG3	FUNCTION: May play a role in plant defense against pathogens
TRINITY_DN246123_c0_g6	4.25	CP74A	Allene oxide synthase, chloroplastic (EC 4.2.1.92) (Cytochrome P450 74A) (Hydroperoxide dehydrase)
TRINITY_DN250576_c2_g1	3.78	CRK10	Cysteine-rich receptor-like protein kinase 10 (Cysteine-rich RLK10) (EC 2.7.11.-) (Receptor-like protein kinase 4)
TRINITY_DN262950_c0_g3	6.38	CRK10	
TRINITY_DN269199_c5_g3	2.96	CRK8	Cysteine-rich receptor-like protein kinase 8 (Cysteine-rich RLK8) (EC 2.7.11.-)
TRINITY_DN269928_c5_g3	2.98	CRK8	
TRINITY_DN265279_c0_g1	3.87	CRK8	
TRINITY_DN248337_c1_g1	4.20	CRK8	
TRINITY_DN246730_c3_g1	3.16	DLO2	FUNCTION: Converts salicylic acid (SA) to 2,3-dihydroxybenzoic acid (2,3-DHBA) (By similarity)
TRINITY_DN246730_c4_g1	3.81	DMR6	FUNCTION: Converts salicylic acid (SA) to 2,3-dihydroxybenzoic acid (2,3-DHBA) (By similarity)
TRINITY_DN263235_c4_g1	2.69	DTX16	Protein DETOXIFICATION 16 (AtDTX16) (Multidrug and toxic compound extrusion protein 16) (MATE protein 16)
TRINITY_DN252600_c0_g4	4.22	DTX16	
TRINITY_DN265084_c1_g1	4.61	DTX16	
TRINITY_DN247869_c0_g1	4.10	HEVL	FUNCTION: Fungal growth inhibitors
TRINITY_DN246095_c2_g1	9.71	HS901	FUNCTION: Molecular chaperone involved in R gene-mediated disease resistance
TRINITY_DN255432_c3_g5	11.88	HS901	
TRINITY_DN246527_c0_g1	4.48	HSP7C	FUNCTION: In cooperation with other chaperones, Hsp70s are key components that facilitate folding of de novo synthesized proteins, assist translocation of precursor proteins into organelles, and are responsible for degradation of damaged protein under stress conditions
TRINITY_DN245625_c3_g4	6.29	HSP7C	
TRINITY_DN242645_c2_g6	9.08	HSP7C	
TRINITY_DN264830_c4_g2	6.62	HSP7J	FUNCTION: Chaperone involved in the maturation of iron-sulfur [Fe-S] cluster-containing proteins. Has a low intrinsic ATPase activity which is markedly stimulated by HSCB and ISU1 (By similarity). In cooperation with other chaperones, Hsp70s are key components that facilitate folding of de novo synthesized proteins, assist translocation of precursor proteins into organelles, and are responsible for degradation of damaged protein under stress conditions (Probable)
TRINITY_DN260172_c6_g1	8.39	HSP7J	

TRINITY_DN259917_c0_g3	7.72	LRK42	FUNCTION: Required during pollen development. FUNCTION: Involved in resistance response to the pathogenic bacteria.
TRINITY_DN250308_c4_g1	5.77	LRK91	FUNCTION: Promotes hydrogen peroxide production and cell death. FUNCTION: Involved in resistance response to the pathogenic oomycetes
TRINITY_DN265881_c6_g4	12.59	MD37E	FUNCTION: Component of the Mediator complex, a coactivator involved in the regulated transcription of nearly all RNA polymerase II-dependent genes. FUNCTION: Heat shock protein probably involved in defense response. Chaperone involved in protein targeting to chloroplasts. May cooperate with SGT1 and HSP90 in R gene-mediated resistance towards oomycete
TRINITY_DN265954_c3_g2	5.28	MLO1	FUNCTION: May be involved in modulation of pathogen defense and leaf cell death. Activity seems to be regulated by calcium-dependent calmodulin binding and seems not to require heterotrimeric G proteins (By similarity)
TRINITY_DN258508_c1_g4	6.52	NQR	FUNCTION: The enzyme apparently serves as a quinone reductase in connection with conjugation reactions of hydroquinones involved in detoxification pathways
TRINITY_DN261672_c3_g6	2.97	OSL3	Osmotin-like protein OSM35
TRINITY_DN252743_c1_g1	3.05	OSL3	
TRINITY_DN255368_c0_g1	5.73	PLP2	FUNCTION: Possesses non-specific lipolytic acyl hydrolase (LAH) activity. Negatively affects disease resistance to the necrotic fungal pathogen and the avirulent bacteria by promoting cell death and reducing the efficiency of the hypersensitive response, respectively.
TRINITY_DN255368_c0_g2	6.01	PLP2	
TRINITY_DN266073_c0_g4	10.57	PLP2	
TRINITY_DN245093_c3_g2	5.11	PME41	FUNCTION: Acts in the modification of cell walls via demethylesterification of cell wall pectin
TRINITY_DN245797_c0_g7	4.69	PR1	FUNCTION: Partially responsible for acquired pathogen resistance.
TRINITY_DN264656_c4_g8	7.95	PR1	
TRINITY_DN245797_c0_g1	8.65	PR1	
TRINITY_DN269215_c2_g1	3.93	SBT33	FUNCTION: Serine protease that plays a role in the control of the establishment of immune priming and systemic induced resistance
TRINITY_DN257497_c1_g5	4.63	SBT33	FUNCTION: Serine protease that plays a role in the control of the establishment of immune priming and systemic induced resistance
TRINITY_DN250027_c0_g1	3.08	SODC1	FUNCTION: Destroys radicals which are normally produced within the cells and which are toxic to biological systems
unique			
TRINITY_DN253255_c0_g1	2.89	AB1G	ABC transporter G family member 1 (ABC transporter ABCG.1) (AtABCG1) (White-brown complex homolog protein 1) (AtWBC1)
TRINITY_DN258066_c1_g4	3.59	AB1G	
TRINITY_DN265642_c0_g4	4.60	AB4C	FUNCTION: Involved in the regulation of stomatal aperture. May function as a high-capacity pump for folates
TRINITY_DN247352_c0_g1	5.74	AB4C	
TRINITY_DN249308_c0_g1	2.13	AB9C	FUNCTION: Pump for glutathione S-conjugates
TRINITY_DN269910_c7_g1	4.65	AB9C	
TRINITY_DN256277_c3_g3	2.07	AHL20	FUNCTION: Transcription factor that specifically binds AT-rich DNA sequences related to the nuclear matrix attachment regions (MARs) (By similarity). Negatively regulates plant innate immunity (PTI) to pathogens through the down-regulation of the PAMP-triggered NHO1 and FRK1 expression
TRINITY_DN256789_c1_g2	2.29	AHL20	
TRINITY_DN263651_c0_g1	2.63	ANT1	FUNCTION: Translocates aromatic and neutral amino acids such as tyrosine, tryptophan, phenylalanine, histidine, proline, leucine, valine, glutamine, as well as arginine. Transports the auxins indole-3-acetic acid (IAA) and 2,4-dichlorophenoxyacetic acid (2,4-D)

TRINITY_DN257942_c1_g1	3.98	BAH1	FUNCTION: Mediates E2-dependent protein ubiquitination. Plays a role in salicylic acid-mediated negative feedback regulation of salicylic acid (SA) accumulation. May be involved in the overall regulation of SA, benzoic acid and phenylpropanoid biosynthesis. Controls the adaptability to nitrogen limitation by channeling the phenylpropanoid metabolic flux to the induced anthocyanin synthesis
TRINITY_DN220901_c0_g1	9.07	BAS1A	FUNCTION: Thiol-specific peroxidase that catalyzes the reduction of hydrogen peroxide and organic hydroperoxides to water and alcohols, respectively. Plays a role in cell protection against oxidative stress by detoxifying peroxides. May be an antioxidant enzyme particularly in the developing shoot and photosynthesizing leaf
TRINITY_DN230275_c0_g1	3.05	BAS1B	
TRINITY_DN229046_c3_g1	9.21	BAS1B	
TRINITY_DN263448_c1_g1	2.13	BECN1	FUNCTION: Required for normal plant development, pollen germination. Required for autophagic activity. Required to limit the pathogen-associated cell death response
TRINITY_DN269470_c2_g3	4.14	BGL42	FUNCTION: Involved in the secretion of root-derived phenolics upon iron ions (Fe) depletion. Promotes disease resistance toward pathogens. Required during rhizobacteria-mediated (e.g. P.fluorescens WCS417r) broad-spectrum induced systemic resistance (ISR) against several pathogens
TRINITY_DN267239_c0_g3	2.60	C81D1	Cytochrome P450 81D1 (EC 1.14.-.-)
TRINITY_DN265902_c0_g1	3.56	C81D1	
TRINITY_DN256851_c2_g2	2.49	CCT14	Cyclin-T1-4 (CycT1;4) (Protein AtCycT-like2)
TRINITY_DN262027_c0_g2	2.28	CE101	FUNCTION: Promotes the expression of genes involved in photosynthesis at least in dedifferentiated calli
TRINITY_DN268790_c1_g5	2.53	CE101	
TRINITY_DN259898_c0_g1	2.44	CER1	FUNCTION: Aldehyde decarbonylase involved in the conversion of aldehydes to alkanes. Core component of a very-long-chain alkane synthesis complex. Involved in epicuticular wax biosynthesis and pollen fertility.
TRINITY_DN246596_c0_g2	3.84	CHIA	FUNCTION: This protein functions as a defense against chitin containing fungal pathogens
TRINITY_DN248488_c3_g3	3.89	CHIA	
TRINITY_DN252720_c2_g4	2.30	CRK35	Putative cysteine-rich receptor-like protein kinase 35 (Cysteine-rich RLK35) (EC 2.7.11.-)
TRINITY_DN254705_c0_g1	3.33	CRK5	FUNCTION: Involved in multiple distinct defense responses. May function as a disease resistance (R) protein
TRINITY_DN247994_c3_g2	2.32	CRK7	Cysteine-rich receptor-like protein kinase 7 (Cysteine-rich RLK7) (EC 2.7.11.-)
TRINITY_DN247994_c3_g1	3.08	CRK7	
TRINITY_DN253246_c0_g1	2.15	CRPK1	FUNCTION: Negative regulator of freezing tolerance that phosphorylates 14-3-3 proteins (e.g. GRF6) thus triggering their translocation from the cytosol to the nucleus in response to cold stress
TRINITY_DN264297_c1_g1	2.33	CRPK1	
TRINITY_DN266066_c0_g2	2.85	DRP1E	FUNCTION: Microtubule-associated force-producing protein that is targeted to the tubulo-vesicular network of the forming cell plate during cytokinesis. Plays also a major role in plasma membrane maintenance and cell wall integrity with an implication in vesicular trafficking, polar cell expansion, and other aspects of plant growth and development
TRINITY_DN266066_c0_g1	2.90	DRP1E	
TRINITY_DN252762_c0_g2	3.14	EFR	FUNCTION: Constitutes the pattern-recognition receptor (PPR) that determines the specific perception of elongation factor Tu (EF-Tu), a potent elicitor of the defense response to pathogen-associated molecular patterns (PAMPs)
TRINITY_DN259554_c2_g1	4.96	EULS3	FUNCTION: Lectin which binds carbohydrates in vitro. Interacts through its lectin domain with some glycan structures. May play a role in abiotic stress responses (Probable). May play a role in abscisic acid-induced stomatal closure. May play a role in disease resistance against bacteria
TRINITY_DN255773_c2_g1	5.78	EULS3	
TRINITY_DN263759_c1_g2	2.15	FERON	FUNCTION: Receptor-like protein kinase that mediates the female control of male gamete delivery during fertilization, including growth cessation of compatible pollen tubes ensuring a reproductive isolation barriers, by regulating MLO7 subcellular polarization upon pollen tube perception in the female gametophyte synergids. Required for cell elongation during vegetative growth, mostly in a brassinosteroids- (BR-) independent manner. Acts as an upstream regulator for the Rac/Rop-signaling pathway that controls ROS-mediated root hair
TRINITY_DN263759_c1_g1	4.06	FERON	

			development. Seems to regulate a cross-talk between brassinosteroids and ethylene signaling pathways during hypocotyl elongation. Negative regulator of brassinosteroid response in light-grown hypocotyls, but required for brassinosteroid response in etiolated seedlings. Mediates sensitivity to powdery mildew (e.g. Golovinomyces orontii). Positive regulator of auxin-promoted growth that represses the abscisic acid (ABA) signaling via the activation of ABI2 phosphatase. Required for RALF1-mediated extracellular alkalinization in a signaling pathway preventing cell expansion.
TRINITY_DN255960_c2_g4	2.11	FRI1	FUNCTION: Stores iron in a soluble, non-toxic, readily available form. Important for iron homeostasis. Has ferroxidase activity. Iron is taken up in the ferrous form and deposited as ferric hydroxides after oxidation (By similarity)
TRINITY_DN248640_c0_g1	3.51	GDU3	FUNCTION: Probable subunit of an amino acid transporter involved in the regulation of the amino acid metabolism. Stimulates amino acid export by activating nonselective amino acid facilitators. Acts upstream genes involved in the salicylic acid (SA) pathway
TRINITY_DN262177_c0_g1	2.41	GWD1	FUNCTION: Acts as an overall regulator of starch mobilization. Required for starch degradation, suggesting that the phosphate content of starch regulates its degradability
TRINITY_DN245625_c3_g1	4.73	HSP7E	FUNCTION: In cooperation with other chaperones, Hsp70s are key components that facilitate folding of de novo synthesized proteins, assist translocation of precursor proteins into organelles, and are responsible for degradation of damaged protein under stress conditions
TRINITY_DN252185_c2_g4	8.99	HSP7E	
TRINITY_DN258901_c2_g3	2.67	HSR4	Protein HYPER-SENSITIVITY-RELATED 4 (AtHSR4) (EC 3.6.1.3) (BCS1-like protein)
TRINITY_DN239947_c0_g1	5.35	HSR4	
TRINITY_DN267302_c1_g1	2.24	IOS1	FUNCTION: Regulates negatively the abscisic acid (ABA) signaling pathway. Required for full susceptibility to filamentous (hemi)biotrophic oomycetes and fungal pathogens, probably by triggering the repression of ABA-sensitive COLD REGULATED and RESISTANCE TO DESICCATION genes during infection, but independently of immune responses. Involved in BAK1-dependent and BAK1-independent microbe-associated molecular patterns (MAMPs)-triggered immunity (PTI) leading to defense responses, including callose deposition and MAPK cascade activation, toward pathogenic bacteria. Required for chitin-mediated PTI.
TRINITY_DN268832_c2_g1	3.81	IOS1	
TRINITY_DN257134_c2_g1	3.19	IPYR6	Soluble inorganic pyrophosphatase 6, chloroplastic (EC 3.6.1.1) (Inorganic pyrophosphatase 6) (Pyrophosphate phospho-hydrolase 6) (PPase 6)
TRINITY_DN260602_c0_g1	2.10	ISPG	FUNCTION: Enzyme of the plastid non-mevalonate pathway for isoprenoid biosynthesis that converts 2-C-methyl-D-erythritol 2,4-cyclodiphosphate (Me-2,4cPP) into 1-hydroxy-2-methyl-2-(E)-butenyl 4-diphosphate. Is essential for chloroplast development and required for the salicylic acid (SA)-mediated disease resistance to biotrophic pathogens
TRINITY_DN253825_c1_g1	2.50	LRKS4	FUNCTION: Involved in resistance response to the pathogenic oomycetes and to the pathogenic bacteria
TRINITY_DN267363_c3_g1	5.06	MD37D	FUNCTION: Component of the Mediator complex, a coactivator involved in the regulated transcription of nearly all RNA polymerase II-dependent genes. Mediator functions as a bridge to convey information from gene-specific regulatory proteins to the basal RNA polymerase II transcription machinery. The Mediator complex, having a compact conformation in its free form, is recruited to promoters by direct interactions with regulatory proteins and serves for the assembly of a functional preinitiation complex with RNA polymerase II and the general transcription factors (By similarity). FUNCTION: In cooperation with other chaperones, Hsp70s are key components that facilitate folding of de novo synthesized proteins, assist translocation of precursor proteins into organelles, and are responsible for degradation of damaged protein under stress conditions.
TRINITY_DN265380_c1_g4	6.81	MD37D	
TRINITY_DN268959_c1_g3	2.43	NPR1	FUNCTION: May act as a substrate-specific adapter of an E3 ubiquitin-protein ligase complex (CUL3-RBX1-BTB) which mediates the ubiquitination and subsequent proteasomal degradation of target proteins (By similarity). Key positive regulator of the SA-dependent signaling pathway that negatively regulates JA-dependent signaling pathway. Mediates the binding of TGA factors to the as-1 motif found in the pathogenesis-related PR-1 gene, leading to the transcriptional regulation of the gene defense. Controls the onset of systemic acquired resistance

			(SAR). Upon SAR induction, a biphasic change in cellular reduction potential occurs, resulting in reduction of the cytoplasmic oligomeric form to a monomeric form that accumulates in the nucleus and activates gene expression. Phosphorylated form is target of proteasome degradation
TRINITY_DN261612_c0_g5	4.69	NRPD2	FUNCTION: DNA-dependent RNA polymerase catalyzes the transcription of DNA into RNA using the four ribonucleoside triphosphates as substrates. Proposed to contribute to the polymerase catalytic activity and forms the polymerase active center together with the largest subunit. Also required for full erasure of methylation when the RNA trigger is withdrawn. Required for intercellular RNA interference (RNAi) leading to systemic post-transcriptional gene silencing. Involved in the maintenance of post-transcriptional RNA silencing. During interphase, mediates siRNA-independent heterochromatin association and methylation into chromocenters and condensation and cytosine methylation at pericentromeric major repeats. Required for complete maintenance of the 35S promoter homology-dependent TGS in transgenic plants and for the initial establishment of DNA methylation
TRINITY_DN253577_c4_g1	5.24	PCKA	Phosphoenolpyruvate carboxykinase (ATP) (PEP carboxykinase) (PEPCK) (EC 4.1.1.49)
TRINITY_DN262564_c0_g1	2.39	PCRK1	FUNCTION: Involved in the activation of early immune responses. Plays a role in pattern-triggered immunity (PTI) induced by pathogen-associated molecular patterns (PAMPs) and damage-associated molecular patterns (DAMPs).
TRINITY_DN246707_c1_g1	6.13	PER53	FUNCTION: Removal of hydrogen peroxide, oxidation of toxic reductants, biosynthesis and degradation of lignin, suberization, auxin catabolism, response to environmental stresses such as wounding, pathogen attack and oxidative stress. These functions might be dependent on each isozyme/isoform in each plant tissue.
TRINITY_DN251687_c1_g1	7.57	PGKY3	Phosphoglycerate kinase 3, cytosolic (EC 2.7.2.3)
TRINITY_DN240782_c7_g1	2.36	PLDB1	FUNCTION: Hydrolyzes glycerol-phospholipids at the terminal phosphodiesteric bond to generate phosphatidic acids (PA). Plays an important role in various cellular processes, including phytohormone action, vesicular trafficking, secretion, cytoskeletal arrangement, meiosis, tumor promotion, pathogenesis, membrane deterioration and senescence. Modulates defense responses to bacterial and fungal pathogens
TRINITY_DN269024_c0_g1	2.88	PLDB1	
TRINITY_DN251887_c2_g3	3.51	PLDB1	
TRINITY_DN254637_c0_g1	2.66	PR5K	FUNCTION: Possesses kinase activity in vitro
TRINITY_DN264338_c1_g3	3.41	PR5K	
TRINITY_DN268049_c2_g1	5.94	PR5K	
TRINITY_DN245797_c0_g5	7.72	PRB1	FUNCTION: Probably involved in the defense reaction of plants against pathogens
TRINITY_DN269300_c4_g1	2.03	PTR36	Probable peptide/nitrate transporter At3g43790 (Protein ZINC INDUCED FACILITATOR-LIKE 2)
TRINITY_DN250124_c0_g1	3.39	PTR36	
TRINITY_DN269875_c1_g3	3.66	PTR36	
TRINITY_DN269875_c1_g1	4.29	PTR36	
TRINITY_DN249309_c0_g2	2.42	RAP23	FUNCTION: Probably acts as a transcriptional activator. Binds to the GCC-box pathogenesis-related promoter element. May be involved in the regulation of gene expression by stress factors and by components of stress signal transduction pathways (By similarity)
TRINITY_DN255972_c2_g4	2.18	RENT2	FUNCTION: Recruited by UPF3 associated with the EJC core at the cytoplasmic side of the nuclear envelope and the subsequent formation of an UPF1-UPF2-UPF3 surveillance complex (including UPF1 bound to release factors at the stalled ribosome) is believed to activate NMD. In cooperation with UPF3 stimulates both ATPase and RNA helicase activities of UPF1. Binds spliced mRNA (By similarity). Involved in nonsense-mediated decay (NMD) of mRNAs containing premature stop codons by associating with the nuclear exon junction complex (EJC). Required for plant development and adaptation to environmental stresses, including plant defense and response to wounding
TRINITY_DN253650_c0_g1	2.96	RENT2	
TRINITY_DN259644_c1_g1	5.54	SAG12	FUNCTION: Cysteine protease that may have a developmental senescence specific cell death function during apoptosis, heavy metal detoxification, and hypersensitive response
TRINITY_DN254997_c0_g3	2.19	TET8	FUNCTION: May be involved in the regulation of cell differentiation

TRINITY_DN264416_c1_g1	2.37	TGA1	FUNCTION: Transcriptional activator that binds specifically to the DNA sequence 5'-TGACG-3'. Binding to the as-1-like cis elements mediate auxin- and salicylic acid-inducible transcription. May be involved in the induction of the systemic acquired resistance (SAR) via its interaction with NPR1
TRINITY_DN269605_c3_g2	2.63	TGA3	FUNCTION: Transcriptional activator that binds specifically to the DNA sequence 5'-TGACG-3'. Recognizes ocs elements like the as-1 motif of the cauliflower mosaic virus 35S promoter. Binding to the as-1-like cis elements mediate auxin- and salicylic acid-inducible transcription. Required to induce the systemic acquired resistance (SAR) via the regulation of pathogenesis-related genes expression. Binding to the as-1 element of PR-1 promoter is salicylic acid-inducible and mediated by NPR1.
TRINITY_DN269154_c2_g2	2.45	TGA9	FUNCTION: Together with TGA10, basic leucine-zipper transcription factor required for anther development. Required for signaling responses to pathogen-associated molecular patterns (PAMPs) such as flg22 that involves chloroplastic reactive oxygen species (ROS) production and subsequent expression of hydrogen peroxide-responsive genes
TRINITY_DN223389_c0_g1	6.06	WAKLI	FUNCTION: Serine/threonine-protein kinase that may function as a signaling receptor of extracellular matrix component. Required during plant's response to pathogen infection
TRINITY_DN249459_c2_g3	3.26	WRK50	FUNCTION: Transcription factor. Interacts specifically with the W box (5'-(T)TGAC[CT]-3'), a frequently occurring elicitor-responsive cis-acting element (By similarity)
TRINITY_DN267640_c2_g1	3.35	WRK53	FUNCTION: Transcription factor. Interacts specifically with the W box (5'-(T)TGAC[CT]-3'), a frequently occurring elicitor-responsive cis-acting element. May regulate the early events of leaf senescence Negatively regulates the expression of ESR/ESP. Together with WRKY46 and WRKY70, promotes resistance to bacteria, probably by enhancing salicylic acid (SA)- dependent genes. Contributes to the suppression of jasmonic acid (MeJA)-induced expression of PDF1.2.
TRINITY_DN255329_c1_g2	3.47	WRK53	
TRINITY_DN259059_c2_g1	2.61	Y1743	Probable LRR receptor-like serine/threonine-protein kinase At1g74360 (EC 2.7.11.1)
TRINITY_DN267959_c1_g4	2.28	YSL3	FUNCTION: May be involved in the lateral transport of nicotianamine-chelated metals in the vasculature
TRINITY_DN240038_c0_g1	3.47	ZIF1	FUNCTION: Major facilitator superfamily (MFS) transporter involved in zinc tolerance by participating in vacuolar sequestration of zinc

REFERENCES

1. Adie, B. A. T., Pérez-Pérez, J., Pérez-Pérez, M. M., Godoy, M., Sánchez-Serrano, J. J., Schmelz, E. A., and Solano, R. 2007. ABA is an essential signal for plant resistance to pathogens affecting JA biosynthesis and the activation of defenses in *Arabidopsis*. Plant Cell 19:1665-1681.

2. Afzal, A. J., da Cunha, L., and Mackey, D. 2011. Separable fragments and membrane tethering of *Arabidopsis* RIN4 regulate its suppression of PAMP-triggered immunity. Plant Cell 23:3798-3811.

3. Aguileta, G., de Vienne, D. M., Ross, O. N., Hood, M. E., Giraud, T., Petit, E., and Gabaldón, T. 2014. High variability of mitochondrial gene order among fungi. Genome Biology and Evolution 6:451-465.

4. Ahn, I. P., Kim, S., Lee, Y. H., and Suh, S. C. 2007. Vitamin B1-induced priming is dependent on hydrogen peroxide and the NPR1 gene in *Arabidopsis*. Plant Physiol 143:838-848.

5. Aimanianda, V., Bayry, J., Bozza, S., Kniemeyer, O., Perruccio, K., Elluru, S. R., Clavaud, C., Paris, S., Brakhage, A. A., Kaveri, S. V., Romani, L., and Latge, J. P. 2009. Surface hydrophobin prevents immune recognition of airborne fungal spores. Nature 460:1117-1121.

6. Allan, A. C., and Fluhr, R. 1997. Two distinct sources of elicited reactive oxygen species in tobacco epidermal cells. Plant Cell 9:1559-1572.

7. Alves, M. S., Dadalto, S. P., Gonçalves, A. B., de Souza, G. B., Barros, V. A., and Fietto, L. G. 2014. Transcription factor functional protein-protein interactions in plant defense responses. Proteomes 2:85-106.

8. Andlar, M., Rezić, T., Marđetko, N., Kracher, D., Ludwig, R., and Šantek, B. 2018. Lignocellulose degradation: An overview of fungi and fungal enzymes involved in lignocellulose degradation. Engineering in Life Sciences 18:768-778.

9. Andrews, S. 2010. FastQC: a quality control tool for high throughput sequence data. Available online at: http://www.bioinformatics.babraham.ac.uk/projects/fastqc.

10. Anonymous. 1960. Index of Plant Diseases in the United States. U.S.D.A. Agric. Handb. 165:1-531.

11. Arnaud, M. B., Cerqueira, G. C., Inglis, D. O., Skrzypek, M. S., Binkley, J., Chibucos, M. C., Crabtree, J., Howarth, C., Orvis, J., Shah, P., Wymore, F., Binkley, G., Miyasato, S. R., Simison, M., Sherlock, G., and Wortman, J. R. 2012. The Aspergillus Genome Database (AspGD): recent developments in comprehensive multispecies curation, comparative genomics and community resources. Nucleic Acids Research 40:D653-D659.

12. Asada, K. 2006. Production and scavenging of reactive oxygen species in chloroplasts and their functions. Plant Physiol 141:391-396.

13. Asai, T., Tena, G., Plotnikova, J., Willmann, M. R., Chiu, W. L., Gomez-Gomez, L., Boller, T., Ausubel, F. M., and Sheen, J. 2002. MAP kinase signalling cascade in *Arabidopsis* innate immunity. Nature 415:977-983.

14. Ashtamker, C., Kiss, V., Sagi, M., Davydov, O., and Fluhr, R. 2007. Diverse subcellular locations of cryptogein-induced reactive oxygen species production in tobacco Bright Yellow-2 cells. Plant Physiol 143:1817-1826.

15. Axtell, M. J., and Staskawicz, B. J. 2003. Initiation of RPS2-specified disease resistance in *Arabidopsis* is coupled to the AvrRpt2-directed elimination of RIN4. Cell 112:369-377.

16. Aylward, J., Steenkamp, E. T., Dreyer, L. L., Roets, F., Wingfield, B. D., and Wingfield, M. J. 2017. A plant pathology perspective of fungal genome sequencing. IMA fungus 8:1-15.

17. Backer, R., Naidoo, S., and van den Berg, N. 2019. The NONEXPRESSOR OF PATHOGENESIS-RELATED GENES 1 (NPR1) and related family: mechanistic insights in plant disease resistance. Frontiers in Plant Science 10:102.

18. Bajaj, R., Huang, Y., Gebrechristos, S., Mikolajczyk, B., Brown, H., Prasad, R., Varma, A., and Bushley, K. E. 2018. Transcriptional responses of soybean roots to colonization with the root endophytic fungus *Piriformospora indica* reveals altered phenylpropanoid and secondary metabolism. Scientific Reports 8:10227.

19. Baker, C. J., and Orlandi, E. W. 1995. Active oxygen in plant pathogenesis. Annu Rev Phytopathol 33:299-321.

20. Balazadeh, S., Parlitz, S., Mueller-Roeber, B., and Meyer, R. C. 2008. Natural developmental variations in leaf and plant senescence in *Arabidopsis thaliana*. Plant Biology 10:136-147.

21. Bankevich, A., Nurk, S., Antipov, D., Gurevich, A. A., Dvorkin, M., Kulikov, A. S., Lesin, V. M., Nikolenko, S. I., Pham, S., Prjibelski, A. D., Pyshkin, A. V., Sirotkin, A. V., Vyahhi, N., Tesler, G., Alekseyev, M. A., and Pevzner, P. A. 2012. SPAdes: a new genome assembly algorithm and its applications to single-cell sequencing. Journal of Computational Biology 19:455-477.

22. Bari, R., and Jones, J. D. 2009. Role of plant hormones in plant defence responses. Plant Mol Biol 69:473-488.

23. Bayry, J., Aimanianda, V., Guijarro, J. I., Sunde, M., and Latge, J. P. 2012. Hydrophobins--unique fungal proteins. PLoS Pathog 8:e1002700.

24. Beers, E. P. 1997. Programmed cell death during plant growth and development. Cell Death and Differentiation 4:649-661.

25. Bellin, D., Asai, S., Delledonne, M., and Yoshioka, H. 2013. Nitric oxide as a mediator for defense responses. Molecular Plant-Microbe Interactions 26:271-277.

26. Bigeard, J., Colcombet, J., and Hirt, H. 2015. Signaling mechanisms in Pattern-Triggered Immunity (PTI). Molecular Plant 8:521-539.

27. Birker, D., Heidrich, K., Takahara, H., Narusaka, M., Deslandes, L., Narusaka, Y., Reymond, M., Parker, J. E., and O'connell, R. 2009. A locus conferring resistance to *Colletotrichum higginsianum* is shared by four geographically distinct *Arabidopsis* accessions. Plant Journal 60:602-613.

28. Bohlool, B. B., and Schmidt, E. L. 1974. Lectins: A possible basis for specificity in the *Rhizobium*-legume root nodule symbiosis. Science 185:269-271.

29. Bolger, A. M., Lohse, M., and Usadel, B. 2014. Trimmomatic: a flexible trimmer for Illumina sequence data. Bioinformatics 30:2114-2120.

30. Boller, T., and Felix, G. 2009. A renaissance of elicitors: perception of microbe-associated molecular patterns and danger signals by pattern-recognition receptors. Annu Rev Plant Biol 60:379-406.

31. Boraston, A. B., Bolam, D. N., Gilbert, H. J., and Davies, G. J. 2004. Carbohydrate-binding modules: fine-tuning polysaccharide recognition. The Biochemical Journal 382:769-781.

32. Bradford, M. M. 1976. A rapid and sensitive method for the quantitation of microgram quantities of protein utilizing the principle of protein-dye binding. Analytical Biochemistry 72:248-254.

33. Bringans, S., Hane, J. K., Casey, T., Tan, K.-C., Lipscombe, R., Solomon, P. S., and Oliver, R. P. 2009. Deep proteogenomics; high throughput gene validation by multidimensional liquid chromatography and mass spectrometry of proteins from the fungal wheat pathogen *Stagonospora nodorum*. BMC Bioinformatics 10:301.

34. Broekaert, W. F., Terras, F. R. G., and Cammue, B. P. A. 2000. Induced and Preformed Antimicrobial Proteins. Pages 371-477. In: Mechanisms of Resistance to Plant Diseases. A. J. Slusarenko, R. S. S. Fraser and L. C. van Loon, eds. Springer Netherlands, Dordrecht.

35. Busey, P., and Myers, B. J. 1979. Growth rates of turfgrasses propagated vegetatively. Agronomy Journal 71:817-821.

36. Caarls, L., Pieterse, C. M. J., and Van Wees, S. C. M. 2015. How salicylic acid takes transcriptional control over jasmonic acid signaling. Frontiers in Plant Science 6:170.

37. Caasi, O. C., Walker, N. R., Marek, S. M., Enis, J. N., and Mitchell, T. K. 2010. Infection and colonization of turf-type bermudagrass by Ophiosphaerella herpotricha expressing green or red fluorescent proteins. Phytopathology 100:415-423.

38. Caillaud, M.-C., Asai, S., Rallapalli, G., Piquerez, S., Fabro, G., and Jones, J. D. G. 2013. A downy mildew effector attenuates salicylic acid-triggered immunity in *Arabidopsis* by interacting with the host mediator complex. PLoS biology 11:e1001732-e1001732.

39. Camara, M. P. S., O'Neill, N. R., van Berkum, P., and Dernoeden, P. H. 2000. *Ophiosphaerella agrostis* sp. nov. and its relationship to other *Ophiosphaerella* species pathogenic to grasses. Mycologia 92:317-325.

40. Campos, M. L., Kang, J.-H., and Howe, G. A. 2014. Jasmonate-triggered plant immunity. Journal of Chemical Ecology 40:657-675.

41. Cantarel, B. L., Coutinho, P. M., Rancurel, C., Bernard, T., Lombard, V., and Henrissat, B. 2009. The Carbohydrate-Active EnZymes database (CAZy): an expert resource for glycogenomics. Nucleic Acids Research 37:D233-D238.

42. Capella-Gutierrez, S., Silla-Martinez, J. M., and Gabaldon, T. 2009. trimAl: a tool for automated alignment trimming in large-scale phylogenetic analyses. Bioinformatics 25:1972-1973.

43. Carlile, A. J., Bindschedler, L. V., Bailey, A. M., Bowyer, P., Clarkson, J. M., and Cooper, R. M. 2000. Characterization of SNP1, a cell wall-degrading trypsin, produced during infection by *Stagonospora nodorum*. Molecular Plant-Microbe Interactions 13:538-550.

44. Caspary, M. R. 1865. Remarks on the protective sheath and on the formation of the stem of the root. Annals and Magazine of Natural History 16:382-383.

45. Catanzariti, A.-M., Dodds, P. N., Ve, T., Kobe, B., Ellis, J. G., and Staskawicz, B. J. 2010. The AvrM effector from flax rust has a structured C-terminal domain and interacts directly with the M resistance protein. Molecular Plant-Microbe Interactions 23:49-57.

46. Cesari, S., Bernoux, M., Moncuquet, P., Kroj, T., and Dodds, P. N. 2014. A novel conserved mechanism for plant NLR protein pairs: the "integrated decoy" hypothesis. Frontiers in Plant Science 5:606.

47. Cesari, S., Kanzaki, H., Fujiwara, T., Bernoux, M., Chalvon, V., Kawano, Y., Shimamoto, K., Dodds, P., Terauchi, R., and Kroj, T. 2014. The NB - LRR proteins RGA 4 and RGA 5 interact functionally and physically to confer disease resistance. EMBO Journal 33:1941-1959.

48. Cesari, S., Thilliez, G., Ribot, C., Chalvon, V., Michel, C., Jauneau, A., Rivas, S., Alaux, L., Kanzaki, H., Okuyama, Y., Morel, J.-B., Fournier, E., Tharreau, D., Terauchi, R., and Kroj, T. 2013. The rice resistance protein pair RGA4/RGA5 recognizes the *Magnaporthe oryzae* effectors AVR-Pia and AVR1-CO39 by direct binding. The Plant Cell 25:1463-1481.

49. Chaisson, M. J., and Tesler, G. 2012. Mapping single molecule sequencing reads using basic local alignment with successive refinement (BLASR): application and theory. BMC Bioinformatics 13:238.

50. Charpenteau, M., Jaworski, K., Ramirez, B. C., Tretyn, A., Ranjeva, R., and Ranty, B. 2004. A receptor-like kinase from *Arabidopsis thaliana* is a calmodulin-binding protein. Biochemical Journal 379:841-848.

51. Chen, S., Songkumarn, P., Venu, R. C., Gowda, M., Bellizzi, M., Hu, J., Liu, W., Ebbole, D., Meyers, B., Mitchel, T., and Wang, G. L. 2013. Identification and characterization of in planta-expressed secreted effector proteins from *Magnaporthe oryzae* that induce cell death in rice. Molecular Plant-Microbe Interactions 26:191-202.

52. Chinchilla, D., Bauer, Z., Regenass, M., Boller, T., and Felix, G. 2006. The *Arabidopsis* receptor kinase FLS2 binds flg22 and determines the specificity of flagellin perception. Plant Cell 18:465-476.

53. Christians, N. E. 2007. Fundamentals of turfgrass management. 3rd ed. John Wiley & Sons, Hoboken, NJ.

54. Christians, N. E., and Engelke, M. C. 1994. Choosing the right grass to fit the environment. In: Handbook of Integrated Pest Management for Turfgrass and Ornamentals. Lewis Publishers, Boca Raton, FL.

55. Coll, N. S., Epple, P., and Dangl, J. L. 2011. Programmed cell death in the plant immune system. Cell Death Differ 18:1247-1256.

56. Collemare, J., Pianfetti, M., Houlle, A. E., Morin, D., Camborde, L., Gagey, M. J., Barbisan, C., Fudal, I., Lebrun, M. H., and Bohnert, H. U. 2008. *Magnaporthe grisea* avirulence gene ACE1 belongs to an infection-specific gene cluster involved in secondary metabolism. New Phytol 179:196-208.

57. Condon, B. J., Leng, Y., Wu, D., Bushley, K. E., Ohm, R. A., Otillar, R., Martin, J., Schackwitz, W., Grimwood, J., MohdZainudin, N., Xue, C., Wang, R., Manning, V. A., Dhillon, B., Tu, Z. J., Steffenson, B. J., Salamov, A., Sun, H., Lowry, S., LaButti, K., Han, J., Copeland, A., Lindquist, E., Barry, K., Schmutz, J., Baker, S. E., Ciuffetti, L. M., Grigoriev, I. V., Zhong, S., and Turgeon, B. G. 2013. Comparative genome structure, secondary metabolite, and effector coding capacity across *Cochliobolus* pathogens. PLoS genetics 9:e1003233-e1003233.

58. Conrath, U., Beckers, G. J. M., Langenbach, C. J. G., and Jaskiewicz, M. R. 2015. Priming for Enhanced Defense. Annual Review of Phytopathology 53:97-119.

59. Corina Vlot, A., Dempsey, D. A., and Klessig, D. F. 2009. Salicylic acid, a multifaceted hormone to combat disease. Annual Review of Phytopathology 47:177-206.

60. Crahay, J. N., Derdoeden, P. H., and O'Neill, N. R. 1988. Growth and pathogenicity of *Leptosphaeria korrae* in bermudagrass. Plant Disease 72:945-949.

61. Dale, J. L., and Diaz, C. 1963. A new disease of bermudagrass turf. Arkansas Farm Research 12:6.

62. Dangl, J. L., and Jones, J. D. G. 2001. Plant pathogens and integrated defence responses to infection. Nature 411:826-833.

63. Dangl, J. L., and McDowell, J. M. 2006. Two modes of pathogen recognition by plants. Proceedings of the National Academy of Sciences 103:8575.

64. De Coninck, B., Timmermans, P., Vos, C., Cammue, B. P., and Kazan, K. 2015. What lies beneath: belowground defense strategies in plants. Trends Plant Sci 20:91-101.

65. De Jonge, R., Bolton, M. D., and Thomma, B. P. 2011. How filamentous pathogens co-opt plants: the ins and outs of fungal effectors. Curr Opin Plant Biol 14:400-406.

66. De Jonge, R., Van Esse, H. P., Kombrink, A., Joosten, M. H. A. J., Thomma, B. P. H. J., Shinya, T., Desaki, Y., Shibuya, N., Bours, R., and Van Der Krol, S. 2010. Conserved fungal LysM effector Ecp6 prevents chitin-triggered immunity in plants. Science 329:953-955.

67. De Vleesschauwer, D., Xu, J., and Höfte, M. 2014. Making sense of hormone-mediated defense networking: From rice to *Arabidopsis*. Frontiers in Plant Science 5:611.

68. De Wit, P. J. 2007. How plants recognize pathogens and defend themselves. Cellular and Molecular Life Sciences 64:2726-2732.

69. De-La-Peña, C., Badri, D. V., Lei, Z., Watson, B. S., Brandão, M. M., Silva-Filho, M. C., Sumner, L. W., and Vivanco, J. M. 2010. Root secretion of defense-related proteins is development-dependent and correlated with flowering time. The Journal of Biological Chemistry 285:30654.

70. De-La-Peña, C., Lei, Z., Watson, B. S., Sumner, L. W., and Vivanco, J. M. 2008. Root-microbe communication through protein secretion. The Journal of Biological Chemistry 283:25247.

71. Dean, R. A., Talbot, N. J., Ebbole, D. J., Farman, M. L., Mitchell, T. K., Orbach, M. J., Thon, M., Kulkarni, R., Xu, J.-R., Pan, H., Read, N. D., Lee, Y.-H., Carbone, I., Brown, D., Oh, Y. Y., Donofrio, N., Jeong, J. S., Soanes, D. M., Djonovic, S., Kolomiets, E., Rehmeyer, C., Li, W., Harding, M., Kim, S., Lebrun, M.-H., Bohnert, H., Coughlan, S., Butler, J., Calvo, S., Ma, L.-J., Nicol, R., Purcell, S., Nusbaum, C., Galagan, J. E., and Birren, B. W. 2005. The genome sequence of the rice blast fungus *Magnaporthe grisea*. Nature 434:980-986.

72. Dennis, R. W. G. 1978. British Ascomycetes. J. Cramer, Vaduz.

73. Dernoeden, P. H., Crahay, J. N., and Davis, D. B. 1991. Spring dead spot and bermudagrass quality as influenced by nitrogen source and potassium. Crop Science 31:1674-1680.

74. Deshmukh, S., Hückelhoven, R., Schäfer, P., Imani, J., Sharma, M., Weiss, M., Waller, F., and Kogel, K.-H. 2006. The root endophytic fungus *Piriformospora indica* requires host cell death for proliferation during mutualistic symbiosis with barley. Proceedings of the National Academy of Sciences of the United States of America 103:18450.

75. Desikan, R., A.-H.-Mackerness, S., Hancock, J. T., and Neill, S. J. 2001. Regulation of the *Arabidopsis* transcriptome by oxidative stress. Plant Physiology 127:159-172.

76. Desikan, R., Hancock, J. T., Bright, J., Harrison, J., Weir, I., Hooley, R., and Neill, S. J. 2005. A role for ETR1 in hydrogen peroxide signaling in stomatal guard cells. Plant Physiology 137:831-834.

77. Dodds, P. N., and Rathjen, J. P. 2010. Plant immunity: towards an integrated view of plant–pathogen interactions. Nature Reviews Genetics 11:539.

78. Dodds, P. N., Lawrence, G. J., Catanzariti, A. M., Teh, T., Wang, C. I. A., Ayliffe, M. A., Kobe, B., and Ellis, J. G. 2006. Direct protein interaction underlies gene-for-gene specificity and coevolution of the flax resistance genes and flax rust avirulence genes. Proceedings of the National Academy of Sciences of the United States of America 103:8888-8893.

79. Dodds, P., Lawrence, G., Ayliffe, M., and Ellis, J. 2004. The *Melampsora lini* AvrL567 avirulence genes are expressed in haustoria and their products are recognized inside plant cells. Plant Cell 16:755-768.

80. Doidge, E. M. 1950. The South African fungi and lichens to the end of 1945. Bothalica 5:1-1094.

81. Doornbos, R., Loon, L., and Bakker, P. 2012. Impact of root exudates and plant defense signaling on bacterial communities in the rhizosphere. A review. Agronomy for Sustainable Development 32:227-243.

82. Douglas, P. 2018. TransDecoder (Find Coding Regions Within Transcripts). Available from: https://github.com/TransDecoder/TransDecoder/wiki.

83. Eaton, C. J., Cox, M. P., and Scott, B. 2011. What triggers grass endophytes to switch from mutualism to pathogenism? Plant Science 180:190-195.

84. Edgar, R. C. 2004. MUSCLE: multiple sequence alignment with high accuracy and high throughput. Nucleic Acids Research 32:1792-1797.

85. Endo, R. M., Ohr, H. D., and Krausman, E. M. 1984. The cause of spring dead spot disease (SDS) of *Cynodon dactylon* (L) Pers. in California. Phytopathology 74:812.

86. Endo, R. M., Ohr, H. D., and Krausman, E. M. 1985. *Leptosphaeria korrae*, a cause of the spring dead spot disease of bermudagrass in California. Plant Disease 69:235-237.

87. Erwig, J., Ghareeb, H., Kopischke, M., Hacke, R., Matei, A., Petutschnig, E., and Lipka, V. 2017. Chitin-induced and chitin elicitor receptor kinase1 (CERK1) phosphorylation-dependent endocytosis of *Arabidopsis thaliana* lysin motif-containing receptor-like kinase5 (LYK5). New Phytologist 215:382-396.

88. Evert, R. F. 2013. Raven Biology of plants. Eighth edition.. ed. New York : W.H. Freeman and Company Publishers, New York.

89. Farr, D. F., and Rossman, A. Y. Fungal Databases, Systematic Mycology and Microbiology Laboratory. U.S. National Fungus Collections, ARS, USDA. Retrieved August 8, 2018, from https://nt.ars-grin.gov/fungaldatabases/.

90. Fedoroff, N. 2006. Redox regulatory mechanisms in cellular stress responses. Annals of Botany 98:289-300.

91. Felix, G., Duran, J. D., Volko, S., and Boller, T. 1999. Plants have a sensitive perception system for the most conserved domain of bacterial flagellin. Plant J 18:265-276.

92. Felix, G., Regenass, M., and Boller, T. 1993. Specific perception of subnanomolar concentrations of chitin fragments by tomato cells: induction of extracellular alkalinization, changes in protein phosphorylation, and establishment of a refractory state. The Plant Journal 4:307-316.

93. Flor, H. H. 1971. Current Status of the Gene-For-Gene Concept. Annual Review of Phytopathology 9:275-296.

94. Flores, F. 2014. Etiology of spring dead spot of bermudagrass (Order No. 3727702), Available from ProQuest Dissertations & Theses Global. (1733691360). Retrieved from http://argo.library.okstate.edu/login?url=https://search-proquest-com.argo.library.okstate.edu/docview/1733691360?accountid=4117.

95. Flores, F. J., Marek, S. M., Anderson, J. A., Mitchell, T. K., and Walker, N. R. 2015. Infection and colonization of several bermudagrasses by Ophiosphaerella korrae. Phytopathology 105:656-661.

96. Flores, F. J., Marek, S. M., Orquera, G., and Walker, N. R. 2017. Molecular identification and multilocus phylogeny of species associated with spring dead spot of bermudagrass. Crop Science 57:1-13.

97. Flores, F., Marek, S., Anderson, J., Mitchell, T., and Walker, N. 2016. Reactive oxygen species production in response to Ophiosphaerella spp. colonization of bermudagrass roots. Acta Horticulturae 1122:41-48.

98. Foley, R. C., Gleason, C. A., Anderson, J. P., Hamann, T., and Singh, K. B. 2013. Genetic and genomic analysis of *Rhizoctonia solani* interactions with *Arabidopsis*; Evidence of resistance mediated through NADPH oxidases. PLoS ONE 8.

99. Frazee, A. C., Pertea, G., Jaffe, A. E., Langmead, B., Salzberg, S. L., and Leek, J. T. 2015. Ballgown bridges the gap between transcriptome assembly and expression analysis. Nature Biotechnology 33:243-246.

100. Friesen, T. L., Faris, J. D., Solomon, P. S., and Oliver, R. P. 2008. Host-specific toxins: effectors of necrotrophic pathogenicity. Cell Microbiol 10:1421-1428.

101. Friesen, T. L., Meinhardt, S. W., and Faris, J. D. 2007. The *Stagonospora nodorum*-wheat pathosystem involves multiple proteinaceous host-selective toxins and corresponding host sensitivity genes that interact in an inverse gene-for-gene manner. Plant J 51:681-692.

102. Fu, Z. Q., and Dong, X. 2013. Systemic acquired resistance: Turning local infection into global defense. Annual Review of Plant Biology 64:839-863.

103. Fu, Z. Q., Guo, M., Jeong, B.-r., Tian, F., Elthon, T. E., Cerny, R. L., Staiger, D., and Alfano, J. R. 2007. A type III effector ADP-ribosylates RNA-binding proteins and quells plant immunity. Nature 447:284.

104. Galagan, J. E., Calvo, S. E., Cuomo, C., Ma, L.-J., Wortman, J. R., Batzoglou, S., Lee, S.-I., Baştürkmen, M., Spevak, C. C., Clutterbuck, J., Kapitonov, V., Jurka, J., Scazzocchio, C., Farman, M., Butler, J., Purcell, S., Harris, S., Braus, G. H., Draht, O., Busch, S., D'Enfert, C., Bouchier, C., Goldman, G. H., Bell-Pedersen, D., Griffiths-Jones, S., Doonan, J. H., Yu, J., Vienken, K., Pain, A., Freitag, M., Selker, E. U., Archer, D. B., Peñalva, M. Á., Oakley, B. R., Momany, M., Tanaka, T., Kumagai, T., Asai, K., Machida, M., Nierman, W. C., Denning, D. W., Caddick, M., Hynes, M., Paoletti, M., Fischer, R., Miller, B., Dyer, P., Sachs, M. S., Osmani, S. A., and Birren, B. W. 2005. Sequencing of *Aspergillus nidulans* and comparative analysis with *A. fumigatus* and *A. oryzae*. Nature 438:1105-1115.

105. Galhano, R., Illana, A., Ryder, L. S., Rodríguez-Romero, J., Demuez, M., Badaruddin, M., Martinez-Rocha, A. L., Soanes, D. M., Studholme, D. J., Talbot, N. J., and Sesma, A. 2017. Tpc1 is an important Zn(II)2Cys6 transcriptional regulator required for polarized growth and virulence in the rice blast fungus. PLoS Pathogens 13(7):e1006516.

106. Galletti, R., Ferrari, S., and de Lorenzo, G. 2011. *Arabidopsis* MPK3 and MPK6 play different roles in basal and oligogalacturonide-or flagellin-induced resistance against *Botrytis cinerea*. Plant Physiology 157:804-814.

107. Gao, Q.-M., Zhu, S., Kachroo, P., and Kachroo, A. 2015. Signal regulators of systemic acquired resistance. Frontiers in Plant Science 6:228.

108. Gapper, C., and Dolan, L. 2006. Control of plant development by reactive oxygen species. Plant Physiology 141:341-345.

109. Gay, N. J., and Gangloff, M. 2007. Structure and function of Toll receptors and their ligands. Annual Review of Biochemistry 76:141.

110. Geldner, N. 2013. Casparian strips. Current Biology 23:R1025-R1026.

111. Geldner, N. 2013. The Endodermis. Annual Review of Plant Biology 64:531-558.

112. Ghassemi-Golezani, K., and Farhangi-Abriz, S. 2018. Foliar sprays of salicylic acid and jasmonic acid stimulate H+-ATPase activity of tonoplast, nutrient uptake and salt tolerance of soybean. Ecotoxicology and Environmental Safety 166:18-25.

113. Ginns, J. H. 1986. Compendium of plant diseases and decay fungi in Canada 1960-1980. Res. Br. Can. Agric. Publ. 1813:416.

114. Gómez-Gómez, L., and Boller, T. 2000. FLS2: An LRR receptor-like kinase involved in the perception of the bacterial elicitor flagellin in *Arabidopsis*. Molecular Cell 5:1003-1011.

115. Gómez-Gómez, L., Felix, G., and Boller, T. 1999. A single locus determines sensitivity to bacterial flagellin in *Arabidopsis thaliana*. Plant Journal 18:277-284.

116. Grabherr, M. G., Haas, B. J., Yassour, M., Levin, J. Z., Thompson, D. A., Amit, I., Adiconis, X., Fan, L., Raychowdhury, R., Zeng, Q., Chen, Z., Mauceli, E., Hacohen, N., Gnirke, A., Rhind, N., di Palma, F., Birren, B. W., Nusbaum, C., Lindblad-Toh, K., Friedman, N., and Regev, A. 2011. Full-length transcriptome assembly from RNA-Seq data without a reference genome. Nature biotechnology 29:644-652.

117. Grant, J. J., and Loake, G. J. 2000. Role of reactive oxygen intermediates and cognate redox signaling in disease resistance. Plant Physiology 124:21-29.

118. Green II, D. E., Fry, J. D., Pair, J. C., and Tisserat, N. A. 1993. Pathogenicity of *Rhizoctonia solani* AG-2-2 and *Ophiosphaerella herpotricha* on zoysiagrass. Plant Disease 77:1040-1044.

119. Grigoriev, I. V., Cullen, D., Goodwin, S. B., Hibbett, D., Jeffries, T. W., Kubicek, C. P., Kuske, C., Magnuson, J. K., Martin, F., Spatafora, J. W., Tsang, A., and Baker, S. E. 2011. Fueling the future with fungal genomics. Mycology 2:192-209.

120. Grigoriev, I. V., Nikitin, R., Haridas, S., Kuo, A., Ohm, R., Otillar, R., Riley, R., Salamov, A., Zhao, X., Korzeniewski, F., Smirnova, T., Nordberg, H., Dubchak, I., and Shabalov, I. 2014. MycoCosm portal: gearing up for 1000 fungal genomes. Nucleic Acids Research 42:D699-D704.

121. Gullino, M. L., Mocioni, M., and Titone, P. 2007. First repot of *Ophiosphaerella korrae* causing spring dead spot ot bermudagrass in Italy. Plant Disease 91:1200.

122. Gunes, A., Inal, A., Alpaslan, M., Eraslan, F., Bagci, E. G., and Cicek, N. 2007. Salicylic acid induced changes on some physiological parameters symptomatic for oxidative stress and mineral nutrition in maize (*Zea mays* L.) grown under salinity. Journal of Plant Physiology 164:728-736.

123. Gupta, R., and Luan, S. 2003. Redox control of protein tyrosine phosphatases and mitogen-activated protein kinases in plants. Plant Physiology 132:1149-1152.

124. Gurevich, A., Saveliev, V., Vyahhi, N., and Tesler, G. 2013. QUAST: quality assessment tool for genome assemblies. Bioinformatics 29:1072-1075.

125. Haas, B. J., Papanicolaou, A., Yassour, M., Grabherr, M., Blood, P. D., Bowden, J., Couger, M. B., Eccles, D., Li, B., Lieber, M., MacManes, M. D., Ott, M., Orvis, J., Pochet, N., Strozzi, F., Weeks, N., Westerman, R., William, T., Dewey, C. N., Henschel, R., LeDuc, R. D., Friedman, N., and Regev, A. 2013. *De novo* transcript sequence reconstruction from RNA-seq using the Trinity platform for reference generation and analysis. Nature Protocols 8:1494-1512.

126. Haas, B. J., Salzberg, S. L., Zhu, W., Pertea, M., Allen, J. E., Orvis, J., White, O., Buell, C. R., and Wortman, J. R. 2008. Automated eukaryotic gene structure annotation using EVidenceModeler and the Program to Assemble Spliced Alignments. Genome Biology 9:R7.

127. Hajam, I. A., Dar, P. A., Shahnawaz, I., Jaume, J. C., and Lee, J. H. 2017. Bacterial flagellin—a potent immunomodulatory agent. Experimental & Molecular Medicine 49:e373.

128. Hancock, J., Desikan, R., Harrison, J., Bright, J., Hooley, R., and Neill, S. 2006. Doing the unexpected: Proteins involved in hydrogen peroxide perception. Journal of Experimental Botany 57:1711-1718.

129. Hane, J. K., Lowe, R. G. T., Solomon, P. S., Tan, K.-C., Schoch, C. L., Spatafora, J. W., Crous, P. W., Kodira, C., Birren, B. W., Galagan, J. E., Torriani, S. F. F., McDonald, B. A., and Oliver, R. P. 2007. Dothideomycete–plant interactions illuminated by genome sequencing and EST analysis of the wheat pathogen *Stagonospora nodorum*. The Plant Cell 19:3347-3368.

130. Hatsugai, N., Iwasaki, S., Tamura, K., Kondo, M., Fuji, K., Ogasawara, K., Nishimura, M., and Hara-Nishimura, I. 2009. A novel membrane fusion-mediated plant immunity against bacterial pathogens. Genes Dev 23:2496-2506.

131. Henry, C. M., and Deacon, J. W. 1981. Natural (non-pathogenic) death of the cortex of wheat and barley seminal roots, as evidenced by nuclear staining with acridine orange. Plant and Soil 60:255-274.

132. Hermanns, M., Slusarenko, A. J., and Schlaich, N. L. 2003. Organ-specificity in a plant disease is determined independently of R gene signaling. Molecular Plant-Microbe Interactions 16:752-759.

133. Hirt, H. 2000. Connecting oxidative stress, auxin, and cell cycle regulation through a plant mitogen-activated protein kinase pathway. Proceedings of the National Academy of Sciences of the United States of America 97:2405-2407.

134. Hogenhout, S. A., Van Der Hoorn, R. A. L., Terauchi, R., and Kamoun, S. 2009. Emerging concepts in effector biology of plant-associated organisms. Molecular Plant-Microbe Interactions 22:115-122.

135. Hong, S. K., Choi, H. W., Lee, Y. K., and Ham, H. H. 2019. First report of *Ophiosphaerella korrae* causing root rot of *Hordeum vulgare* in Korea. Plant Disease 103:158.

136. Hsiang, T., Chen, F., and Goodwin, P. H. 2003. Detection and phylogenetic analysis of mating type genes of *Ophiosphaerella korrae*. Canadian Journal of Botany 81:307-315.

137. Hu, Y., Dong, Q., and Yu, D. 2012. Arabidopsis WRKY46 coordinates with WRKY70 and WRKY53 in basal resistance against pathogen *Pseudomonas syringae*. Plant Science 185-186:288-297.

138. Huerta-Cepas, J., Forslund, K., Coelho, L. P., Bork, P., von Mering, C., Szklarczyk, D., and Jensen, L. J. 2017. Fast genome-wide functional annotation through orthology assignment by eggNOG-Mapper. Molecular Biology and Evolution 34:2115-2122.

139. Ichimura, K., Shinozaki, K., Tena, G., Sheen, J., Henry, Y., Champion, A., Kreis, M., Zhang, S., Hirt, H., Wilson, C., Heberle-Bors, E., Ellis, B. E., Morris, P. C., Innes, R. W., Ecker, J. R., Scheel, D., Klessig, D. F., Machida, Y., Mundy, J., Ohashi, Y., and Walker, J. C. 2002. Mitogen-activated protein kinase cascades in plants: A new nomenclature. Trends in Plant Science 7:301-308.

140. Inderbitzin, P., Asvarak, T., and Turgeon, B. G. 2010. Six new genes required for production of T-toxin, a polyketide determinant of high virulence of *Cochliobolus heterostrophus* to maize. Molecular Plant-Microbe Interactions 23:458-472.

141. Iriarte, F. B., Wetzel III, H. C., Fry, J. D., Martin, D. L., and Tisserat, N. A. 2004. Genetic diversity and aggressiveness of *Ophiosphaerella korrae*, a cause of spring dead spot of bermudagrass. Plant Disease 88:1341-1346.

142. Iriti, M., and Faoro, F. 2009. Chitosan as a MAMP, searching for a PRR. Plant Signaling and Behavior 4:66-68.

143. Jackson, N. 1993. Geographic distribution, host range, and symptomatology of patch disease caused by ectotrophic fungi. in: Turfgrass patch disease caused by ectotrophic root-infecting fungi. B. B. Clarke and A. B. Gould, eds. APS Press, St. Paul, MN.

144. Jelenska, J., Yao, N., Vinatzer, B. A., Wright, C. M., Brodsky, J. L., and Greenberg, J. T. 2007. A J-domain virulence effector of *Pseudomonas syringae* remodels host chloroplasts and suppresses defenses. Current Biology 17:499-508.

145. Jia, Y., McAdams, S. A., Bryan, G. T., Hershey, H. P., and Valent, B. 2000. Direct interaction of resistance gene and avirulence gene products confers rice blast resistance. EMBO Journal 19:4004-4014.

146. Jones, J. D. G., and Dangl, J. L. 2006. The plant immune system. Nature 444:323-329.

147. Jones, J. D. G., Vance, R. E., and Dangl, J. L. 2016. Intracellular innate immune surveillance devices in plants and animals. Science 354:aaf6395.

148. Kader, M. A., and Lindberg, S. 2014. Cytosolic calcium and pH signaling in plants under salinity stress. Plant Signaling & Behavior 5:233-238.

149. Kaku, H., Nishizawa, Y., Ishii-Minami, N., Akimoto-Tomiyama, C., Dohmae, N., Takio, K., Minami, E., and Shibuya, N. 2006. Plant cells recognize chitin fragments for defense signaling through a plasma membrane receptor. Proceedings of the National Academy of Sciences of the United States of America 103:11086-11091.

150. Kaminski, J. E., Dernoeden, P. H., Mischke, S., and O'Neill, N. R. 2006. Genetic diversity among *Ophiosphaerella agrostis* strains causing dead spot in creeping bentgrass. Plant Disease 90:146-154.

151. Kanehisa, M., Sato, Y., Kawashima, M., Furumichi, M., and Tanabe, M. 2016. KEGG as a reference resource for gene and protein annotation. Nucleic Acids Research 44:D457-D462.

152. Kang, C. H., Jung, W. Y., Kang, Y. H., Kim, J. Y., Kim, D. G., Jeong, J. C., Baek, D. W., Jin, J. B., Lee, J. Y., Kim, M. O., Chung, W. S., Mengiste, T., Koiwa, H., Kwak, S. S., Bahk, J. D., Lee, S. Y., Nam, J. S., Yun, D. J., and Cho, M. J. 2006. AtBAG6, a novel calmodulin-binding protein, induces programmed cell death in yeast and plants. Cell Death & Differentiation 13:84-95.

153. Kawano, T., and Muto, S. 2000. Mechanism of peroxidase actions for salicylic acid-induced generation of active oxygen species and an increase in cytosolic calcium in tobacco cell suspension culture. Journal of Experimental Botany 51:685-693.

154. Khaldi, N., Seifuddin, F. T., Turner, G., Haft, D., Nierman, W. C., Wolfe, K. H., and Fedorova, N. D. 2010. SMURF: Genomic mapping of fungal secondary metabolite clusters. Fungal Genetics and Biology 47:736-741.

155. Khan, M. I. R., Fatma, M., Per, T. S., Anjum, N. A., and Khan, N. A. 2015. Salicylic acid-induced abiotic stress tolerance and underlying mechanisms in plants. Frontiers in Plant Science 6:462.

156. Kim, D., Langmead, B., and Salzberg, S. L. 2015. HISAT: a fast spliced aligner with low memory requirements. Nature Methods 12:357-360.

157. Kim, S., Ahn, I. P., Rho, H. S., and Lee, Y. H. 2005. MHP1, a *Magnaporthe grisea* hydrophobin gene, is required for fungal development and plant colonization. Mol Microbiol 57:1224-1237.

158. Klessig, D. F., Choi, H. W., and Dempsey, D. A. 2018. Systemic acquired resistance and salicylic acid: Past, present, and future. Molecular Plant-Microbe Interactions 31:871-888.

159. Klessig, D. F., Durner, J., Noad, R., Navarre, D. A., Wendehenne, D., Kumar, D., Zhou, J. M., Shah, J., Zhang, S., Kachroo, P., Trifa, Y., Pontier, D., Lam, E., and Silva, H. 2000. Nitric oxide and salicylic acid signaling in plant defense. Proceedings of the National Academy of Sciences of the United States of America 97:8849-8855.

160. Knapp, D. G., Németh, J. B., Barry, K., Hainaut, M., Henrissat, B., Johnson, J., Kuo, A., Lim, J. H. P., Lipzen, A., Nolan, M., Ohm, R. A., Tamás, L., Grigoriev, I. V., Spatafora, J. W., Nagy, L. G., and Kovács, G. M. 2018. Comparative genomics provides insights into the lifestyle and reveals functional heterogeneity of dark septate endophytic fungi. Scientific Reports 8:6321.

161. Knepper, C., Savory, E. A., and Day, B. 2011. The role of NDR1 in pathogen perception and plant defense signaling. Plant Signaling and Behavior 6:1114-1116.

162. Koren, S., Walenz, B. P., Berlin, K., Miller, J. R., Bergman, N. H., and Phillippy, A. M. 2017. Canu: scalable and accurate long-read assembly via adaptive k-mer weighting and repeat separation. Genome Research 27:722-736.

163. Kosslak, R. M., Chamberlin, M. A., Palmer, R. G., and Bowen, B. A. 1997. Programmed cell death in the root cortex of soybean root necrosis mutants. Plant Journal 11:729-745.

164. Kourtev, P. S., Ehrenfeld, J. G., and Häggblom, M. 2003. Experimental analysis of the effect of exotic and native plant species on the structure and function of soil microbial communities. Soil Biology and Biochemistry 35:895-905.

165. Kozelnicky, G. M. 1974. Updating 20 years of research: Spring dead spot. USGA Green Section Record May:12-15.

166. Kozlov, A., Darriba, D., Flouri, T., Morel, B., and Stamatakis, A. 2018. RAxML-NG: A fast, scalable, and user-friendly tool for maximum likelihood phylogenetic inference. bioRxiv:447110.

167. Kriventseva, E. V., Zdobnov, E. M., Simão, F. A., Ioannidis, P., and Waterhouse, R. M. 2015. BUSCO: assessing genome assembly and annotation completeness with single-copy orthologs. Bioinformatics 31:3210-3212.

168. Kroj, T., Chanclud, E., Michel-Romiti, C., Grand, X., and Morel, J. B. 2016. Integration of decoy domains derived from protein targets of pathogen effectors into plant immune receptors is widespread. New Phytologist 210:618-626.

169. Kück, P., and Meusemann, K. 2010. FASconCAT: Convenient handling of data matrices. Molecular Phylogenetics and Evolution 56:1115-1118.

170. Kudla, J., Batistic, O., and Hashimoto, K. 2010. Calcium signals: the lead currency of plant information processing. Plant Cell 22:541-563.

171. Kunze, G., Zipfel, C., Robatzek, S., Niehaus, K., Boller, T., and Felix, G. 2004. The N-terminus of bacterial elongation factor Tu elicits innate immunity in *Arabidopsis* plants. Plant Cell 16:3496-3507.

172. Kushalappa, A. C., Yogendra, K. N., and Karre, S. 2016. Plant innate immune response: qualitative and quantitative resistance. Critical Reviews in Plant Sciences 35:38-55.

173. Lai, Z., Wang, F., Zheng, Z., Fan, B., and Chen, Z. 2011. A critical role of autophagy in plant resistance to necrotrophic fungal pathogens. The Plant Journal 66:953-968.

174. Lamotte, O., Gould, K., Lecourieux, D., Sequeira-Legrand, A., Lebrun-Garcia, A., Durner, J., Pugin, A., and Wendehenne, D. 2004. Analysis of nitric oxide signaling functions in tobacco cells challenged by the elicitor cryptogein. Plant Physiology 135:516-529.

175. Landshoot, P. J. 1993. Ecology and epidemiology of ectotrophic root-infecting fungi associated with patch diseases of turfgrass. In: Turfgrass patch disease caused by ectotrophic root-infecting fungi. B. B. Clarke and A. B. Gould, eds. APS Press, St. Paul, MN.

176. Lang, B. F., Laforest, M.-J., and Burger, G. 2007. Mitochondrial introns: a critical view. Trends in Genetics 23:119-125.

177. Lang, F. n.d. About RNAweasel and MFannot. Retrieved February 26 2019, from http://megasun.bch.umontreal.ca/RNAweasel/.

178. Larroque, M., Belmas, E., Martinez, T., Vergnes, S., Ladouce, N., Lafitte, C., Gaulin, E., and Dumas, B. 2013. Pathogen-associated molecular pattern-triggered immunity and resistance to the root pathogen *Phytophthora parasitica* in *Arabidopsis*. J Exp Bot 64:3615-3625.

179. Lascaris, D., and Deacon, J. W. 1991. Relationship between root cortical senescence and growth of wheat as influenced by mineral nutrition, *Idriella bolleyi* (Sprague) von Arx and pruning of leaves. New Phytologist 118:391-396.

180. Latgé, J.-P., Cole, G. T., Horisberger, M., and PréVost, M.-C. 1986. Ultrastructure and chemical composition of the ballistospore wall of *Conidiobolus obscurus*. Experimental Mycology 10:99-113.

181. Lechner, M., Findeiß, S., Steiner, L., Marz, M., Stadler, P. F., and Prohaska, S. J. 2011. Proteinortho: Detection of (Co-)orthologs in large-scale analysis. BMC Bioinformatics 12:124.

182. Lecourieux-Ouaked, F., Pugin, A., and Lebrun-Garcia, A. 2000. Phosphoproteins involved in the signal transduction of cryptogein, an elicitor of defense reactions in tobacco. Molecular Plant-Microbe Interactions 13:821-829.

183. Lee, H. A., and Yeom, S. I. 2015. Plant NB-LRR proteins: Tightly regulated sensors in a complex manner. Briefings in Functional Genomics 14:233-242.

184. Lenne, J. M. 1990. World list of fungal diseases of tropical pasture species. Phytopathol. Pap. 31:1-162.

185. Léon-Kloosterziel, K. M., Verhagen, B. W. M., Keurentjes, J. J. B., Van Pelt, J. A., Rep, M., Van Loon, L. C., and Pieterse, C. M. J. 2005. Colonization of the *Arabidopsis* rhizosphere by fluorescent *Pseudomonas* spp. activates a root-specific, ethylene-responsive PR-5 gene in the vascular bundle. Plant Molecular Biology 57:731-748.

186. Leuchtmann, A. 1984. Uber *Phaeosphaeria* Miyake und andere bitunicate Ascomyceten mit mehrfach querseptierten Ascosporen. Sydowia 37:75-194.

187. Levasseur, A., Drula, E., Lombard, V., Coutinho, P. M., and Henrissat, B. 2013. Expansion of the enzymatic repertoire of the CAZy database to integrate auxiliary redox enzymes. Biotechnology for Biofuels 6:41.

188. Levine, A., Pennell, R. I., Alvarez, M. E., Palmer, R., and Lamb, C. 1996. Calcium-mediated apoptosis in a plant hypersensitive disease resistance response. Current Biology 6:427-437.

189. Li, B., and Dewey, C. N. 2011. RSEM: accurate transcript quantification from RNA-Seq data with or without a reference genome. BMC Bioinformatics 12:323.

190. Li, Y., Kabbage, M., Liu, W., and Dickman, M. B. 2016. Aspartyl protease-mediated cleavage of BAG6 is necessary for autophagy and fungal resistance in plants. The Plant Cell 28:233-247.

191. Liljeroth, E., and Bryngelsson, T. 2001. DNA fragmentation in cereal roots indicative of programmed root cortical cell death. Physiologia Plantarum 111:365-372.

192. Liljeroth, E., Franzon-Almgren, I., and Gunnarsson, T. 1996. Root colonization by *Bipolaris sorokiniana* in different cereals and relations to lesion development and natural root cortical cell death. Journal of Phytopathology 144:301-307.

193. Liljeroth, E., Franzon-Almgren, I., and Gustafsson, M. 1994. Effect of prehelminthosporol, a phytotoxin produced by *Bipolaris sorikinaiana*, on barley roots. Canadian Journal of Botany 72:558-563.

194. Lindermayr, C., Sell, S., Müller, B., Leister, D., and Durner, J. 2010. Redox regulation of the NPR1-TGA1 system of *Arabidopsis thaliana* by nitric oxide. Plant Cell 22:2894-2907.

195. Liu, J. Z., Horstman, H. D., Braun, E., Graham, M. A., Zhang, C., Navarre, D., Qiu, W. L., Lee, Y., Nettleton, D., Hill, J. H., and Whitham, S. A. 2011. Soybean homologs of MPK4 negatively regulate defense responses and positively regulate growth and development. Plant Physiology 157:1363-1378.

196. Liu, W., Liu, J., Ning, Y., Ding, B., Wang, X., Wang, Z., and Wang, G. L. 2013. Recent progress in understanding PAMP- and effector-triggered immunity against the rice blast fungus *Magnaporthe oryzae*. Mol Plant 6:605-620.

197. Liu, Y., Schiff, M., Czymmek, K., Tallóczy, Z., Levine, B., and Dinesh-Kumar, S. P. 2005. Autophagy regulates programmed cell death during the plant innate immune response. Cell 121:567-577.

198. Liu, Z., Faris, J. D., Oliver, R. P., Tan, K. C., Solomon, P. S., McDonald, M. C., McDonald, B. A., Nunez, A., Lu, S., Rasmussen, J. B., and Friesen, T. L. 2009. SnTox3 acts in effector triggered susceptibility to induce disease on wheat carrying the Snn3 gene. PLoS Pathog 5:e1000581.

199. Lohse, M., Drechsel, O., Kahlau, S., and Bock, R. 2013. OrganellarGenomeDRAW—a suite of tools for generating physical maps of plastid and mitochondrial genomes and visualizing expression data sets. Nucleic Acids Research 41:W575-W581.

200. Lombard, V., Golaconda Ramulu, H., Drula, E., Coutinho, P. M., and Henrissat, B. 2014. The carbohydrate-active enzymes database (CAZy) in 2013. Nucleic Acids Research 42:D490-D495.

201. Lotan, T., Ori, N., and Fluhr, R. 1989. Pathogenesis-related proteins are developmentally regulated in tobacco flowers. The Plant Cell 1:881-887.

202. Lucas, L. T. 1980. Spring deadspot of bermudagrass. USGA Green Section Record 18:4-6.

203. Luna, E., Pastor, V., Robert, J., Flors, V., Mauch-Mani, B., and Ton, J. 2010. Callose deposition: A multifaceted plant defense response. Molecular Plant-Microbe Interactions 24:183-193.

204. Lundell, T. K., Mäkelä, M. R., and Hildén, K. 2010. Lignin-modifying enzymes in filamentous basidiomycetes – ecological, functional and phylogenetic review. Journal of Basic Microbiology 50:5-20.

205. Ma, Z., Zhu, L., Song, T., Wang, Y., Zhang, Q., Xia, Y., Qiu, M., Lin, Y., Li, H., Kong, L., Fang, Y., Ye, W., Wang, Y., Dong, S., Zheng, X., Tyler, B. M., and Wang, Y. 2017. A paralogous decoy protects apoplastic effector PsXEG1 from a host inhibitor. Science 355:710-714.

206. Macho, A. P., and Zipfel, C. 2014. Plant PRRs and the activation of innate immune signaling. Molecular Cell 54:263-272.

207. Mackey, D., Holt, B. F., Wiig, A., and Dangl, J. L. 2002. RIN4 interacts with *Pseudomonas syringae* type III effector molecules and is required for RPM1-mediated resistance in *Arabidopsis*. Cell 108:743.

208. Malik, S., and Van Der Hoorn, R. A. L. 2016. Inspirational decoys: a new hunt for effector targets. New Phytologist 210:371-373.

209. Manning, V. A., Pandelova, I., Dhillon, B., Wilhelm, L. J., Goodwin, S. B., Berlin, A. M., Figueroa, M., Freitag, M., Hane, J. K., Henrissat, B., Holman, W. H., Kodira, C. D., Martin, J., Oliver, R. P., Robbertse, B., Schackwitz, W., Schwartz, D. C., Spatafora, J. W., Turgeon, B. G., Yandava, C., Young, S., Zhou, S., Zeng, Q., Grigoriev, I. V., Ma, L. J., and Ciuffetti, L. M. 2013. Comparative genomics of a plant-pathogenic fungus, *Pyrenophora tritici-repentis*, reveals transduplication and the impact of repeat elements on pathogenicity and population divergence. G3 3:41-63.

210. Mardis, E. R. 2011. A decade's perspective on DNA sequencing technology. Nature 470:198-203.

211. Medzhitov, R. 2009. Approaching the asymptote: 20 years later. Immunity 30:766-775.

212. Mészáros, T., Helfer, A., Hatzimasoura, E., Magyar, Z., Serazetdinova, L., Rios, G., Bardóczy, V., Teige, M., Koncz, C., Peck, S., and Bögre, L. 2006. The *Arabidopsis* MAP kinase kinase MKK1 participates in defence responses to the bacterial elicitor flagellin. Plant Journal 48:485-498.

213. Milesi, C., Elvidge, C. M., Dieta, J. B., Tuttle, B. T., Nemani, R. R., and Running, S. W. 2005. A strategy for mapping and modeling ecological effects of US lawns. Journal of Turfgrass Management 1:83-97.

214. Millet, Y. A., Danna, C. H., Clay, N. K., Songnuan, W., Simon, M. D., Werck-Reichhart, D., and Ausubel, F. M. 2010. Innate immune responses activated in *Arabidopsis* roots by microbe-associated molecular patterns. Plant Cell 22:973-990.

215. Mishina, T. E., and Zeier, J. 2007. Pathogen-associated molecular pattern recognition rather than development of tissue necrosis contributes to bacterial induction of systemic acquired resistance in Arabidopsis. Plant Journal 50:500-513.

216. Miya, A., Albert, P., Shinya, T., Desaki, Y., Ichimura, K., Shirasu, K., Narusaka, Y., Kawakami, N., Kaku, H., and Shibuya, N. 2007. CERK1, a LysM receptor kinase, is essential for chitin elicitor signaling in *Arabidopsis*. Proceedings of the National Academy of Sciences of the United States of America 104:19613-19618.

217. Möller, E. M., Bahnweg, G., Sandermann, H., and Geiger, H. H. 1992. A simple and efficient protocol for isolation of high molecular weight DNA from filamentous fungi, fruit bodies, and infected plant tissues. Nucleic Acid Research 20:6115-6116.

218. Morita, Y., Hyon, G. S., Hosogi, N., Miyata, N., Nakayashiki, H., Muranaka, Y., Inada, N., Park, P., and Ikeda, K. 2013. Appressorium-localized NADPH oxidase B is essential for aggressiveness and pathogenicity in the host-specific, toxin-producing fungus *Alternaria alternata* Japanese pear pathotype. Molecular Plant Pathology 14:365-378.

219. Morris, K. 2003. The National Turfgrass Research Initiative. Retrieved August 8, 2018, from http://www.turfresearch.org/initiative.htm.

220. Mueller, D. S., Wise, K. A., Dufault, N. S., Bradley, C. A., and Chilvers, M. I. 2013. Fungicides for Field Crops. The American Phytopathological Society, St. Paul, MN.

221. Munk, A. 1957. Danish Pyrenomycetes. A Preliminary Flora. Dansk Bot. Ark. 17:1-491.

222. Muria-Gonzalez, M. J., Chooi, Y. H., Breen, S., and Solomon, P. S. 2015. The past, present and future of secondary metabolite research in the Dothideomycetes. Mol Plant Pathol 16:92-107.

223. Muthamilarasan, M., and Prasad, M. 2013. Plant innate immunity: an updated insight into defense mechanism. Journal of Biosciences 38:433-449.

224. Mutlu, S., Karadağoğlu, Ö., Atici, Ö., and Nalbantoğlu, B. 2013. Protective role of salicylic acid applied before cold stress on antioxidative system and protein patterns in barley apoplast. Biologia Plantarum 57:507-513.

225. Narusaka, M., Shirasu, K., Noutoshi, Y., Kubo, Y., Shiraishi, T., Iwabuchi, M., and Narusaka, Y. 2009. RRS1 and RPS4 provide a dual resistance-gene system against fungal and bacterial pathogens. Plant Journal 60:218-226.

226. Naumann, T. A., Wicklow, D. T., and Price, N. P. 2011. Identification of a chitinase-modifying protein from *Fusarium verticillioides*: truncation of a host resistance protein by a fungalysin metalloprotease. J Biol Chem 286:35358-35366.

227. Navarro, L., Zipfel, C., Rowland, O., Keller, I., Robatzek, S., Boller, T., and Jones, J. D. G. 2004. The transcriptional innate immune response to flg22. Interplay and overlap with Avr gene-dependent defense responses and bacterial pathogenesis. Plant Physiology 135:1113-1128.

228. Neale, A. D., Wahleithner, J. A., Lund, M., Bonnett, H. T., Kelly, A., Meeks-Wagner, D. R., James Peacock, W., and Dennis, E. S. 1990. Chitinase, β-1,3-glucanase, osmotin, and extensin are expressed in tobacco explants during flower formation. Plant Cell 2:673-684.

229. Neill, S. J., Desikan, R., and Hancock, J. T. 2003. Nitric oxide signalling in plants. New Phytologist 159:11-35.

230. Neill, S., Desikan, R., and Hancock, J. 2002. Hydrogen peroxide signalling. Current Opinion in Plant Biology 5:388-395.

231. Newman, M.-A., Sundelin, T., Nielsen, J., and Erbs, G. 2013. MAMP (microbe-associated molecular pattern) triggered immunity in plants. Frontiers in Plant Science 4:139.

232. Nishimura, M. T., Stein, M., Hou, B. H., Vogel, J. P., Edwards, H., and Somerville, S. C. 2003. Loss of a callose synthase results in salicylic acid-dependent disease resistance. Science 301:969-972.

233. Nurk, S., Bankevich, A., Antipov, D., Gurevich, A. A., Korobeynikov, A., Lapidus, A., Prjibelski, A. D., Pyshkin, A., Sirotkin, A., Sirotkin, Y., Stepanauskas, R., Clingenpeel, S. R., Woyke, T., McLean, J. S., Lasken, R., Tesler, G., Alekseyev, M. A., and Pevzner, P. A. 2013. Assembling single-cell genomes and mini-metagenomes from chimeric MDA products. Journal of Computational Biology 20:714-737.

234. O'Connell, R. J., Thon, M. R., Hacquard, S., Amyotte, S. G., Kleemann, J., Torres, M. F., Damm, U., Buiate, E. A., Epstein, L., Alkan, N., Altmüller, J., Alvarado-Balderrama, L., Bauser, C. A., Becker, C., Birren, B. W., Chen, Z., Choi, J., Crouch, J. A., Duvick, J. P., Farman, M. A., Gan, P., Heiman, D., Henrissat, B., Howard, R. J., Kabbage, M., Koch, C., Kracher, B., Kubo, Y., Law, A. D., Lebrun, M.-H., Lee, Y.-H., Miyara, I., Moore, N., Neumann, U., Nordström, K., Panaccione, D. G., Panstruga, R., Place, M., Proctor, R. H., Prusky, D., Rech, G., Reinhardt, R., Rollins, J. A., Rounsley, S., Schardl, C. L., Schwartz, D. C., Shenoy, N., Shirasu, K., Sikhakolli, U. R., Stüber, K., Sukno, S. A., Sweigard, J. A., Takano, Y., Takahara, H., Trail, F., van der Does, H. C., Voll, L. M., Will, I., Young, S., Zeng, Q., Zhang, J., Zhou, S., Dickman, M. B., Schulze-Lefert, P., Ver Loren van Themaat, E., Ma, L.-J., and Vaillancourt, L. J. 2012. Lifestyle transitions in plant pathogenic *Colletotrichum* fungi deciphered by genome and transcriptome analyses. Nature Genetics 44:1060-1065.

235. Ohm, R. A., Feau, N., Henrissat, B., Schoch, C. L., Horwitz, B. A., Barry, K. W., Condon, B. J., Copeland, A. C., Dhillon, B., Glaser, F., Hesse, C. N., Kosti, I., LaButti, K., Lindquist, E. A., Lucas, S., Salamov, A. A., Bradshaw, R. E., Ciuffetti, L., Hamelin, R. C., Kema, G. H. J., Lawrence, C., Scott, J. A., Spatafora, J. W., Turgeon, B. G., de Wit, P. J. G. M., Zhong, S., Goodwin, S. B., and Grigoriev, I. V. 2012. Diverse lifestyles and strategies of plant pathogenesis encoded in the genomes of eighteen Dothideomycetes fungi. PLoS pathogens 8:e1003037-e1003037.

236. Ökmen, B., Kemmerich, B., Hilbig, D., Wemhöner, R., Aschenbroich, J., Perrar, A., Huesgen, P. F., Schipper, K., and Doehlemann, G. 2018. Dual function of a secreted fungalysin metalloprotease in *Ustilago maydis*. New Phytologist 220:249-261.

237. Okubara, P. A., and Paulitz, T. C. 2005. Root defense responses to fungal pathogens: A molecular perspective. Plant and Soil 274:215-226.

238. Onions, J., Hermann, S., and Grundström, T. 2000. A novel type of calmodulin interaction in the inhibition of basic helix−loop−helix transcription factors. Biochemistry 39:4366-4374.

239. Park, H. C., Kim, M. L., Lee, S. M., Bahk, J. D., Yun, D. J., Lim, C. O., Hong, J. C., Lee, S. Y., Cho, M. J., and Chung, W. S. 2007. Pathogen-induced binding of the soybean zinc finger homeodomain proteins GmZF-HD1 and GmZF-HD2 to two repeats of ATTA homeodomain binding site in the calmodulin isoform 4 (GmCaM4) promoter. Nucleic Acids Res 35:3612-3623.

240. Patel, S., and Dinesh-Kumar, S. P. 2008. *Arabidopsis* ATG6 is required to limit the pathogen-associated cell death response. Autophagy 4:20-27.

241. Paulus, J. K., van der Hoorn, R. A. L., and Zipfel, C. 2018. Tricked or trapped—Two decoy mechanisms in host–pathogen interactions. PLoS Pathogens 14(2):e1006761.

242. Perchepied, L., Balagué, C., Riou, C., Claudel-Renard, C., Rivière, N., Grezes-Besset, B., and Roby, D. 2010. Nitric oxide participates in the complex interplay of defense-related signaling pathways controlling disease resistance to *Sclerotinia sclerotiorum* in *Arabidopsis thaliana*. Molecular Plant-Microbe Interactions 23:846-860.

243. Pertea, M., Kim, D., Pertea, G. M., Leek, J. T., and Salzberg, S. L. 2016. Transcript-level expression analysis of RNA-seq experiments with HISAT, StringTie and Ballgown. Nature Protocols 11:1650-1667.

244. Pertea, M., Pertea, G. M., Antonescu, C. M., Chang, T. C., Mendell, J. T., and Salzberg, S. L. 2015. StringTie enables improved reconstruction of a transcriptome from RNA-seq reads. Nature Biotechnology 33:290-295.

245. Peškan-Berghöfer, T., Shahollari, B., Giong, P. H., Hehl, S., Markert, C., Blanke, V., Kost, G., Varma, A., and Oelmüller, R. 2004. Association of *Piriformospora indica* with *Arabidopsis thaliana* roots represents a novel system to study beneficial plant–microbe interactions and involves early plant protein modifications in the endoplasmic reticulum and at the plasma membrane. Physiologia Plantarum 122:465-477.

246. Petersen, M., Brodersen, P., Naested, H., Andreasson, E., Lindhart, U., Johansen, B., Nielsen, H. B., Lacy, M., Austin, M. J., Parker, J. E., Sharma, S. B., Klessig, D. F., Martienssen, R., Mattsson, O., Jensen, A. B., and Mundy, J. 2000. *Arabidopsis* MAP kinase 4 negatively regulates systemic acquired resistance. Cell 103:1111-1120.

247. Petersen, T. N., Brunak, S., von Heijne, G., and Nielsen, H. 2011. SignalP 4.0: discriminating signal peptides from transmembrane regions. Nature Methods 8:785-786.

248. Phookamsak, R., Liu, J.-K., McKenzie, E. H. C., Manamgoda, D. S., Ariyawansa, H., Thambugala, K. M., Dai, D.-Q., Camporesi, E., Chukeatirote, E., Wijayawardene, N. N., Bahkali, A. H., Mortimer, P. E., Xu, J.-C., and Hyde, K. D. 2014. Revision of *Phaeosphaeriaceae*. Fungal Diversity 68:159-238.

249. Pieterse, C. M. J., Zamioudis, C., Berendsen, R. L., Weller, D. M., Van Wees, S. C. M., and Bakker, P. A. H. M. 2014. Induced systemic resistance by beneficial microbes. Annual Review of Phytopathology 52:347-375.

250. Pitzschke, A., Schikora, A., and Hirt, H. 2009. MAPK cascade signalling networks in plant defence. Current Opinion in Plant Biology 12:421-426.

251. Price, A. H., Taylor, A., Ripley, S. J., Griffiths, A., Trewavas, A. J., and Knight, M. R. 1994. Oxidative signals in tobacco increase cytosolic calcium. Plant Cell 6:1301-1310.

252. Pusztahelyi, T. 2018. Chitin and chitin-related compounds in plant-fungal interactions. Mycology 9:189-201.

253. Pusztahelyi, T., Holb, I. J., and Pocsi, I. 2015. Secondary metabolites in fungus-plant interactions. Front Plant Sci 6:573.

254. Qiu, J. L., Fiil, B. K., Petersen, K., Nielsen, H. B., Botanga, C. J., Thorgrimsen, S., Palma, K., Suarez-Rodriguez, M. C., Sandbech-Clausen, S., Lichota, J., Brodersen, P., Grasser, K. D., Mattsson, O., Glazebrook, J., Mundy, J., and Petersen, M. 2008. *Arabidopsis* MAP kinase 4 regulates gene expression through transcription factor release in the nucleus. EMBO Journal 27:2214-2221.

255. Qiu, J. L., Zhou, L., Yun, B. W., Nielsen, H. B., Fiil, B. K., Petersen, K., MacKinlay, J., Loake, G. J., Mundy, J., and Morris, P. C. 2008. *Arabidopsis* mitogen-activated protein kinase kinases MKK1 and MKK2 have overlapping functions in defense signaling mediated by MEKK1, MPK4, and MKS1. Plant Physiology 148:212-222.

256. Quinlan, A. R., and Hall, I. M. 2010. BEDTools: a flexible suite of utilities for comparing genomic features. Bioinformatics 26:841-842.

257. Radoshevich, L., Murrow, L., Chen, N., Fernandez, E., Roy, S., Fung, C., and Debnath, J. 2010. ATG12 conjugation to ATG3 regulates mitochondrial homeostasis and cell death. Cell 142:590-600.

258. Rasmussen, M. W., Roux, M., Petersen, M., and Mundy, J. 2012. MAP kinase cascades in *Arabidopsis* innate immunity. Front Plant Sci 3:169.

259. Raven, P. H. 1992. Biology of plants. 5th ed.. ed. New York, N.Y. : Worth Publishers, New York, N.Y.

260. Rawlings, N. D., Barrett, A. J., and Bateman, A. 2010. MEROPS: the peptidase database. Nucleic Acids Research 38:D227-D233.

261. Reddy, A. S., Ali, G. S., Celesnik, H., and Day, I. S. 2011. Coping with stresses: roles of calcium- and calcium/calmodulin-regulated gene expression. Plant Cell 23:2010-2032.

262. Richards, J. K., Wyatt, N. A., Liu, Z., Faris, J. D., and Friesen, T. L. 2017. Reference quality genome assemblies of three *Parastagonospora nodorum* isolates differing in virulence on wheat. G3 8:393-399.

263. Ridley, B. L., O'Neill, M. A., and Mohnen, D. 2001. Pectins: Structure, biosynthesis, and oligogalacturonide-related signaling. Phytochemistry 57:929-967.

264. Robinson, G. E., Hackett, K. J., Purcell-Miramontes, M., Brown, S. J., Evans, J. D., Goldsmith, M. R., Lawson, D., Okamuro, J., Robertson, H. M., and Schneider, D. J. 2011. Creating a buzz about insect genomes. Science 331:1386.

265. Robinson, M. D., McCarthy, D. J., and Smyth, G. K. 2009. edgeR: A Bioconductor package for differential expression analysis of digital gene expression data. Bioinformatics 26:139-140.

266. Rose, S. H., Yun, T., Asvarak, S. W., Lu, O., Yoder, B., and Turgeon, B. 2002. A decarboxylase encoded at the *Cochliobolus heterostrophus* translocation-associated Tox1B locus is required for polyketide (T-toxin) biosynthesis and high virulence on T-cytoplasm maize. Molecular Plant-Microbe Interactions 15:883-893.

267. Roux, M., Schwessinger, B., Albrecht, C., Chinchilla, D., Jones, A., Holton, N., Malinovsky, F. G., Tör, M., de Vries, S., and Zipfel, C. 2011. The *Arabidopsis* leucine-rich repeat receptor–like kinases BAK1/SERK3 and BKK1/SERK4 are required for innate immunity to hemibiotrophic and biotrophic pathogens. The Plant Cell 23(6) 2440-2455.

268. Sanchez-Vallet, A., Saleem-Batcha, R., Kombrink, A., Hansen, G., Valkenburg, D. J., Thomma, B. P., and Mesters, J. R. 2013. Fungal effector Ecp6 outcompetes host immune receptor for chitin binding through intrachain LysM dimerization. Elife 2:e00790.

269. Schardl, C. L. 2001. *Epichloë festucae* and related mutualistic symbionts of grasses. Fungal Genetics and Biology 33:69-82.

270. Schatz, M. C., Witkowski, J., and McCombie, W. R. 2012. Current challenges in *de novo* plant genome sequencing and assembly. Genome Biology 13:243.

271. Schenck, N. C. 1972. *Phaeosphaeria herpotricha* on southern corn leaf blight-infected plants in Florida. Pl. Dis. Reporter 56:276-281.

272. Schikora, A., Schenk, S. T., Stein, E., Molitor, A., Zuccaro, A., and Kogel, K. H. 2011. N-acyl-homoserine lactone confers resistance toward biotrophic and hemibiotrophic pathogens via altered activation of AtMPK6. Plant Physiology 157:1407-1418.

273. Schwessinger, B., Roux, M., Kadota, Y., Ntoukakis, V., Sklenar, J., Jones, A., and Zipfel, C. 2011. Phosphorylation-dependent differential regulation of plant growth, cell death, and innate immunity by the regulatory receptor-like kinase BAK1. PLoS Genet 7:e1002046.

274. Scott, B., Takemoto, D., and Tanaka, A. 2007. Fungal endophyte production of reactive oxygen species is critical for maintaining the mutualistic symbiotic interaction between *Epichloë festucae* and perennial ryegrass. Plant signaling & behavior 2:171-173.

275. Senthil-Kumar, M., and Mysore, K. S. 2013. Nonhost resistance against bacterial pathogens: retrospectives and prospects. Annual Review of Phytopathology 51:407-427.

276. Shimizu, T., Nakano, T., Takamizawa, D., Desaki, Y., Ishii-Minami, N., Nishizawa, Y., Minami, E., Okada, K., Yamane, H., Kaku, H., and Shibuya, N. 2010. Two LysM receptor molecules, CEBiP and OsCERK1, cooperatively regulate chitin elicitor signaling in rice. Plant J 64:204-214.

277. Shoemaker, R. A., and Babcock, C. E. 1989. *Phaeosphaeria*. Canadian Journal of Botany 67:1500-1599.

278. Sill Jr., W. H., Hansing, E. D., Kramer, C. L., and King, C. L. 1961. Kansas Phytopathological Notes: 1960. Transactions of the Kansas Academy of Science 64:292.

279. Smiley, R. W., Dernoeden, P. H., and Clarke, B. B. 2005. Compendium of Turfgrass Diseases. 3rd ed. The American Phytopathological Society, St. Paul, MN.

280. Smith, A. M. 1965. *Ophiobolus herpotrichus* a cause of spring dead spot in couch turf. The Agricultural Gazette Dezember:753-758.

281. Smith, A. M. 1971. Control of spring dead spot of couch grass turf in New South Wales. The Journal of the Sports Turf Research Institute 47:54-59.

282. Snedden, W. A., and Fromm, H. 2001. Calmodulin as a versatile calcium signal transducer in plants. New Phytologist 151:35-66.

283. Sperschneider, J., Catanzariti, A.-M., DeBoer, K., Petre, B., Gardiner, D. M., Singh, K. B., Dodds, P. N., and Taylor, J. M. 2017. LOCALIZER: subcellular localization prediction of both plant and effector proteins in the plant cell. Scientific Reports 7:44598.

284. Sperschneider, J., Dodds, P. N., Singh, K. B., and Taylor, J. M. 2018. ApoplastP: prediction of effectors and plant proteins in the apoplast using machine learning. New Phytologist 217:1764-1778.

285. Sperschneider, J., Gardiner, D. M., Dodds, P. N., Tini, F., Covarelli, L., Singh, K. B., Manners, J. M., and Taylor, J. M. 2016. EffectorP: predicting fungal effector proteins from secretomes using machine learning. New Phytologist 210:743-761.

286. Stael, S., Kmiecik, P., Willems, P., Van Der Kelen, K., Coll, N. S., Teige, M., and Van Breusegem, F. 2015. Plant innate immunity - sunny side up? Trends in Plant Science 20:3-11.

287. Stajich, J. E., Wilke, S. K., Ahrén, D., Au, C. H., Birren, B. W., Borodovsky, M., Burns, C., Canbäck, B., Casselton, L. A., Cheng, C. K., Deng, J., Dietrich, F. S., Fargo, D. C., Farman, M. L., Gathman, A. C., Goldberg, J., Guigó, R., Hoegger, P. J., Hooker, J. B., Huggins, A., James, T. Y., Kamada, T., Kilaru, S., Kodira, C., Kües, U., Kupfer, D., Kwan, H. S., Lomsadze, A., Li, W., Lilly, W. W., Ma, L.-J., Mackey, A. J., Manning, G., Martin, F., Muraguchi, H., Natvig, D. O., Palmerini, H., Ramesh, M. A., Rehmeyer, C. J., Roe, B. A., Shenoy, N., Stanke, M., Ter-Hovhannisyan, V., Tunlid, A., Velagapudi, R., Vision, T. J., Zeng, Q., Zolan, M. E., and Pukkila, P. J. 2010. Insights into evolution of multicellular fungi from the assembled chromosomes of the mushroom *Coprinopsis cinerea* (*Coprinus cinereus*). PNAS 107:11889-11894.

288. Stanke, M., Keller, O., Gunduz, I., Hayes, A., Waack, S., and Morgenstern, B. 2006. AUGUSTUS: *ab initio* prediction of alternative transcripts. Nucleic Acids Research 34:W435-W439.

289. Stergiopoulos, I., Collemare, J., Mehrabi, R., and De Wit, P. J. 2013. Phytotoxic secondary metabolites and peptides produced by plant pathogenic Dothideomycete fungi. FEMS Microbiol Rev 37:67-93.

290. Stotz, H. U., Mitrousia, G. K., de Wit, P. J., and Fitt, B. D. 2014. Effector-triggered defence against apoplastic fungal pathogens. Trends Plant Sci 19:491-500.

291. Sun, Y., Li, L., Macho, A. P., Han, Z., Hu, Z., Zipfel, C., Zhou, J. M., and Chai, J. 2013. Structural basis for flg22-induced activation of the *Arabidopsis* FLS2-BAK1 immune complex. Science 342:624-628.

292. Syme, R. A., Hane, J. K., Friesen, T. L., and Oliver, R. P. 2013. Resequencing and comparative genomics of *Stagonospora nodorum*: sectional gene absence and effector discovery. G3 3:959-969.

293. Szklarczyk, D., Gable, A. L., Lyon, D., Junge, A., Wyder, S., Huerta-Cepas, J., Simonovic, M., Doncheva, N. T., Morris, J. H., Bork, P., Jensen, L. J., and Von Mering, C. 2019. STRING v11: Protein-protein association networks with increased coverage, supporting functional discovery in genome-wide experimental datasets. Nucleic Acids Research 47:D607-D613.

294. Taliaferro, C. M. 1995. Diversity and vulnerability of bermuda turfgrass species. Crop Science 35:327-332.

295. Taliaferro, C., Roquette Jr, F., and Mislevy, P. 2004. Bermudagrass and stargrass. Pages 417-475 in: Warm-season (C4) grasses. L. Moser, L. Sollenberger and B. Burson, eds. American Society of Agronomy, Madison, MI.

296. Thulasi Devendrakumar, K., Li, X., and Zhang, Y. 2018. MAP kinase signalling: interplays between plant PAMP- and effector-triggered immunity. Cellular and Molecular Life Sciences 75:2981-2989.

297. Tischner, R., Koltermann, M., Hesse, H., and Plath, M. 2010. Early responses of *Arabidopsis thaliana* to infection by *Verticillium longisporum*. Physiological and Molecular Plant Pathology 74:419-427.

298. Tisserat, N. A., Pair, J. C., and Nus, A. 1989. *Ophiosphaerella herpotricha*, a cause of spring dead spot of bermudagrass in Kansas. Plant Disease 73:933-937.

299. Tisserat, N. A., Wetzel III, H., Fry, J., and Martin, D. L. 1999. Spring dead spot of buffalograss caused by *Ophiosphaerella herpotricha* in Kansas and Oklahoma. Plant Disease 83:199.

300. Torres, M. A., Jones, J. D., and Dangl, J. L. 2006. Reactive oxygen species signaling in response to pathogens. Plant Physiol 141:373-378.

301. Travassos, L. H., Carneiro, L. A. M., Ramjeet, M., Hussey, S., Kim, Y.-G., Magalhães, J. G., Yuan, L., Soares, F., Chea, E., Le Bourhis, L., Boneca, I. G., Allaoui, A., Jones, N. L., Nuñez, G., Girardin, S. E., and Philpott, D. J. 2009. Nod1 and Nod2 direct autophagy by recruiting ATG16L1 to the plasma membrane at the site of bacterial entry. Nature Immunology 11:55.

302. Treangen, T. J., and Salzberg, S. L. 2011. Repetitive DNA and next-generation sequencing: computational challenges and solutions. Nature Reviews Genetics 13:36-46.

303. Tredway, L. P., and Butler, E. L. 2007. First report of spring dead spot of zoysiagrass caused by *Ophiosphaerella korrae* in the United States. Plant Disease 91:1684.

304. Tredway, L. P., Butler, M. D., Soika, M. D., and Bunting, M. L. 2008. Etiology and management of spring dead spot of hybrid bermudagrass in North Carolina, USA. Acta Horticulturae 783:535-546.

305. Tsukagoshi, H. 2016. Control of root growth and development by reactive oxygen species. Current Opinion in Plant Biology 29:57-63.

306. Tsukagoshi, H., Busch, W., and Benfey, P. N. 2010. Transcriptional regulation of ROS controls transition from proliferation to differentiation in the root. Cell 143:606-616.

307. Tyburski, J., Dunajska, K., and Tretyn, A. 2009. Reactive oxygen species localization in roots of *Arabidopsis thaliana* seedlings grown under phosphate deficiency. Plant Growth Regulation 59:27-36.

308. Uma, B., Swaroopa Rani, T., and Podile, A. R. 2011. Warriors at the gate that never sleep: non-host resistance in plants. Journal of Plant Physiology 168:2141-2152.

309. Unamuno, P. L. M. 1941. Enumeracion y distribucion geografica de los ascomicetos de la Peninsula Iberica y de las Islas Baleares. Mem. Real Acad. Ci. Exact. Madrid 8:1-403.

310. Urban, M., Cuzick, A., Rutherford, K., Irvine, A., Pedro, H., Pant, R., Sadanadan, V., Khamari, L., Billal, S., Mohanty, S., and Hammond-Kosack, K. E. 2017. PHI-base: a new interface and further additions for the multi-species pathogen-host interactions database. Nucleic Acids Research 45:D604-D610.

311. Vaaje-Kolstad, G., Westereng, B., Horn, S. J., Liu, Z., Zhai, H., Sørlie, M., and Eijsink, V. G. H. 2010. An oxidative enzyme boosting the enzymatic conversion of recalcitrant polysaccharides. Science 330:219-222.

312. Valenzuela-Lopez, N., Cano-Lira, J. F., Guarro, J., Sutton, D. A., Wiederhold, N., Crous, P. W., and Stchigel, A. M. 2018. Coelomycetous *Dothideomycetes* with emphasis on the families *Cucurbitariaceae* and *Didymellaceae*. Stud. Mycol 90:1-69.

313. Van der Biezen, E. A., and Jones, J. D. 1998. The NB-ARC domain: a novel signalling motif shared by plant resistance gene products and regulators of cell death in animals. Current Biology 8:R226-227.

314. Van Der Hoorn, R., and Kamoun, S. 2008. From guard to decoy: A new model for perception of plant pathogen effectors. Plant Cell 20:2009-2017.

315. Van Doorn, W. G., Beers, E. P., Dangl, J. L., Franklin-Tong, V. E., Gallois, P., Hara-Nishimura, I., Jones, A. M., Kawai-Yamada, M., Lam, E., Mundy, J., Mur, L. A., Petersen, M., Smertenko, A., Taliansky, M., Van Breusegem, F., Wolpert, T., Woltering, E., Zhivotovsky, B., and Bozhkov, P. V. 2011. Morphological classification of plant cell deaths. Cell Death Differ 18:1241-1246.

316. Van Loon, L. C., Rep, M., and Pieterse, C. M. J. 2006. Significance of inducible defense-related proteins in infected plants. Annu Rev Phytopathol. 44:135-162.

317. Van Wetter, M.-A., Wösten, H. A. B., Sietsma, J. H., and Wessels, J. G. H. 2000. Hydrophobin gene expression affects hyphal wall composition in *Schizophyllum commune*. Fungal Genetics and Biology 31:99-104.

318. Vandenabeele, S., Van Der Kelen, K., Dat, J., Gadjev, I., Boonefaes, T., Morsa, S., Rottiers, P., Slooten, L., Van Montagu, M., Zabeau, M., Inzé, D., and Van Breusegem, F. 2003. A comprehensive analysis of hydrogen peroxide-induced gene expression in tobacco. Proceedings of the National Academy of Sciences of the United States of America 100:16113-16118.

319. Venkatasubbaiah, P., Tisserat, N. A., and Chilton, W. S. 1994. Metabolites of *Ophiosphaerella herpotricha*, a cause of spring dead spot of bermudagrass. Mycopathologia 128:155-159.

320. Vranová, E., Inzé, D., and Van Breusegem, F. 2002. Signal transduction during oxidative stress. Journal of Experimental Botany 53:1227-1236.

321. Wadsworth, D. F., and Young, H. C. 1960. Spring dead spot of bermudagrass. Plant Disease Reporter 44:516-518

322. Walker, J. 1980. *Gaeumannomyces*, *Linocarpon*, *Ophiobolus* and several other genera of scolecospored ascomycetes and *Phialophora* conidial states, with a note on hyphopodia. Mycotaxon 11:1-129.

323. Walker, J., and Smith, A. M. 1972. *Leptosphaeria namari* and *L. korrae* sp. npv., two long-spored pathogens of grasses in Australia. Transactions of the British Mycological Society 58:459-466.

324. Walker, N. 2006. Viability of dormant bermudagrass in spring dead spot patches caused by *Ophiosphaerella herpotricha* during winter months. Phytopathology 96:S119.

325. Walker, N. R., Mitchell, T. K., Morton, A. N., and Marek, S. M. 2006. Influence of temperature and time of year on colonization of bermudagrass roots by *Ophiosphaerella herpotricha*. Plant Disease 90:1326-1330.

326. Wallen, R. M., and Perlin, M. H. 2018. An overview of the function and maintenance of sexual reproduction in dikaryotic fungi. Frontiers in Microbiology 9:503.

327. Waller, F., Achatz, B., Baltruschat, H., Fodor, J., Becker, K., Fischer, M., Heier, T., Hückelhoven, R., Neumann, C., von Wettstein, D., Franken, P., and Kogel, K.-H. 2005. The endophytic fungus *Piriformospora indica* reprograms barley to salt-stress tolerance, disease resistance, and higher yield. Proceedings of the National Academy of Sciences of the United States of America 102:13386.

328. Wan, J., Tanaka, K., Zhang, X. C., Son, G. H., Brechenmacher, L., Nguyen, T. H., and Stacey, G. 2012. LYK4, a lysin motif receptor-like kinase, is important for chitin signaling and plant innate immunity in *Arabidopsis*. Plant Physiol 160:396-406.

329. Wang, C., Du, X., and Mou, Z. 2016. The Mediator complex subunits MED14, MED15, and MED16 are involved in defense signaling crosstalk in *Arabidopsis*. Frontiers in Plant Science 7:1947.

330. Wang, H., Li, J., Bostock, R. M., and Gilchrist, D. G. 1996. Apoptosis: A functional paradigm for programmed plant cell death induced by a host-selective phytotoxin and invoked during development. Plant Cell 8:375-391.

331. Wang, Y., Li, J., Hou, S., Wang, X., Li, Y., Ren, D., Chen, S., Tang, X., and Zhou, J. M. 2010. A *Pseudomonas syringae* ADP-ribosyltransferase inhibits arabidopsis mitogen-activated protein kinase kinases. Plant Cell 22:2033-2044.

332. Wehmeyer, L. E. 1963. Some Himalayan ascomycetes of the Punjab and Kashmir. Mycologia 55:309-336.

333. Wessels, J. G. H. 1994. Developmental regulation of fungal cell wall formation. Annual Review of Phytopathology 32:413-437.

334. Wetterstrand, K. A. DNA Sequencing Costs: Data from the NHGRI Genome Sequencing Program (GSP). Retrieved from. Retrieved February 22, 2019, from www.genome.gov/sequencingcostsdata.

335. Wetzel III, H. C., Dernoeden, P. H., and Millner, P. D. 1996. Identification of darkly pigmented fungi associated with turfgrass roots by mycelial characteristics and RAPD-PCR. Plant Disease 80:359-364.

336. Wetzel III, H. C., Hulbert, S. H., and Tisserat, N. A. 1999. Molecular evidence for the presence of *Ophiosphaerella narmari* n. comb., a cause of spring dead spot of Bermuda grass, in North America. Mycological Research 103:981-989.

337. Wetzel III, H. C., Skinner, D. Z., and Tisserat, N. A. 1999. Geographic distribution and genetic diversity of three *Ophiosphaerella* species that cause spring dead spot of bermudagrass. Plant Disease 83:1160-1166.

338. Wilken, P. M., Steenkamp, E. T., Wingfield, M. J., de Beer, Z. W., and Wingfield, B. D. 2017. Which MAT gene? Pezizomycotina (Ascomycota) mating-type gene nomenclature reconsidered. Fungal Biology Reviews 31:199-211.

339. Wilton, M., Subramaniam, R., Elmore, J., Felsensteiner, C., Coaker, G., and Desveaux, D. 2010. The type III effector HopF2 Pto targets *Arabidopsis* RIN4 protein to promote *Pseudomonas syringae* virulence. Proceedings of the National Academy of Sciences of the United States of America 107:2349-2354.

340. Wolpert, T. J., Dunkle, L. D., and Ciuffetti, L. M. 2002. Host-selective toxins and avirulence determinants: what's in a name? Annu Rev Phytopathol 40:251-285.

341. Wong, P. T. W., Dong, C., Martin, P. M., and Sharp, P. J. 2015. Fairway patch - a serious emerging disease of couch (syn. bermudagrass) [*Cynodon dactylon*] and kikyuy (*Pennisetum clandestinum*) turf in Australiua caused by *Phialocephala bamuru* P.T.W. Wong & C. Dong sp. nov. Australasian Plant Pathology 44:545-555.

342. Wösten, H. A. B. 2001. Hydrophobins: multipurpose proteins. Annual Reviews in Microbiology 55:625-646.

343. Wu, C. H., Krasileva, K. V., Banfield, M. J., Terauchi, R., and Kamoun, S. 2015. The “sensor domains” of plant NLR proteins: More than decoys? Frontiers in Plant Science 6:134.

344. Wu, D., Oide, S., Zhang, N., Choi, M. Y., and Turgeon, B. G. 2012. ChLae1 and ChVel1 regulate T-toxin production, virulence, oxidative stress response, and development of the maize pathogen *Cochliobolus heterostrophus*. PLoS Pathog 8:e1002542.

345. Xu, N., Luo, X., Li, W., Wang, Z., and Liu, J. 2017. The bacterial effector AvrB-induced RIN4 hyperphosphorylation is mediated by a receptor-like cytoplasmic kinase complex in *Arabidopsis*. Mol Plant Microbe Interact 30:502-512.

346. Yamada, K., Yamaguchi, K., Shirakawa, T., Nakagami, H., Mine, A., Ishikawa, K., Fujiwara, M., Narusaka, M., Narusaka, Y., Ichimura, K., Kobayashi, Y., Matsui, H., Nomura, Y., Nomoto, M., Tada, Y., Fukao, Y., Fukamizo, T., Tsuda, K., Shirasu, K., Shibuya, N., and Kawasaki, T. 2016. The *Arabidopsis* CERK1-associated kinase PBL27 connects chitin perception to MAPK activation. EMBO Journal 35:2468-2483.

347. Yang, S. L., and Chung, K. R. 2013. Similar and distinct roles of NADPH oxidase components in the tangerine pathotype of *Alternaria alternata*. Molecular Plant Pathology 14:543-556.

348. Yang, Y., Li, L., and Qu, L.-J. 2016. Plant Mediator complex and its critical functions in transcription regulation. Journal of Integrative Plant Biology 58:106-118.

349. Zaccaron, A. Z., and Bluhm, B. H. 2017. The genome sequence of *Bipolaris cookei* reveals mechanisms of pathogenesis underlying target leaf spot of sorghum. Sci Rep 7:17217.

350. Zeilmaker, T., Ludwig, N. R., Elberse, J., Seidl, M. F., Berke, L., Van Doorn, A., Schuurink, R. C., Snel, B., and Van den Ackerveken, G. 2015. DOWNY MILDEW RESISTANT 6 and DMR6-LIKE OXYGENASE 1 are partially redundant but distinct suppressors of immunity in *Arabidopsis*. The Plant Journal 81:210-222.

351. Zhang, H., Yohe, T., Huang, L., Entwistle, S., Wu, P., Yang, Z., Busk, P. K., Xu, Y., and Yin, Y. 2018. dbCAN2: a meta server for automated carbohydrate-active enzyme annotation. Nucleic Acids Research 46:W95-W101.

352. Zhang, X., Yao, J., Zhang, Y., Sun, Y., and Mou, Z. 2013. The *Arabidopsis* Mediator complex subunits MED14/SWP and MED16/SFR6/IEN1 differentially regulate defense gene expression in plant immune responses. The Plant Journal 75:484-497.

353. Zhang, Y., Guenzi, A. C., Anderson, M. P., Taliaferro, C. M., and Gonzales, R. A. 2006. Enrichment of bermudagrass genes associates with tolerance to the spring dead spot fungus *Ophiosphaerella herpotricha*. Physiological and Molecular Plant Pathology 68:105-118.

354. Zheng, Z., Qamar, S. A., Chen, Z., and Mengiste, T. 2006. *Arabidopsis* WRKY33 transcription factor is required for resistance to necrotrophic fungal pathogens. Plant Journal 48:592-605.

355. Zipfel, C., and Rathjen, J. 2008. Plant immunity: AvrPto targets the frontline. Current Biology 18:R218-R220.

356. Zipfel, C., Kunze, G., Chinchilla, D., Caniard, A., Jones, J. D., Boller, T., and Felix, G. 2006. Perception of the bacterial PAMP EF-Tu by the receptor EFR restricts *Agrobacterium*-mediated transformation. Cell 125:749-760.

357. Zipfel, C., Robatzek, S., Navarro, L., Oakeley, E. J., Jones, J. D., Felix, G., and Boller, T. 2004. Bacterial disease resistance in *Arabidopsis* through flagellin perception. Nature 428:764-767.

358. Zottini, M., Costa, A., De Michele, R., Ruzzene, M., Carimi, F., and Lo Schiavo, F. 2007. Salicylic acid activates nitric oxide synthesis in *Arabidopsis*. Journal of Experimental Botany 58:1397-1405.

APPENDICES

Table A-1. DNA extraction protocol and modifications that were tested in order to achieve high yield high molecular weight nucleic acid of *Ophiosphaerella* spp.

Protocol	Modification
Weising *et al.* [1] with previous modifications by G. Orquera-Tornakian	• Using fresh and freeze-dried mycelium • Treatment with proteinase K (50 ug/ml) • Phenol:chloroform:isoamyl alcohol 25:24:1 • 5M potassium acetate with isopropanol
Möller *et al.* [2]	• Using fresh and freeze-dried mycelium • Removing proteins in acetone • 1% PVP and 0.2% 2-mercaptoethanol to TES Buffer • Omitting ammonium acetate • Phenol:chloroform:isoamyl alcohol 25:24:1 • Increased the temperature on CTAB step to 85ºC • Adding 0.3M sodium chloride to isopropanol step • Aspiration of supernatant • Cleaning the wall of tubes with a sterile kimwipe to remove traces of proteins • Retrieving the DNA pellet with a loop into a new tube

References:

1. Weising, K., Nybom, H., Wolff, K., Meyer, W. 1995. DNA fingerprinting in plant and fungi. CRC Press, Boca Raton, FL.

2. Möller, E. M., Bahnweg, G., Sandermann, H., and Geiger, H. H. 1992. A simple and efficient protocol for isolation of high molecular weight DNA from filamentous fungi, fruit bodies, and infected plant tissues. Nucleic Acid Research 20(22):6115-6116

Table A-2. Prediction of secreted effectors of *Ophiosphaerella herpotricha* and their location in the host cell during bermudagrass hosts 'Tifway' (susceptible) and 'U3 biotype' (resistant) root colonization. The secretome, produced by SignalP, of *O. herpotricha* was subjected to EffectorP prediction of candidate effectors. Subsequently, candidate effectors were subjected to ApoplastP and LOCALIZER to predict their location. Candidate effectors that had at least one predicted location were considered to be potential effectors.

Total Candidate Effectors	Predicted location of candidate effectors			
	Apoplast	**Chloroplast**	**Mitochondria**	**Nucleous**
421	357	52	10	53

Table A-3. Candidate secreted secreted effectors of *Ophiosphaerella herpotricha* that were predicted to localize exclusively in the apoplast during bermudagrass hosts 'Tifway' (susceptible) and 'U3 biotype' (resistant) root colonization.

Total	Candidate effector gene/identifier
305	g5617.t1, g10491.t1, MSTRG.8890.1, g1360.t1, MSTRG.10409.1, g8550.t1, g13212.t1, MSTRG.4270.1, MSTRG.7880.2, MSTRG.12710.1, MSTRG.1887.1, MSTRG.9480.2, MSTRG.5066.5, MSTRG.5066.6, MSTRG.12035.2, g12712.t1, g4201.t1, MSTRG.12166.1, MSTRG.9996.1, g4749.t1, MSTRG.9092.1, MSTRG.1545.1, g9781.t1, g4612.t1, g6235.t1, MSTRG.2558.1, MSTRG.11819.1, MSTRG.11819.2, g3570.t1, g2559.t1, g1355.t1, MSTRG.4479.1, g3156.t1, g5606.t1, MSTRG.7084.1, g2123.t1, MSTRG.6528.3, MSTRG.1662.1, MSTRG.1745.1, g3611.t1, g2470.t1, MSTRG.9737.5, g2202.t1, g5951.t1, MSTRG.2492.1, MSTRG.8864.1, g7429.t1, g7999.t1, MSTRG.1738.1, MSTRG.8779.1, g1358.t1, g6884.t1, g10206.t1, g4105.t1, g9336.t1, MSTRG.2073.2, MSTRG.2073.1, g1517.t1, g777.t1, g6695.t1, MSTRG.6069.1, g10213.t1, g10176.t1, MSTRG.5066.1, g6814.t1, MSTRG.5412.1, g2918.t1, MSTRG.3522.1, g4158.t1, g10325.t1, MSTRG.11485.2, MSTRG.11485.1, g589.t1, g9848.t1, g11771.t1, g7100.t1, MSTRG.1890.1, g4000.t1, g2226.t1, MSTRG.9226.1, g7219.t1, MSTRG.9871.1, MSTRG.9871.2, MSTRG.3946.1, g12917.t1, g11705.t1, g10006.t1, g7818.t1, MSTRG.1762.3, MSTRG.1762.2, MSTRG.1762.1, MSTRG.1762.4, MSTRG.3352.1, MSTRG.3352.2, MSTRG.3352.3, MSTRG.4755.3, MSTRG.2873.1, g8657.t1, g1350.t1, g11068.t1, MSTRG.4131.2, g6676.t1, MSTRG.9874.1, MSTRG.6658.1, MSTRG.9224.1, MSTRG.9224.2, MSTRG.1384.1, g12803.t1, g1617.t1, g7647.t1, g6030.t1, MSTRG.12035.1, g8930.t1, MSTRG.2074.1, g205.t1, MSTRG.4067.1, MSTRG.2788.2, MSTRG.2788.3, MSTRG.2455.1, g7345.t1, MSTRG.4693.1, MSTRG.4693.2, MSTRG.223.1, g12477.t1, g11040.t1, MSTRG.2377.1, g10618.t1, g7648.t1, g2483.t1, MSTRG.9421.1, g6384.t1, g1200.t1, g3365.t1, MSTRG.10731.1, MSTRG.9378.1, MSTRG.1908.1, g3003.t1, MSTRG.5224.9, MSTRG.1416.1, MSTRG.2763.3, MSTRG.2763.1, MSTRG.2763.4, MSTRG.1638.1, g11679.t1, g4455.t1, g7072.t1, MSTRG.1007.4, g2775.t1, g1751.t1, MSTRG.11829.1, g12235.t1, g1996.t1, g164.t1, g9874.t1, g1246.t1, g12730.t1, g9143.t1, g12579.t1, MSTRG.3263.1, g3840.t1, g903.t1, g92.t1, g6854.t1, g8622.t1, g5722.t1, g5427.t1, MSTRG.12098.1, MSTRG.4211.1, g12087.t1, g9443.t1, g4114.t1, g5179.t1, g8670.t1, MSTRG.1908.2, MSTRG.4813.2, MSTRG.2118.1, g2636.t1, g2827.t1, g3623.t1, g9643.t1, g11942.t1, g4549.t1, g10109.t1, MSTRG.5078.1, g1960.t1, MSTRG.12361.1, MSTRG.7690.1, g3044.t1, g6413.t1, MSTRG.11142.1, MSTRG.2827.1, MSTRG.11420.1, g4905.t1, MSTRG.6120.3, MSTRG.6120.1, MSTRG.2334.3, MSTRG.1676.1, MSTRG.5384.1, g3632.t1, MSTRG.11091.1, g1789.t1, MSTRG.10198.2, MSTRG.10198.1, g7294.t1, g4101.t1, g2795.t1, g10613.t1, MSTRG.9331.1, g5407.t1, MSTRG.9225.1, g6169.t1, g10016.t1, g4200.t1, MSTRG.5812.1, g8328.t1, MSTRG.3093.1, g737.t1, g8845.t1, g5806.t1, g2334.t1, MSTRG.7561.1, g10095.t1, g2568.t1, MSTRG.2557.1, g1326.t1, MSTRG.6722.3, MSTRG.6658.6, g9421.t1, g1681.t1, MSTRG.6894.1, g7927.t1, MSTRG.5229.1, MSTRG.5229.2, g3469.t1, MSTRG.12983.2, MSTRG.4549.1, MSTRG.3500.1, MSTRG.6528.1, MSTRG.1546.2, g10263.t1, MSTRG.11684.1, MSTRG.3339.1, g1217.t1, g12150.t1, MSTRG.8136.1, MSTRG.1482.2, g9871.t1, MSTRG.10019.1, MSTRG.570.1, g13097.t1, MSTRG.694.2, MSTRG.694.1, MSTRG.13096.1, g6434.t1, MSTRG.10185.3, MSTRG.6555.6, MSTRG.10599.1, g4537.t1, g11340.t1, MSTRG.7083.1, MSTRG.12786.1, g9588.t1, g10066.t1, g936.t1, g3693.t1, g8125.t1, g9849.t1, MSTRG.4131.1, g9117.t1, MSTRG.3107.2, MSTRG.3964.1, g8948.t1, g1229.t1, g9578.t1, g950.t1, MSTRG.127.1, MSTRG.795.1, MSTRG.1416.5, MSTRG.1416.4, MSTRG.1416.3, MSTRG.1416.2, g4452.t1, MSTRG.5619.1, g3590.t1, g1909.t1, MSTRG.4656.1, g10412.t1, g5472.t1, MSTRG.8091.1, g2931.t1, g2300.t1, g9548.t1, g1120.t1, MSTRG.12263.1, g993.t1, MSTRG.1514.4, MSTRG.1514.5, MSTRG.1514.3, MSTRG.1514.8, g10279.t1, MSTRG.7097.2, g7649.t1, g11757.t1, MSTRG.7856.1, g12843.t1

Table A-4. Candidate secreted secreted effectors of *Ophiosphaerella herpotricha* that were predicted to localize exclusively in the cytoplasm during bermudagrass hosts 'Tifway' (susceptible) and 'U3 biotype' (resistant) root colonization.

Total	Predicted location of candidate effectors		
	Chloroplast	Mitochondria	Nucleous
63	g10595.t1 MSTRG.303.1 MSTRG.9235.2 MSTRG.9235.3 g1967.t1 g9840.t1 MSTRG.4471.1 MSTRG.6141.1 MSTRG.1760.1 MSTRG.2012.1 MSTRG.2012.2 MSTRG.4332.2 MSTRG.4332.1 g9603.t1 g10729.t1 MSTRG.9180.2 g1585.t1	MSTRG.10139.1 MSTRG.4600.1 MSTRG.2096.4 MSTRG.8762.1 MSTRG.10032.3 MSTRG.10032.4 g6170.t1	MSTRG.10258.1 MSTRG.10258.2 MSTRG.12287.2 MSTRG.12287.3 MSTRG.12287.1 g6132.t1 g4867.t1 g2472.t1 g8547.t1 g12063.t1 g6635.t1 MSTRG.7555.1 MSTRG.10259.1 g4208.t1 g7531.t1 g13093.t1 g1516.t1 MSTRG.3259.1 MSTRG.6191.1 MSTRG.12288.1 g5315.t1 g6244.t1 MSTRG.6086.7 MSTRG.6086.6 MSTRG.6086.5 MSTRG.6086.4 MSTRG.6086.3 MSTRG.6086.2 MSTRG.6086.1 MSTRG.6086.8 MSTRG.12322.2 MSTRG.11139.1 MSTRG.12626.1 MSTRG.7981.2 MSTRG.12121.1 g12673.t1 g2566.t1 MSTRG.12083.1 g10072.t1

Table A-5. Candidate secreted secreted effectors of *Ophiosphaerella herpotricha* that were predicted to localize in the apoplast and in the cytoplasm during bermudagrass hosts 'Tifway' (susceptible) and 'U3 biotype' (resistant) root colonization.

Total	Predicted location of candidate effectors		
	Chloroplast	Mitochondria	Nucleous
52	MSTRG.6306.1 g1245.t1 g9991.t1 g769.t1 MSTRG.9465.2 MSTRG.9465.1 g7736.t1 g5952.t1 g6025.t1 g9271.t1 g11733.t1 g12291.t1 MSTRG.5244.1 MSTRG.6565.1 MSTRG.4493.1 MSTRG.8035.2 MSTRG.8035.1 MSTRG.5700.1 MSTRG.4662.1 MSTRG.11587.1 MSTRG.11587.2 g8263.t1 g7571.t1 g2351.t1 MSTRG.357.1 g12939.t1 MSTRG.357.2 g10876.t1 MSTRG.12435.1 MSTRG.5417.1 MSTRG.7104.5 MSTRG.7104.4 MSTRG.7104.3 MSTRG.7104.2 MSTRG.7104.1	g7738.t1 g13260.t1 MSTRG.10483.1	g12620.t1 MSTRG.9746.1 MSTRG.9746.3 MSTRG.9746.2 MSTRG.401.2 g1577.t1 g2509.t1 g9224.t1 MSTRG.3302.1 g248.t1 MSTRG.7997.3 MSTRG.7997.4 MSTRG.9395.5 g11677.t1

VITA

Nathalia Graf Grachet

Candidate for the Degree of

Doctor of Philosophy

Dissertation: HOST-PATHOGEN INTERACTION IN THE SPRING DEAD SPOT OF BERMUDAGRASS PATHOSYSTEM

Major Field: Plant Pathology

Biographical:

Education:

Completed the requirements for the Doctor of Philosophy in Plant Pathology at Oklahoma State University, Stillwater, Oklahoma in July, 2019.

Completed the requirements for the Master of Science in Entomology and Plant Pathology at Oklahoma State University, Stillwater, Oklahoma in 2015.

Completed the requirements for the Bachelor of Science in Agricultural Engineering at Federal University of Sao Carlos, Araras, Sao Paulo, Brazil in 2012.

Experience:
Graduate Research Assistant, Department of Entomology and Plant Pathology, Oklahoma State University, Stillwater, OK, January 2013 to July 2019.
Visiting Research Scholar, Department of Entomology and Plant Pathology, Oklahoma State University, Stillwater, OK, March to October 2012.
Undergraduate Field Intern, Farm & Ranch Zurita, Araras, Sao Paulo, Brazil, December 2011 to February 2012.

Professional Memberships:
American Phytopathological Society (APS)
Honor Society Phi Kappa Phi
Genetics Society of America (GSA)
International Turfgrass Society (ITS)